# DISSERTATION

# Comprehensive analytical methods for lipid profiling in biological systems

submitted by

## Dipl.-Ing. Alexander Fauland

For the Doctoral Degree of

Technical Sciences

at the

## Graz University of Technology

under Supervision of

## Ao.Univ.-Prof. Dipl.-Ing. Dr.techn. Ernst Lankmayr

**2012**

# STATUTORY DECLARATION

I declare that I have authored this thesis independently, that I have not used other than the declared sources / resources, and that I have explicitly marked all material which has been quoted either literally or by content from the used sources.

………………………………                      …………………………………………………..

         date                                                                (signature)

# Acknowledgements

First of all I express my deep thanks to everyone at the Institute of Analytical Chemistry and Food Chemistry for providing a great platform for my PhD work.

Especially, I thank to my supervisor, Prof. Ernst Lankmayr for guiding me throughout the four years of my PhD studies. He managed to maintain the fine balance of giving me useful directions and advices but taking me serious enough and allowed me to freely try my own ideas. For this I am very grateful to him.

I want to thank also my colleague Prof. Xinghua Guo for his supportive suggestions and being always helpful.

My dissertation has created a new connection between our institute and the Core Facility for Mass Spectrometry in the Center for Medical Research at the Medical University of Graz. This work has greatly benefitted from the outstanding expertise of the director, Dr. Harald Köfeler. His broad knowledge and experience were essential for completing this work.

Special thanks to my outdoor-friend and colleague, Dr. Martin Trötzmüller for his creative attitude and endless theoretical and practical suggestions which always proved to work. I can honestly state that the time with him brought me a good scientific practice and irreplaceable experience in the field of organic analytical chemistry.

I express my deepest thanks to all members of the Core Facility team for providing an inspiring atmosphere.

Dear Viki, thank you for your continuous support in my life as well as in my doctoral study.

My dearest family, without your support and believe in me I would have not completed my dissertation.

# Table of contents

# Comprehensive analytical methods for lipid profiling in biological systems

Lipids are a class of biomolecules with enormous structural diversity and a huge number of different biological functions. Lipid molecules are involved in various cellular regulation cycles of biological systems; the multiple roles of lipids are demonstrated by human diseases. Impaired lipid metabolism is associated with diseases such as diabetes, atherosclerosis, cancer, chronic inflammation and neurodegenerative diseases. The system-based study of all lipids including their interaction partners and the functions of lipids within the cell is called lipidomics, an emerging research field. Novel analytical methodologies, in particular atmospheric pressure ionization mass spectrometry coupled with enhanced chromatographic separation techniques enables new possibilities in lipid analysis.

Despite advanced analytical instrumentation technologies, sample preparation is still an essential part in lipid research. Especially innovative techniques such as solid-phase extraction (SPE) can be used either for separation of contaminants, for the enrichment of low concentrated components or for chromatographic pre-separation of individual target analytes. Thus, in this work, a rapid and universal SPE method has been developed, which is highly suitable for the separation and identification of phospholipids derived from complex biological samples. For the separation step, sequential combination of silica gel - aminopropyl - silica gel SPE cartridges is applied prior to the LC-MS measurement. The centerpiece of this work comprises the development of an analytical platform for high throughput lipidomic analysis. The instrumental setup includes a one dimensional reversed-phase HPLC coupled to a Fourier transform ion cyclotron resonance mass spectrometer (LTQ-FT), and Lipid Data Analyzer (LDA) software. Identification and quantification of lipid species, shown here paradigmatically for murine lipid droplets, is based on retention time, mass resolution of 200,000, and mass accuracy below 2 ppm. Data analysis in a quantitative manner is performed by LDA. In addition, the automatically generated MS/MS spectra provide structural information at molecular level. Extension of 1D to 2D chromatography improves chromatographic separation, yet it is still time consuming. Additionally, this work involves the characterization of ionic chemical background noise typically present in negative ESI LC-MS mode. Chemical background noise is one of the major problems in organic trace analysis, since they tend to interfere with target analytes during measurement. Systematic investigation of the ionic chemical background noise for typical eluents in LC-MS leads to further significant noise reduction.

# Umfassende analytische Methoden zur Lipidbestimmung in biologischen Systemen

Lipide sind Biomoleküle, die eine enorme strukturelle Vielfalt aufweisen und unterschiedliche, biologische Funktionen besitzen. Sie spielen eine zentrale Rolle in der Regulation und Kontrolle zellulärer Prozesse und bei menschlichen Krankheiten. Störungen des Lipidstoffwechsels sind Auslöser sowie Begleiterscheinungen vieler Krankheiten wie zum Beispiel Diabetes, Arteriosklerose, Krebserkrankungen aber auch chronische, inflammatorische oder neurodegenerative Krankheiten. Das junge Forschungsgebiet der Lipidomik umfasst die Erforschung der Gesamtheit der Lipide in einer Zelle, einem Gewebe, oder einem gesamten Organismus. Dazu gehören auch systematische Untersuchungen physiologischer und pathophysiologischer Funktionen von Lipiden und ihren Metaboliten. Enorme Fortschritte in der Analytik, wie zum Beispiel hochauflösende Massenspektrometer in Kombination mit Ionisation unter Atmosphärendruck und auch verbesserte chromatographische Trenntechniken (LC-MS) revolutionieren die Lipidanalytik.

Trotz der schnellen Entwicklung methodischer Techniken bleibt die Probenvorbereitung ein integraler Bestandteil in der Lipidforschung. Innovative Methoden wie die Festphasen-extraktion (SPE), bestechen durch ihre mannigfaltigen Anwendungsmöglichkeiten. So können mithilfe der SPE gewünschte Zielanalyten angereichert bzw. störende Matrixkomponenten weitgehend entfernt werden, was eine anschließende, massenspektrometrische Bestimmung wesentlich vereinfacht. Des Weiteren besteht die Möglichkeit, individuelle Zielanalyten mittels SPE chromatographisch aufzutrennen, was auch in dieser Arbeit zur Anwendung kommt. Dieser Teil der Arbeit beschreibt die Entwicklung einer universellen SPE Methode, die speziell für die Fraktionierung und Identifizierung von Phospholipiden aus komplexen, biologischen Proben geeignet ist. Die chromatographische Auftrennung erfolgt mittels sequentieller Kombination beginnend mit einer Silikagel-, gefolgt von einer Aminopropyl- und wiederum gefolgt von einer Silikagel SPE Kartusche. Die Bestimmung der Analyten erfolgt abschließend mittels LC-MS. Das Herzstück dieser Arbeit ist die Entwicklung einer analytischen Plattform für „High-Throughput" Lipidomik. Diese besteht aus einer eindimensionalen Umkehrphasen-HPLC Methode, gekoppelt mit einem Fourier Transformations Ionenzyklotron Resonanz Massenspektrometer (LTQ-FT) und einer Auswertesoftware, dem Lipid Data Analyzer (LDA). Die Bestimmung verschiedenster Lipidspezies wird beispielhaft an Lipidtropfen aus murinen Hepatozyten gezeigt. Die Identifizierung der Lipide wird durch die erhaltenen Informationen aus chromatographischer Retentionszeit, der hohen Massenauflösung bis zu 200.000 und der Massengenauigkeit unter 2 ppm ermöglicht. Die quantitative Datenauswertung wird mittels LDA durchgeführt. Zusätzlich geben die automatisch generierten MS/MS Spektren Auskunft

über die Lipidstruktur auf molekularem Level. Die Erweiterung der 1D chromatographischen Methode auf eine 2D Chromatographie hat zwar eine verbesserte Auftrennung der aller Analyten zur Folge, ist jedoch zeitintensiver. Des Weiteren umfasst die Arbeit die Charakterisierung der chemischen Untergrund-Ionen die im negativen ESI LC-MS Modus ubiquitär vorhandenen sind. Chemisches Untergrundrauschen ist eines der Hauptprobleme in der organischen Spurenanalytik, da sie mit den Zielanalyten während der Messung häufig interferieren. Systematische Untersuchungen des chemischen Untergrundes mit gängigen Laufmitteln zur LC-MS sind hilfreich für eine signifikante Reduzierung der chemischen Untergrund-Ionen.

# List of abbreviations

| Abbreviation | Definition |
| --- | --- |
| 2D IT | two dimensional ion trap |
| 3D-IT | three-dimensional ion trap |
| AGC | automatic gain control |
| APCI | atmospheric pressure chemical ionization |
| API | atmospheric pressure ionization |
| APPI | atmospheric pressure photo ionization |
| CAD | collision activated dissociation |
| CEM | chemical measurement process |
| CI | chemical ionization |
| CID | collision induced dissociation |
| CMP | chemical measurement process |
| CRM | charged residue model |
| DART | direct analysis in real time |
| DC | direct current |
| DDA | data dependent acquisition |
| DESI | desorption electrospray ionization |
| EI | electron impact ionization |
| EMC | enhanced multiply charged |
| EMS | enhanced Q3 single MS |
| EPI | enhanced product ion |
| ER | enhanced resolution Q3 single MS |
| ESCi | ESI-APCI |
| ESI | electrospray ionization |
| FAB | fast atom bombardment |
| FID | free induced decay |
| FT-ICR-MS | Fourier transform ion cyclotron resonance mass spectrometry |
| FWHM | full width at half maximum |
| GC | gas chromatography |
| GC-MS | gas chromatography - mass spectrometry |
| HILIC | hydrophilic interaction liquid chromatography |
| HPLC | high performance liquid chromatography |
| IDA | information dependent aquisition |
| IEC | ion exchange chromatography |

| | |
|---|---|
| IEV | ion evaporation model |
| LC | liquid chromatography |
| LC-MS | liquid chromatography - mass spectrometry |
| LDA | Lipid Data Analyzer |
| LIT | linear ion trap |
| LLE | liquid-liquid extraction |
| LTQ | linear ion trap quadrupole |
| LTQ-FT | linear ion trap quadrupole - Fourier transform ion cyclotron resonance mass spectrometer |
| MAE | microwave-assisted extraction |
| MALDI | matrix assisted laser desorption ionization |
| MCP | multichannel plates |
| MESI | membrane extraction with a sorbent interface |
| MMLLE | microporous membrane liquid-liquid extraction |
| MS | mass spectrometry |
| NL | neutral loss |
| NP-LC | normal phase-liquid chromatography |
| PB | particle beam |
| PC | precursor ion scan |
| PIS | product ion scan |
| PS-DVB | polystyrene divinylbenzene polymer |
| PTFE | polytetrafluoroethylene |
| PV-PPS | polyvinyl pyridine-polystyrene polymer |
| QIT | quadrupole ion trap |
| QqQ | triple quadrupole |
| QqQLIT | triple quadrupole linear ion trap |
| QqTOF | quadrupole time of flight hybrid instrument |
| RF | radiofrequency |
| RP | reversed phase |
| RP-LC | reversed phase-liquid chromatography |
| SAE | sonication-assisted extraction |
| SBSE | stir bar sorptive extraction |
| SEC | size exclusion chromatography |
| SFE | supercritical fluid extraction |
| SIM | selected ion monitoring |
| SLE | supported liquid extraction |
| SLM | supported liquid membrane extraction |

| | |
|---|---|
| SPE | solid-phase extraction |
| SPME | solid-phase micro extraction |
| SRM | selected reaction monitoring |
| TDF | time delayed fragmentation |
| TLC | thin layer chromatography |
| TOF | time of flight |
| TSP | thermospray |
| UHPLC | ultra high performance liquid chromatography |
| UV/VIS | ultraviolet/visible spectrophotometry |

# A. Introduction

## A.1. General aspects of analytical chemistry

*"Analytical chemistry is a scientific discipline which develops and applies methods, instruments and strategies to obtain information on the composition and nature of matter in space and time".[1]*

Analytical chemistry can be divided into two fields, namely the basic and the applied analytical chemistry. The task of basic analytical chemistry is introducing innovations in chemical analysis. Such innovations include the development of new analytical tools and methods or the preparation of reference materials of high metrological quality. Optimization of new calibration procedures and chemometric approaches also belongs to the basic analytical chemistry discipline. In contrast, applied analytical chemistry deals with solving problems occurring in economic and social areas including industry, environment, food science, technology and pharmaceutical or clinical analysis.

Analytical chemistry is an information discipline which fundamentally aims to extract the intrinsic (bio)chemical information from a target object or system. This information which retains or alters its composition in space and/or in time is typically the sort of information to be addressed by an analytical chemist. This important analytical information includes qualitative, quantitative and structural compositions which are closely related to each other. Thus, some qualitative knowledge of a complex sample is required for assessing further quantitative analysis. Conversely, structural analyses are related to qualitative and quantitative information previously obtained from a certain sample. For collecting this intrinsic chemical information it is substantially important to select the most proper chemical measurement process. This measurement process includes the right choice of already available analytical methods or optionally the development of new analytical procedures. The final quality of analytical results and processes depends on the applied analytical properties. These properties are quality indicators for a variety of systems, objects, tools and outputs in (bio)chemical measurements that allow comparison and validation of both the analytical processes and the provided data. The quality indicators are accuracy, representativeness, and precision, as well as robustness, expenditure of time, automatization, sensitivity and selectivity. These determinants have to be always optimized for numerous analytical parameters in a chemical measurement process.

---

[1] Definition of the DAC (Division of Analytical Chemistry) and FECS (Federation of European Chemical Societies.

A general overview of chemical measurement process in analytical chemistry is shown in Figure 1. This can be explained as a set of operations taking place between the uncollected - unmeasured - untreated sample and the final results. A chemical measurement process can be generally divided into four major steps. The first two steps are the preliminary operations and the measurement and transducing of the analytical signal. The third part is the acquisition and processing of the data while the last step involves calibration operations using measurement standards as input.
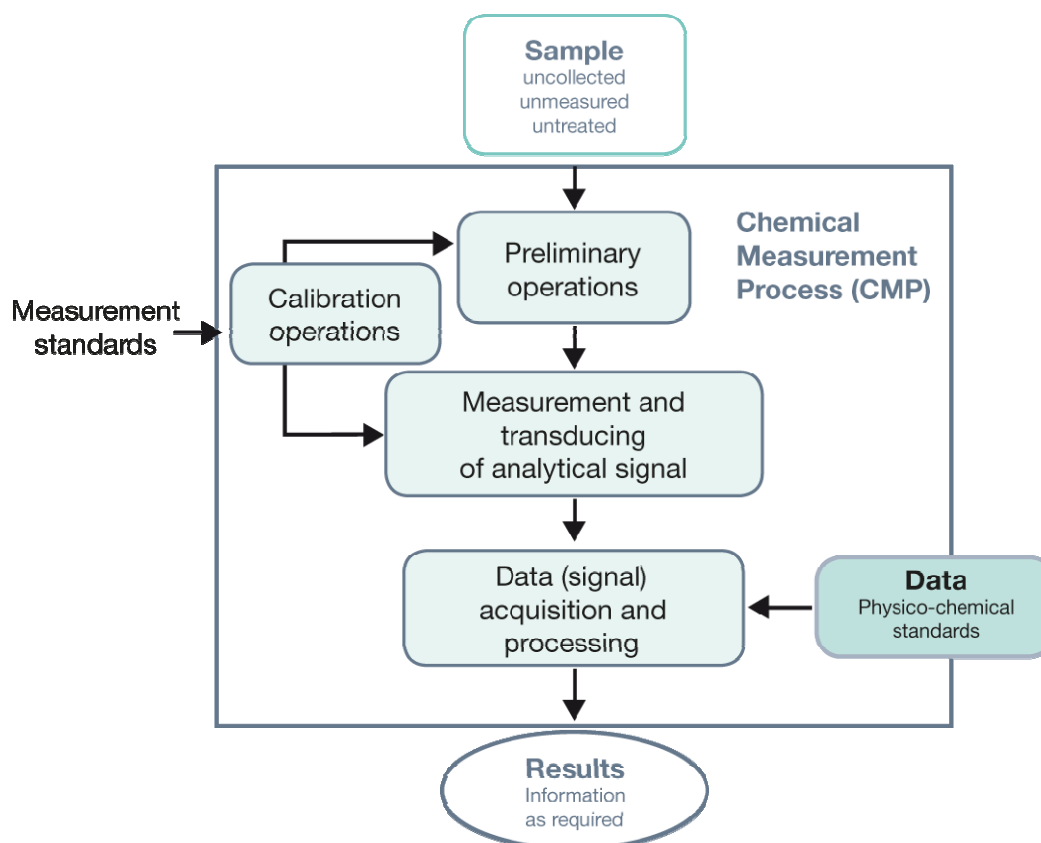


**Figure 1**. Main steps of a chemical measurement process (CMP). The CMP consists of three major steps, starting with preliminary operation, followed by measurement and transducing of analytical signal and finally data acquisition and processing. In addition the fourth step comprises calibration operations. The image is reproduced and slightly modified with the kind permission of © Wiley-VCH Verlag GmbH & Co. KGaA (1).

The first step, preliminary operations of the analytical process are subdivided into the sampling and the sample preparation step. Both are described more in detail in chapter B.1 and B.2. Their main purpose is preparing the sample for further measurements. Generally, preliminary operations are widely variable in nature due to the diversity of the samples. They can be derived from different physical conditions and can possess an organic, inorganic or biological matrix. Furthermore, analytes can also be inorganic, organic or biochemical of nature, and are represented at variable concentrations. This variability requires a specific

approach for each individual sample-analyte pair. The complexity of preliminary operations demands intensive human participation and are generally difficult to automate. In addition this step is the greatest source of both systematic and random errors which have a crucial influence on the quality of the results. Typical errors in this context arise from non-representative samples, incomplete removal of interfering compounds or inappropriate sample storage conditions.

The second step of the analytical process involves the use of an instrument that receives an aliquot of the processed sample from the first step and measures and transduces the analytical signal related to the presence and/or amount of the analyte. The measured signal is a response of the instrument to chemical (reactivity) or physico-chemical properties of the analyte or its reaction products. This signal can be of various sorts, including optical (e.g. UV/VIS spectrophotometer) electrochemical (e.g. pH-meter), mass (e.g. mass spectrometer) or thermal (e.g. thermogravimetric balance) signals.

The next step in the analytical process encompasses the transformation of the analytical signals produced by instruments into the analytical results in a required format, according to client's prerequisites. The acquisition of transduced signals can be achieved simply by inspecting the color of a precipitate or reading of the burette scale. Such data can also be acquired semi-automatically, for example by using instruments providing output information such as a chromatogram or spectrum, but also automatically with computer processing information.

The first three steps, which have the sample as input are frequently integrated, either partly (gas-liquid chromatography integrating the first two steps) or completely (e.g. strips for the in situ determination of glucose in blood). The fourth essential step of a chemical measurement process involves calibration operations and has measurement standard as input. Equipment calibration is necessary to ensure correct performance of the instrument and all apparatuses. On the other hand, method calibration is carried out to establish qualitative and quantitative relationships between the analytes and the signals provided by the analytical instruments. Method calibration is mainly connected to the second step of the process (1, 2).

## A.2. Scope of work

The aim of this work is based on the development of a high throughput analytical method for the comprehensive analysis of different lipid species in various biological matrices. The here established universally applicable analytical platform include: 1) simple and versatile sample

preparation steps 2) highly sensitive and selective mass spectrometry based approaches in combination with chromatographic separation for structure determination, identification and quantification of various lipid species at different concentration levels. 3) a data processing software for automatic lipid profiling. In addition to this platform, typical chemical background noise in LC-MS is studied which is a major drawback in organic trace analysis.

In detail, the first level of a successful lipid profiling requires proper sample preparation steps. Due to the complexity of the biological matrices it is necessary to separate interfering compounds from analytes with suitable extraction procedures. Next to simple sample preparation steps like liquid-liquid extraction, centrifugation and filtration, innovative techniques such as solid-phase extraction (SPE) are applied, as exemplified in chapter C.3.

Secondly, mass spectrometry based approaches in combination with chromatographic separation were applied for determination of different lipid components. The biological samples might contain a high diversity of lipids, which urges successful determination of all components of interest, including the ones at low concentration levels too. Hence, online coupling high performance liquid chromatography (HPLC) to high resolution Fourier transform ion cyclotron resonance mass spectrometry (FT-ICR-MS) in combination with electrospray ionization (ESI) is the method of choice. The development of a fast, highly reproducible, sensitive and selective LC-MS approach which allows analyzing complex biological samples in a quantitative manner constitutes the main part of this work (chapter C.4). Additionally, for optimal chromatographic separation of target analytes one or two dimensional LC approaches are applied. Due to the multiplicity of various lipids in biological samples, a complete successful separation of all lipid species from different lipid classes is hardly manageable with a one dimensional chromatographic approach. Although alleviated by chromatography, adverse effects caused by overlapping masses and ion suppression are still encountered in such an LC-MS setting. Therefore, two dimensional chromatographic separation can decrease the problem of ion suppression, yet it is more time consuming. An additional point, which should be considered, is that SPE can also be used for chromatographic separation of individual lipid classes prior to LC-MS analysis. Chapter C.3 describes a simple and fast SPE method which allows the separation of phospholipid classes into different fractions. A further combination to the one dimensional LC approach enables an improved separation without ion suppression.

The third level of the analytical platform is the high throughput sample analysis. To this end, data dependent acquisition (DDA), a special mode of operation of ion trap mass spectrometer instruments like the linear ion trap quadrupole coupled to a Fourier transform

ion cyclotron resonance mass spectrometer (LTQ-FT), is applied here. The DDA mode circumvents the need of measuring samples separately to obtain MS and MS/MS data. Since those sophisticated and modern mass spectrometers easily generate a huge volume of spectra, data processing becomes the bottleneck of a high throughput analytical method. Manual extraction of relevant information to address certain biological questions can be extremely time consuming and hence an automatic data processing is simply indispensable. Therefore, I take benefit of the flexible in-house developed software, the so called Lipid Data Analyzer (LDA), which is especially suitable for the determination of lipids.

Another major problem in organic trace analysis is discussed in this work, which is related to the presence of ionic chemical background noise. In the procedure of atmospheric pressure ionization LC-MS, ionic background chemicals appear unavoidably. These omnipresent by-products are traces of ionized contaminants and stable clusters, which render even more difficult e.g. qualitative studies for the identification of trace components almost useless. These background ions completely overshadow the target analytes in chromatograms or mass spectra. The study of chemical background ions which are typically detected in negative ESI mode is shown in chapter C.5.

# B. Theoretical fundamentals in organic trace analysis

## B.1. Sampling

The initial sample collection step plays an essential role, since the quality of the analytical results relies on both accuracy and representativeness. As shown in Figure 2, sampling is the major source of errors in the analytical process and an accurate result which is not representative will not be a proper result anyway. Optimal sampling is a complex operation which can entail various problems. Hence, sampling represents one of the most difficult procedures of an analytical process.
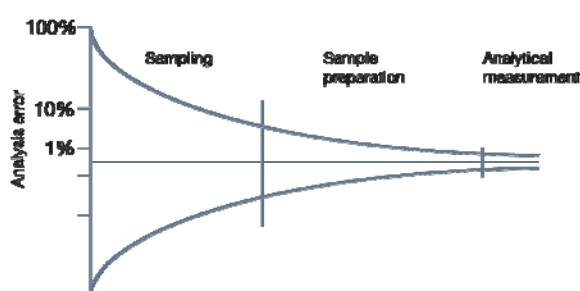


**Figure 2**. Error sources of an analytical process. Sampling is the major source of error in the analytical process. The image is reproduced and slightly modified with the kind permission of © Springer Spektrum (3).

Prior to sample collection, one needs an accurate definition of the required information that will be extracted from the object. An important issue in addressing the analytical problem is the nature of the desired information, whether it is uniform or shows spatial or temporal variability. The individual properties of the target object are highly relevant to sampling. Sampling becomes an elaborate problem in the analytical process in case the target object is not uniform or homogeneous. Heterogeneity in the object directly influences the precision of the results. Thus, collection of higher sample numbers is required in order to ensure representativeness and minimize random errors, which would directly influence the precision of the result expressed as a standard deviation. Additionally, the aggregate state of the target object (solid, liquid, gaseous or mixed) plays also a crucial role and fosters dedicated sampling procedures. Sampling is further strongly affected by the type of matrix of the target object (inorganic, organic or biological) and by the nature and concentration of the target analytes. Moreover, the sampling approach of choice strongly depends on the variability of the target object in time, which is commonly referred to as stability. If the composition of the object is time-dependent, collection of higher sample numbers will be necessary. A further source of problems in sampling can occur due to improper sample storage and transport

conditions. These systematic sampling errors affect directly the accuracy of the results. Inappropriate sampling equipment or storage conditions can lead to losses of analytes through interaction of the sample with the container walls or reaction with the atmosphere agents (e.g. $CO_2$ or $H_2O$).

Taken together, sampling should be done in a way which ensures that the sample aliquot, the ultimate subject of the other steps of the analytical process, represents the original composition of the source object as close as possible (1-3).

## B.2. Sample preparation

The analytes of interest are rarely ready to measure without a sufficient sample preparation. Pre-treatment of the sample before the actual measurement is frequently required, such as extraction of the analyte from a complex matrix or its enrichment to a suitable concentration that could be easier detected. The appropriate choice of sample preparation improves selectivity, detectability, reliability, accuracy and reproducibility of the analysis. The selection of a sample preparation method is on one hand largely influenced by the nature of the sample and on the other hand by the analytical instrumentation technique which is planned to be used for determination of the analytes. Typically, the first steps of sample treatment involve homogenization, evaporation of the sample, filtration, centrifugation, mixing, etc., often followed by the suitable extraction procedures (e.g. liquid-liquid extraction, solid-phase extraction or solid-liquid extraction). In this context chromatographic separation techniques like thin layer chromatography (TLC), high performance liquid chromatography (HPLC) or gas chromatography (GC) are also regarded as sample preparation techniques. However, the proper combination of dedicated detection methods is necessary for these techniques too. Additionally, chemical modification of the analyte molecules is many times used to improve detectability and extraction efficiency.

The sample preparation step is essential because even the best analytical instrumentation cannot fix problems generated by improper sample handling. Along with sampling, the sample preparation is a key step prior to the analytical determination of the target analytes. Choosing the most optimal sample preparation procedure can be very difficult if a combination of several different preparation techniques is required. Figure 3 shows a general strategy for sample pre-treatment of solid and liquid samples including a huge variety of different sample preparation techniques.
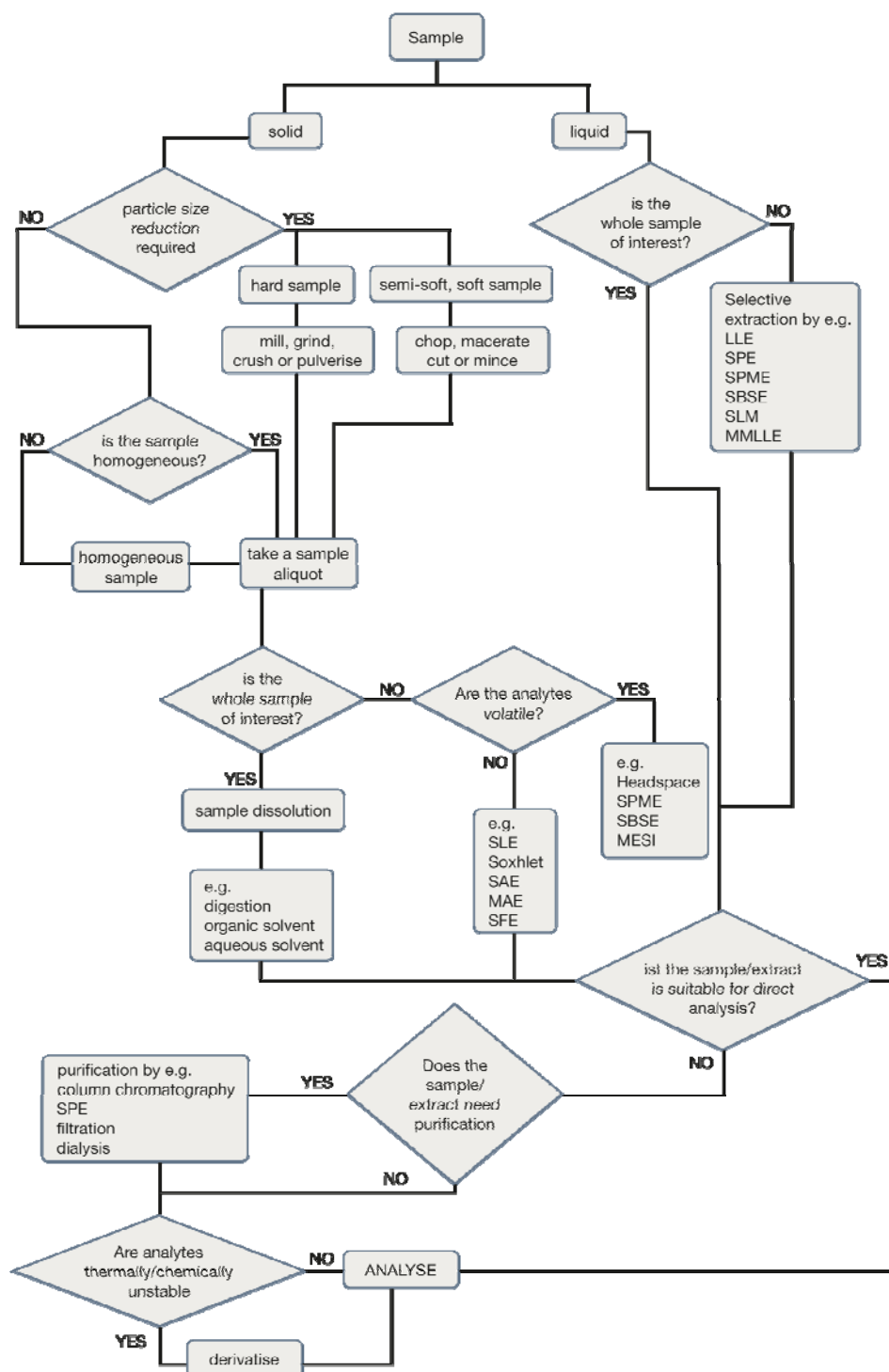
**Figure 3**. Simplified general strategy for the selection of a sample preparation procedure for solid and liquid samples. LLE: liquid-liquid extraction, SPE: solid-phase extraction, SPME: solid-phase micro extraction, SBSE: stir bar sorptive extraction, SLM: supported liquid membrane extraction, MMLLE: microporous membrane liquid-liquid extraction, MESI: membrane extraction with a sorbent interface, SLE: supported liquid extraction, SAE: sonication-assisted extraction, MAE: microwave-assisted extraction, SFE: supercritical fluid extraction. The image is reproduced and slightly modified with the kind permission of © Wiley-VCH Verlag GmbH & Co. KGaA (1).

The following chapters B.2.1, B.2.2, B.2.3 and B.2.4 describe certain sample preparation techniques including extraction methods and also chromatographic separation techniques which were applied in the present work (1-3).

### B.2.1. Liquid-liquid extraction

Liquid-liquid extraction (LLE) is the most common organic solvent extraction technique for the isolation of analytes solved in a liquid sample. This extraction method enables separation of analytes from interfering compounds by partioning the sample between two immiscible liquids or phases. In practice most of the extractions are performed from aqueous samples. Therefore, the aqueous phase is combined with a suitable organic solvent where the analytes get favourably solved. The simplest way to accomplish LLE is pouring the two phases in a separation funnel and shaking the mixture manually. The theory of LLE is based on the Nernst distribution law, which defines the distribution coefficient for the analyte between the particular phases as the crucial parameter with respect to the extraction yield. A distribution coefficient is dependent on the chemical nature of the analytes, the two liquid phases, the pH and on the temperature. Higher extraction efficiency can be reached by repeating LLE with small amounts of solvents for a few times instead of using a large amount of organic solvent one time. The purity of organic solvents for the extraction is of particular importance, as contamination of the solvents can disturb subsequent measurements of the analytes. Typical disadvantages of LLE are the high dilution factor of the extract and big amounts of solvent requirement. Additionally, the formation of emulsions is a drawback of LLE, which appears mainly if an organic extraction solvent with intermediate polarity is used or if the volume ratio of organic solvent to aqueous phase is rather small (1, 2, 4, 5).

### B.2.2. Solid-phase extraction

The beginning of solid-phase extraction (SPE) dates back to the early 1970s when columns were commonly packed with polymeric sorbent particles to concentrate organic particles from water samples. The name "solid-phase extraction" was first used by the J.T. Baker Chemical Company in 1982.

SPE is a multistage separation technique used for concentration and isolation of analytes from liquid and gaseous samples and for the separation of interferences from the samples as so called sample clean-up. SPE is often applied as sample pre-treatment step before HPLC. Generally, SPE enables removal of chemical constituents from a flowing liquid sample via retention of the analytes on a solid sorbent and by subsequent recovery of selected analytes

by elution from the sorbent. SPE is typically performed in small cartridges which are commonly made of polytetrafluoroethylene (PTFE), polypropylene or glass. The size of the cartridges is in the range of 0.5 to 60 mL and the packing weights of the solid sorbent in the cartridges vary usually from 30 mg to 10 g. To avoid sample cross-contamination SPE cartridges are generally used only once. The principle of SPE is based on the different distribution of the analytes between a mobile phase and a stationary phase similarly to liquid chromatography separation. However, SPE chromatographic separation of the analytes is performed on very short columns having a low number of theoretical plates but involving compounds with very distinguishable distribution coefficients. The interactions between analytes and the sorbent material are for instance hydrogen bonding, dipole-dipole interactions, hydrophobic dispersion forces or electrostatic interactions (Coulomb interactions).

A large variety of different sorbent materials are applied in SPE. The choice of the sorbent material is determined by the polarity of the analytes and the nature of the sample matrix. Sorbents are classified as nonpolar, polar and ion-exchange types. Polar materials like silica, alumina or polar-functionalized bonded silica are mainly used in normal-phase SPE. For reversed-phase applications, common bonded phases like hydrophobic, aliphatic alkyl groups or aromatic phenyl groups covalently bound to the silica backbone are produced. Furthermore, various ion exchange sorbents with carboxylic acid or sulfonic acid as ionic functional groups, polymers or other special packing materials for different applications are available. Special mixed-mode phases are also popular, which represent dual characteristics of, e.g. reversed-phase and ionic sorbent.

There are several advantages of the SPE method compared to LLE. SPE is much faster, easy to automate and manipulate. SPE offers an ample spectrum of extractions and interfering compounds can be washed off or retained more efficiently. The time consuming steps in LLE like shaking, waiting for the emulsion to break, careful separation of the two liquid phases or back extraction are not required at all in SPE. Reduced amounts of organic solvents are sufficient, which is an important environmental issue. SPE also provides much higher concentrated extracts compared to LLE, concentration factors of 1000 or even higher are manageable.

### B.2.2.1. The four steps of SPE

In practice the SPE procedure can be divided into four main steps, which are conditioning, adsorption, washing, and elution. The SPE process is illustrated in Figure 4. Each step is described in the following section.
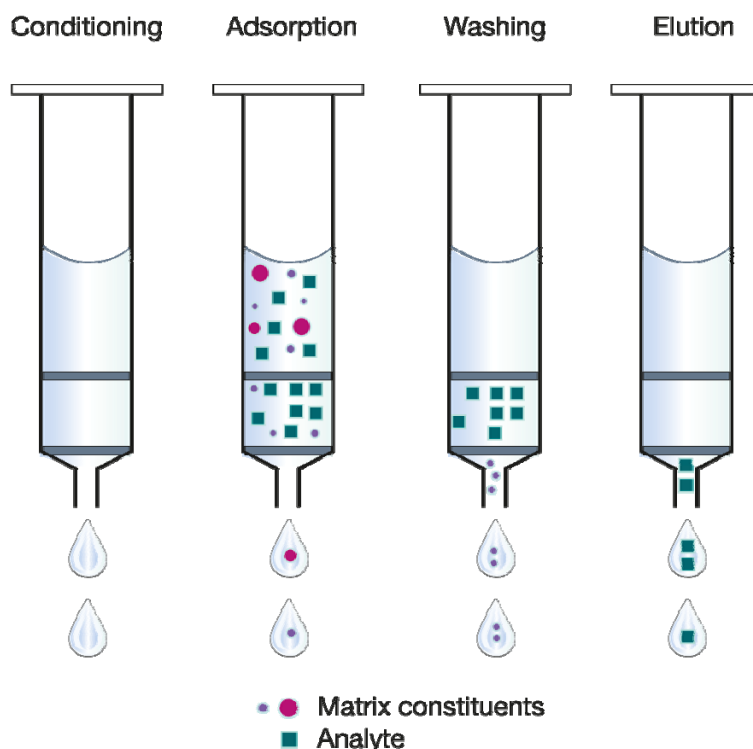


**Figure 4**. The four steps in SPE comprising of the conditioning, adsorption, washing and elution step. The image is reproduced and slightly modified with the kind permission of © Wiley-VCH Verlag GmbH & Co. KGaA (6).

*Conditioning*

Before applying the sample, the adsorbent material first has to be conditioned with a suitable solvent to ensure high reproducibility. This handling step allows the sorbent to be solvated and promotes better surface contact between the solid and liquid phase. Thus, conditioning increases the active surface area.

*Adsorption*

The volume of the liquid to be extracted should be minimized for the separation from interfering impurities. For the proper enrichment of analytes on the sorbent a slow and constant flow rate is used. Sometimes a sufficient sample clean-up can be achieved only by applying these first two steps of the SPE procedure. In this process, the sample passes

through the cartridge and only the interfering impurities are strongly retained on the sorbent, whereas the analytes are weakly held on the cartridge and collected for further treatments. In this case no further washing and elution step is necessary.

*Washing*

If both, analyte and interfering impurities are strongly retained on the cartridge, interferences can be removed in a washing step with a suitable solvent or solvent mixture. This wash solution should be strong enough to elute undesirable matrix components but the analytes should remain at the sorbent material. The washing step is an optional step of the SPE procedure.

*Elution*

In the elution step the target compounds are selectively collected from the adsorbent material with a strong elution solvent which is passed through the packed column (1, 2, 4-6).

### B.2.3. Thin-layer chromatography

Thin-layer chromatography (TLC) can be seen as a modified form of liquid chromatography. Compared to column chromatography the TLC technique is a planar method of chromatography. TLC is a separation system which can be carried out very quickly and it is easy to handle. Thus, this technique is often chosen as a preliminary test prior to column chromatographic separation and frequently used for screening in chemical, industrial, clinical, pharmaceutical, biomedical and biological laboratories.

Stationary phases used in TLC can be common sorbents like normal-phase (e.g. silica or alumina) and a variety of different reversed-phase sorbents. Further sorbents available nowadays for different applications are for example kieselgur, cellulose, polyamides or cyclodextrin. The separation of the analytes in TLC is based on adsorption, partition, ion-exchange and size exclusion. The development of the chromatogram is performed in a closed development chamber, where the mobile phase must be moved across the stationary phase. Various visualization techniques allow the detection and identification of the analytes on the plate. As one possibility, the layer bed of the TLC plate can be impregnated with a fluorescent indicator substance which enables detection of the analytes as nonfluorescent spots under UV light. Analytes themselves do also have fluorescence characteristic and can be used for detection. For detection, a variety of group- or substance specific spraying and dipping reagents (e.g. ninhydrin to visualize $NH_2$ groupings) can be applied. Additionally, the

selectivity of TLC separation can be improved by developing the plate in two dimensions using separated mobile phases in each direction. Compared to other chromatographic separation techniques like HPLC or GC, TLC allows simultaneous development of several samples on one single plate. This possibility triggers a widespread application of this technique as an easily handled "high throughput screening" method (1, 2, 7).

### B.2.4. High-performance liquid chromatography

Initially, simple column chromatography was first introduced by Tsweet in 1903 which is dated back as the beginning of the liquid chromatography era. Since that time, various liquid chromatography techniques represent one of the most commonly used separation techniques. Despite improved and novel chromatographic methods, the easy and simple column chromatography from that time is still used today in large-scale preparative work or for preliminary experiments to liquid chromatography. Importantly, the most frequently used application in liquid chromatography is high-performance liquid chromatography, known as HPLC for short.

High performance liquid chromatography (HPLC, also known as high pressure liquid chromatography) is typically applied in analytical chemistry as well as in biochemistry for the separation, identification and quantification of different compounds of interest. Generally HPLC is an ideal alternative to gas chromatography (GC). Although GC is widely used, this technique is restricted to samples that are thermally stable and easily volatized. Some nonvolatile samples can be analyzed by GC only after a suitable chemical derivatisation. However, a large number of organic compounds cannot be vaporized without thermal decomposition. Consequently, the determination of such substances with GC becomes impossible. The only criterion for HPLC is solubility of organic compounds in certain solvents suitable for HPLC applications. Hence, the determination of almost all kinds of organic compounds, except of cross-linked macromolecules, is manageable by using HPLC.

HPLC is a fully automated instrumentation consisting of solvent reservoirs, a degassing unit, solvent delivering pumps, an injection port, a column, an optional column oven and a detector. The modules of a HPLC unit are illustrated in Figure 5. After degassing the solvent (mobile phase) the pump pushes the eluents through the column (stationary phase) at a defined flow rate. The most commonly used pumps in HPLC systems are displacement and reciprocating pumps. The sample is injected by using a six-way valve with an attached sample loop. Upon injection of the sample, the eluents pass through the injector and transfer the sample into the column. In most of the HPLC instruments, the temperature of the eluent

13

and column can be controlled too. The sample components will be separated on the column due to different interaction between analytes and the sorbent material followed by analysis using the proper detector. Peak broadening effects should be reduced; therefore, the dead volume of the unit in the injection system and in the detector must be kept minimal. Retention time of the analytes is influenced by the interactions between the stationary phase, all other molecules being analyzed and the mobile phase. Such interactions are for example hydrogen bonding, dipole-dipole interactions, hydrophobic dispersion forces or electrostatic interactions (Coulomb interactions). HPLC separations can be monitored with several types of detectors including UV detectors, photodiode array detectors, fluorescence, evaporative light scattering detectors or refractive index detectors. In addition, coupling of HPLC to mass spectrometry attracts a growing interest due to the additional information provided by mass spectrometry. In this latter approach, next to the retention time of the detected compounds, information of the molecular mass as well as structural information, given by the fragmentation pattern can be used additionally for identifying the detected analytes. Up to now, various LC-MS coupling techniques are already well established and almost completely replaced the traditional UV detection in many bioanalytical laboratories. LC-MS is also the main instrumentation setup used in this work and described in detail in chapter B.4.
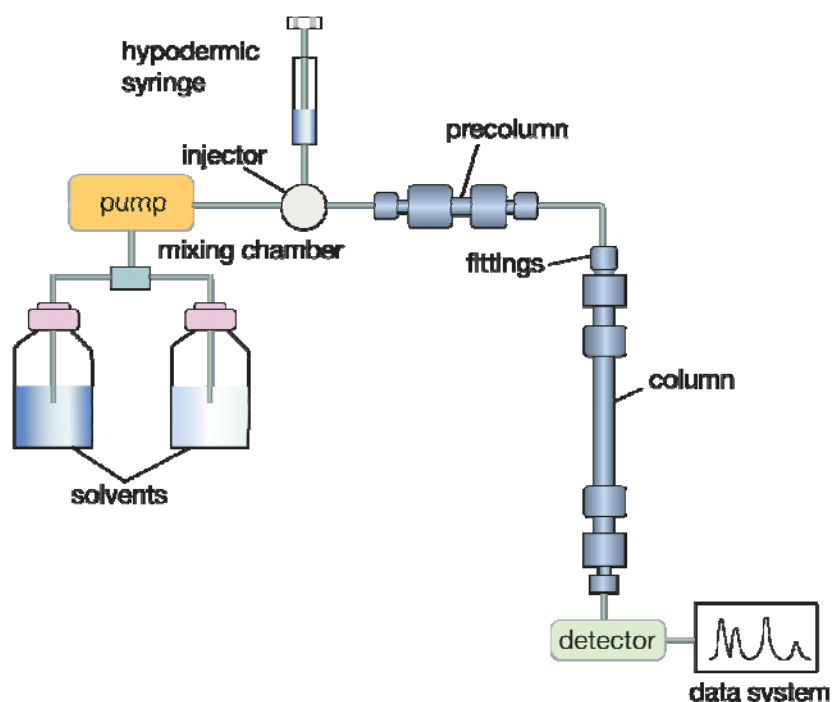


**Figure 5**. Sketch of a HPLC unit with a precolumn. Generally, HPLC hardware consists of solvent reservoirs, a degassing unit, solvent delivering pumps, an injection port, a column, an optional column oven and a detector. The image is reproduced and slightly modified with the kind permission of © Wiley-VCH Verlag GmbH & Co. KGaA (1).

Since the column is the core of the HPLC instrument, different types of HPLC systems can be classified based on the dimension and particle size of the applied column. Hence, HPLC systems are divided into preparative, analytical, micro and nano HPLC. The start of modern HPLC column and packing material development dates back to the mid-`60s. The very first materials used in HPLC columns were irregularly formed particles of silica and reversed-phase bonded silica in a size range of 15-10 μm. In the same time, pellicular HPLC packing materials were developed too, which consisted of a solid core of 30-40 μm glass and were coated with microfine sorbent material. Following this initial time, the majority of particles used for HPLC are spherical due to their better fit at packing into a column compared to the previously used irregularly-formed particles. Over the years the particle size has been strongly reduced as well as the columns become much shorter in length. Reduced particle size allows faster and better separation without the loss of efficiency. Moreover, the productivity is increased with a combination of lower cost per analysis. However, reduced particle size and inner diameter of the column lead to a sharp increase of the back pressure inside the column. The capability of a pump thus determines the practical limits of column dimension and particle size. Conversely, the five years ago developed ultra-HPLC (UHPLC) systems overcome this difficulty because these systems can stand high back pressure and allow sub-2 μm particles to be used in HPLC columns.

Today, over 30 different column sizes are available with various sorbent materials and particle sizes. The type of stationary phase is chosen according to the applied technique. Important general characteristics of the stationary phase are the shape, size, porosity and particle size distribution of the supporting material. The supporting material may be composed of non-porous, pellicular, porous or perfusion particles or of monolithic rods. Nowadays, silica-based stationary phases are the most popular supporting materials. Pure silica is often used in adsorption chromatography or as support material for chemical modified materials. Recent developments of particle technology are the so called fused-core particles consisting of a solid core encircled by a porous silica shell. These supporting materials provide significantly improved separation resolution, minimized peak broadening and they enable higher flow rates. Less popular supporting materials are polymeric supports such as polystyrene divinylbenzene polymer (PS-DVB) and polyvinyl pyridine-polystyrene polymer (PV-PPS). Despite of this huge and unclear variety of different types of packing materials, they can be simple classified based on their polarity of the stationary and mobile phases.

### B.2.4.1.    Normal-phase chromatography

In normal phase-liquid chromatography (NP-LC) polar stationary phases and nonpolar mobile phases are used for the separation of moderately polar compounds. Typical packing materials in NP-LC are pure silica or diol-, amino-, cyano-bonded phases. In NP-LC the retention of analytes is determined by the competitive adsorption between the analyte molecules and the strongly eluting solvent molecules for the adsorptive sites on the adsorbent surface.

### B.2.4.2.    Reversed-phase chromatography

Besides NP-LC, reversed phase-liquid chromatography (RP-LC) is the most popularly used separation technique in HPLC. Additionally, there are various separation modes available like ion exchange chromatography (IEC) and size exclusion chromatography (SEC), which are both not described in this work. A wide variety of compounds can be separated by RP-LC, in fact approximately 80% of all separations reported in literature are covered by this kind of chromatography. RP-LC can be performed for the separation of compounds ranging from small to large molecules as well as from nonpolar to intermediate polar analytes. Mainly nonpolar, chemically-modified silica particles and sometimes also different polymeric nonpolar packing materials are used as stationary phase in RP-LC. The bonding reagent consists mostly of a straight-chain alkyl group such as $C_8H_{17}$ or $C_{18}H_{37}$. However, hydrocarbon polymer layers which are covalently bound to the support surface are less frequently applied. In RP-LC, a mixture of an aqueous solution and organic solvent is used as mobile phase. The retention in RP-LC can be considered as a partioning mechanism of the analytes between the moderately polar mobile phase and the nonpolar sorbent. Generally, nonpolar compounds retain longer at the nonpolar RP stationary phase then polar analytes. The nonpolar surface in RP-LC, like bonded alkyl chains can be highly solvated by compounds of the mobile phase. This part can be explained as a selective adsorption of compounds from the eluents. However, the solvation leads to the formation of a thick solid-liquid interface with a complex structure. Since the stationary phase in RP-LC can be regarded as a quasi-liquid layer, a portioning of the analytes between the stationary and the mobile phase similarly to LLE described in chapter B.2.1 is possible.

### B.2.4.3.    Hydrophilic interaction liquid chromatography

Due to the growing demand of analyzing highly hydrophilic, ionic and polar compounds in highly diverse extracts, which is practically not possible by RP chromatography, a suitable

approach, the so called hydrophilic interaction liquid chromatography (HILIC) method was developed. First described around 1990, HILIC is an alternative separation mode to NP chromatography. Polar materials such as amino-, amide-, diol-, zwitterionic silica etc. are used as stationary phase in HILIC. The most frequently occurring functional groups attached to the backbone are cyano-, carbohydrates-, diol- and hydroxyl groups. However, compared to NP-LC the mobile phase in HILIC consists mostly of the mixture of an organic solvent (typically acetonitrile) and a protic solvent (usually water which acts as strong eluting solvent) and additionally of a volatile salt (such as ammonium acetate or ammonium formate). Using 5% to 50% water in eluents offers better solubility of highly polar analytes in HILIC eluents in comparison to the eluents used in NP-LC. Furthermore, the big amount of organic solvent in eluents enables the use of high flow rate of mobile phase without high column back pressure. The retention mechanism in HILIC can be regarded as a mixed retention model composed of partitioning as seen at RP-LC and adsorptive interaction, for instance dipole-dipole or ionic interactions which are commonly used retention mechanisms in NP-LC. Compared to RP chromatography, HILIC shows a quite different elution order of analytes. If the separation of polar analytes is strongly limited with RP-LC, a satisfying separation can still be managed with HILIC. Consequently, this high orthogonality of both techniques is very attractive for multi-column approaches. Online coupling or offline analysis on both RP and HILIC columns broadens the range of compounds which can be analysed in a single chromatographic run. This approach was also used in the present work described in chapter C.4 (1, 2, 5, 8-13).

## B.3. Mass spectrometry in organic trace analysis

Mass spectrometry (MS) is a sensitive analytical technique which is able to precisely quantify known analytes and to identify unknown molecules occurring in picomolar or femtomolar range. A fundamental requirement of MS is the generation of gaseous analyte ions. These ions are then further separated or filtered according to their mass-to-charge (m/z) ratio and are finally detected. The resulting mass spectrum is a plot of the (relative) abundance of the ions produced as a function of the m/z ratio. MS is applied analytically in a great variety of qualitative and quantitative studies. Qualitative applications involve structure elucidation of unknown compounds such as natural or synthetic compounds and metabolites of drugs. MS is substantial for the determination of molecular mass, molecular formula or elemental composition and in structure elucidation. In quantitative analysis, MS is applied in developing definitive and reference methods and in the quantitation of, for example drugs in biological matrices. Mass spectrometers are highly sophisticated and computerized instruments, which basically consist of a sample introduction device, a source to produce ions, one or several

mass analyzers, a detector to measure the abundance of ions and a computerized system for data handling (Figure 6).
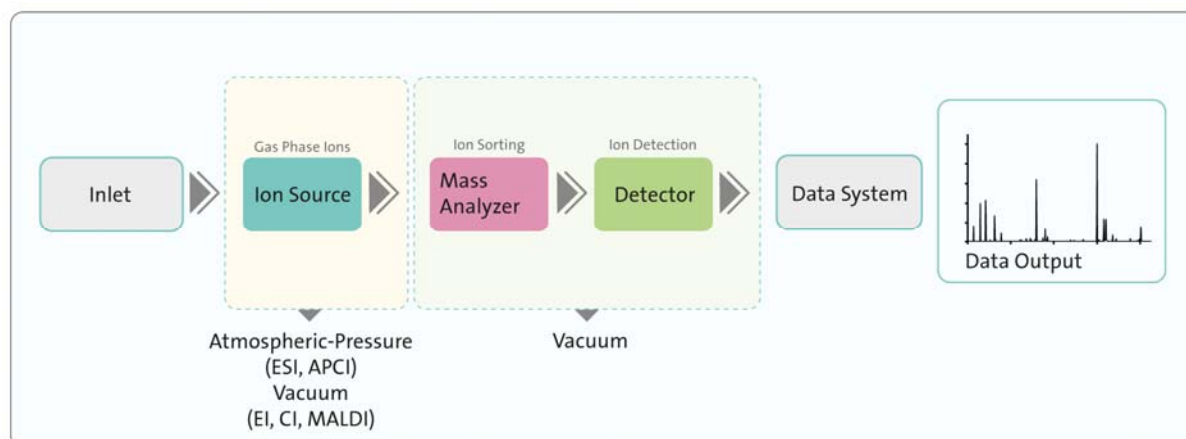


**Figure 6**. General scheme of a mass spectrometry setup comprising of an inlet unit, ion source, mass analyzer, detector and a data system. Ionization of analytes with electrospray ionization (ESI) or atmospheric pressure chemical ionization (APCI) is performed under atmospheric pressure whereas for electron impact (EI), chemical ionization (CI) or matrix assisted laser desorption ionization (MALDI) a high vacuum is required.

In the following chapters (chapter B.3.3) functionality and various designs of different mass spectrometers using different mass analyzers are described, which are especially suitable for coupling to HPLC separation techniques, since the methodological focus of the present work is on LC-MS coupling. Therefore, these chapters attempt to explain in depth the current ionization techniques, different mass analyzers and detectors used in LC-MS and in organic trace analysis. As already mentioned before, coupling MS to separation techniques, like LC has become increasingly important in recent years (more about in chapter B.4). Applications of such hyphenation techniques are already well established and essential methods in life science research as well as in daily routine analysis (1, 2, 12-14).

### B.3.1. Atmospheric Pressure Ionization techniques

Organic trace analysis using mass spectrometry is possible with a wide range of different ionization techniques. Analyte ionization methods in analytical MS can be subdivided as hard and soft ionization techniques. This classification is due to the different extent of fragmentation occurring during the ionization process. A typical hard ionization method is electron impact ionization (EI), generally used for example in GC-MS. The remaining other techniques are mainly soft ionization techniques, like the currently frequently applied electrospray ionization (ESI). Soft ionization techniques are based on the principle of atmospheric pressure ionization (API) and have become of substantial importance,

particularly in LC-MS. Generally, API enables the ionization of labile and non-volatile substances which can be then further examined by MS. Thus, API has become strongly linked to HPLC due to ionization of the eluent on its way into the MS. However, API is also used as a stand-alone inlet for introduction of samples. As indicated by its name, in API the analyte ions are first generated at atmospheric pressure followed by their transfer into the vacuum space. Some API sources enable ionization of neutral molecules in solution or in gas phase prior to ion transfer to the MS. These most notable techniques in API are ESI, atmospheric pressure chemical ionization (APCI) and atmospheric pressure photoionisation (APPI). Alternatively, different ionization sources might be combined with each other. The great advantage is that a broader range of analytes can be acquired simultaneously by combining for instance ESI and APCI, known as ESCi, or ESI and APPI. Important to note are some new techniques in API, the so called desorption electrospray ionization (DESI) and direct analysis in real time (DART) techniques. They offer unique opportunities for the analysis of surface or solid samples. Working principles and certain designs of frequently used API sources utilized in the actual work are discussed in detail in the following chapter (chapter B.3.2) (1, 12, 13, 15).

## B.3.2.  Atmospheric Pressure Ionization - sources and interfaces

An API source consists of five parts. Figure 7 illustrates paradigmatically an ESI source coupled to a quadrupole mass analyzer. Generally, the front part of an API source is a liquid introducing device followed by the actual ion source region. In this area ions are generated under atmospheric pressure by means of ESI, APCI, or other techniques. The rear part of an API source consists of the ion-sampling aperture, followed by the transition region from atmospheric pressure to high vacuum interface. Finally an ion-optical system is used, where ions generated in the source are analyte-enriched and transported towards the MS into the high vacuum region.
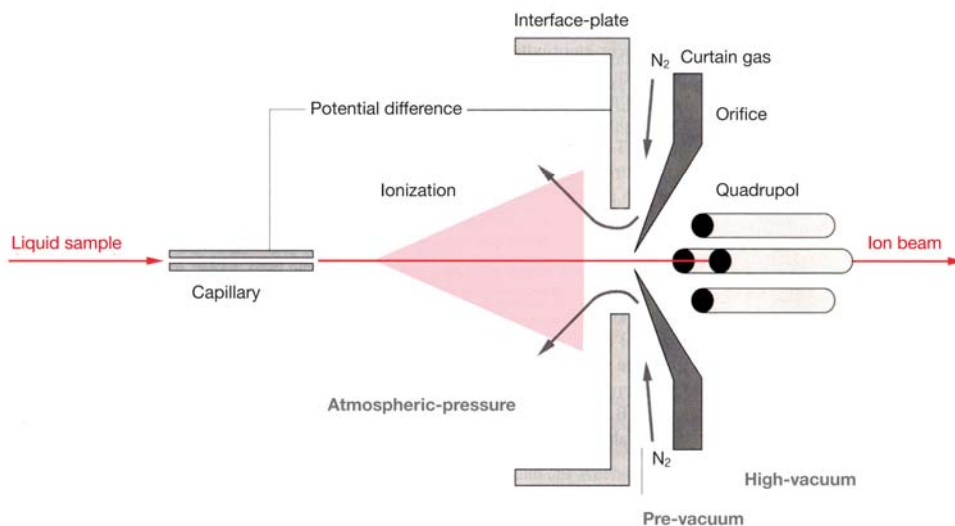
**Figure 7**. Design of an ESI source coupled to a quadrupole mass analyzer. The liquid sample is first introduced in the ion source region where ionization takes place under atmospheric pressure. Generated ions are further transported towards the MS into the high vacuum region. The image is reproduced and slightly modified with kind permission of © Springer-Verlag (16).

Significant pressure reduction is required for transfer of generated ions from the atmospheric pressure into the high vacuum region. A gas stream which is transferred from the ionization source into a vacuum system expands and cools down. In case this gas stream contains ions and solvent vapors, ion-solvent clusters might appear. For achieving good sensitivity and a high quality spectrum a key requirement is the prevention of these cluster formations. To this end, several instrumental setups have been proposed, including single stage pumping or differential stage pumping. Figure 8A displays a typical single stage pumping API interface with curtain gas. The space between the orifice and the curtain plate is flushed with heated pure nitrogen. An electric field is formed between the curtain plate and the orifice and this moves the ions through the curtain gas into the mass analyzer. In this way, neutral solvent molecules cannot penetrate into the high vacuum region, which excludes the formation of cluster ions. An orifice has the size of about 100 µm in diameter and for maintaining high vacuum extreme powerful pumps are applied, like turbo molecular, diffusion or cryogenic pumps. Differential pumping systems were developed in order to reach the desired vacuum in the mass analyzer. In Figure 8B an instrumental design is shown using differential pumping designs with a heated capillary interface. In this system, the ions flow through a heated stainless-steal capillary at first (150-300 °C), which has a typical internal diameter of 0.5 mm, and supports the desolvation process. In the first pumping region, a reduced vacuum is created with the help of a rotary pump. The ions are subsequently pushed through

a skimmer or an orifice into a second vacuum chamber where the high vacuum is provided by a turbo molecular pump. Finally, the ions are analyzed in the mass analyzer. Most modern instruments use differential pumping system either with capillary skimmer or with an orifice skimmer setup with or without curtain gas (2, 12, 13, 17).
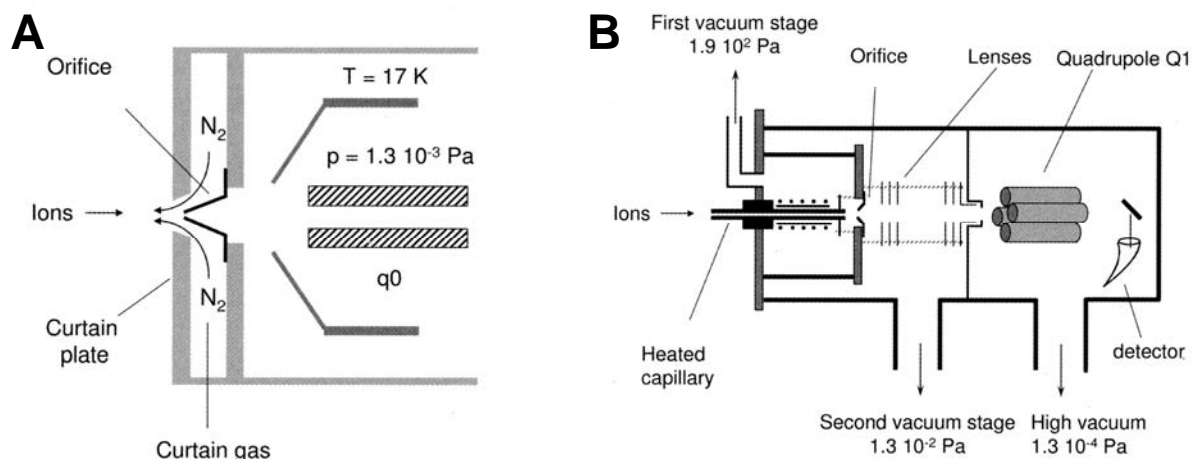


**Figure 8**. Single stage- and differential pumping design of an API interface. (**A**) Single stage pumping with curtain gas and q0, where q0 acts as a focusing quadrupole. The presence of nitrogen gas prevents neutral molecules from being introduced into the mass spectrometer. (**B**) Differential pumping design with heated capillary. This design requires a dual stage pumping system before the ions are introduced into the quadrupole mass analyzer which needs to operate at high vacuum. The function of the lenses is focusing on the ions; these lenses can also be a hexapole or octapole. The images are reproduced with the kind permission of © Wiley-VCH Verlag GmbH & Co. KGaA (13).

### B.3.2.1.    Electrospray Ionization

Electrospray was used long before its application to MS. This technique is of significant importance for the electrostatic dispersion of liquids and creation of aerosols. However, the initial idea of using electrospray as an ionization technique for MS, called today ESI, is originated from Malcolm Dole in the nineteen sixties. The significance of ESI coupled to MS was recognized by the award of a Nobel Prize in 2002 to John Fenn. Today, Fenn is regarded as the major developer of ESI. He continued the work of Dole and finally designed a suitable electrospray source which can be interfaced to MS. ESI-MS could be used very effectively for the analysis of small ions and molecules as well as macromolecules with a molecular mass extending into the megadalton range. Since then, this new ionization approach has gained a big impact in organic trace analysis. In addition, this time was also the start of the ESI-MS revolution which is presently still emerging.

Generally, ESI is a process where charged droplets are generated due to the nebulisation of a solution in an electric field (Figure 9). The liquid is introduced via stainless steel or a fused silica capillary into the ion source while the potential (typically 3-6 kV in positive mode) is applied directly on the capillary or on the counter electrode. In negative mode the applied potential range is always a bit lower (typically 3-4 kV) to avoid discharge. The penetration of the imposed electric field into the liquid near the spray capillary tip leads to formation of an electric double layer at the meniscus. This double layer arises from the polarisability and dipole moments of the solvent molecules. Thus, in positive ionization mode positive ions which are present in the solution are enriched on or near the surface of the meniscus, whereas negative ions are enriched away from the meniscus. The forces due to the polarization cause a destabilization of the meniscus which leads further to the formation of a so called Taylor cone, and a jet charged by an excess of positive ions. This fluid filament splits into charged droplets containing mainly positive ions. The size of the charged droplet is continuously decreasing since the neutral solvent molecules from these charged droplets are evaporated. This in turn leads to a reduction of the distances between the excess charges at the droplet surface. After some time, the surface tension of the liquid droplet can no longer accommodate the increasing Coulomb repulsion between the excess charges at the surface. At a defined limit, called the Rayleigh limit, a Coulomb explosion or field induced electrohydrodynamic disintegration process takes place, which causes disintegration of the droplets. The process of solvent evaporation and electrohydrodynamic droplet disintegration may be repeated a few times, which results in formation of smaller and smaller offspring droplets. Finally, two processes are responsible for the formation of gas phase analyte ions from these microdroplets.
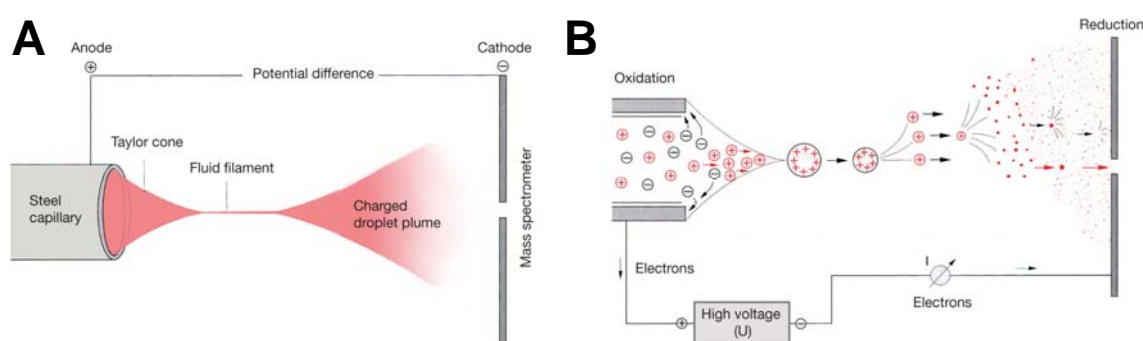


**Figure 9**. Schematic of a macroscopic- and microscopic ESI process. (**A**) The macroscopic ESI process illustrates the typical formation of the Taylor cone followed by the fluid filament and the charged droplet plume before ions are further transferred into the MS. (**B**) The ionization process in positive ESI is illustrated in detail in the figure. At the Rayleigh limit, a Coulomb explosion or field induced electrohydrodynamic disintegration process leads to disintegration of the droplets and finally to charged analyte molecules. The images are reproduced and slightly modified with the kind permission of © Springer-Verlag (16).

The mechanisms for the formation of gas phase ions from droplets are not fully understood yet. Two theories have been recommended to account for the formation of gas-phase ions from the final droplets, namely (i) the charged residue model (CRM) and (ii) the ion evaporation model (IEV). In the CRM, proposed by Dole, it is supposed that analyte molecules are present as preformed ions (e.g. by choosing an appropriate pH). The sequence of solvent evaporation and electrohydrodynamic droplet disintegration is proceeded until microdroplets are formed. A single droplet contains only one preformed analyte ion. After the whole solvent is evaporated, the preformed ion is released to the gas phase. The theory of IEV, suggested by Irbarne and Thomson, is also based on the sequence of solvent evaporation and electrohydrodynamic droplet disintegration, which finally results in the formation of microdroplets. Generation of gas phase ions from highly charged microdroplets requires sufficiently high local field strengths for the emission of preformed ions in solution into the gas phase. In summary, the IEV is experimentally well supported, but only for small ions of the kind that one encounters in inorganic and organic chemistry. However, for ions derived from large molecules like polymers or proteins, the CRM becomes more plausible.

Contrary to APCI and APPI techniques (described in the following part in detail), ESI is a condensed phase ionization process and the ions have to be already in present solution. For the formation of ions, the pH has to be adjusted in such a way that ionisable groups are either mainly protonated $[M+H]^+$ (for positive ESI) or deprotonated $[M-H]^-$ (for negative ESI). In some cases also neutral molecules can be analyzed if they tend to form adducts with ions such as ammonium, sodium, potassium, acetate or silver. Generally, ESI allows an effective ionization of small to high molecular weight compounds without fragmentation during the ionization process. The APCI and APPI techniques are limited to low mass compounds which are thermally stable. However, ESI is more suitable for the ionization of high to moderate polarity compounds, whereas APPI and APCI allow the ionization of low and moderate polarity analytes. Figure 10 shows the application of the three ionization techniques, ESI, APCI and APPI and the relationship between the molecular weight and polarity (2, 12, 13, 17).
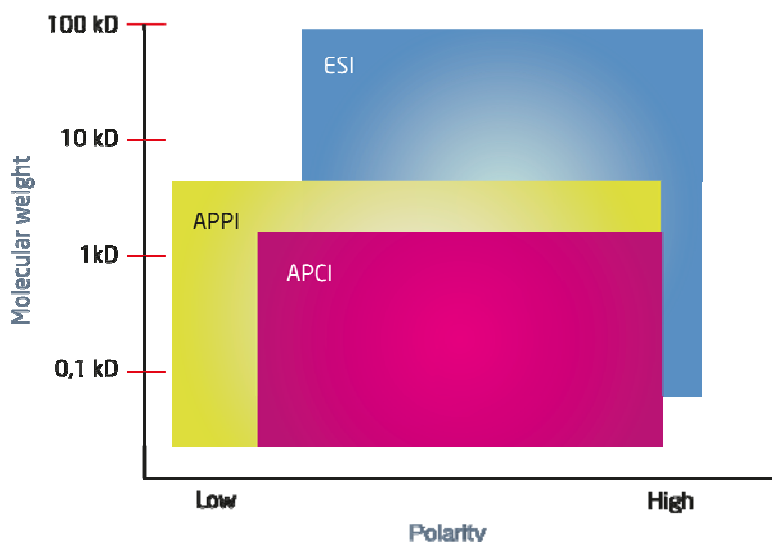
**Figure 10**. Application area of the three most popular API techniques. ESI allows ionization of high molecular weight compounds, whereas APCI and APPI are limited to low mass compounds. In contrast to ESI, APCI and APPI are more suitable for the ionization of low and moderate polarity compounds.

### B.3.2.2. Atmospheric Pressure Chemical Ionization

Atmospheric pressure chemical ionization (APCI) is comparable to the chemical ionization (CI) process used in GC-MS. The main difference is that in APCI the ionization of analytes is performed under atmospheric pressure. APCI is a gas phase ionization process where an ion-molecule reaction between a neutral molecule and reactant ions takes place. For successful ionization, a complete evaporation of the liquid sample is required. Figure 11 illustrates the scheme of an APCI process. Generally, an aerosol is formed with the help of a heated nebulizer using nitrogen as nebulizer gas. The heated nebulizer applied in an APCI source is a concentric pneumatic nebulizer comprising of three concentric tubes, namely a liquid tube in the center, a nebulizer tube and an auxiliary gas tube. The nebulizer is further attached to a heated quartz or ceramic tube, where the aerosol is directly formed and an explosive vaporization of the solvent and the analytes is enabled. The typical temperature of the tube is between 200 - 250 °C. Flow rates of the liquid sample are in the range of 200-1000 µL/min. The ionization of the gaseous solvent and analyte compounds in the APCI source is performed with a needle where a high voltage is applied. The evaporated sample is bombarded with electrons from this needle formed by corona discharge. In positive ionization mode mainly ions such as $N_2^+$ are formed by EI. Subsequently these ions react with water in several steps by charge transfer to form $H_3O^+$. Ionization of analyte A is carried out then by proton transfer. In negative ionization mode ions are formed either by resonance capture of electrons (AB $\rightarrow$ AB$^-$), dissociative capture of electrons (AB $\rightarrow$ B$^-$) or ion molecular reactions

24

(BH → B⁻). In APCI single charged ions [M+H]⁺ in positive and [M-H]⁻ in negative ionization mode are predominately detected.
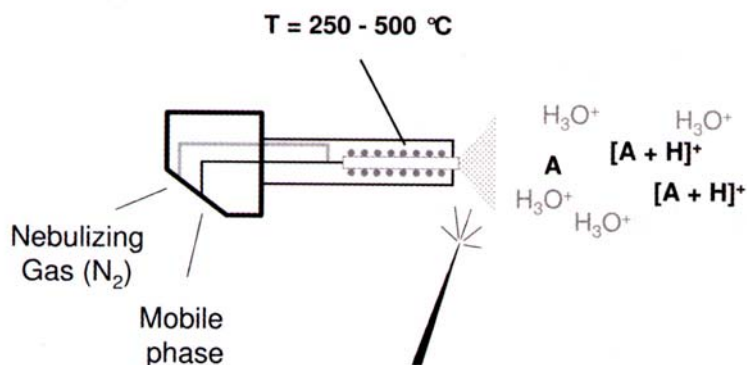


**Figure 11**. Principle of APCI, A=Analyt. Ionization of evaporated liquid is performed with a corona discharge needle. Solvent molecules are first ionized and subsequent ionization of analyte molecules occurs then by charge or ion transfer. The image is reproduced with the kind permission of © Wiley-VCH Verlag GmbH & Co. KGaA (13).

APCI can be accomplished in exactly the same API source as applied for ESI. To this end a corona discharge needle has to be implemented into the source and the inlet probe has to be changed. Compared to ESI, the application of heat in APCI may generate thermal decomposition of the analyte. Thus, as already mentioned above, APCI is limited to rather small thermally stable molecules, having low and moderate polarity (Figure 10) (2, 12, 13).

### B.3.2.3. Atmospheric Pressure Photo Ionization

The setup of an atmospheric pressure photo ionization (APPI) source is closely related to that of APCI. Similarly to APCI the liquid sample is vaporized by the application of a heated pneumatic nebulizer. Instead of using a corona discharge needle the ionization of analytes is performed under APPI by a gas discharge lamp (krypton, 10.0 eV), that generates vacuum ultraviolet photons. The potential of 10 eV is sufficient for a successful ionization of most of the analytes since their ionization potentials are lower. The basic principle of APPI is the absorption of a photon by the molecule and further the ejection of an electron which leads to the formation of a radical cation. Sensitivity can be improved by adding easily ionizable dopants to the mobile phase or to the nebulizing gas. Toluene, acetone or anisole are frequently used as dopants due to their low ionization potential. However, the mechanism of the ionization process after the addition of dopants is not fully understood yet. Two different mechanisms are suggested. On the one hand dopant radical cations may react with the analyte by charge transfer or on the other hand the dopant radical cation ionizes first the

solvent molecules by proton transfer which further ionize the analyte. In addition, APPI is also suitable for negative ionization. Compared to ESI and APCI, APPI proves to be particularly attractive for the analysis of non polar analytes (2, 12, 13).

### B.3.2.4.    Multiple ionization source

The combination of ESI, APCI and APPI ionization sources enables to extend the range of compounds that can be analyzed simultaneously. Generally, positive and negative ESI can be used for the analysis of a big range of compounds of interest. Nevertheless, those compounds which give no signal with ESI, e.g. non polar compounds, may require APCI or APPI for successful determination. However, the combination of an ESI and APCI source, also called ESCi allows alternate online ESI and APCI scans with polarity switching within a single analysis. Thus, this multi-mode ionization source is of particular interest for high speed online LC-MS analysis. During an LC-MS run the high voltage power supply can be switched within 100 ms from the electrospray capillary to the APCI discharge needle. Further combinations of ESI, APCI and APPI either in simultaneous or in switching mode are possible. Especially the combination of ESI with APPI seems to be very attractive, since APPI enables the ionization of very low polarity molecules, whereas ESI covers rather large molecules (12, 13).

### B.3.2.5.    Desorption Electrospray and Direct Analysis in Real Time

The development of techniques to analyze solid samples or analytes on solid surfaces without any sample preparation has always been of particular interest. Desorption electrospray ionization (DESI), allows the generation of molecular ions under atmospheric pressure directly from the solid surface which are directly further transferred into the MS. In Figure 12 the principle of a DESI interface is illustrated. The solid sample to be analyzed is placed in front of the orifice. Charged liquid droplets are directly focused by a high velocity gas jet on the surface of the sample. This leads to desorption of molecular ions from the surface which are further guided into the MS.
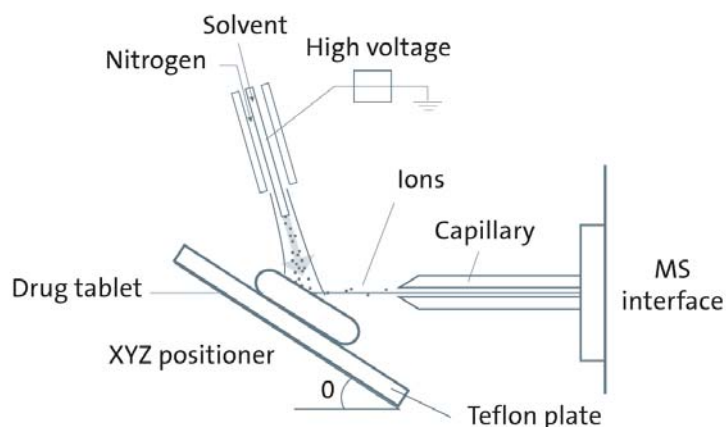
**Figure 12**. Schematic of a desorption electrospray ionization interface (DESI). The sample, for example a pharmaceutical pill, is placed on the drug tablet in front of the orifice. The sample is hit by nebulized droplets which lead to desorption of analyte ions from the pill. The image is reproduced with the kind permission of © Wiley-VCH Verlag GmbH & Co. KGaA (13).

Another method which offers direct analysis of samples without sample preparation is called direct analysis in real time (DART). This new approach is closely related to DESI. The ionization technique of DART is based on the reactions of metastable helium atoms generated by corona discharge with oxygen/water (negative mode) or water clusters (positive mode). The formed reactant ions ionize the analyte molecules either by cluster assisted desorption or proton exchange. Generally both techniques, DESI and DART mainly generate protonated or deprotonated molecular ions. Both new techniques can be used to analyse for instance biological tissues or to determine active ingredients in pharmaceutical samples in tablets without any sample preparation and under atmospheric pressure (13).

### B.3.3. Mass analyzers

Gas phase ions generated from various ionization sources are further separated according to their mass to charge ratio (m/z) in different mass analyzer. However, not all mass analyzers share the same operation principle. Generally gas phase ions are separated in either time or space, which can be performed in different ways. For instance they can be separated in a radio frequency field or according to the time of flight that ions need to cross in a field free tube. Separation can also be achieved via trapping ions in an electric or magnetic ion trap and by using ion path stability for separation by their m/z.

In the last few years the performance of mass analyzers underwent significant improvements. Nowadays, it is common to combine two or more mass analyzers of either the same or different type. The latter kind of combination is called hybrid mass spectrometer. These kind of mass spectrometers offer a higher number of scan possibilities, enhanced sensitivity and selectivity. The following chapters illustrate in more detail the operation principles of frequently used mass analyzers (2, 12, 13).

### B.3.3.1. Linear Quadrupole Analyzer

Linear quadrupole mass filters are the most widely applied mass analyzer in MS, especially due to their low acquisition costs. Common ionization sources such as EI, ESI, APCI and MALDI are used on quadrupole instruments. The mass filter consists of four hyperbolic or circular rods which are placed in parallel with identical diagonal distances from each other, shown in Figure 13. The rods are connected electrically in diagonal from. In addition to the alternating radiofrequency (RF) potential (V), a positive direct current (DC) potential (U) is applied on one pair of rods while a negative potential is applied to the other pair. Followed by the samling of ions into the quadrupole they begin to oscillate in a plane perpendicular to the rod axis as they traverse through the quadrupole filter. At a defined combination of DC and RF applied to the rods, the ions of one particular m/z never get in touch with the rods of the quadrupole. Thus, the trajectories of these ions remain stable in the x and y directions and are finally transmitted towards the detector. Ions with other m/z have unstable trajectories and do not pass the mass filter, because the amplitude of their oscillations becomes infinite. These ions are colliding either with the rods of the quadrupole where they will be discharged or they get lost in the vacuum system. To obtain a mass spectrum, ions of increasing m/z are consecutively guided towards the detector by increasing the magnitude of DC and RF potentials at a constant ratio. Generally, the motion of ions in the quadrupole is quite complex and can be described by the Matthieu equations.
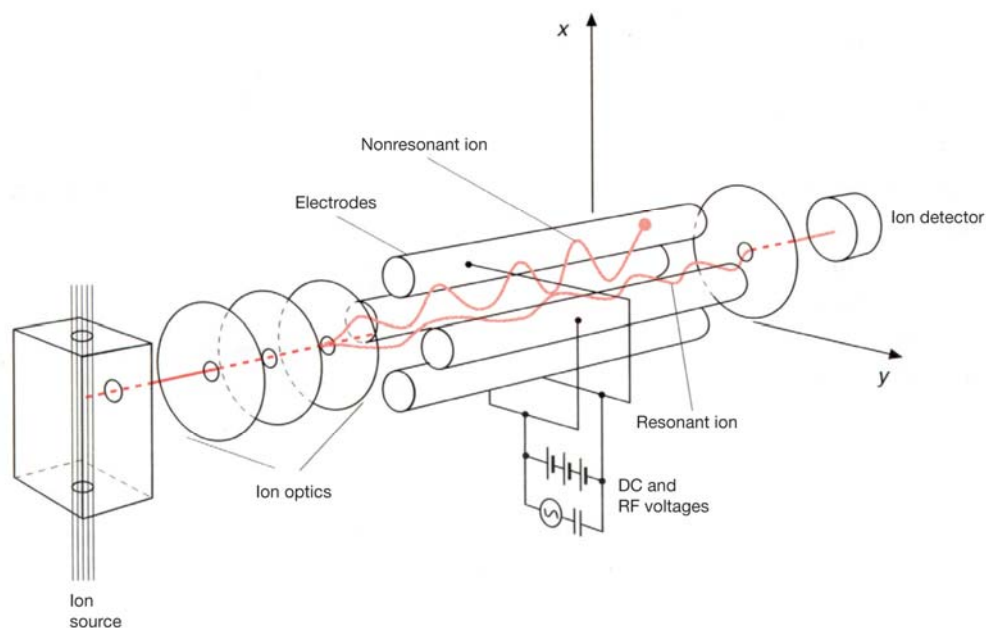
**Figure 13**. Linear quadrupole mass analyzers consist of four circular or hyberpolic rods placed in parallel. Ions generated in the ion source are passing through the ion optics and are guided into the quadrupole mass analyzer. At a given combination of DC and RF applied to the rods, the trajectories of the ions of one particular m/z are stable and reach the detector. The image is reproduced and slightly modified with the kind permission of © Springer-Verlag (3).

Typically, unit mass resolution (FWHM 0.6-0.7 m/z) can be achieved with quadrupole mass filters at a mass range between m/z 5 and m/z 4000. Linear quadrupole mass filters can also be applied as ion guides or collision cells. If the DC voltage of a quadrupole mass filter is set to zero and the RF voltage stays the same, ions can be directed through the filter without mass selection. Generally a linear quadrupole mass analyzer can be operated in two data-acquisition modes. Full scan spectra over the whole mass range can be acquired for qualitative analysis. Selected ion monitoring (SIM) is used for quantitative study. Here only the ion abundance of the preselected ions is measured which results in a much higher sensitivity (2, 12, 13).

### B.3.3.2. Triple Quadrupole Mass Analyzer

Detailed structural determination by using mass spectrometers, e.g. in organic trace analysis, requires special instrumental setups. Tandem mass spectrometry offers various types of MS and MS/MS experiments on ions generated in a soft ionization process. These experiments are particularly helpful for solving structure elucidation problems since they provide additional

mass spectral information. The most versatile and widely used tandem mass spectrometers are triple quadrupole instruments (QqQ) consisting of linear quadrupole mass analyzers as described above. A configuration of a triple quadrupole mass analyzer is illustrated in Figure 14. The instrument consists of two quadrupole mass filters, both operating in RF/DC mode. These two filters are separated by a collision cell which is also a quadrupole, operating in RF-only mode. However, hexapoles, octapoles or ion tunnels can also be applied as collision cells. Before generated ions pass Q1 they are first directed through a focusing quadrupole (q0) which operates in RF-only mode. For MS/MS experiments like the product ion scan mode, one particular precursor ion is selected in the first mass analyzer (Q1). Subsequent fragmentation of the precursor ion takes place in the collision cell (q2). The dissociation of the ions is performed by collisional activation via collisions of the precursor ions with neutral gas molecules such as nitrogen or argon. This process is called collision induced dissociation (CID) or collision activated dissociation (CAD). The generated product ions from q2 are further sorted according to their m/z ratio in the second mass analyzer (Q3) prior to detection. CID can be explained as a two step process. In the first step of the collision event, ion translational energy is converted into ion internal energy, followed by a unimolecular decomposition of the excited ions. This may yield various product ions. Energy redistribution within the ion may take place between the two steps. The collision energy is expressed in electron volts (eV) and is usually not higher than 100 eV. Generally ions are separated in space on a QqQ instrument whereas with ion trap mass analyzers (explained in detail in chapter B.3.3.3) MS/MS experiments are performed in time.



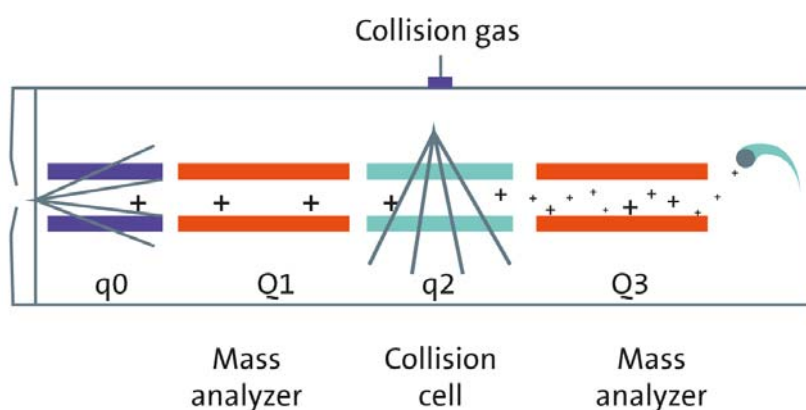**Figure 14**. Principle of a triple quadrupole mass analyzer (QqQ). The analyzer comprises of two mass analyzer quadrupoles, Q1 and Q3, a cllosion cell q2 and a focusing quadrupole q0. In the actual configuration the collision energy is determined by the potential difference between q0 and q2. The image is reproduced and slightly modified with the kind permission of © Wiley-VCH Verlag GmbH & Co. KGaA (13).

The two mass analyzers (Q1 and Q3) of a QqQ can be operated in different ways, resulting in various types of MS and MS/MS experiments. Table 1 shows a summary of various scan modes. Setting either Q1 or Q3 to RF-only mode, MS experiments can be performed, identically like with a single quadrupole mass analyzer. For a product ion scan which is already explained above, the first mass filter Q1 is fixed to an m/z ratio specific to a certain ion of interest. After the fragmentation reactions in the collision cell q2 the fragment ions are scanned in Q3. Product ion scans are widely used in structural elucidation. Further scan modes which are particularly useful in qualitative analysis are precursor and neutral loss scans. Precursor ion scans enable monitoring of compounds which have CID identical characteristic fragments. This scan type is suitable for identification of structural homologues in a complex mixture. In neutral loss scan mode Q1 and Q3 scan at a fixed m/z difference for monitoring compounds that lose a common neutral species. The method of choice in quantification analysis is offered by selected reaction monitoring (SRM) mode, where a selected collision induced fragmentation reaction is monitored. In SRM mode both mass analyzers; Q1 and Q3 scan at one fixed m/z which provides high selectivity and improves the signal to noise ratio significantly (2, 12, 13).

**Table 1**. Scan possibilities of a triple quadrupole mass spectrometer. Different settings of the Q1 and Q3 quadrupoles allow a variety of different MS and MS/MS experiments. The table is reproduced with the kind permission of © Wiley-VCH Verlag GmbH & Co. KGaA (13).

| . Mode | Q1 quadrupole | Q3 quadrupole |
|---|---|---|
| Full scan Q1/single ion monitoring (SIM) Q1 | Scan/fixed | Rf mode |
| Full scan Q3/single ion monitoring (SIM) Q3 | Rf mode | Scan/fixed |
| Product ion scan (PIS) | Fixed | Scan |
| Precursor ion scan (PS) | Scan | Fixed |
| Neutral loss (NL) | Scan | Scan: neutral loss offset |
| Selected reaction monitoring (SRM) | Fixed | Fixed |

### B.3.3.3.    Ion Trap Mass Spectrometry

A further important development of the quadrupole mass filter is the three-dimensional ion trap, also called quadrupole ion trap (QIT or 3D-IT), operating in a three-dimensional quadrupole field. Figure 15 illustrates a QIT consisting of a cylindrical ring electrode, having a

shape similar to a donut. The ring electrode is placed symmetrically between two end-cap electrodes. The 3D quadrupole field is applied to the ring electrode. The electrode ions are guided through the small holes of one end-cap from the ionization source into the ion trap in pulsed mode. The electrode ions are then stored in the ion trap and collide with the helium gas presented there. Thus the ions are focused in the center of the trap and have stabilized trajectories. The holes of the other end-cap electrode are used to transfer ions towards the detector.
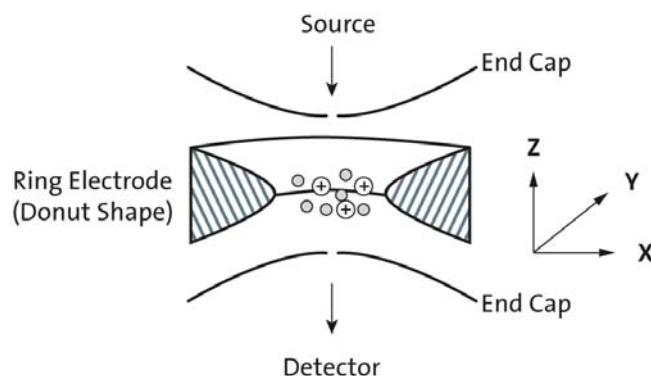


**Figure 15**. Principle of a quadrupole ion trap (QIT). A fundamental RF potential is applied onto the ring electrode to trap ions. The gray circles represent helium gas which is necessary to focus molecular ions in the center of the trap. The image is reproduced with the kind permission of © Wiley-VCH Verlag GmbH & Co. KGaA (13).

To obtain a mass spectrum with a QIT mass analyzer combined with an external ion source a number of sequentially applied steps are necessary. The storage capacity of ions in a QIT is limited due to space-charge effects. Typically around $10^4$ ions can be stored in a trap without affecting the mass resolution and accuracy. The adequate fill time of the trap to maximize sensitivity and minimize resolution losses is determined by an automatic gain control procedure (AGC). To trap and accumulate ions in the trap with an m/z above a low mass cut-off value it is necessary to apply an appropriate RF voltage to the ring electrode. For a full scan mass spectrum ions of different m/z ratios are ejected consecutively from the trap by gradually increasing the RF voltage at the ring electrode. Ions with the lowest m/z are always ejected first out of the trap. Resonant ion ejection, which offers a mass spectrum with a higher mass range, may be supported by additional wave forms applied to the end-cap electrodes. Generally ion ejection can be achieved with unit mass resolution, while an enhanced resolution of a mass spectrum is possible by slowing down the scan speed. Measuring in SIM mode only a selected m/z is stored in the trap and all other ions are ejected from the trap. Thus, the RF storage voltage at the ring electrode is adapted to selectively accumulated ions of a particular m/z in the trap prior to their ejection towards the

detector. In the end of a full scan or SIM measurement, all ions are removed from the trap by a RF pulse to prepare the trap for the next sequence of events.

The quadrupole mass analyzer (described in chapter B.3.3.2) shows some significant differences in contrast to a QIT. QIT can perform full scans with higher sensitivity, because a QIT is able to store ions in the trap before mass analysis. The mass instability scan in QIT enables rapid mass analysis at a scan speed of several thousand m/z units per second. The duty cycle, which represents the time to obtain a mass spectrum, depends on various parameters. These are the injection time (within 0.5 to 500 ms), the scan speed (in the range 5000 to 20,000 units/s), the isolation of the precursor ion and fragmentation in tandem MS or $MS^n$. Compared to a QqQ mass analyzer the duty cycle for MS/MS experiments in a QIT is much shorter. The MS/MS experiments are not performed in space like in a QqQ but in time. The fragmentation process in an ion trap is performed also by CID. However, the CID process is completely different from that of the QqQ mass analyzer. In QIT, helium is used as damping gas instead of nitrogen or argon. The trap is constantly filled with helium which enables fast switching between single MS and MS/MS mode. Moreover, up to 100 collisions takes place in ion traps, whereas QqQ analyzers can handle maximally 10 collisions in a duty cycle. MS/MS experiments are performed in time in the same physical device and can be repeated several times. Thus, $MS^n$ experiments to the 11th level are manageable with the most QIT instruments. The mass range of an ion trap is up to 50,000 which is much higher than with QqQ instruments. A disadvantage of QIT is the low mass cut-off of about one third of the precursor ion mass. Furthermore, only up to 8 SRM transitions/second can be recorded on a QIT, whereas more than 100 SRM transition/second can be performed on a QqQ. Due to the high sensitivity in $MS^n$ mode, ion traps are mostly applied for qualitative analysis in drug metabolism and proteomics study.

Another very important type of an ion trap is the linear ion trap (LIT), also called two dimensional ion trap (2D IT) or linear ion trap quadrupole (LTQ, defined by Thermo Fisher Scientific, Bremen). LIT can be either used as standalone mass analyzer or can also be attractive in  coupling to other mass analyzers such as Fourier transform ion cyclotron (FT-ICR) or a QIT, time of flight (TOF) or an orbitrap mass analyzer. The design of a LIT is similar to a quadrupole mass analyzer, consisting of four hyperbolic or circular rods which are placed parallel in a radial array. In a LIT a DC potential is applied to the end electrodes to avoid axial escaping of the ions. Compared to a QIT the same kind of experiments can be performed with a LIT. In addition LIT offers some advantages for trapping ions compared to the QIT. In a LIT more ions can be trapped before observing space charge effects which results in higher sensitivity. LIT provides enhanced trapping efficiency and instead of

focusing ions to a point, they are strongly focused along the center line. Additionally, LIT has also no quadrupole field along the z-axis.

*Data-dependent operation in MS/MS*

Data-dependent acquisition (DDA), also known as information dependent acquisition (IDA) is a special mode of operation of ion trap systems. In the first step of a DDA experiment a full scan spectrum (survey scan) is acquired to generate a peak list from all detected ions. From this list a certain number of peaks are selected according to user defined criteria. In the second step of the DDA experiment, selected precursor ions are acquired in MS/MS analysis. In LC-MS, the preselected precursor ions from the survey scan depend on the chromatographic retention time. In DDA it is not necessary to perform two subsequent injections for the identification of unknown components in the sample. DDA allows the generation of large MS/MS data of unknown components in a fully automated way. This time saving approach has become state of the art for qualitative analysis and importantly it is also used in the present work, shown in chapter C.3 and C.4 (2, 12, 13).

### B.3.3.4. Triple Quadrupole Linear Ion Trap

In a hybrid mass spectrometer two or more different types of mass analyzers are combined, such a hybrid MS is a triple quadrupole linear ion trap ($QqQ_{LIT}$). The design of a $QqQ_{LIT}$ is based on a QqQ; the mass analyzer consists of a focusing quadrupole (q0), two quadrupole mass filters, Q1 and Q3, and a collision cell q2, similar to a QqQ. However, the Q3 mass filter can be operated either in normal RF/DC mode or as LIT analyzer. Schematic of a $QqQ_{LIT}$ is shown in Figure 16.
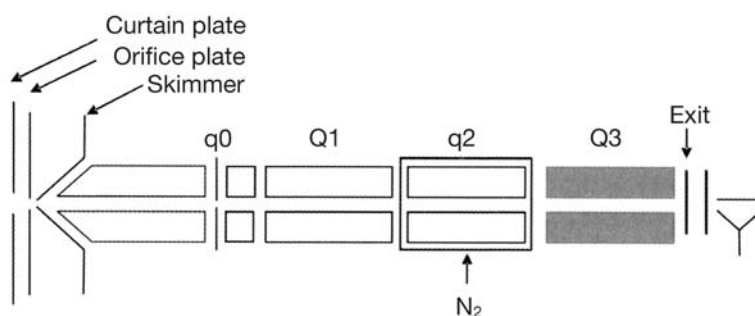


**Figure 16**. Schematic of the triple quadrupole linear ion trap ($QqQ_{LIT}$). Q3 can be either used as a quadrupole mass filter or as a linear ion trap. In both modes ions are ejected in the axial direction. The image is reproduced with the kind permission of © Wiley-VCH Verlag GmbH & Co. KGaA (13).

Similar to QqQ, MS/MS experiments are also performed in space in a QqQ$_{LIT}$ where the LIT in the QqQ$_{LIT}$ instrument is used only as a trapping and mass analyzing device. Generally QqQ$_{LIT}$ mass analyzers offer a huge variety of different scan possibilities which are summarized in Table 2. QqQ$_{LIT}$ can manage MS$^3$ experiments too, which are performed in the following manner. First precursor ions are selected in Q1 and further fragmented in the pressurized q2. Fragment ions and residual precursor ions are further guided into the Q3 mass analyzer which operates as a LIT. Here, next generation precursor ions are trapped, excited and further fragmented. The LIT analyzer offers also enhanced DDA experiments, where the SRM mode can be used as survey scan and the enhanced product ion mode can be selected as dependent scan. This last option enables improved qualitative and quantitative analysis in the same LC-MS run (2, 12, 13).

**Table 2**. Mode of operation of a triple quadrupole linear ion trap. Q3 can be operated either as quadrupole or ion trap mass filter, which offers a higher number of different scan possibilities. The table is reproduced with the kind permission of © Wiley-VCH Verlag GmbH & Co. KGaA (13).

| Mode of operation | Q1 | q2 | Q3 |
|---|---|---|---|
| Q1 scan | Resolving (scan) | RF only | RF only |
| Q3 scan | RF only | RF only | Resolving (scan) |
| Product ion scan (PIS) | Resolving (fixed) | Fragment | Resolving (scan) |
| Precursor ion scan (PC) | Resolving (scan) | Fragment | Resolving (fixed) |
| Neutral loss scan (NL) | Resolving (scan) | Fragment | Resolving (scan offset) |
| Selected reaction monitoring mode (SRM) | Resolving (fixed) | Fragment | Resolving (fixed) |
| Enhanced Q3 single MS (EMS) | RF only | No fragment | Trap/scan |
| Enhanced product ion (EPI) | Resolving (fixed) | Fragment | Trap/scan |
| MS$^3$ | Resolving (fixed) | Fragment | Isolation/fragment trap/scan |
| Time delayed fragmentation (TDF) | Resolving (fixed) | Trap/no fragment | Isolation/trap/scan |
| Enhanced resolution Q3 single MS (ER) | RF only | No fragment | Trap/scan |
| Enhanced multiply charged (EMC) | RF only | No fragment | Trap/scan |

### B.3.3.5. Time of Flight Mass Spectrometry

The principle of a time of flight mass analyzer (TOF) is measurement of the flight time of equally accelerated ions through a field free linear flight tube, illustrated in Figure 17. Compared to other mass analyzers like quadrupole or ion trap, TOF is a non-scanning mass analyzer. At the front end of the flight tube, a package of previously accumulated ions is accelerated by strong electric fields (2-30 kV) in the direction of the detector. Pulsed ion introduction into the TOF analyzer is necessary to avoid that ions of different m/z reach the detector plate simultaneously. The flight time of ions through the tube is proportional to their m/z ratio. Low mass ions have a shorter flight time than high mass ions. Generally, the flight time of ions through the drift region is in the range of 50 to 100 μsec. In addition, due to the good ion transmission, a spectrum acquisition is possible within 100 ms over a theoretically almost unlimited mass range. In combination with soft ionization techniques such as matrix assisted laser desorption ionization (MALDI), the setup enables the detection of large ions up to m/z 200,000 routinely. Since MALDI and TOF are pulsed techniques, TOF is regarded as the ideal mass analyzer for MALDI. However, the mass range of a TOF analyzer is limited since the sensitivity of the detector decreases with increasing m/z of the ions. Another disadvantage of the TOF mass analyzer is that it can achieve only medium mass resolution around 5000. This limitation is caused by the distribution in the flight time of ions with similar m/z. A simple way to improve the mass resolution is to increase the length of the flight tube. Therefore, an ion mirror, also called electrostatic mass reflectron can be used to double the length of the flight tube without increasing the physical size of the instrument. To this end the electrostatic mirror is placed into the drift region which significantly increases the mass resolution up to 15,000. However, the mass range is then limited to several thousand m/z units. Briefly, in reflectron mode ions with high energy penetrate deeper into the mirror region than those with the same m/z at lower energy level. Because of the different trajectories, all ions of one particular m/z reach the detector at the same time resulting in a focussing effect, which further pushes up the resolution of the analyzer. Another possibility to enhance mass resolution is the reduction of the kinetic energy spread of ions leaving the ion source. This can be achieved by a delayed pulsed extraction, which is a time delay between ion formation and acceleration.
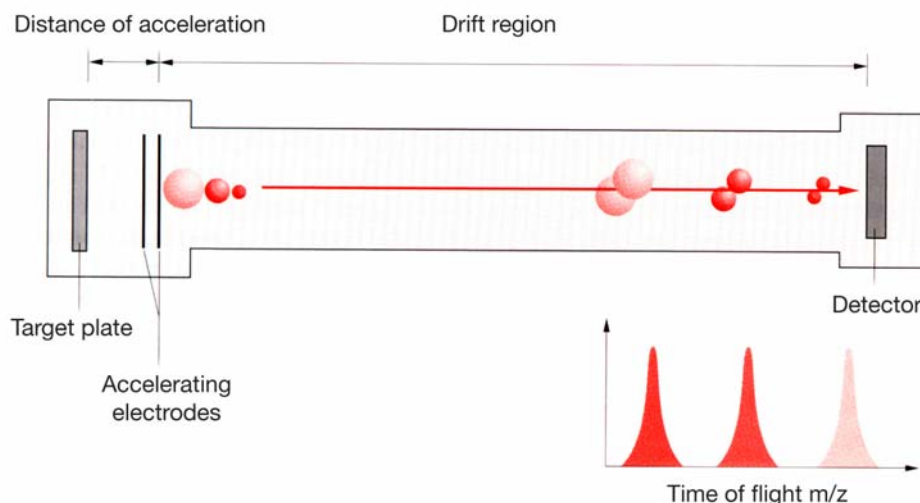
**Figure 17**. Principle of the simplest form of a time of flight mass analyzer (TOF). At the starting point a package of accumulated ions is accelerated by a strong electric field into a free linear flight tube. The image is reproduced and slightly modified with the kind permission of © Springer-Verlag (16).

TOF mass analyzers are also easily combined with other types of mass analyzers. In quadrupole time of flight hybrid instruments (QqTOF) the quadrupole Q3 in a QqQ analyzer is replaced by a TOF analyzer, shown in Figure 18. This powerful combination offers a high mass range (m/z 5 to m/z 40,000), mass resolving power up to 40,000 and high sensitivity. In single MS mode the first quadrupole Q1 is operated in RF-only mode and the ions are guided to the TOF analyzer where mass analysis is performed. For MS/MS experiments like the product ion scan, precursor ions are selected in Q1, further fragmented in the collision cell q2 and fragments are analyzed in the TOF analyzer. Since mass analysis is always performed in the TOF analyzer, the same accurate mass determination and high mass resolution is available in MS and MS/MS mode.
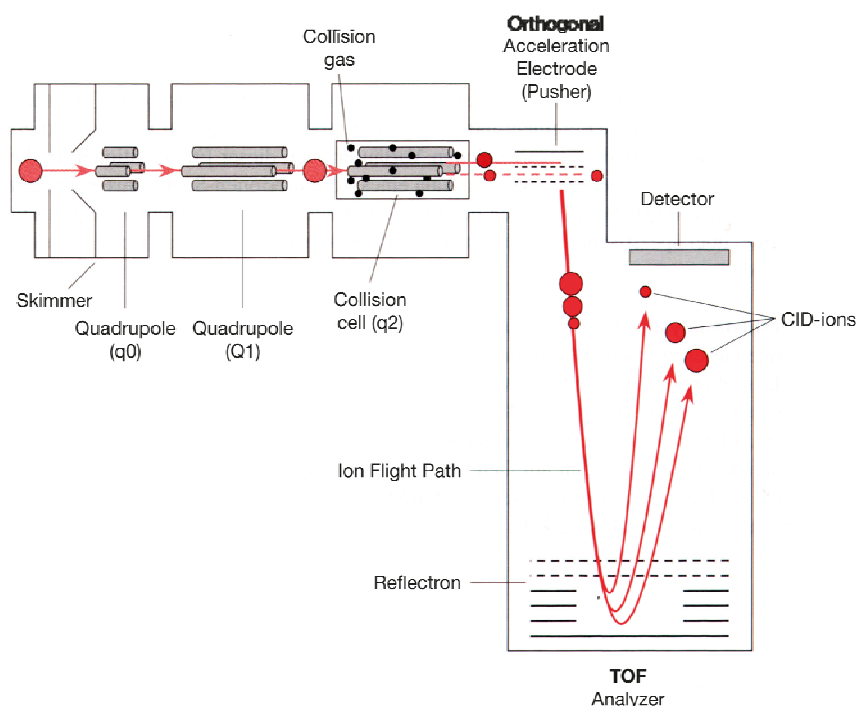
**Figure 18**. Schematic of a quadrupole time of flight instrument (QqTOF). Quadrupole q0 is used for collisional cooling and ion focusing. Nitrogen or argon is generally used as collision gas. The ion modulator, also pusher accelerates the ions orthogonally to their initial direction into the TOF analyzer. The image is reproduced and slightly modified with the kind permission of © Springer-Verlag (16).

QqTOF instruments are an interesting alternative to MALDI-TOF instruments and have gained wide application in LC-MS, especially in peptide sequencing analysis. Next to the QqTOF, there are various other combinations of different mass analyzers with TOF available. For instance the combination of TOF analyzers with ion accumulation devices such as an ion trap offers also $MS^n$ capabilities with accurate mass measurement. Furthermore, TOF can be combined with quadrupole ion traps, linear ion traps and with another TOF, known as TOF-TOF instruments (2, 12, 13).

### B.3.3.6. Fourier Transform - Ion Cyclotron Resonance Mass Spectrometry

Fourier transform ion cyclotron resonance mass spectrometry (FT-ICR-MS) can be regarded as an ion trap system. However, generated ions are not trapped in a quadrupole field like in a LIT but in a magnetic field. Schematic of an ion cyclotron resonance instrument is illustrated in Figure 19. The main components of a FT-ICR-MS analyzer are a superconducting magnet and a cubic or cylindrical cell. Mass analysis is performed in the cell which is placed in the strong magnetic field. The magnetic field strengths (B) are typically in the range of 3.0-12

Tesla. The cell is composed of two opposite trapping plates, two opposite excitation plates and two opposite receiver plates.
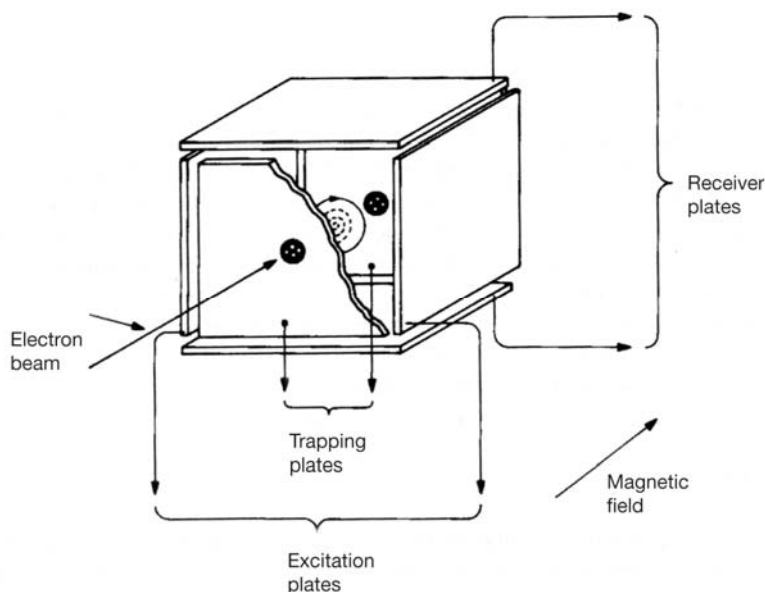


**Figure 19**. Schematic of Fourier transform ion cyclotron resonance cell. Ions are trapped in the cell according to their cyclotronic motion. The image is reproduced and slightly modified with the kind permission of © Wiley-VCH Verlag GmbH & Co. KGaA (1).

Ions from an external ion source are guided into the cell and trapped according to their cyclotronic motion. This motion occurs due to the interaction of an ion with the unidirectional constant homogenous magnetic field. This static magnetic field is directed along the z axis and forces ions due to the cyclotronic motion to rotate around the z-axis in the x-y plane. A low electrostatic potential at the end cap electrodes prevents ions from escaping the cell along the z axis. The cyclotronic motion of ions in the cell is determined by its cyclotron frequency, which ranges from 5 kHz to 5 MHz. This cyclotron frequency depends on the magnetic field, the charge of the ion and the mass of the ion. In contrast to other types of mass spectrometry instruments, ions are detected in a non-destructive way with FT-ICR-MS. The detection of ions is performed by applying a coherent broadband excitation. The ions undergo cyclotron motion as a packet with a larger radius. When the ion packet approaches the detection plates it generates an alternating current, called image current. The resulting signal is generally called the transient free induced decay (FID) and ions of any mass can be detected simultaneously. The image current consists of different frequencies and amplitudes which are converted by applying a Fourier transformation to frequency components and subsequently to a mass spectrum.

FT-ICR-MS instruments offer an extremely high mass resolution even more than 1,000,000 and sub ppm mass accuracy. However, the mass resolution depends on the field strength, the mass of the target ions and the acquisition time. Mass resolution improves with higher field strength, whereas an ion with increasing m/z leads to decreased resolution. Also the length of the transient time has a significant influence on the mass resolution which is typically in the range of 0.1 to 2 seconds. MS/MS experiments can be also performed in a FT-ICR cell, which is similar to ion trap instruments. Thus, target ions are trapped in the cell and further fragmentation of the ions can be induced by various excitation methods. Similar to other mass analyzers, CID is often applied as excitation method. Therefore, the collision gas is introduced via a pulsed valve. However, collision of ions and neutral molecules results in a decrease of the transient time. Hence to avoid this limitation, it is essential to work at a very high vacuum ($1.3 \times 10^{-8}$ Pa). Further excitation methods for fragmentation of molecule ions are laser photodissociation, infrared multiphoton dissociation, electron capture dissociation or surface induced dissociation. The dynamic range of FT-ICR-MS instruments is relatively poor, since the number of ions in the trap must be in a specific range. If the trap is over- or underfilled with ions, the mass shifts towards high and low values, respectively. Conversely, this decreases the dynamic range of the instrument. The combination of an FT-ICR-MS instrument with a LIT mass analyzer allows a better control of the ion population in the cell. The combination of a LIT mass analyzer with an FT-ICR-MS is commercially available in the form of a LTQ-FT hybrid mass spectrometry instrument (Figure 20). LTQ is a generic name by Thermo Fisher Scientific, Bremen but it is actually similar to a LIT. Since the LIT is equipped with two detectors, the analyzer can be operated independently from the FT-ICR-MS. Thus, data can be collected either in the ion trap or in the FT-ICR-MS but also in both analyzers at the same time. Therefore, the LTQ-FT hybrid instrument offers a variety of different operation modes. For example precursor ion selection or fragmentation can be performed in the LIT and further measured in the FT-ICR cell. In this way, the FT-ICR-MS operates only as a high resolution detector for MS or MS$^n$. Furthermore, DDA experiments, described in capture B.3.3.3, can be performed using both analyzers in parallel. While acquiring a high resolution full scan in the FT-ICR cell, a certain number of highly abundant ions are selected in DDA, fragmented in the linear ion trap analyzer and ejected at nominal mass resolution.
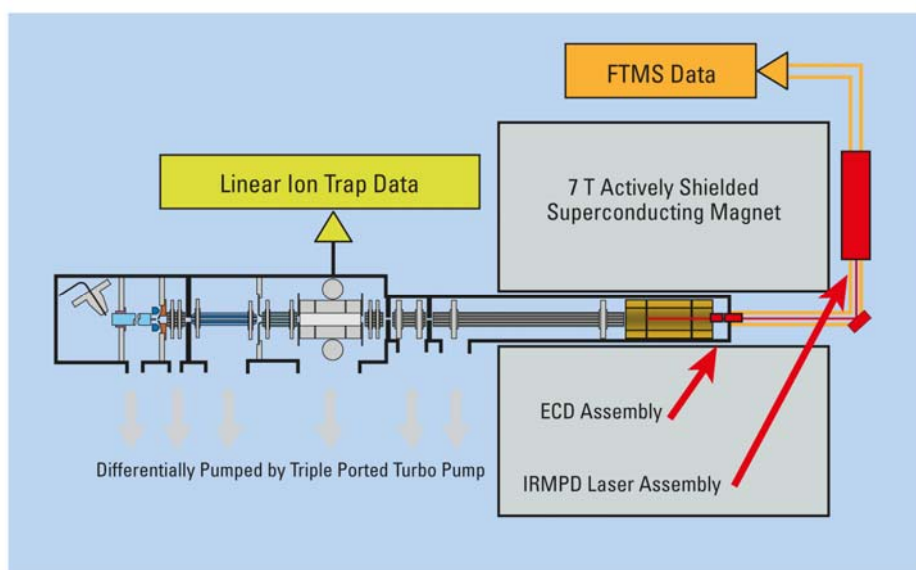
**Figure 20**. Schematic of a LTQ-FT hybrid mass spectrometry instrument. Since the LIT is equipped with two detectors, this mass analyzer can also be used separately from the FT part. The image is reproduced with the kind permission of Thermo Fisher Scientific, Bremen (18).

For the most demanding analysis of complex samples, e.g. lipid profiling in biological samples or analysis of intact proteins, features of high resolution, high mass accuracy and MS/MS experiments are required. Hence, the LTQ-FT hybrid instrument in combination with ESI as ion source provides a very powerful analytical setup, which can be optionally coupled to LC for further chromatographic separation of the analytes. This approach is preferentially used in this work as well (chapter C.3 and C.4). Furthermore, the mass spectrometer provides comprehensive applications from routine compound analysis to the determination of trace-level analytes in complex mixtures. Application of LTQ-FT disables false positive identification much easier than the low resolution mass spectrometers (12, 13, 18).

### B.3.3.7.   Orbitrap Mass Spectrometry

Orbitrap technology is based on a novel type of mass analyzer invented in the year 2005 (Thermo Fisher Scientific, Bremen). The principle of an orbitrap mass analyzer is the orbital trapping of ions around a central electrode in a purely electrostatic field. Schematic of the Orbitrap mass analyzer is illustrated in Figure 21. The mass analyzer consists of a central spindle-like electrode (inner electrode) which is enclosed by an electrode (outer electrode) having the shape of a barrel to create an electrostatic potential. The m/z is a reciprocal proportionate to the frequency of the ions oscillating along the z-axis. Ions are detected by

measuring the current image of the axial ion motion around the inner electrode. The mass spectrum is obtained after Fourier transformation of the image current.
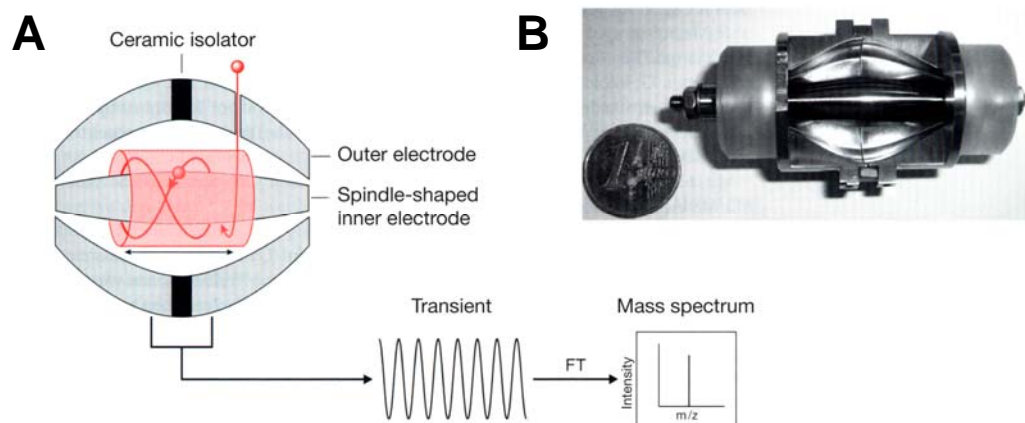


**Figure 21**. Orbitrap mass analyzer. (**A**) Principle of an Orbitrap mass analyzer consisting of a spindle-shaped inner electrode which is enclosed by an outer electrode having the shape of a barrel. Ions are trapped around a central electrode in an electrostatic field. The image is reproduced and slightly modified with the kind permission of © Springer-Verlag (16). (**B**) The full-scale image of an Orbitrap is reproduced with the kind permission of Thermo Fisher Scientific, Bremen (16).

The performances of different mass analyzers described above have been continuously improved in the past decade. Various powerful combinations of existing mass analyzing techniques provide higher sensitivity, faster acquisition rate, capabilities of accurate mass determination and improved resolution. Besides those mass analyzing techniques, the Orbitrap is the first new mass analyzer to be introduced as a commercially available instrument in the last 20 years. The newest generation of Orbitrap mass analyzers (Orbitrap Elite, Thermo Fisher Scientific) offers a high mass resolving power up to 240,000 FWHM and a high mass accuracy of less than 1 ppm.

In addition the Orbitrap can be also combined with other mass analyzers similar to an LTQ-FT hybrid instrument described above. As the name indicates the LTQ-Orbitrap hybrid mass spectrometer (Figure 22) invented by Thermo Fisher Scientific, Bremen consists of the Orbitrap mass analyzer combined with a LIT mass analyzer. Similar to the LTQ-FT instrument, the particularity of the LTQ-Orbitrap mass spectrometer is its possibility of independent operation of the Orbitrap and the LIT, which results in an enlarged number of applications. Compared to the LTQ-FT the LTQ-Orbitrap offers a lower resolution but its maintenance costs are far lower than for an LTQ-FT mass spectrometer. However, the Orbitrap technology offers high space charge capacity combined with superior dynamic range and unsurpassed sensitivity. In addition to the above-mentioned benefits, the

instrument serves a variety of different operation modes which provides a new level of versatility for a wide range of research applications. These are ranging from routine compound identification to the analysis of trace level components of complex mixtures. The LTQ-Orbitrap is expected to make significant contributions to various areas of scientific exploration (9, 12, 13, 16).
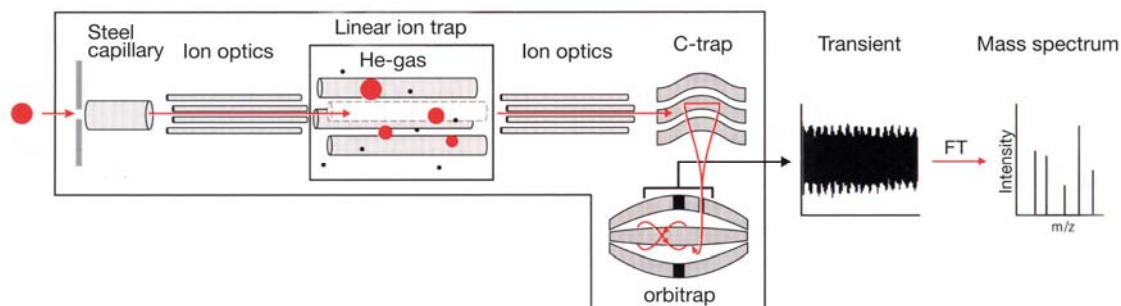


**Figure 22**. Illustration of an LTQ-Orbitrap hybrid mass spectrometer consisting of a linear trap quadrupole and a Orbitrap mass analyzer. The image is reproduced and slightly modified with the kind permission of © Springer-Verlag (16).

### B.3.4. Ion Detectors

An ion detection system is responsible for the detection of all ions of a certain m/z which are selected before by the mass filter. Furthermore, the ion detector converts the detected ions into a suitable signal to finally receive a mass spectrum. Various kinds of electron multipliers are used as ion detectors in mass spectrometry. Figure 23 shows the principle of a discrete-dynode electron multiplier used in mass spectrometer instruments which consists of sequentially arranged dynodes. When the ion beam, coming from the mass analyzer, hits the surface of the conversion dynode (described in detail below) secondary electrons are emitted. These electrons are accelerated down the channel producing additional secondary electrons. They further form an avalanche of electrons generating a measureable current at the end of the detector, which finally provides the mass spectrum.
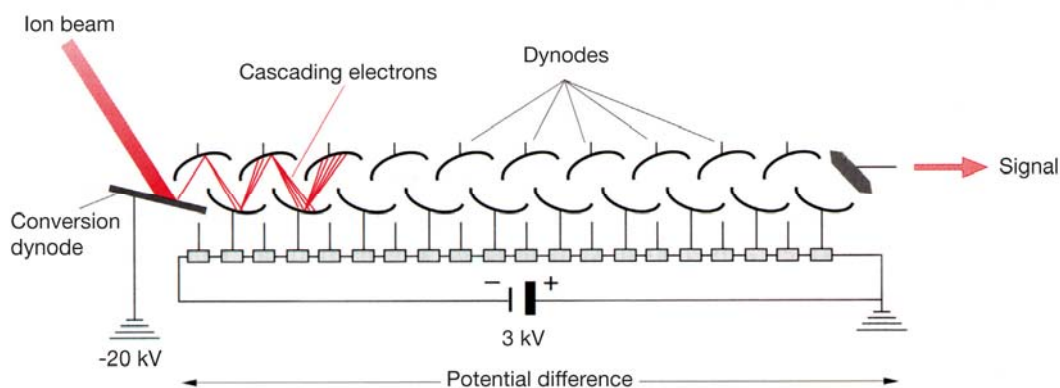
**Figure 23**. Principle of a discrete-dynode electron multiplier comprising sequentially arranged dynodes. Ions from the mass analyzer hit the surface of the conversion dynode which leads to emission of electrons. Thus, an avalanche of electrons is formed which finally generates the signal. The image is reproduced and slightly modified with the kind permission of © Springer-Verlag (16).

Another type of electron multiplier is the channel electron multiplier (CEM). CEM consist of lead silica glass and is the most extended kind of multiplier used in mass spectrometry. CEM can have a straight or a curved form, illustrated in Figure 24. If positive or negative charged ions hit the surface of the electrode, secondary electrons are formed from the surface, which further on generate the measurable current. CEM can be operated either in analog or pulse counting mode. The pulse counting operation mode offers high sensitivity whereas the analog mode is suitable for intense signals.
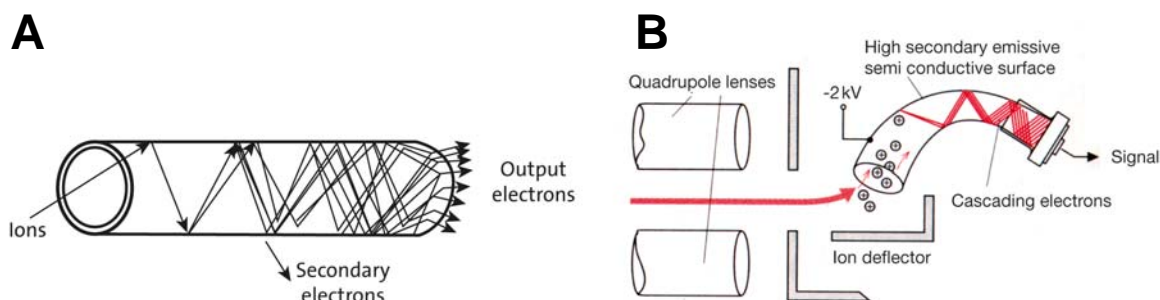


**Figure 24**. Systematic of a straight (**A**) and a curved (**B**) channel electron multiplier. Charged ions hit the surface of the channel electron multiplier and generate secondary electrons. Figure 24A is reproduced with the kind permission of © Wiley-VCH Verlag GmbH & Co. KGaA (13) and Figure 24B is reproduced and slightly modified from © Springer-Verlag (16).

A disadvantage of CEM is the exponential decrease of sensitivity if the mass of ions increases. This problem can be fixed by using a conversion dynode. This conversion dynode,

a metal surface with a constantly high potential of more than 3 kV, accelerates ions before they hit the surface of the CEM. This ensures that also ions with higher masses have an effective conversion into secondary electrons.

Photon multipliers are also used in mass spectrometry. Ions hit first a conversion dynode to generate secondary electrons. These electrons are accelerated towards a phosphorescent screen and converted into photons and detected by a photomultiplier. Compared to CEM, photomultipliers have a much longer lifetime. A CEM has to be replaced after one or two years, whereas photomultipliers have a lifetime of several years. Generally, the above described ion detectors are mainly used in quadrupole instruments and ion traps. In TOF mass spectrometry, mainly array detectors such as multichannel plates (MCP) are used. MCP enables simultaneous multichannel detection, offers high sensitivity and eliminates background noise (13).

## B.4. Liquid chromatography coupled to mass spectrometry

The start of coupling liquid chromatography online with mass spectrometry (LC-MS) dates back to the early 1970´s. In the first 20 years of the LC-MS development most attention was paid to solve the interface problem between LC and MS and to develop new techniques. Nowadays the situation has changed completely. Today researchers who are working on LC-MS are mainly concerned with application of the existing techniques in their field of interest. Generally the efforts and motivation to combine those two different techniques were inspired by the great success of GC-MS in solving analytical problems. But contrarily to GC-MS it was much more difficult to find a proper interface. Electron impact or chemical ionization techniques used in GC-MS were limited to volatile and small molecular weight compounds. Thus, those ionization techniques were not suitable interfaces for LC-MS. Furthermore, MS instruments from that time could not deal with high LC flow rates. Coupling online LC to MS was only possible at LC flow rates of a few microliters per minute. It took almost ten years of exploration and development to find applicable techniques. For example interfaces like particle beam (PB) and thermospray (TSP) enabled routine analysis of small molecules. The analysis of larger molecules became possible using continuous flow fast atom bombardment (FAB). Over the years a wide variety of different interfaces have been developed, but only a few of them were successful and are commercially available today. The history of various developed interfaces for LC-MS instrumentations is shown more in detail in Figure 25. However, today basically only two ionization techniques remained which are both based on the principle of atmospheric pressure ionization. Currently, ESI and APCI techniques, described in chapter B.3.2, are the two predominant interface techniques. Many variations of

ESI and APCI have been developed in the past years to achieve higher ionization efficiency and to better meet the needs of specific applications. But, also other interface techniques are promising for the future, like APPI which has recently expanded the range of analytes that are accessible to LC-MS. In addition, dual- or multimode ion sources (chapter B.3.2.4) gain more and more in importance.
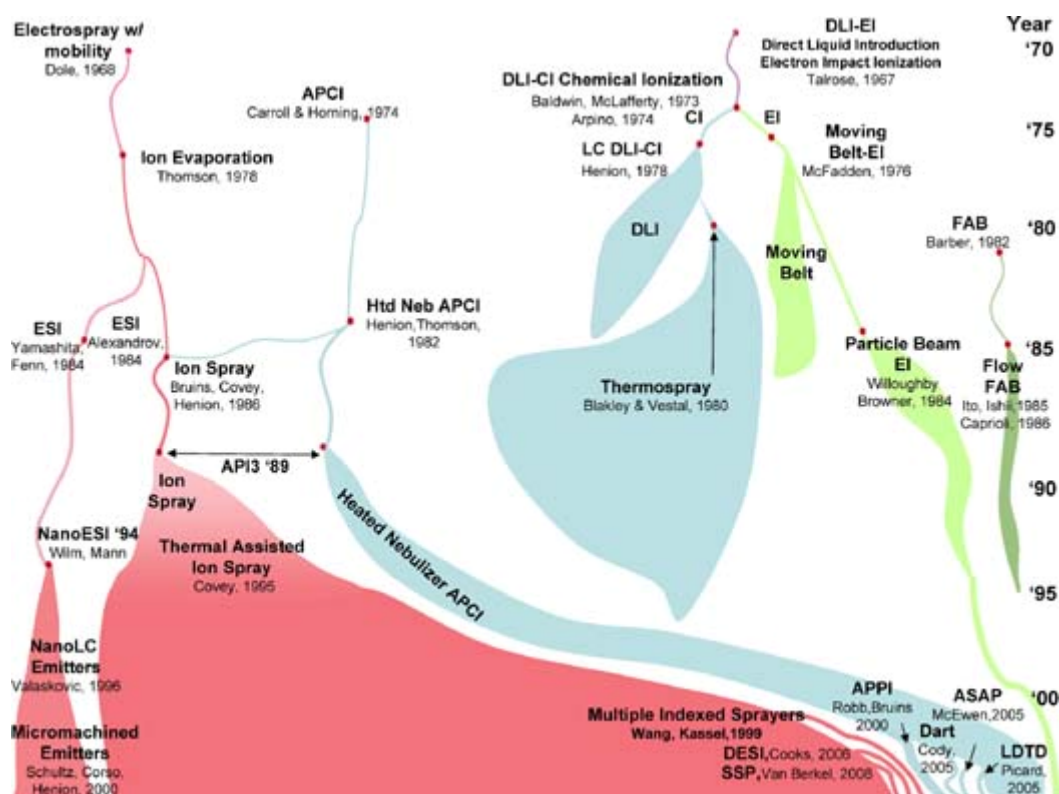


**Figure 25**. A history of the development of LC-MS instrumentation as viewed in histomap format. The "y" axis depicts the years and the "x" axis is the relative adoption of the technique at that point of time estimated by the extent of commercial indicators as well as publications and activity in academic research institutions. The image is reproduced with the kind permission of © Wiley-VCH Verlag GmbH & Co. KGaA (19).

Nowadays coupling liquid chromatography with atmospheric pressure mass spectrometry has become a very powerful, essential and versatile analytical tool which is widely applied in various research areas including chemistry, biochemistry, medicine and pharmaceutics. The increasing demand of qualitative and quantitative analysis from low molecular weight compounds to macromolecules in life science has led to constant improvements and new developments in this analytical technology. Due to its speed, wide dynamic signal range and quantitative capability, LC-MS is the analytical instrumentation of choice for the study of increasingly complex biological samples. Especially tandem mass spectrometry has grown to be an invaluable tool in LC-MS, which enables structure elucidation and peptide/protein sequencing of unknown samples.

Today combinations between HPLC and a broad range of mass analyzers and hybrid mass spectrometers (described in detail in chapter B.3.3) are commercially available. For routine and high-throughput clinical analysis, QqQ mass spectrometers have become the working horses among other mass analyzers. Various types of MS and MS/MS experiments particularly the highly sensitive and selective MRM mode of QqQ instruments provides quantification for hundreds of compounds in one single LC-MS/MS run. Despite many other sophisticated MS techniques with growing versatility, the outstanding performance of QqQ systems will continue to be very important also in the future. However, other mass analyzers like ion traps or especially high resolution instruments like QqTOF, FT-MS and the novel Orbitrap gain more and more importance. Since they have been improved significantly over the last years, they are already used extensively in academic environments. Also other fields, like clinical applications, start to involve these techniques in their analytical workflows. High resolution instruments from today offer improved selectivity, mass accuracy and full-scan data at low duty cycle times and measuring in DDA mode has become state of the art for qualitative analysis.

The chromatographic part in LC-MS underwent also fundamental improvements in the last years, discussed in more detail in chapter B.2.4. Today, LC configuration ranges from nano-LC to conventional bore-LC. Recent developments in LC technology have taken place in the areas of particle size, ultra high pressure resistance (UHPLC), high temperature, monolithic support and fused-core technology. These developments significantly increased the separation efficiency in LC which enables LC peaks with peak widths at half-height below one second. Also the duration of one chromatographic run can be reduced approximately ten times compared to classical LC without reducing the separation efficiency. Thus, MS producing companies face another technical challenge driven by the increasing pace of chromatography to develop the proper instruments (2, 9, 12, 13, 17, 20, 21).

## B.5. References

1. Kellner, R., J. M. Mermet, M. Otto, M. Valcarcel, and H. M. Widmer. 2004. Analytical Chemistry - A Modern Approach to Analytical Science, 2th ed. p.1-864 © Wiley-VCH Verlag GmbH & Co. KGaA, Weinheim. Reproduced with permission.

2. Trötzmüller, M. 2009. Dissertation: Methodenentwicklung zur Identifizierung und spurenanalytischen Bestimmung von organischen Verbindungen. Graz University of Technology.

3. Cammann, K. 2001. Instrumentelle Analytische Chemie Verfahren-Anwendung-Qualitätssicherung. Spektrum Akademischer Verlag GmbH, Berlin, Heidelberg. Reproduced with permission.

4. Begerow, J., and L. Dunemann. 2001. Sample Preparation for Trace Analysis. p.77-104 In: Günzler, H., and A. Williams, editor. Handbook of Analytical Techniques. © Wiley-VCH Verlag GmbH & Co. KGaA, Weinheim. Reproduced with permission.

5. Waksmundzka-Hajnos, M., and J. Sherma. 2011. High Performance Liquid Chromatography in Phytochemical Analysis. CRC Press Taylor and Francis Group, Boca Raton, FL.

6. Fritz, J. S. 1999. Analytical Solid-Phase Extraction. John Wiley & Sons Ltd, Chichester.

7. Touchstone, J. C. 2001. Thin Layer Chromatography. p.327-344 In: Günzler, H., and A. Williams, editor. Handbook of Analytical Techniques. © Wiley-VCH Verlag GmbH & Co. KGaA, Weinheim. Reproduced with permission.

8. Lembke, P., G. Henze, K. Cabrera, W. Brünner, and E. Müller. 2001. Liquid Chromatography. p.261-323 In: Günzler, H., and A. Williams, editor. Handbook of Analytical Techniques. © Wiley-VCH Verlag GmbH & Co. KGaA, Weinheim. Reproduced with permission.

9. Guo, X. 2011. Habilitation Thesis: Developments of Liquid Chromatography (LC-MS) for Trace Bioanalysis. Graz University of Technology.

10. Harvey, D. 2000. Modern Analytical Chemistry. McGraw-Hill Companies, New York City Inc., NY.

11. Wu, J. 2009. Dissertation: Development and evaluation of new silica based polar and / or mixed modal stationary phases for HPLC. University of Vienna.

12. Niessen, W. M. A. 2006. Liquid Chromatography-Mass Spectrometry, 3rd ed. CRC Press Taylor and Francis Group, Boca Raton, FL.

13. Hopfgartner, G. 2007. Mass Spectrometry in Bioanalysis - Methods, Principles and Instrumentation. p.3-62 In: Wanner, K.T., and G. Höfner, editor. Mass Spectrometry in Medicinal Chemistry. © Wiley-VCH Verlag GmbH & Co. KGaA, Weinheim. Reproduced with permission.

14. Barker, J. 1999. Mass Spectrometry, 2nd ed. John Wiley & Sons Ltd, Chichester.

15. Herbert, C. G., and R. A. W. Johnstone. 2003. Mass Spectrometry Basics. CRC Press LLC, Boca Raton, FL.

16. Lottspeich, F., and J. W. Engels. 2012. Bioanalytik, 3.Auflage. © Springer-Verlag, Berlin, Heidelberg. Reproduced with permission.

17. Kebarle, P., and U. H. Verkerk. 2010. A Brief Overview of the Mechanisms Involved in Electrospray Mass Spectrometry. p.1-35 In: Santos, L.S., editor. Reactive Intermediates - MS Investigations in Solution. © Wiley-VCH Verlag GmbH & Co. KGaA, Weinheim. Reproduced with permission.

18. LTQ FT Ultra - Product Specifications. 2006. Thermo Fisher Scientific, Bremen.

19. Covey, T. R., B. A. Thomson, and B. B. Schneider. 2009. Atmospheric pressure ion sources. *Mass Spectrom Rev* **28**: 870-897. © Wiley-VCH Verlag GmbH & Co. KGaA, Weinheim. Reproduced with permission.

20. Hopfgartner, G. 2011. Can MS fully exploit the benefits of fast chromatography? *Bioanalysis* **3**: 121-123.

21. Himmelsbach, M. 2012. 10 years of MS instrumental developments - Impact on LC-MS/MS in clinical chemistry. *Chromatogr B Analyt Technol Biomed Life Sci* **883**: 3-17.

# C. New strategies in lipid trace analysis

## C.1. Introduction

Lipids, in former days also called lipine, lipin or lipoid, are a large group of naturally occurring compounds with an immense combinatorial structural diversity arising from the various combinations of fatty acids with backbone structures. This huge number of chemically distinct molecular species makes the precise definition of lipids very challenging. In many textbooks for example, lipids are defined as a group of molecules which are highly soluble in organic solvents such as chloroform, benzene, ethers and alcohols. However, this definition can be misleading since many classes of lipid molecules such as the very polar phosphoinositides may be more soluble in the aqueous than in the organic phase during LLE. Another classification was suggested by Christie, who restricted the use of "lipids" to fatty "acids". He stated that "Lipids are fatty acids and their derivates, and substances related biosynthetically or functionally to these compounds." A further definition has been proposed by the LIPID MAPS (LIPID Metabolites And Pathways Strategy) consortium. They define lipids as hydrophobic or amphipathic small molecules that originate entirely or in part by carbanion-based condensations of thioesters and/or by carbocation-based condensations of isoprene units. However, using the approach of LIPID MAPS, lipids can be generally categorized into eight major groups according to their nature of the various constituent parts of the molecules, listed in Figure 26.

For a long time, lipids were only considered to be an uninteresting heterogeneous group of molecules with some specific functions. Nevertheless, it was already established in 1925 that most of the lipids are main structural components of cell membranes as they build the lipid bilayer. Especially in aqueous environment the formation of lipid bilayers from single lipids is an energetically preferred process. Today we know that membrane lipids are not only passive elements of the cell membrane matrix. Lipids are additionally involved in membrane trafficking, they regulate membrane proteins and cellular architecture. Furthermore, lipids provide the membrane cover of separate specific subcompartments, the so called cellular organelles which fulfil important intracellular functions. Besides membrane forming lipids, other lipid molecules have multiple important biological functions such as energy storing or taking part in cell signaling procedures. Energy storing lipids in cells are the triacylglycerols, which appear mainly in adipose tissue in mammals. Signal transduction pathways initiated with activation of receptors like the G protein-coupled receptors or various nuclear receptors utilize lipid molecules as secondary messengers. For example sphingosine-1-phosphate, a sphingolipid derived from ceramide is a potent messenger molecule involved in regulation of calcium mobilization, cell growth, and apoptosis.
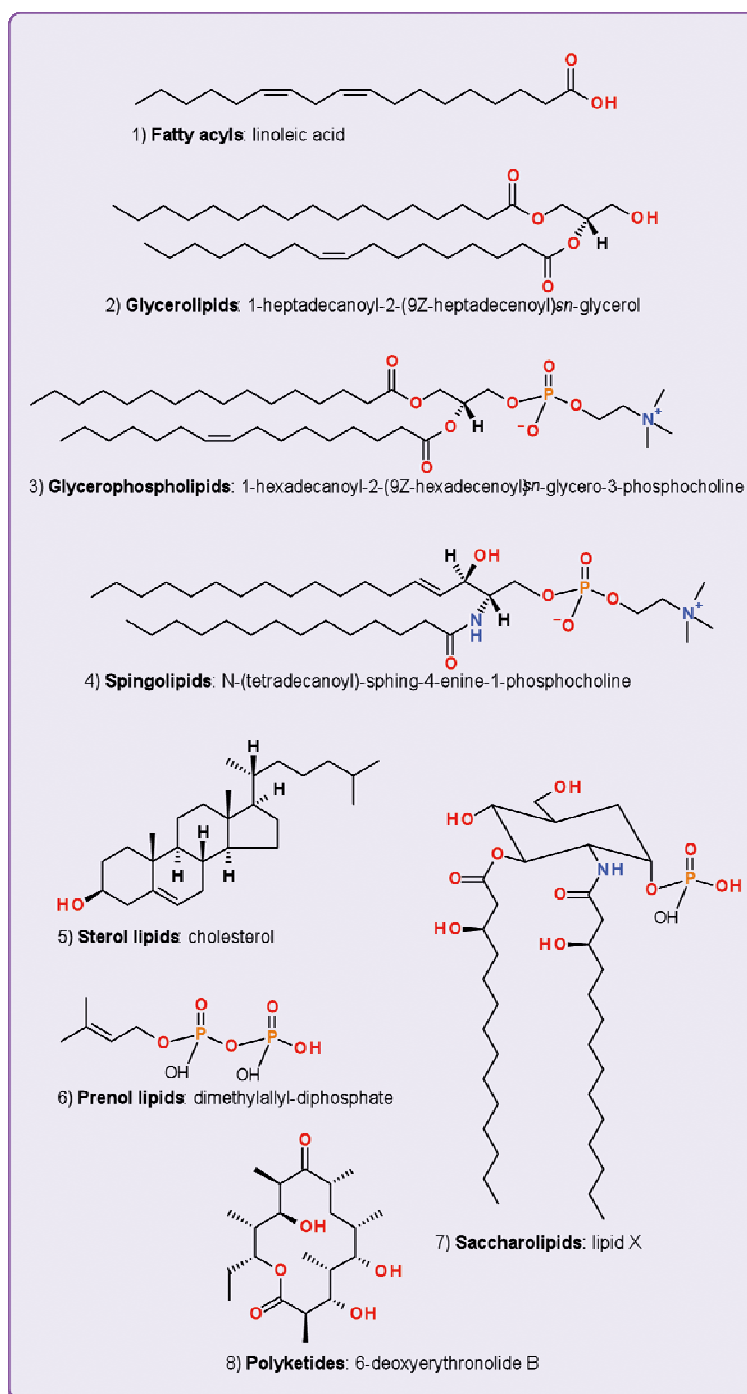
**Figure 26.** Lipid classification comprising of eight lipid categories. For every lipid class one specific representative lipid species is illustrated in the figure.

Additionally, fat soluble vitamin A, D, E and K, which are isoprene-based lipids, fulfil a wide range of important biological functions. These vitamins are important nutrients and mainly stored in the liver and fatty tissues. Carnitines and their acyl esters (acylcarnitines) are essential elements of the transport and metabolism of fatty acids in and out of the mitochondria. The general importance of lipids has been emphasized during the past decades in a huge number of different studies. These outcomes have evidenced the

fundamental role of lipids in cell, tissue and organ physiology. The physiological relevance of lipids has been evidenced by human diseases which are caused by dysfunction of lipid metabolic enzymes and abolished pathways involving lipids. Lipid abnormalities contribute to numerous diseases including cancer, diabetes and obesity as well as neurodegenerative and inflammatory diseases. These recent discoveries about essential lipid functions in various biological processes highly motivated the detailed research of these compounds. Hence, lipidomics has emerged, which is the system-based analysis of lipid molecular species and their interacting partners. Complete characterization of all lipid species in a complex cellular network contributes toward understanding how lipids operate in biological systems. Furthermore lipidomic research, along with genomics, proteomics and metabolomics, provides a powerful tool for elucidating the mechanism of lipid-based diseases. Lipidomics further enables biomarker screening and monitoring of pharmacological therapies.

The driving force of recognizing lipidomics as an autonomic discipline was the appearance of novel chromatography- and mass spectrometry-based analytical technologies. These instrumentations are highly sophisticated and powerful, e.g. the newest generation of mass analyzers (QqQ, QIT, QqQ$_{LIT}$, QqTOF, FT-ICR-MS or LTQ-Orbitrap, described in chapter B.3.3) offer high sensitivity and provide quantitative data. In addition, online coupling of chromatographic separation to selective mass spectrometry, which is possible by the most popular atmospheric pressure ionization techniques ESI or APCI, opens completely new analytical perspectives in lipid research. However, since direct sample injection into the ion source is also possible, extensive sample preparation or chromatographic separation is not always required. Furthermore, tandem MS applications greatly enhance the obtainable information. Although these instruments are still costly, they are becoming more and more affordable, thus meanwhile they can be found as part of the standard laboratory infrastructure.

Detailed explanations of various instrumental setups and functionalities are described in chapter B.3. Moreover different strategies in lipidomic research ranging from shotgun lipidomics to LC-MS approaches are discussed and summarized in chapter C.2. The main part of this work (chapter C.3 and C.4) demonstrates newly developed applications of high throughput lipid profiling in different biological samples. These experimental setups involve high resolution LC-MS and MS/MS approaches combined with fast and efficient working sample preparation techniques, like SPE. In addition, negative background ions typically appearing in ESI LC-MS are characterized (chapter C.5). The motivation for such analysis is the chemical background noise which appears in atmospheric pressure ionization liquid chromatography-mass spectrometry (API LC-MS) approaches, which in turn is actually also

their major drawback. These ubiquitous by-products rise from the efficient and generic nature of this soft ionization technique. Traces of ionized contaminants and clustered ions derived from various sources like HPLC solvents as well as additives or tubing materials, can be such by-products. Ionic chemical background noise may have a huge negative impact on trace analysis even by using modern mass spectrometry techniques. Especially the determination of very low concentrated unknown components of various extracts and biological samples can be complicated due to background ions. Furthermore, identification of molecules having poor ionization efficiency could also be disturbed due to ionic chemical background noise. The presence of these by-products may completely overshadow the appearance of target analytes in chromatograms and even in mass spectra. Therefore, we studied the typical background ions in negative ESI LC-MS. This phenomenon might also occur in lipidomic research and thus it has to be considered too. Prevention and reduction of chemical noise allows precision and high sensitivity which are both very important for the determination of minor and low abundant lipid molecules (1-7).

## C.2. Mass spectrometry based lipidomics: An overview about technological platforms

Harald Köfeler [1], Alexander Fauland [2], Gerald N. Rechberger [3] and Martin Trötzmüller [1]

[1]Core Facility for Mass Spectrometry, Center for Medical Research, Medical University of Graz, Graz, Austria

[2]Institute of Analytical Chemistry and Food Chemistry, Graz University of Technology, Graz, Austria

[3] Department for Molecular Biosciences, University of Graz, Graz, Austria

**ABSTRACT**

One decade after the genomic and the proteomic life science revolution new 'omics' fields are emerging. The metabolome encompasses the entity of small molecules, most often end products of a catalytic process regulated by genes and proteins, with the lipidome being its fat soluble subdivision. Within recent years, lipids are more and more regarded not only as energy storage compounds but also as interactive players in various cellular regulation cycles and thus attain rising interest in the bio-medical community. The field of lipidomics is on one hand fuelled by analytical technology advance, particularly mass spectrometry and chromatography, but on the other hand new biological questions also drive analytical technology developments. Compared to fairly standardized genomic or proteomic high-throughput protocols, the high degree of molecular heterogeneity adds a special analytical challenge to lipidomic analysis. In this review we will take a closer look at various mass spectrometric platforms for lipidomic analysis. We will focus on the advantages and limitations of various experimental setups like 'shotgun lipidomics', liquid chromatography – mass spectrometry (LC-MS) and matrix assisted laser desorption ionization- time of flight (MALDI-TOF) based approaches. We will also examine available software packages for data analysis, which nowadays is in fact the rate limiting step for most 'omics' workflows.

## INTRODUCTION

Biological systems such as cells comprise thousands of individual molecular lipid species, called the lipidome of an organism, which can be classified into 8 major lipid categories and dozens of lipid classes and subclasses (1). Generally, lipids fulfil three major tasks in cellular systems: Energy storage, structural functions and cellular signaling (2, 3).Within the recent decade it became increasingly evident that lipids are not only energy storing bystanders in cellular processes but are a vital part of cellular regulation processes by themselves. As their biological properties strongly depend upon their chemical structure, each molecular lipid species has an individual role in a living system. An imbalance in this system can lead to various pathophysiological conditions such as diabetes, atherosclerosis, liver steatosis, chronic inflammation and also neurodegenerative diseases to name just a few (4, 5).

Improved lipidomic technologies greatly enhance the knowledge about lipid functions at the level of individual species (6). Thin layer chromatography (TLC), the classical standard in lipid analysis, is cheap and fast, but it is very limited when it comes to identification issues below the level of lipid classes. Due to its sensitivity and selectivity mass spectrometry (MS) is the method of choice for qualitative and quantitative lipidomic analysis. Although it is yet not possible to detect and quantify all individual lipids in a given cellular system, the aim of lipidomic analysis is to determine as many individual lipids as possible.

Compared to biopolymers such as DNA, RNA, carbohydrates or proteins, lipids show much less standardized fragment mass spectra. Each lipid class has its own rules for fragmentation and its specific ionization efficiency (7), which makes development of standardized 'all inclusive' methods a daunting challenge. Depending on the instrumental setup, different layers of information about the molecular structure are to be discovered. Survey approaches sometimes only determine the number of fatty acyl carbons and the number of fatty acyl double bonds, whereas more focused in depth methods are able to determine structural details down to fatty acid double bond position. Due to the diversity in molecular structures there is no single mass spectrometric approach which could cover detection of the whole lipidome of an organism, but usually it is rather a combination of different experimental platforms. The following article will focus on mass spectrometry instrumentation using electrospray ionization (ESI), atmospheric pressure chemical ionization (APCI) and MALDI, because these are nowadays the ionization techniques of choice for complex lipids with a molecular weight above 500 Da.

## DIRECT INFUSION

The first ones to propose lipidomic analysis by ESI were Han and Gross in 1994 (8). This concept utilized the emerging combination of ESI with a triple quadrupole analyzer. Sample injection was done by a syringe pump. A few years later the same instrumentation was

successfully used for lipid analysis in combination with the first prototypes of a static nano ESI source (9) without syringe pump. The nano ESI source with a flow rate of about 80 nL/min resulted in higher ionization efficiencies than a syringe pump running at several µL/min. Although this method now widely termed 'shotgun lipidomics' improved a lot in the last 15 years the basic concept behind it remains the same. It is based on precursor ion and constant neutral loss scans of readily ionizable phospholipid headgroups, resulting in lipid class specific fragments (10). Shotgun lipidomics avoids difficulties with concentration alterations and chromatographic abnormalities. Another advantage compared to LC-MS is the literally unlimited time which can be spent on each lipid class specific scan type. Addition of one internal standard per lipid class was shown to be sufficient for quantitation (11), because ionization of lipids is largely dependent on the class specific head group and not so much on the fatty acyl chains. One drawback of this system are isobaric overlaps of the M+2 isotope with the monoisotopic peak of the compound with one double bond less. This can be overcome by deisotoping algorithms (12). The output format of data usually indicates the sum of fatty acyl carbons and the sum of double bonds but not the individual composition of fatty acids.

Multi dimensional mass spectrometry based shotgun lipidomics (MDMS-SL) is a further development of shotgun lipidomics taking into account the concept of building blocks in lipid structures (13). MDMS-SL takes advantage of differential intrasource separation properties with various additives like $Li^+$, $NH_4^+$ or $Na^+$, and unique fragments for each lipid class. Glycerolipids without class specific fragments are detected by constant neutral losses of fatty acids and information about the intact lipid is drawn from the combinatorial possibilities of all monitored fatty acid neutral losses (14). Coupled with an Advion NanoMate the MDMS-SL concept proves to be a powerful high throughput device because of its high degree of automatization and the enhanced sensitivity provided by a nano ESI source. The MDMS-SL system covers quantitative analysis of various classes of glycerophospholipids, sphingolipids and glycerolipids (10).

Flow injection lipidomic analysis, a variation of shotgun lipidomics is proposed by the group of Liebisch (15). In contrast to classical shotgun lipidomic methods this experimental setup utilizes an HPLC apparatus coupled to a triple quadrupole analyzer. The HPLC pump runs at microflow rates and the autosampler injects samples automatically into the flow, which delivers the sample directly into the ESI source without HPLC column. The HPLC autosampler offers a higher degree of automatization than a syringe pump. Furthermore it results in a short and concentrated sample pulse for about one minute, which can be used for data acquisition with precursor ion and constant neutral loss scans. Depending on the number of scans necessary multiple injections per sample are possible. Quantitation is achieved by a standard addition method with multiple standard curves, featuring one internal

standard and sets of lipids with different fatty acyl chain lengths and degrees of unsaturation (16). The method is very robust, highly automated and was applied on various subclasses of glycerophospholipids, sphingolipids and sterols (16-19). As for all low resolution direct infusion technologies it runs into its limits when isobaric nominal mass compounds derived from the same phospholipid subclass occur, like e.g. diacyl and acyl-alkyl glycerophospholipids.

Another direct infusion approach encompasses coupling of a syringe pump and a triple quadrupole analyzer in multiple reaction monitoring (MRM) mode (20). In this experimental setup the anticipated precursor and product ions have to be known. It allows a quick and reliable quantitation of major lipid components in a given lipid extract. On the downside, this method has a limited capability for detection of unexpected lipid species and is particularly vulnerable for overlapping isobaric compounds.

In contrast to low resolution instruments high resolution mass spectrometers deliver accurate mass and elemental composition of ions with very high confidence. Most lipid classes have an unambiguous fingerprint due to a certain and invariable number of the heteroatoms N, O, P and S. Due to this fact, the elemental composition of precursor and often also product ions contains highly valuable information about the lipid class. The Multiple Precursor Ion Scans (MPIS) method developed on a quadrupole-TOF instrument by the group of Shevchenko (21, 22) combines high resolution precursor ion scans on glycerophospholipid headgroups and fatty acyl moieties, resulting in the individual fatty acyl composition of glycerophospholipid species. The high resolving power is particularly helpful in the case of ambiguous product ions with mass differences in the first or second digit. The MPIS concept was successfully applied for quantitative global lipidome analysis in various cell systems including glycerophospholipids, glycerolipids, sphingolipids, sterols and various glycolipids (23-25). The method has its limitations when one lipid class like triacylglycerol (TG) is present in bulk amounts and possibly suppresses ionization of other minor lipid classes (26).

A further development of the MPIS concept is shotgun lipidomics with a hybrid LTQ-Orbitrap instrument coupled to an Advion NanoMate ion source (27). A schematic workflow of this platform is shown in Figure 1. This system relies on accurate mass down to sub ppm range for both, precursor and product ions. With the recent development of higher energy collision-induced dissociation (HCD) even the low mass cut off problem of product ion spectra acquired in the LTQ could be overcome (28). The Advion NanoMate provides plenty of time to be spent on each sample with only a few microliters of it consumed. This opens up the avenue for data dependent acquisition of product ion spectra on all possible precursor ions, resulting in full scan precursor spectra and product ion spectra of literally every detectable lipid species at a resolution of 100,000 or more. Additionally, exact assignment of fatty acyl side chains can be achieved on a regular basis with this system. Quantitation is done by one

internal standard per lipid class (29), which is sufficient to compensate for varying ionization efficiencies.



**Figure 1.** Schematic outline of a high throughput shotgun lipidomics platform consisting of an LTQ-Orbitrap mass spectrometer coupled to a NanoMate.

An interesting alternative to gas chromatography-mass spectrometry (GC-MS) analysis of fatty acids is published by the Welti group (30). The CID-TOF system uses a quadrupole-TOF analyzer coupled to negative ESI direct infusion. Thereby mass selection in Q1 is turned off, Q2 fragments all ions and the TOF analyzer records intact fatty acid carboxylates with accurate mass. This provides the fingerprint of fatty acids including modified fatty acids without any prior derivatisation step being necessary. Mentionable, this method only works for lipids which generate negative ions in ESI, but nevertheless comparison with GC-flame ionization detector (GC-FID) data shows good correlation (30).

**LC-MS**

**Low resolution mass spectrometry**

The invention of ESI enabled coupling of HPLC with mass spectrometry in a highly efficient manner for the first time (31). This instrumental combination opened up completely new analytical perspectives in lipid research by combining the separation power of HPLC with the selectivity of mass spectrometry. Complex lipid classes like glycerolipids, glycerophospho-lipids or even glycolipids were analytically amenable on a regular basis by chromatography coupled to mass spectrometry, now termed LC-MS. Compared to direct infusion systems HPLC adds retention time as another layer of selectivity. On one hand this results in increased specificity for lipid identification, but on the other hand it complicates quantitation, because every spectrum in an LC-MS run has to be regarded as a single event with unique matrix effects and solvent composition (Figure 2). Therefore quantitative aspects are generally more difficult to be standardized than for direct infusion methods.
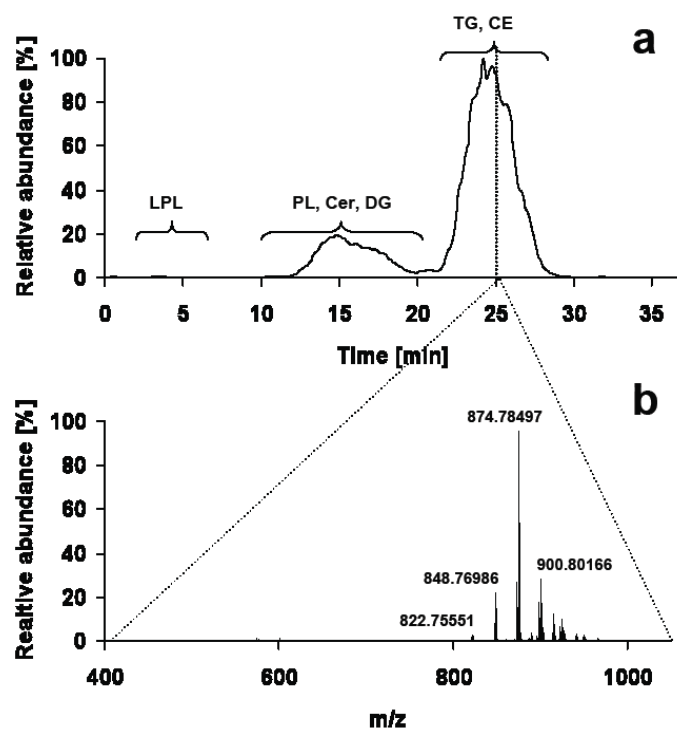
**Figure 2. (a)** Total ion chromatogram of a lipid droplet extract acquired on C-18 reversed phase HPLC coupled to an LTQ-FT in positive ESI mode, **(b)** consisting of 487 individual full scan mass spectra at a resolution of 200,000.

Excellent examples of lipidomic LC-MS analysis have recently been shown for human plasma (32) and subcellular organelle lipidomics of TLR-4 activated macrophages (33) by the LIPID MAPS consortium. These publications show very well that the whole lipidome of an organism or tissue can not be determined by a single experimental setup but rather by a combination of various methods, most of them LC-MS based.

The fastest and simplest way to monitor changes in a lipid profile by LC-MS is LC/single ion monitoring (SIM)/MS (34). This method is based on ESI full scan quadrupole MS of intact molecular adduct ions. Plotting of retention time versus m/z and intensity provides a 3D lipidomic fingerprint of a sample, which can be used to monitor changes between statistical groups by differential profiles in a fast and comprehensive manner.

A very efficient way to maximize sensitivity is targeted lipidomics with HPLC-triple quadrupole instrumentation in MRM mode. Due to the instruments high dynamic range and the selectivity of retention time in conjunction with known precursor / product ion pairs it is the method of choice for lipid quantitation. Recent developments in scan speed of triple quadrupole mass spectrometers result in a duty cycle of up to 100 Hz, which provides the basis for fast and reliable quantitation of whole lipid classes within one chromatographic run (35-37). In some rare cases molecular species of lipids are composed of exactly the same building blocks, resulting in the same elemental composition and the same fragments, which

renders MRM analysis basically useless. In this case good chromatographic separation is mandatory as shown for bis(monoacylglycero)phosphate (BMP) and cardiolipin (CL) by the group of Liebisch (38).

A good compromise between targeted and non targeted analysis on a triple quadrupole instrument are precursor ion- and constant neutral loss scans. Although sensitivity for such scans might not be as high as in MRM mode it opens the possibility to find unexpected species within the lipid classes surveyed by the respective precursor or constant neutral loss scans. Such systems are quite frequently used with ESI and reversed phase HPLC coupling. An excellent example of this technique is shown by Retra et al. (39). The applied very shallow 60 min gradient results in baseline separation of glycerophospholipid species. The use of constant neutral loss scans for phosphatidylinositol phosphate (PIP) identification and quantitation is shown by Clark et al. (40).

Identification of lipid molecular species with low resolution instrumentation is best achieved by MS$^n$ analysis, because this kind of analysis provides a high degree of structural information. The preferred instrumentation is either (linear) ion trap or triple quadrupole technology. Usually acquisition time for a certain compound is limited in LC-MS approaches and as acquisition of product ion spectra takes much longer than for MRM spectra the number of lipids to be covered is a potential bottleneck. Nevertheless, in cases of a defined number of lipids this can be a highly specific identification strategy as shown successfully for oxysterols (41), positional isomer analysis of phospholipids (42) and in depth analysis of PIP species (43).

While chromatographic separation of lipids is often performed on reversed phase HPLC according to fatty acyl chains, this strategy runs into its limits when cholesterol esters (CE) are to be analyzed in the presence of bulk amounts of TG. Due to their very similar hydrophobicity CE and TG are hardly separated on reversed phase and hydrophilic interaction liquid chromatography (HILIC) columns, resulting in suppression of low abundant CE by TG. In contrast, silica based normal phase HPLC provides separation of these lipid classes by their polar functional groups, but usually highly non polar solvents with low ionization capacity have to be used. Hutchins et al. (44) use APCI and post column addition of a polar solvent to increase ionization properties of the non polar solvent eluting from normal phase HPLC. This results in a practicable online bridging between normal phase HPLC and triple quadrupole mass spectrometry, which can either be used in precursor ion, MRM or single quadrupole mode for determination of neutral lipids (32, 45).

**High resolution mass spectrometry**

Quadrupole-TOF mass spectrometry offers several advantages. On one hand this instrumentation provides resolution of up to 40,000 and mass accuracy of better 5 ppm,

which is sufficient for pinning down many of the elemental compositions encountered in lipidomic analysis. On the other hand TOF analyzers have a very high scan rate and acquire full product ion spectra very fast and efficient. On the downside is the usually limited dynamic range of the detector, which limits quantitation to a rather narrow concentration range. Nevertheless this kind of instrumentation is a valuable tool when coupled to reversed phase HPLC. Successful application of this experimental setup was used for analysis of TG and oxidized TG species. In this case it was even possible to determine the actual fatty acid composition of TG molecular species by product ion spectra on all major species (46). An excellent example for an integrated lipidomic platform relying on reversed phase ultra performance liquid chromatography (UPLC) quadrupole-TOF is shown by the group of Oresic (47), whereby a combination of retention time, exact precursor mass and product ion spectra are used for identification of lipids from various lipid classes. In contrast to widely used gradient elution, the group of Wenk present a profiling method based on quadrupole-TOF and isocratic reversed phase HPLC (48) used for determination of anionic glycerophospholipids, glycolipids, fatty acids, prenols and sphingolipids.

Fourier transform ion cyclotron resonance mass spectrometry (FT-ICR-MS) offers literally unlimited mass resolution and sub ppm mass accuracy. Its combination with a linear ion trap (LTQ-FT) has become a high end standard instrumentation in proteomic research, but a few groups also use it in lipidomic research. The instruments hybrid character holds the possibility to run the linear ion trap and the FT-ICR-MS as two instruments in parallel, resulting in high resolution precursor spectra and low resolution product ion spectra at an increased duty cycle. Coupled to HPLC this experimental platform delivers retention time, exact sub ppm precursor masses and product ion spectra as means for identification (Figure 3). High mass accuracy paired with retention time is particularly helpful for identification of lipids with too little intensity for reliable fragment spectra. Such an integrated experimental platform is successfully used for quantitative determination of various lipid classes in lipid droplet preparations (49). MS/MS spectra are triggered in a data dependent manner on the four most intensive ions in the preview scan, resulting in MS/MS coverage of 66%. Owing to the ultra high resolving power and mass accuracy it is possible to confidently detect lipid species in crude lipid extracts at extremely low quantities, even when no MS/MS spectra are available for the precursor. Extension of reversed phase HPLC by a preceding HILIC fractionation of certain lipid classes results in higher sensitivity for lipid classes previously suppressed by PC. Other successful applications of similar instrumental setup are methods for quantitation of glycerophospholipids and TG in plasma samples (50) and for identification of glycerophospholipids in yeast (51). The disadvantages of such systems are their still rather slow duty cycle of about 3s at 200,000 mass resolution, and the low mass cutoff in the linear ion trap, which might cause loss of some low mass diagnostic fragment ions.
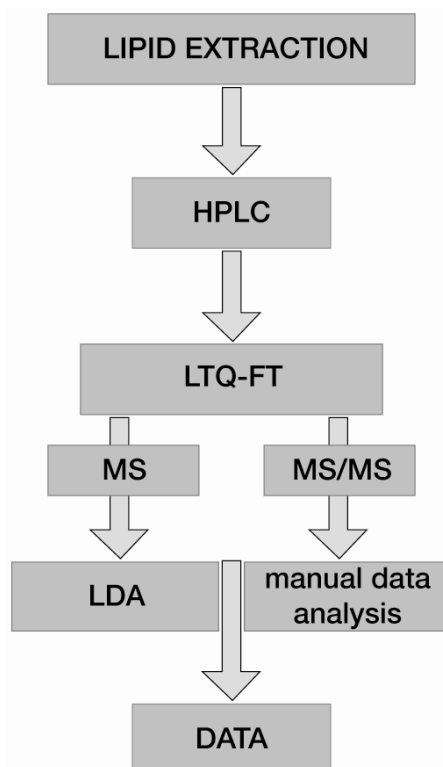
**Figure 3.** Workflow of a high resolution LC-MS platform relying on an LTQ-FT mass spectrometer. Full scan MS and MS/MS data are acquired parallel in data dependent acquisition mode. Full scan MS data are automatically processed and quantified by Lipid Data Analyzer (LDA), whereas MS/MS data have to be manually inspected for fatty acid assignment.

Within recent years Orbitrap technology started to stepwise replace the LTQ-FT. Originally designed for small molecule identification and quantitation this technology has a lot of advantages in store for lipidomic applications, especially when hyphenated with the fragmentation power of linear ion trap or quadrupole technology. Although resolving power and mass accuracy are less than at the LTQ-FT, they are still sufficient to provide unambiguous elemental compositions for most applications. Mass accuracy can even be increased into the sub ppm range by use of constant background signals as internal lock mass calibrants. The addition of an HCD quadrupole alleviates the low mass cutoff limitations of the LTQ and provides high resolution MS/MS spectra, although at a much slower speed than for example a quadrupole-TOF analyzer. Another advantage of the most recent LTQ-Orbitrap models in comparison to the LTQ-FT is the faster scan speed of the linear ion trap at uncompromised sensitivity, allowing acquisition of up to 20 low resolution MS/MS spectra per cycle. The combination of LTQ-Orbitrap with reversed phase HPLC is successfully used by the group of Taguchi for determination of glycerophospholipids and PIP, either just by full scan of molecular ions (52) or by a combination of high resolution precursor full scans and low resolution product ion scans (52, 53). Sato et al. even expanded

this platform by separation of glycerophospholipids into three fractions with solid-phase extraction (SPE) prior to LC-MS analysis (54).

Eicosanoids are an analytical challenge because they comprise a plethora of isomeric compounds. An excellent approach by reversed phase HPLC and LTQ-Orbitrap is shown by the group of Volmer (35), whereby retention time, exact mass and MS/MS fragment intensities all have to be taken into account for successful identification of various isomers. A faster but somewhat less specific variant of this experimental setup is shown by the same group on an Orbitrap Exactive instrument coupled to reversed phase HPLC (55). Although this instrumentation lacks any MS/MS capabilities sub ppm mass accuracies and retention time are sufficient for identification of certain glycerophospholipid classes in fast survey scans.

**Digging deeper into structural details**

Beyond the actual fatty acid composition of a lipid species, the fatty acid *sn*-position can be of importance for many biological functions. Most direct infusion and LC-MS methods in lipidomics are not able to separate lipid molecular species at the level of positional isomers. However, some very sophisticated chromatographic methods are able to obtain insight on lipid molecular geometry at this level. Separation of positional TG isomers was successfully achieved by use of silver-ion HPLC (56). This publication describes a setup for serial connection of three HPLC columns to attain the necessary chromatographic resolution. Another excellent example of a highly specialized HPLC setup by the same group uses a 2D approach (57). A first HILIC dimension separates and fractionates lipids by their respective lipid classes, and a second reversed phase dimension further separates lipid classes by their individual molecular composition. While these HPLC methods are very efficient and highly specific for separation of individual lipid molecular species, they are only suitable for a limited number of samples due to their long chromatographic separation times, particularly in 2D HPLC.

Another highly specific LC-MS strategy is proposed by the group of Blair (58). This experimental platform couples chiral normal phase HPLC to negative APCI-MS for separation and determination of regioisomeric and enantiomeric forms of eicosanoids. Beyond enhanced separation selectivity, this method also provides very sensitive detection of eicosanoid pentafluorobenzyl derivatives by electron capture APCI and subsequent MRM analysis by triple quadrupole MS.

An important feature of molecular lipid species is the position of fatty acid double bonds. Gas phase reaction of ozone with double bonds results in primary and secondary ozonides, which fragment further to aldehydes, carboxylates and hydroperoxides indicative for the position of the double bond in the fatty acyl chain (59). Recently the group of Blanksby introduced

custom modified instrumentation for ozone induced dissociation (OzID), at which either a linear ion trap (60) or a quadrupole collision cell (61) are able to be filled with ozone. Either sequential multistage dissociation with an inert collision induced dissociation (CID) gas and ozone, or single stage dissociation by a mixture of ozone and CID gas, results in a double bond position specific fragmentation pattern. The main limitation of this method is the specialized non commercial equipment needed. Additionally, no high throughput standardized data analysis software is available for such an approach.

**MALDI-TOF**

Although not as widely used as ESI instruments, MALDI-TOF is a good complementary choice for lipids in the mass range above m/z 500. The soft ionization properties of MALDI result in intact molecular adduct ions. Paired with the speed of MALDI-TOF analysis this fact renders the technology very suitable for fast screening of lipids. MALDI-TOF instruments equipped with a reflectron nowadays regularly achieve 10,000 resolution and 30 ppm mass accuracy, which is sufficient for assigning intact molecular ions of lipid species. Choice of the right MALDI matrix is an important step for good sensitivity. 2,5-dihydroxy benzoic acid, α-cyano-4-hydroxy-cinnamic acid, 9-ami-noacridine and 2-mercaptobenzothiazole are often used matrix compounds. On the downside of this technology, the mass range below m/z 500 is usually not amenable due to matrix interferences.

MALDI-TOF has been used for analysis of various lipid classes (62), but, the same as ESI, also MALDI has certain quantitative limits for crude mixtures due to ion suppression effects (63). This effect can become quite severe, particularly as MALDI does not allow any chromatographic separation to be coupled directly to the instrument. Recently TLC/MALDI was proposed by several groups as an interesting alternative (64, 65). Instead of a MALDI target a developed TLC plate with separated lipid spots is used as target. This approach is very promising, because TLC is still widely used in lipid analysis and coupling with MALDI-TOF vastly increases identification certainty of TLC spots. In such a setup visualization of TLC spots has to be reversible and non destructive and is either achieved by dyes non covalently bound to lipids (65, 66) or by immunodetection with antibodies (67, 68). Conventional UV lasers are used with most MALDI instruments and do only penetrate the applied MALDI matrix but not the silica gel itself. Therefore UV lasers are prone to distortion of results, because only lipids at the surface of the silica particles can be detected. In contrast, IR lasers do penetrate silica gel particles and are thus certainly the better choice for TLC/MALDI targets. Although this technology is still in its infancy, there are already promising results on glycosphingolipids (67, 68) and glycerophospholipids (69). Further technological progress could develop TLC/MALDI-TOF into a fast and easy to use survey method for lipidomic analysis.

While most instruments nowadays are equipped with low energy CID devices, MALDI-TOF/TOF offers an alternative for high energy CID. The advantage of high energy CID at 20 keV is induction of abundant charge remote fragmentation, which in turn allows structural analysis of lipids at the level of fatty acyl *sn* position and double bond location (70). With the decline of sector instruments in lipid mass spectrometry, MALDI-TOF/TOF has the potential to fill this gap. Pittenauer et al. show the use of MALDI-TOF/TOF for such applications in an excellent manner (71, 72). Alkali cationized TG show a wealth of structure specific fragments indicative for location of fatty acids and their double bonds (Figure 4). One challenge still to be solved is the quite wide isolation window of about 4 Da which makes precursor selection especially in biological lipid extracts problematic. Although this application is clearly no high throughput method and lacks automated software solutions, it is still highly useful for structural determination of selected lipid species.
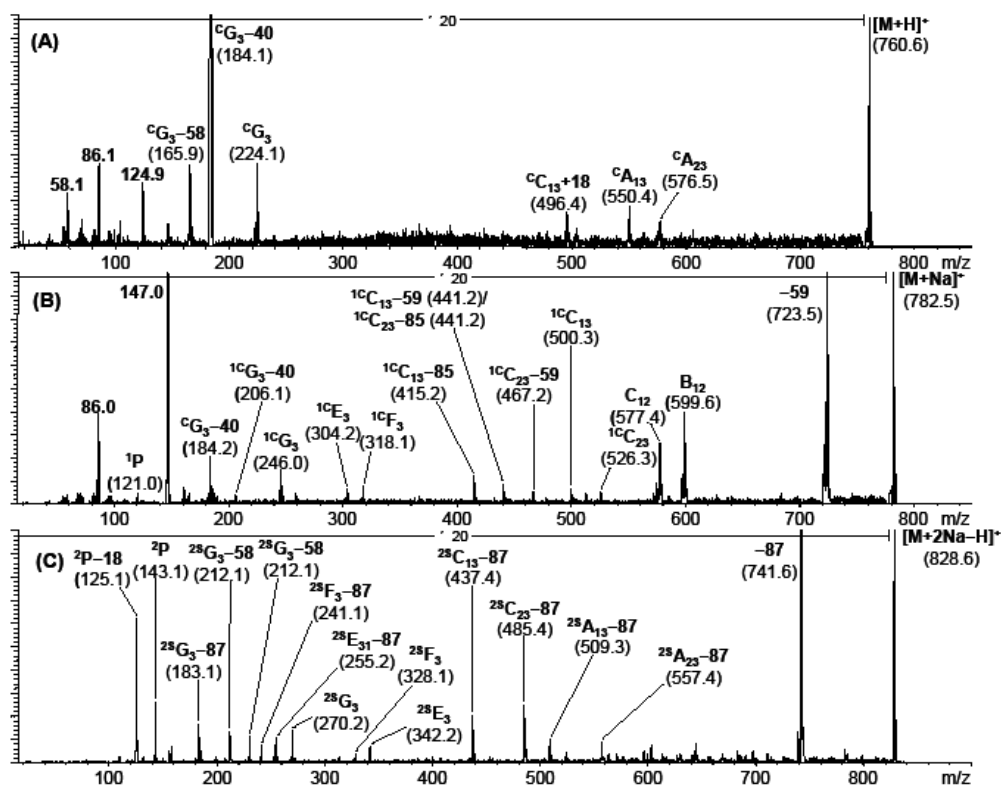


**Figure 4.** (**A**) High-energy CID-TOF/RTOF-spectrum of the [M+H]$^+$ precursor ion of 1-palmitoyl-2-oleoyl-glycero-phosphatidylcholine (m/z 760.6), (**B**) of the corresponding [M+Na]$^+$-precursor ion of 1-palmitoyl-2-oleoyl-glycerophosphytidylcholine (m/z 782.5), (**C**) both originating from commercial hen egg lecithine, and of the [M+2Na−H]$^+$ precursor ion of 1-palmitoyl-2-arachidonoyl-glycerophosphatidylserine (synthetic origin).

**DATA ANALYSIS**

Within the last decade a constantly increasing amount of information is accessible by lipid mass spectrometry. The bottleneck in translation of acquired mass raw data into useful quantitative biological information is data processing. Data processing encompasses primarily identification and quantitation of lipid species. Inevitably, some tradeoffs like semi quantitation instead of accurate quantitation are necessary when processing up to hundreds of lipids per analytical run. Unfortunately no platform independent commercial lipidomic data processing software is available so far. Nevertheless, some open source software packages offer solutions for data processing.

Recently the group of Shevchenko has launched LipidXplorer, an informatics concept based on molecular fragmentation query language (MFQL) (73). LipidXplorer is designed for shotgun lipidomics and takes MS full scan data and product ion scans into account. Although it is also possible to process low resolution data, this program is primarily developed for high resolution spectra and was shown to work best with LTQ-Orbitrap or quadrupole-TOF instrumentation. In contrast to other shotgun lipidomics software packages LipidXplorer does not rely on a database for MS/MS spectra but rather depends on the concept of fragmentation queries, which reflects the variability of MS/MS spectra due to different experimental settings much better. The software allows a lot of freedom for the user, like for example customized adjustment to various experimental parameters, but this requires some dedication.

Processing of LC-MS generated data is usually more challenging because retention time adds another dimension of information. Originally developed for metabolomic data acquired by mass spectrometry (74, 75), m/zMine and its sequel m/zMine2 were also successfully applied on lipidomic data (76). Following peak detection, identification of lipids is performed by searches in public libraries or customized internal databases containing exact mass and approximate retention times. Furthermore also isotopic distributions and adducts can be taken into account for lipid identification. Although originally applied on quadrupole-TOF LC-MS data, m/zMine2 has become a versatile and highly flexible software, which can be used for data generated with various experimental platforms.

In contrast to other software solutions Lipid Data Analyzer (LDA) is based on a 3D algorithm (m/z, retention time, intensity) for peak detection (77). This offers the advantage to detect peaks with overlapping retention time and m/z values which might have remained undetected in a 2D plot. Identification of lipids is performed by exact mass, retention time and isotopic distribution of a compound, resulting in very high identification certainty (Figure 5). Originally designed for an FT-ICR-MS instrument the software is highly dependent on exact mass and works best at a resolution of 100,000 or more. Nevertheless it was also shown to perform well with quadrupole TOF data. A desirable expansion of the program would be automatic

processing of MS/MS data acquired in data dependent fashion on the most abundant m/z values of each high resolution full scan spectrum. Quantitation of lipids is performed with sets of internal standards covering the whole elution range of the respective lipid class. Subsequently the software performs calculation of either the mean or the median intensity of all internal standards. This procedure allows for compensation of internal standard intensity fluctuations arising from variable ion suppression effects in each elution profile.



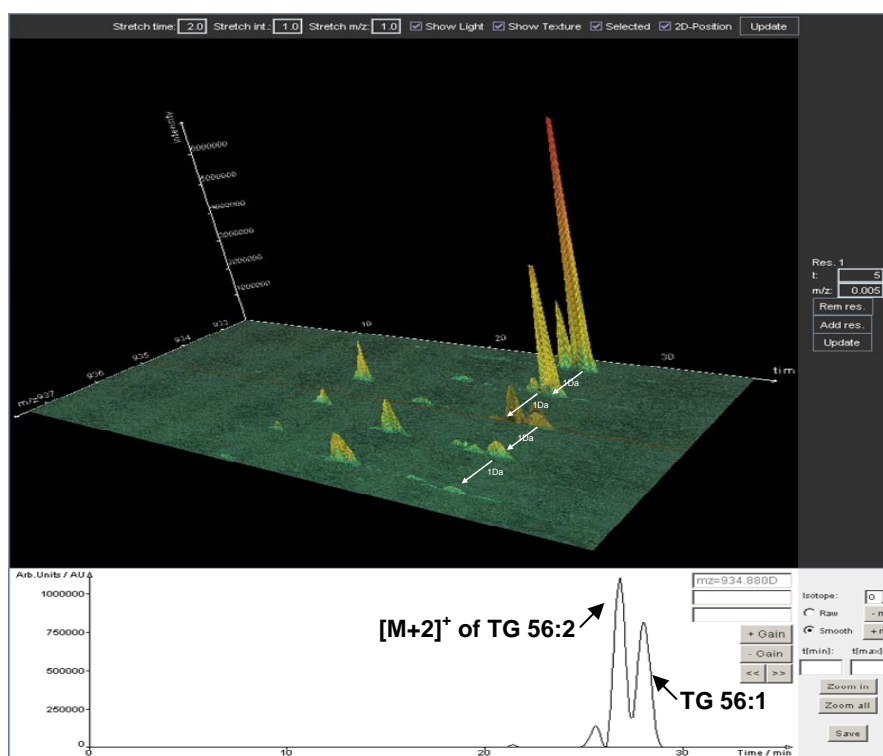**Figure 5.** 3D plot (m/z, retention time, intensity) of high resolution LTQ-FT data generated by Lipid Data Analyzer. Depicted are TG 56:1 and TG 56:2 including their isotopic distribution. Unambiguous identification of elemental composition is accomplished by a 3D algorithm which relies on combination of accurate mass, retention time and isotopic pattern. The lower panel shows a 2 D plot (retention time, intensity) of m/z 934.88.

**CONCLUSION**

Although various experimental platforms and approaches are nowadays established, lipidomic analysis still remains a challenge for analytical chemists and bioinformaticians alike. The biggest issue in the years to come will be standardization of data acquisition and data processing. Unlike genomic or proteomic protocols, lipidomics still stays highly diversified in instrumentation and the degree of information to be deduced from mass spectrometric data. In this respect, a standardized shorthand lipid nomenclature will be needed for database development. Furthermore data processing is highly dependent on customized software solutions, although some promising software tools have been developed recently. Despite these challenges, it can be expected that mass spectrometry based lipidomics will constantly develop into a high throughput technology and advance our understanding of molecular biological processes with increasing impact.

**ACKNOWLEDGMENTS**

**REFERENCES**

1. Fahy, E., S. Subramaniam, H. A. Brown, C. K. Glass, A. H. Merrill, R. C. Murphy, C. R. H. Raetz, D. W. Russell, Y. Seyama, W. Shaw, T. Shimizu, F. Spener, G. van Meer, M. S. VanNieuwenhze, S. H. White, J. L. Witztum, and E. A. Dennis. 2005. A comprehensive classification system for lipids. *J Lipid Res* **46**: 839-861.

2. Wymann, M. P., and R. Schneiter. 2008. Lipid signalling in disease. *Nat Rev Mol Cell Biol* **9**: 162-176.

3. van Meer, G., D. R. Voelker, and G. W. Feigenson. 2008. Membrane lipids: Where they are and how they behave. *Nat Rev Mol Cell Biol* **9**: 112-124.

4. Eckel, R., S. Grundy, and P. Zimmet. 2005. The metabolic syndrome - Reply. *Lancet* **366**: 1923-1923.

5. Bochkov, V. N., O. V. Oskolkova, K. G. Birukov, A.-L. Levonen, C. J. Binder, and J. Stoeckl. 2010. Generation and Biological Activities of Oxidized Phospholipids. *Antioxid Redox Signal* **12**: 1009-1059.

6. Wenk, M. R. 2010. Lipidomics: New Tools and Applications. *Cell* **143**: 888-895.

7. Hsu, F. F., and J. Turk. 2009. Electrospray ionization with low-energy collisionally activated dissociation tandem mass spectrometry of glycerophospholipids: Mechanisms of fragmentation and structural characterization. *J Chromatogr B Analyt Technol Biomed Life Sci* **877**: 2673-2695.

8. Han, X. L., and R. W. Gross. 1994. Electrospray ionization mass spectroscopic analysis of human erythrocyte plasma membrane phospholipids. *Proc Natl Acad Sci U S A* **91**: 10635-10639.

9. Bruegger, B., G. Erben, R. Sandhoff, F. T. Wieland, and W. D. Lehmann. 1997. Quantitative analysis of biological membrane lipids at the low picomole level by nano-electrospray ionization tandem mass spectrometry. *Proc Natl Acad Sci U S A* **94**: 2339-2344.

10. Han, X., K. Yang, and R. W. Gross. 2011. Multi-dimensional mass spectrometry-based shotgun lipidomics and novel strategies for lipidomic analyses. *Mass Spectrom Rev*: doi: 10.1002/mas.20342.

11. Yang, K., Z. D. Zhao, R. W. Gross, and X. L. Han. 2009. Systematic analysis of choline-containing phospholipids using multi-dimensional mass spectrometry-based shotgun lipidomics. *Chromatogr B Analyt Technol Biomed Life Sci* **877**: 2924-2936.

12. Han, X. L., J. Y. Yang, H. Cheng, H. P. Ye, and R. W. Gross. 2004. Toward fingerprinting cellular lipidomes directly from biological samples by two-dimensional electrospray ionization mass spectrometry. *Anal Biochem* **330**: 317-331.

13. Han, X. L., and R. W. Gross. 2005. Shotgun lipidomics: multidimensional MS analysis of cellular lipidomes. *Expert Rev Proteomics* **2**: 253-264.

14. Han, X. L., and R. W. Gross. 2001. Quantitative analysis and molecular species fingerprinting of triacylglyceride molecular species directly from lipid extracts of biological samples by electrospray ionization tandem mass spectrometry. *Anal Biochem* **295**: 88-100.

15. Wiesner, P., K. Leidl, A. Boettcher, G. Schmitz, and G. Liebisch. 2009. Lipid profiling of FPLC-separated lipoprotein fractions by electrospray ionization tandem mass spectrometry. *J Lipid Res* **50**: 574-585.

16. Liebisch, G., B. Lieser, J. Rahtenberg, W. Drobnik, and G. Schmitz. 2005. High-throughput quantification of phosphatidylcholine and sphingomyelin by electrospray ionization tandem mass spectrometry coupled with isotope corrections algorithim (vol 1686, pg 108, 2004). *Biochim Biophys Acta* **1734**: 86-89.

17. Liebisch, G., W. Drobnik, B. Lieser, and G. Schmitz. 2002. High-throughput quantification of lysophosphatidylcholine by electrospray ionization tandem mass spectrometry. *Clin Chem* **48**: 2217-2224.

18. Liebisch, G., W. Drobnik, M. Reil, B. Trumbach, R. Arnecke, B. Olgemoller, A. Roscher, and G. Schmitz. 1999. Quantitative measurement of different ceramide species from crude cellular extracts by electrospray ionization tandem mass spectrometry (ESI-MS/MS). *J Lipid Res* **40**: 1539-1546.

19. Liebisch, G., M. Binder, R. Schifferer, T. Langmann, B. Schulz, and G. Schmitz. 2006. High throughput quantification of cholesterol and cholesteryl ester by electrospray ionization tandem mass spectrometry (ESI-MS/MS). *Biochim Biophys Acta* **1761**: 121-128.

20. Guan, X. L., X. He, W. Y. Ong, W. K. Yeo, G. H. Shui, and M. R. Wenk. 2006. Non-targeted profiling of lipids during kainate-induced neuronal injury. *Faseb J* **20**: 1152-1161.

21. Schwudke, D., J. Oegema, L. Burton, E. Entchev, J. T. Hannich, C. S. Ejsing, T. Kurzchalia, and A. Shevchenko. 2006. Lipid profiling by multiple precursor and neutral loss scanning driven by the data-dependent acquisition. *Anal Chem* **78**: 585-595.

22. Ejsing, C. S., E. Duchoslav, J. Sampaio, K. Simons, R. Bonner, C. Thiele, K. Ekroos, and A. Shevchenko. 2006. Automated identification and quantification of glycerophospholipid molecular species by multiple precursor ion scanning. *Anal Chem* **78**: 6202-6214.

23. Ejsing, C. S., J. L. Sampaio, V. Surendranath, E. Duchoslav, K. Ekroos, R. W. Klemm, K. Simons, and A. Shevchenko. 2009. Global analysis of the yeast lipidome by quantitative shotgun mass spectrometry. *Proc Natl Acad Sci U S A* **106**: 2136-2141.

24. Kalvodova, L., J. L. Sampaio, S. Cordo, C. S. Ejsing, A. Shevchenko, and K. Simons. 2009. The Lipidomes of Vesicular Stomatitis Virus, Semliki Forest Virus, and the Host

Plasma Membrane Analyzed by Quantitative Shotgun Mass Spectrometry. *J Virol* **83**: 7996-8003.

25. Sampaio, J. L., M. J. Gerl, C. Klose, C. S. Ejsing, H. Beug, K. Simons, and A. Shevchenko. 2011. Membrane lipidome of an epithelial cell line. *Proc Natl Acad Sci U S A* **108**: 1903-1907.

26. Stahlman, M., C. S. Ejsing, K. Tarasov, J. Perman, J. Borén, and K. Ekroos. 2009. High-throughput shotgun lipidomics by quadrupole time-of-flight mass spectrometry. *J Chromatogr B Analyt Technol Biomed Life Sci* **877**: 2664-2672.

27. Schwudke, D., J. T. Hannich, V. Surendranath, V. Grimard, T. Moehring, L. Burton, T. Kurzchalia, and A. Shevchenko. 2007. Top-down lipidomic screens by multivariate analysis of high-resolution survey mass spectra. *Anal Chem* **79**: 4083-4093.

28. Schuhmann, K., R. Herzog, D. Schwudke, W. Metelmann-Strupat, S. R. Bornstein, and A. Shevchenko. 2011. Bottom-Up Shotgun Lipidomics by Higher Energy Collisional Dissociation on LTQ Orbitrap Mass Spectrometers. *Anal Chem* **83**: 5480-5487.

29. Graessler, J., D. Schwudke, P. E. H. Schwarz, R. Herzog, A. Shevchenko, and S. R. Bornstein. 2009. Top-Down Lipidomics Reveals Ether Lipid Deficiency in Blood Plasma of Hypertensive Patients. *PLoS One* **4**: 13.

30. Esch, S. W., P. Tamura, A. A. Sparks, M. R. Roth, S. P. Devaiah, E. Heinz, X. Wang, T. D. Williams, and R. Welti. 2007. Rapid characterization of the fatty acyl composition of complex lipids by collision-induced dissociation time-of-flight mass spectrometry. *J Lipid Res* **48**: 235-241.

31. Whitehouse, C. M., R. N. Dreyer, M. Yamashita, and J. B. Fenn. 1985. Electrospray Interface for Liquid Chromatographs and Mass Spectrometers. *Anal Chem* **57**: 675-679.

32. Quehenberger, O., A. M. Armando, A. H. Brown, S. B. Milne, D. S. Myers, A. H. Merrill, S. Bandyopadhyay, K. N. Jones, S. Kelly, R. L. Shaner, C. M. Sullards, E. Wang, R. C. Murphy, R. M. Barkley, T. J. Leiker, C. R. H. Raetz, Z. Q. Guan, G. M. Laird, D. A. Six, D. W. Russell, J. G. McDonald, S. Subramaniam, E. Fahy, and E. A. Dennis. 2010. Lipidomics reveals a remarkable diversity of lipids in human plasma. *J Lipid Res* **51**: 3299-3305.

33. Andreyev, A. Y., E. Fahy, Z. Q. Guan, S. Kelly, X. A. Li, J. G. McDonald, S. Milne, D. Myers, H. Park, A. Ryan, B. M. Thompson, E. Wang, Y. H. Zhao, H. A. Brown, A. H. Merrill, C. R. H. Raetz, D. W. Russell, S. Subramaniam, and E. A. Dennis. 2010. Subcellular organelle lipidomics in TLR-4-activated macrophages. *J Lipid Res* **51**: 2785-2797.

34. Shui, G., X. L. Guan, C. P. Low, G. H. Chua, J. S. Y. Goh, H. Yang, and M. R. Wenk. 2010. Toward one step analysis of cellular lipidomes using liquid chromatography

coupled with mass spectrometry: application to Saccharomyces cerevisiae and Schizosaccharomyces pombe lipidomics. *Mol Biosyst* **6**: 1008-1017.

35. Masoodi, M., M. Eiden, A. Koulman, D. Spaner, and D. A. Volmer. 2010. Comprehensive Lipidomics Analysis of Bioactive Lipids in Complex Regulatory Networks. *Anal Chem* **82**: 8176-8185.

36. Scherer, M., A. Bottcher, G. Schmitz, and G. Liebisch. 2011. Sphingolipid profiling of human plasma and FPLC-separated lipoprotein fractions by hydrophilic interaction chromatography tandem mass spectrometry. *Biochim Biophys Acta* **1811**: 68-75.

37. Merrill, A. H., T. H. Stokes, A. Momin, H. Park, B. J. Portz, S. Kelly, E. Wang, M. C. Sullards, and M. D. Wang. 2009. Sphingolipidomics: A valuable tool for understanding the roles of sphingolipids in biology and disease. *J Lipid Res* **50**: S97-S102.

38. Scherer, M., G. Schmitz, and G. Liebisch. 2010. Simultaneous Quantification of Cardiolipin, Bis(monoacylglycero)phosphate and their Precursors by Hydrophilic Interaction LC-MS/MS Including Correction of Isotopic Overlap. *Anal Chem*.

39. Retra, K., O. B. Bleijerveld, R. A. van Gesteil, A. G. M. Tielens, J. J. van Hellemond, and J. F. Brouwers. 2008. A simple and universal method for the separation and identification of phospholipid molecular species. *Rapid Commun Mass Spectrom* **22**: 1853-1862.

40. Clark, J., K. E. Anderson, V. Juvin, T. S. Smith, F. Karpe, M. J. O. Wakelam, L. R. Stephens, and P. T. Hawkins. 2011. Quantification of PtdInsP(3) molecular species in cells and tissues by mass spectrometry. *Nat Methods* **8**: 267-U120.

41. Karu, K., J. Turton, Y. Q. Wang, and W. J. Griffiths. 2011. Nano-liquid chromatography-tandem mass spectrometry analysis of oxysterols in brain: monitoring of cholesterol autoxidation. *Chem Phys Lipids* **164**: 411-424.

42. Nakanishi, H., Y. Iida, T. Shimizu, and R. Taguchi. 2009. Analysis of oxidized phosphatidylcholines as markers for oxidative stress, using multiple reaction monitoring with theoretically expanded data sets with reversed-phase liquid chromatography/tandem mass spectrometry. *J Chromatogr B Analyt Technol Biomed Life Sci* **877**: 1366-1374.

43. Pettitt, T. R., S. K. Dove, A. Lubben, S. D. J. Calaminus, and M. J. O. Wakelam. 2006. Analysis of intact phosphoinositides in biological samples. *J Lipid Res* **47**: 1588-1596.

44. Hutchins, P. M., R. M. Barkley, and R. C. Murphy. 2008. Separation of cellular nonpolar neutral lipids by normal-phase chromatography and analysis by electrospray ionization mass spectrometry. *J Lipid Res* **49**: 804-813.

45. Murphy, R. C., T. J. Leiker, and R. M. Barkley. 2011. Glycerolipid and cholesterol ester analyses in biological samples by mass spectrometry. *Biochim Biophys Acta* **1811**: 776-783.

46. Ikeda, K., Y. Oike, T. Shimizu, and R. Taguchi. 2009. Global analysis of triacylglycerols including oxidized molecular species by reverse-phase high resolution LC/ESI-QTOF MS/MS. *J Chromatogr B Analyt Technol Biomed Life Sci* **877**: 2639-2647.

47. Nygren, H., T. Seppanen-Laakso, S. Castillo, T. Hyotylainen, and M. Oresic. 2011. Liquid Chromatography-Mass Spectrometry (LC-MS)-Based Lipidomics for Studies of Body Fluids and Tissues. *In* Metabolic Profiling: Methods and Protocols. T. Metz, editor. 247-257.

48. Shui, G. H., A. K. Bendt, K. Pethe, T. Dick, and M. R. Wenk. 2007. Sensitive profiling of chemically diverse bioactive lipids. *J Lipid Res* **48**: 1976-1984.

49. Fauland, A., H. Köfeler, M. Trötzmüller, A. Knopf, J. Hartler, A. Eberl, C. Chitraju, E. Lankmayr, and F. Spener. 2011. A comprehensive method for lipid profiling by liquid chromatography-ion cyclotron resonance mass spectrometry. *J Lipid Res* **52**: 2314-2322.

50. Hu, C. X., J. van Dommelen, R. van der Heijden, G. Spijksma, T. H. Reijmers, M. Wang, E. Slee, X. Lu, G. W. Xu, J. van der Greef, and T. Hankemeier. 2008. RPLC-Ion-Trap-FTMS Method for Lipid Profiling of Plasma: Method Validation and Application to p53 Mutant Mouse Model. *J Proteome Res* **7**: 4982-4991.

51. Hein, E. M., L. M. Blank, J. Heyland, J. I. Baumbach, A. Schmid, and H. Hayen. 2009. Glycerophospholipid profiling by high-performance liquid chromatography/mass spectrometry using exact mass measurements and multi-stage mass spectrometric fragmentation experiments in parallel. *Rapid Commun Mass Spectrom* **23**: 1636-1646.

52. Ogiso, H., T. Suzuki, and R. Taguchi. 2008. Development of a reverse-phase liquid chromatography electrospray ionization mass spectrometry method for lipidomics, improving detection of phosphatidic acid and phosphatidylserine. *Anal Biochem* **375**: 124-131.

53. Taguchi, R., and M. Ishikawa. 2010. Precise and global identification of phospholipid molecular species by an Orbitrap mass spectrometer and automated search engine Lipid Search. *J Chromatogr A* **1217**: 4229-4239.

54. Sato, Y., T. Nakamura, K. Aoshima, and Y. Oda. 2010. Quantitative and Wide-Ranging Profiling of Phospholipids in Human Plasma by Two-dimensional Liquid Chromatography/Mass Spectrometry. *Anal Chem* **82**: 9858-9864.

55. Koulman, A., G. Woffendin, V. K. Narayana, H. Welchman, C. Crone, and D. A. Volmer. 2009. High-resolution extracted ion chromatography, a new tool for metabolomics and lipidomics using a second-generation orbitrap mass spectrometer. *Rapid Commun Mass Spectrom* **23**: 1411-1418.

56. Holcapek, M., H. Dvorakova, M. Lisa, A. J. Giron, P. Sandra, and J. Cvacka. 2010. Regioisomeric analysis of triacylglycerols using silver-ion liquid chromatography

atmospheric pressure chemical ionization mass spectrometry: Comparison of five different mass analyzers. *J Chromatogr A* **1217**: 8186-8194.

57. Lisa, M., E. Cifkova, and M. Holcapek. 2011. Lipidomic profiling of biological tissues using off-line two-dimensional high-performance liquid chromatography mass spectrometry. *J Chromatogr A* **1218**: 5146-5156.

58. Lee, S. H., and I. A. Blair. 2009. Targeted chiral lipidomics analysis of bioactive eicosanoid lipids in cellular systems. *BMB Rep* **42**: 401-410.

59. Brown, S. H. J., T. W. Mitchell, and S. J. Blanksby. 2009. Analysis of unsaturated lipids by ozone-induced dissociation. *Biochim Biophys Acta* **1811**: 807-817.

60. Thomas, M. C., T. W. Mitchell, D. G. Harman, J. M. Deeley, J. R. Nealon, and S. J. Blanksby. 2008. Ozone-induced dissociation: Elucidation of double bond position within mass-selected lipid ions. *Anal Chem* **80**: 303-311.

61. Ellis, S. R., C. P. Wu, J. M. Deeley, X. J. Zhu, R. J. W. Truscott, M. I. H. Panhuis, R. G. Cooks, T. W. Mitchell, and S. J. Blanksby. 2010. Imaging of Human Lens Lipids by Desorption Electrospray Ionization Mass Spectrometry. *J Am Soc Mass Spectrom* **21**: 2095-2104.

62. Fuchs, B., R. Suss, and J. Schiller. 2010. An update of MALDI-TOF mass spectrometry in lipid research. *Prog Lipid Res* **49**: 450-475.

63. Petkovic, M., J. Schiller, M. Muller, S. Benard, S. Reichl, K. Arnold, and J. Arnhold. 2001. Detection of individual phospholipids in lipid mixtures by matrix-assisted laser desorption/ionization time-of-flight mass spectrometry: Phosphatidylcholine prevents the detection of further species. *Anal Biochem* **289**: 202-216.

64. Luftmann, H., M. Aranda, and G. E. Morlock. 2007. Automated interface for hyphenation of planar chromatography with mass spectrometry. *Rapid Commun Mass Spectrom* **21**: 3772-3776.

65. Dreisewerd, K., J. Muthing, A. Rohlfing, I. Meisen, Z. Vukelic, J. Peter-Katalinic, F. Hillenkamp, and S. Berkenkamp. 2005. Analysis of gangliosides directly from thin-layer chromatography plates by infrared matrix-assisted laser desorption/ionization orthogonal time-of-flight mass spectrometry with a glycerol matrix. *Anal Chem* **77**: 4098-4107.

66. Stuebiger, G., E. Pittenauer, O. Belgacem, P. Rehulka, K. Widhalm, and G. Allmaier. 2009. Analysis of human plasma lipids and soybean lecithin by means of high-performance thin-layer chromatography and matrix-assisted laser desorption/ionization mass spectrometry. *Rapid Commun Mass Spectrom* **23**: 2711-2723.

67. Souady, J., J. Soltwisch, K. Dreisewerd, J. Haier, J. Peter-Katalinic, and J. Muething. 2009. Structural Profiling of Individual Glycosphingolipids in a Single Thin-Layer Chromatogram by Multiple Sequential Immunodetection Matched with Direct IR-MALDI-o-TOF Mass Spectrometry. *Anal Chem* **81**: 9481-9492.

68. Muesken, A., J. Souady, K. Dreisewerd, W. Zhang, U. Distler, J. Peter-Katalinic, H. Miller-Podraza, H. Karch, and J. Muething. 2010. Application of thin-layer chromatography/infrared matrix-assisted laser desorption/ionization orthogonal time-of-flight mass spectrometry to structural analysis of bacteria-binding glycosphingolipids selected by affinity detection. *Rapid Commun Mass Spectrom* **24**: 1032-1038.

69. Rohlfing, A., J. Muthing, G. Pohlentz, U. Distler, J. Peter-Katalinic, S. Berkenkamp, and K. Dreisewerd. 2007. IR-MALDI-MS analysis of HPTLC - Separated phospholipid mixtures directly from the TLC plate. *Anal Chem* **79**: 5793-5808.

70. Cheng, C. F., E. Pittenauer, and M. L. Gross. 1998. Charge-remote fragmentations are energy-dependent processes. *J Am Soc Mass Spectrom* **9**: 840-844.

71. Pittenauer, E., and G. Allmaier. 2011. A universal product ion nomenclature for M-H (-), M+H (+) and M+nNa-(n-1)H (+) (n=1-3) glycerophospholipid precursor ions based on high-energy CID by MALDI-TOF/RTOF mass spectrometry. *Int J Mass Spectrom* **301**: 90-101.

72. Pittenauer, E., and G. Allmaier. 2009. The Renaissance of High-Energy CID for Structural Elucidation of Complex Lipids: MALDI-TOF/RTOF-MS of Alkali Cationized Triacylglycerols. *J Am Soc Mass Spectrom* **20**: 1037-1047.

73. Herzog, R., D. Schwudke, K. Schuhmann, J. L. Sampaio, S. R. Bornstein, M. Schroeder, and A. Shevchenko. 2011. A novel informatics concept for high-throughput shotgun lipidomics based on the molecular fragmentation query language. *Genome Biol* **12**.

74. Pluskal, T., S. Castillo, A. Villar-Briones, and M. Oresic. 2010. MZmine 2: Modular framework for processing, visualizing, and analyzing mass spectrometry-based molecular profile data. *BMC Bioinformatics* **11**.

75. Katajamaa, M., J. Miettinen, and M. Oresic. 2006. MZmine: toolbox for processing and visualization of mass spectrometry based molecular profile data. *Bioinformatics* **22**: 634-636.

76. Pietilainen, K. H., M. Sysi-Aho, A. Rissanen, T. Seppanen-Laakso, H. Yki-Jarvinen, J. Kaprio, and M. Oresic. 2007. Acquired Obesity Is Associated with Changes in the Serum Lipidomic Profile Independent of Genetic Effects - A Monozygotic Twin Study. *Plos One* **2**: 14.

77. Hartler, J., M. Trötzmüller, C. Chitraju, F. Spener, H. C. Köfeler, and G. G. Thallinger. 2011. Lipid Data Analyzer: Unattended Identification and Quantitation of Lipids in LC-MS Data. *Bioinformatics* **27**: 572-577.

## C.3. An improved SPE method for fractionation and identification of phospholipids

Alexander Fauland[1], Martin Trötzmüller[2, *], Anita Eberl[2], Somaieh Afiuni-Zadeh[3], Harald Köfeler[2], Xinghua Guo[1] and Ernst Lankmayr[1]

[1] Institute of Analytical Chemistry and Food Chemistry, Graz University of Technology, Graz, Austria

[2] Core Facility for Mass Spectrometry, Center for Medical Research, Medical University of Graz, Graz, Austria

[3] Department of Biochemistry, Molecular Biology and Biophysics, University of Minnesota, Minneapolis, USA

**Abbreviations:** CL: cardiolipin, CV: coefficient of variation, DDA: data dependent acquisition, LPC: lysophosphatidylcholine, LTQ-FT: hybrid linear ion trap - Fourier transform ion cyclotron resonance mass spectrometer, MRM: multiple reaction monitoring, PA: phosphatidic acid, PC: phosphatidylcholine, PE: phosphatidylethanolamine, PG: phosphatidylglycerol, PI: phosphatidylinositol, PS: phosphatidylserine, Q-Trap: quadrupole linear ion trap mass spectrometer, SM: sphingomyelin,

Shorthand notation of lipid species: Abbreviation for lipid class is followed by number of acyl carbons: number of double bounds.

**ABSTRACT**

This work reports about a rapid and universal SPE method developed for separation and identification of phospholipids derived from complex biological samples. For the separation step, sequential combination of silica gel - aminopropyl - silica gel SPE cartridges are applied. This setup enables separation of phosphatidylcholine (PC), lysophosphatidylcholine (LPC), phosphatidylethanolamine (PE), phosphatidylglycerol (PG), phosphatidic acid (PA), phosphatidylinositol (PI), phosphatidylserine (PS), cardiolipin (CL) and sphingomyelin (SM) into four fractions according to the polarity of their headgroups. Sample acquisition of the SPE fractions is performed by a high mass resolution LC-MS system consisting of a hybrid linear ion trap - Fourier transform ion cyclotron resonance mass spectrometer (LTQ-FT) coupled to RP-HPLC. The unequivocal advantage of this SPE sample preparation setup is avoidance of analyte signal overlapping in the hyphenation step with RP-HPLC and MS. Overlapping phospholipid signals would otherwise exert adverse ion suppression effects. An additional benefit of this method is the elimination of polar and non polar (e.g. neutral lipids) contaminants from the phospholipid fractions, which highly reduces contamination of the LC-MS system. The method was validated with fermentation samples of organic waste, where 78 distinct phospholipid and sphingomyelin species belonging to six lipid classes were successfully identified.

## INTRODUCTION

Phospholipids are complex lipids and play an important role in fundamental biological functions (1). They are present in all organisms, represent the major components of all cellular membranes and have important structural and biological properties. Phospholipid bilayers in cellular membranes provide a platform for proteins which are involved in cell signaling and intercellular adhesion for example (2, 3).

Besides various other techniques in lipid analysis (4, 5), mass spectrometry has emerged as an indispensable tool for characterization, identification and quantitation of lipids (5-7), often coupled to ESI as the ionization technique of choice (8-11). In addition, a variety of different chromatographic separation techniques has been developed to achieve better mass spectrometric detection sensitivity (4, 12). Thus, liquid chromatography coupled to mass spectrometry (LC-ESI/MS) based methods have emerged in the past decade (13-19). This setup provides the ability to alleviate ion suppression effects in electrospray and allows also detection of less abundant lipids (20, 21).

A practical aspect often neglected in LC-MS of lipids is the contamination often deposited in expensive analytical equipment by acquisition of total lipid extracts. SPE is a solution to this problem by pre-separating analytes from the bulk of contaminations and other lipid classes not of interest in the particular sample (4). The second important aspect of an efficient pre-separation is a better detection limit for certain minor lipid classes which would otherwise be suppressed by lipid classes with higher abundance co-eluting at the same retention time in LC-MS. Particularly PC shows high ionization efficiency in positive ESI mode and tends to suppress the ionization of other analytes (20). Generally, separation and isolation of phospholipids from other lipids like di- and triglycerides and free fatty acids is performed on aminopropyl cartridges (22-26) or silicagel phases (27). SPE on aminopropyl cartridges or on a combination of silica gel and aminopropyl-bonded phases allows also the separation of different phospholipids (28-31). Furthermore, coupling of a SPE separation to an LTQ Orbitrap mass spectrometer was applied for identifying different phospholipid species (21).

In the following study we describe an efficient and flexible SPE sample preparation method developed for simultaneous separation of different phospholipid classes, which is applicable on various biological samples. The separated analytes are detected by an LC-MS approach based on RP chromatography coupled to a high resolution LTQ-FT instrument (32). The developed SPE method was tested with fermentation samples of organic waste, since such highly complex samples are rich in phospholipid species with odd and even fatty acyl carbon numbers. The lack of sufficient sample preparation and chromatographic separation would result in increased occurrence of overlapping isobaric phospholipid species having the same exact mass. Such mass overlapping would extendedly complicate analyte determination by

MS (33). Hence, our developed SPE method in combination with the LC-MS approach allows separation of phospholipids into their classes and prevents mass overlapping and ion suppression effects.

## MATERIALS AND METHODS

### Chemicals and Lipid Standards

An aqueous fermentation sample of organic waste was used as sample for experiments. Therefore, homogenized and sanitized leftovers were used as substrate and seeding sludge as inoculum, both obtained form a biogas plant (Ökopark Hartberg, Styria, Austria). Detailed description of the fermentation process is published elsewhere (34).

### Lipid standards:

L-α-phosphatidylinositols (soy) (sodium salt), 1-palmitoyl-2-oleoyl-*sn*-glycero-3-[phospho-*rac*-(1-glycerol)] (sodium salt) (PG 16:0/18:1), 1-palmitoyl-2-oleyl-*sn*-glycero-3-phosphate (monosodium salt) (PA 16:0/18:1), sphingomyelines (chicken egg), 1,1,2,2-tetramyristol cardiolipin (ammonium salt) (CL (14:0/14:0)(14:0/14:0)) were supplied by Avanti Polar Lipids (Alabaster, AL, USA). 1,2-dipalmitoyl-*sn*-glycero-3-phospho-L-serine (sodium salt) (PS 16:0/16:0) and 1,2-Dioleoyl-*sn*-glycero-3-phosphoethanolamine (synthetic, approx. 99%,) PE (18:1/18:1) were purchased from Sigma Aldrich (Steinheim, Germany). 1-myristoyl-*sn*-glycero-3-phosphocholine (LPC 14:0) and 1,2-diarachidoyl-*sn*-glycero-3-phosphocholine (PC 20:0/20:0) were provided by the institute of biochemistry, TU Graz (Graz, Austria). Lipid standards were dissolved in chloroform/methanol (2:1, v/v) at a concentration of 1 mM and stored at -18°C.

HPLC gradient grade methanol, acetonitrile, pestilyse acetone, cyclohexane and dichloromethane (Rotisolv) were supplied by Carl Roth (Karlsruhe, Germany). Ammonia solution (25 %) p.a., diethyl ether p.a. and petroleum ether were purchased from Merck KGaA (Darmstadt, Germany). Ammonium acetate puriss. p.a. for HPLC, ammonium formate puriss. p.a. for HPLC and 2-propanol LC-MS grade were supplied by Fluka (Steinheim, Germany). Molybdenum blue was supplied by Sigma-Aldrich Chemie GmbH (Steinheim, Germany). Nitrogen (purity 5.0) was obtained from Air Liquide (Graz, Austria). Ultra pure water purified by Milli-Q Gradient system (Millipore, Bedford, USA) was used for all experiments (resistivity > 18MΩcm).

### Sample preparation

The fermentation sample was homogenized with an Ultra Turrax (Ultra Turrax T25, Janke & Kunkel IKA Labortechnik Staufen, Germany). 10 mL of homogenized sample was extracted two times, starting with a mixed solution of 100 mL chloroform/methanol (3:1, v/v) followed by 100 mL chloroform/methanol (6:1, v/v). After extraction, the organic layer was filtrated using a teflon filter and centrifuged at 1360 g at room temperature for 10 min. The remaining aqueous layer was removed and the organic phase was concentrated to about 1 mL by

means of a rotary evaporator without heating the water bath. The rest of the organic solvent was removed by a gentle stream of nitrogen and dissolved again in 1 mL chloroform/methanol (3:1, v/v). For recovery experiments, 10 mL of homogenized sample were spiked with the prepared stock standard solutions of nine different phospholipids (listed in Materials and Methods) prior to lipid extraction. The amount of added lipid standards equates to the final concentration 5 µM dissolved in 200 µL chloroform/methanol (2:1, v/v) before measurement. Sample preparation was performed as described above.

**Pre-cleaning step for high concentrated polar compounds**

For sample pre-cleaning, a 500 mg/6 mL silica cartridge was preconditioned with 15 mL chloroform and the fermentation sample extract (1 mL) was loaded on the cartridge and washed with 15 mL chloroform. Consecutively, the column was eluted with 15 mL chloroform/methanol (3:1; v/v) and 5 mL methanol. The eluate was concentrated by means of a rotary evaporator to 1 mL and the remaining solvent was completely volatilized under nitrogen. The dried sample was redissolved in 1 mL cyclohexane/chloroform/methanol (95:3:2, v/v). For separation, the sample was allowed to adsorb to the sorbent by percolation through the cartridge by gravity.

**SPE fractionation procedure**

The SPE fractionation procedure illustrated in Figure 1 is based on the use of one SPE aminopropyl-bonded silica gel cartridge ($NH_2$-cartridge; 200 mg/3 mL) purchased from Phenomenex (California, USA) and two SPE silica gel cartridges (SI-cartridge; 200 mg/3 mL) provided by GracePure (Ontario, Canada).
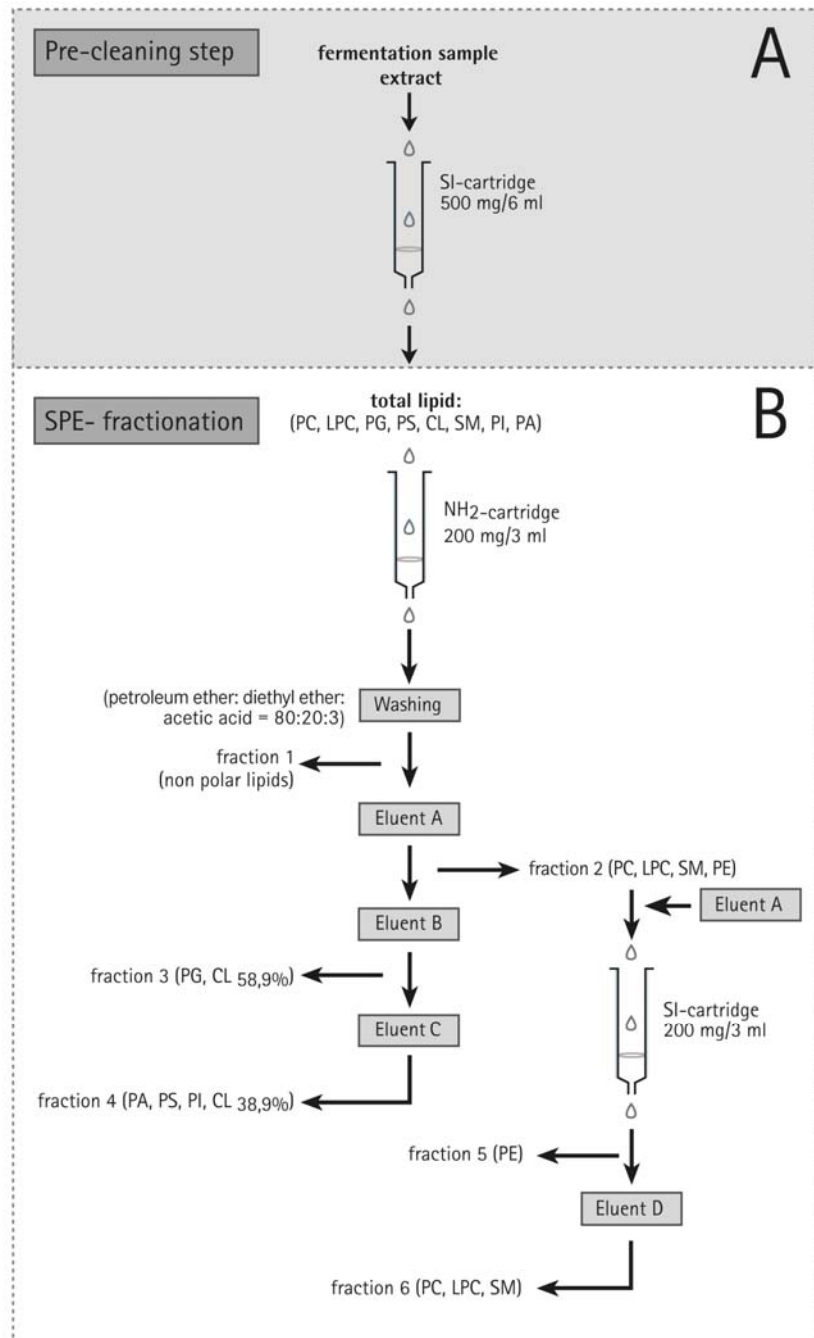
**Figure 1.** Elution scheme of the SPE procedure. (**A**) A single pre-cleaning step for highly concentrated polar compounds is accomplished with a silica cartridge. (**B**) The separation of the phospholipids is carried out on an aminopropyl-bonded silica gel cartridge ($NH_2$) in combination with a silica gel cartridge (SI). After the pre-cleaning step the concentrated lipid extract is first applied on the $NH_2$ cartridge. The washing step is used to remove non polar lipids. The following elution with Eluent A results in fraction 2, containing PC, LPC, SM and PE. Fraction 2 is further applied on an SI cartridge to separate PE (fraction 5) form choline containing phospholipids (fraction 6). The remaining anionic phospholipids PG, CL PA, PS and PI are separated on the $NH_2$ cartridge in two different fractions, fraction 3 and 4.

<u>NH$_2$-cartridge:</u>

Prior to loading the eluat from the pre-cleaning step, the NH$_2$-cartridge was preconditioned with a mixture of 15 mL cyclohexane/chloroform/methanol (95:3:2; v/v). Then the column was further washed with 30 mL petroleum ether/diethyl ether/acetic acid (80:20:3; v/v) and the eluate, containing undesirable components like non polar lipids such as di- and triglycerides, waxes and cholesterol esters, was collected as fraction 1. Subsequently, the cartridge was eluted with 10 mL of eluent A (chloroform/methanol 2:1 (v/v)) resulting in fraction 2 (PC, LPC, SM, PE) and further eluted with the solvent system of eluent B, consisting of eluent B1 (chloroform/methanol/28% ammonium hydroxide 4:1:0.1 (v/v)) and B2 (chloroform/methanol/0.05 M ammonium acetate 4:1 (v/v)). To this end the cartridge was first eluted with 20 mL of eluent B1 followed by 4 mL of eluent B2, thereby collecting fraction 3 (PG, CL$_{58.9\%}$). Eventually, the cartridge was eluted with 7 mL of eluent C (chloroform/methanol/0.02 M ammonium acetate 4:1 (v/v)) resulting in fraction 4 (PA, PS, PI, CL$_{38.9\%}$,).

<u>Silica gel (SI)-cartridge :</u>

The silica gel phase was preconditioned with 6 mL chloroform. Then, fraction 2 was directly applied to the silica gel phase without a concentration step and additionally eluted with 3 mL eluent A to obtain fraction 5 (PE). Subsequent elution with 15 mL of eluent D (methanol) resulted in fraction 6 (PC, LPC, SM).

After fractionation, all eluates were evaporated to 1 mL volume by a rotary evaporator and further concentrated by a gentle stream of nitrogen to complete dryness and all fractions except fraction 4 were taken up in 200 µL of chloroform/methanol (2:1; v/v). The high amount of ammonium acetate in fraction 4, which is insoluble in the organic solvent mixture, required an additional re-extraction step with deionised water. To this end, 600 µL of each chloroform/methanol (2:1; v/v) and deionised water were added to fraction 4. The solution was shaken for 5 min and phase separation was induced. The upper aqueous phase was removed and the organic layer was evaporated with nitrogen to complete dryness and resuspended in 200 µL of chloroform/methanol (2:1; v/v). Finally all solutions were shaken carefully on a vortex for about 1 min to completely dissolve the analytes; samples were then transferred into vials and stored at -18°C before measurement.

**High Performance Liquid Chromatography / QTrap Mass Spectrometric Analysis**

SPE fractionation performance control of spiked fermentation samples with reference phospholipids was carried out on an Agilent Series 1100 LC system (Waldbronn, Germany) coupled to a hybrid triple quadrupole linear ion trap mass spectrometer (API 4000 QTrap, AB

Sciex, Concord, Canada). The QTrap is equipped with a Turbo V source ion spray and operated in negative ESI mode. Multiple reaction monitoring (MRM) was used with the optimized parameters displayed in supplementary Table 1S. The spray voltage was set to -4.5 kV, the curtain gas to 12 arbitrary units, ion source gas 1 to 50 and ion source gas 2 to 60 arbitrary units, collision gas pressure to medium and the ion source heater was set to 600°C. Chromatography was performed on a RP column (RP-C8, Hypersil GOLD C8, 5 µm, 150 x 2.1 mm, Thermo Fisher Scientific, Germany) by a binary gradient consisting of mobile phase A (1.2 mM ammonium acetate in methanol) and mobile phase B (1.2 mM ammonium acetate in aqueous solution). After 2min of equilibration at 15% A, the binary gradient started from 15% to 90% A in 2 min and remained at this composition for 6 min, then was further raised up to 93% A in 6 min and to 96% A in another 9 min where it remained for the following 10 min. Finally the gradient was decreased to 15% A within 2 min. allowing 4 min re-equalibration time at this composition. The LC flow rate was set to 650µL/min, the oven temperature to 50°C and the tray temperature to 5°C. The injection volume was 5 µL.

**Ultra High Performance Liquid Chromatography / LTQ-FT Mass Spectrometric Analysis**

Lipid identification after SPE fractionation was carried out on a UHPLC coupled to a LTQ-FT system (32).The Accela UHPLC system was equipped with a RP-C18 column (RP-C18; 100 x 1 mm i.d., 1.9 µm particle size), both from Thermo Fisher Scientific, San Jose, CA, USA. Aqueous mobile phase A was 10 mM ammonium acetate containing 0.1% formic acid. Mobile phase B was acetonitrile/2-propanol 5:2 (v/v) containing 10 mM ammonium acetate and 0.1% formic acid. The binary gradient started with 35% to 70% B in 4 min, then was further raised up to 100% B in another 16 min and held for 10 min. The flow rate was 250 µL/min, the oven temperature was 50°C and tray temperature 10°C. For analysis 5 µL extract were injected. After each run the column was flushed 5 min with 35% B before the next run was started.

A 7.0 Tesla hybrid linear ion trap Fourier transform ion cyclotron resonance mass spectrometer (LTQ-FT, Thermo Fisher Scientific, Bremen, Germany) equipped with an ESI source was used. The instrument was operated in preview mode for parallel MS/MS spectra in the linear ion trap, while running the ion cyclotron in full scan mode at 200,000 resolution (m/z 400) from m/z 400 to 1050 in positive and from m/z 350 to1050 in negative ESI mode. Helium was used as damping gas for linear ion trap collision-induced dissociation spectra. From the LTQ-FT preview scan the 4 most abundant ions were selected in data dependent acquisition, fragmented in the linear ion trap analyzer and ejected at nominal mass resolution. The following parameters were used for positive and negative ESI-MS/MS experiments: Normalized collision energy was 35%, the repeat count was 2 and the

exclusion duration 60 s. The activation Q was at 0.2 and the isolation width 2. For positive ESI spray the voltage was set to 5 kV and the tube lens offset was at 120 V. For negative ESI spray the voltage was - 4.8 kV and the tube lens offset was - 87 V. The sheath gas flow was set to 50 arbitrary units, auxiliary gas flow to 20 arbitrary units, sweep gas flow to 2 arbitrary units and the capillary temperature to 250°C.

**Data Analysis**

Identification of lipids was performed by Lipid Data Analyzer, a platform independent Java application (32, 33). Briefly, the algorithm identifies peaks in the three dimensional LC-MS data space (retention time, m/z and intensity). It determines the peak borders in m/z as well as in time dimension, and integrates the intensities within the borders. Furthermore, the algorithm uses a theoretically calculated isotopic intensity distribution as peak selection criterion in order to improve the specificity.

**RESULTS**

**SPE fractionation procedure for phospholipid identification**

Comprehensive profiling of lipid species is only possible with highly sophisticated instrumentations as we have shown previously (32). Since such instruments are very sensitive and easily contaminated, development of suitable sample preparation techniques is highly important.

There are particular challenges in the determination of different phospholipid species in biological samples with LC-MS, especially when interfering components have overlapping retention times. Often encountered complications are overlapping masses and ion suppression effects which results in lower specificity and sensitivity. This phenomenon requires an appropriate separation technique prior to LC-MS determination. Our SPE approach allows separation of phospholipid classes into 4 fractions and additionally includes a washing step for removing undesirable non polar components. Prior to SPE fractionation the sample is initially cleaned from highly polar and ionic contaminations by a silica cartridge. This cartridge retains all these compounds while the total lipids are eluted with a suitable solvent and collected for SPE fractionation. Fraction 1 represents also a washing step, where no phospholipids have been found (Table 1). Washing steps are of particular importance with crude fermentation samples containing all kinds of contaminants. The principle of SPE-based separation of analytes is their polarity, which enables separation of neutral and ionic phospholipids (Figure 1). The aim of this optimized SPE method was the pre-separation of those phospholipid classes which would not have been separated sufficiently with an RP-LC-MS approach. Especially phosphatidylcholine, usually highly abundant in biological membranes, tends to suppress ionization of co-eluting compounds due to its superior ionization efficiency in positive ESI (32). Therefore, our proposed SPE pre-fractionation should be beneficial for more sensitive determination of all lipids co-eluting with PC species in RP chromatography. In fraction 2, the neutral and cationic phospholipids PC, LPC, SM and PE are completely separated from the acidic phospholipids using the $NH_2$ cartridge with eluent A. Subsequently, eluent A is applied for successful separation of PE from the SI-cartridge (fraction 5), whereas PC, LPC and SM are retained on the cartridge due to their cationic phosphocholine headgroup. Following that, an increase in polarity of eluent D enables the elution of PC, LPC and SM in one single fraction, fraction 6. Nevertheless, some insignificant traces of PE were detected in fraction 6. In preliminary tests, the increase of the elution volume of eluent A from 3 mL to 5 mL resulted in a mixed fraction, where considerable amounts of PC, LPC and SM were detected in fraction 5 which should be avoided. As shown in Figure 1, PG and CL (58.9 %, see also Table 1) elute in fraction 3 and acidic phospholipid classes like PA, PS and PI are mainly found in fraction 4. These latter steps are accomplished by increasing the salt concentration first to 0.05 M ammonium

acetate which results in elution of PG and CL (58.9%, seeTable 1), and then to 0.2 M ammonium acetate for elution of PA, PS, PI and CL (38.9%, see Table 1) . As part of the SPE method optimization, a rapid and selective one dimensional thin layer chromatography detection method with reference phospholipids has been used (35, 36). This time-saving method enabled a simple check of fractions for phospholipids in the process of method development.

**Table 1.** Recovery [%] of the spiked reference phospholipids in the aqueous fermentation samples of waste. Data were acquired in MRM mode on a 4000QTrap system coupled to HPLC.

| Phospholipid species | Fraction 1 [%] | Fraction 3 [%] | Fraction 4 [%] | Fraction 5 [%] | Fraction 6 [%] |
|---|---|---|---|---|---|
| PG 18:1/16:0 | <1 | **92.9** | 5.5 | <1 | <1 |
| PA 16:0/18:1 | n.d. | n.d. | **92.5** | 7.5 | n.d. |
| CL 14:0 | <1 | **58.9** | **38.9** | 1.2 | <1 |
| PI 18:2/16:0 | n.d. | n.d. | **99.3** | n.d. | <1 |
| PE 18:1/18:1 | n.d. | <1 | <1 | **96.6** | 1.6 |
| PS 16:0/16:0 | n.d. | n.d. | **98** | n.d. | 2 |
| PC 20:0/20:0 | n.d. | 1 | n.d. | n.d. | **99** |
| LPC 14:0 | n.d. | 1.4 | 1.4 | n.d. | **97.2** |
| SM d18:1/16:0 | n.d. | 2.1 | n.d. | n.d. | **97.9** |

**SPE performance control with spiked fermentation sample**

The performance of the SPE method was tested with a fermentation sample spiked with 9 reference phospholipids. Lipids were extracted with chloroform/methanol to enrich them in the organic phase and SPE fractions were collected according to the procedure elaborated above. Following that, the sample was analyzed with HPLC coupled to a 4000 QTrap mass spectrometer in MRM mode. Detailed MRM settings are described in supplementary Table 1S. The results in Table 1 depict the data obtained from this experiment. Detailed recoveries given in % of spiked reference phospholipids in each single fraction are shown in Table 1. Most importantly the spiked PC, LPC and SM species are to be found in one fraction clearly separated from all other phospholipid classes. Also the other spiked phospholipid species show very good correlation with the expected elution pattern, which proves the applicability of the method in real analytical matrix samples.

**SPE method application and phospholipid identification in fermentation samples**

The application of SPE fractionation was done by acquisition of non-spiked fermentation samples. To that end the actual phospholipid composition in the fermentation samples subjected to the SPE procedure is verified by a high resolution LTQ-FT coupled to an Accela UHPLC as described in Materials and Methods. Ultra-high mass resolution and sub ppm mass accuracy ($\leq$ 3 ppm) of the LTQ-FT enables identification by determination of elemental composition. Additionally, MS/MS spectra acquired in data dependent acquisition provide valuable structural information for identification of molecular lipid species (32).

Figure 2 exemplifies the data obtained by the LTQ-FT. Figure 2A illustrates a negative ESI high resolution LTQ-FT spectra containing [M-H]$^-$ ions of PA 34:0 (m/z 675.49815), PA 34:1 (m/z 673.48245), PA 34:2 (m/z 671.46626) and PA 34:3 (m/z 699.45058). The negative ESI unit resolution MS/MS spectrum of PA 34:2 in Figure 2B represents carboxylate anions at m/z 255,4 [$R_1$COO]$^-$ and 279,4 [$R_2$COO]$^-$ which correspond to FA 16:0 and FA 18:2, respectively. The neutral loss of fatty acids from the deprotonated molecular ion [M-H]$^-$ is reflected by fragment ions m/z 391,4 [M-H-$R_2$COOH]$^-$ and m/z 415,4 [M-H-$R_1$COOH]$^-$. Fragment ions at m/z 409,4 [M-H-$R_2$CH=C=O]$^-$ and m/z 433,4 [M-H-$R_1$CH=C=O]$^-$ correspond to ketene loss of fatty acids (6). The ion at m/z 153.0 [$CH_2C(OH)CH_2HPO_4$]$^-$ is characteristic for glycerophospholipids, and particularly so for PA. Detailed MS and MS/MS spectra interpretation for all detected phospholipid classes is exemplified in Figures 1S-5S (supplementary data).
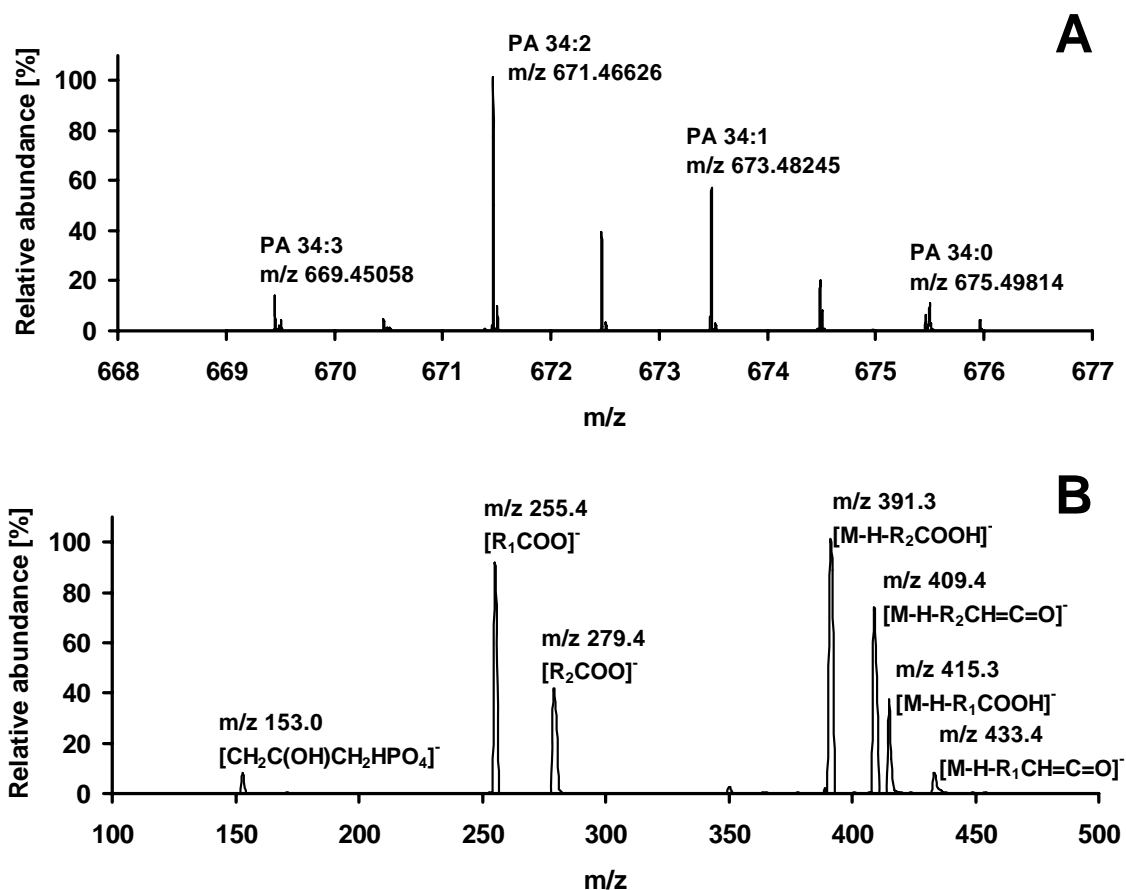
**Figure 2.** Identification and structural elucidation of PA (representative fermentation sample) in negative ESI mode. (**A**) MS data from PA 34:0, PA 34:1, PA 34:2 and PA 34:3 of an LTQ-FT high resolution full scan. Data were generated with the RP-HPLC/LTQ-FT system. (**B**) Low resolution LTQ-MS/MS spectrum of m/z 671.5 (PA 34:2) indicating the following fragment ions and neutral losses: m/z 255.4 corresponds to the carboxylate anion of the fatty acid 16:0; m/z 279.4 corresponds to the carboxylate anion of the fatty acid 18:2; m/z 153.0 corresponds to the lipid class characteristic low mass ion $[CH_2C(OH)CH_2HPO_4]^-$; m/z 391.4 corresponds to NL of fatty acid 18:2; m/z 415.4 corresponds to NL of fatty acid 16:0; m/z 409.4 corresponds to NL of the fatty acid 18:2 as ketene; m/z 433.4 corresponds to the NL of the fatty acid 16:0 as ketene.

**Precision and concentration range for phospholipid identification**

An example for the high reproducibility of the method is shown in Figure 3 for PG. Relative precision was determined for three replicas (n=3). Representative for identified phospholipids the coefficient of variation for PG ranges from 5 to 19%. Generally, these results show a good reproducibility of the SPE fractionation method. An approximate evaluation of the concentration range of some identified phospholipids in the fermentation sample was performed by comparison of peak intensity between reference phospholipids and detected analytes. Thus, concentrations range for PA from 0.4 to 56 nmol/resuspended sample, for PI

from 0.1 to 1.6 nmol/resuspended sample, for PC from 40 to 80 pmol/resuspended sample and for PE from 0.2 to 8.2 nmol/resuspended sample.
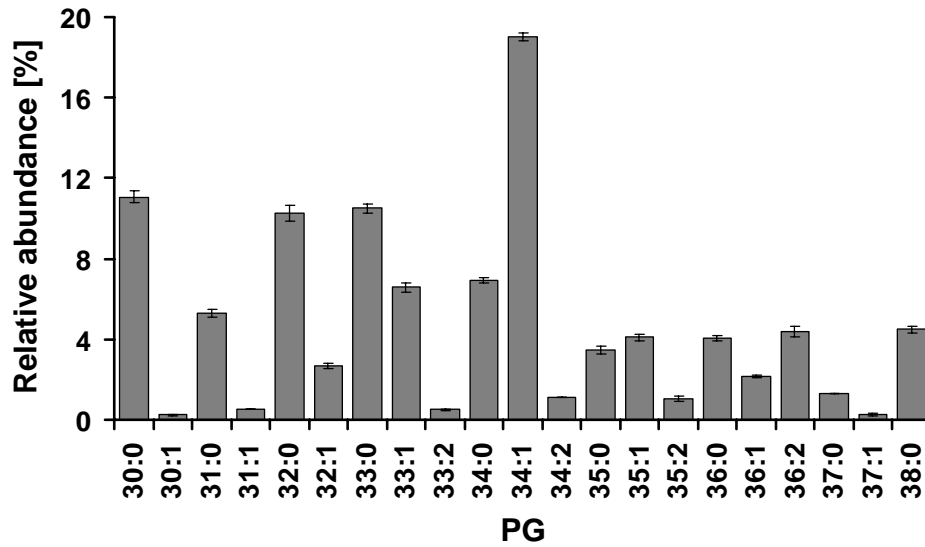


**Figure 3.** Figure illustrates detected PG species relatively to the total PG amount. Calculation of relative precision is done for PG. Lipid species are determined by RP-HPLC/LTQ-FT and values are automatically calculated by LDA (n=3).

## DISCUSSION

The SPE fractionation procedure allows a simultaneous separation of different classes of phospholipids using a combination of silica gel and aminopropyl bonded phase cartridges. This simplifies the identification of individual phospholipids by mass spectrometry in our complex fermentation samples but also other biological samples. In specific cases SPE pre-separation is able to separate isobaric phospholipid species with the same elemental composition like PC 32:1 and PE 35:1 ($C_{40}H_{78}O_8N_1P_1$) which may suffer from overlapping retention times during RP separation. Especially in samples enriched with phospholipids of bacterial origin containing odd carbon numbered fatty acids, the resulting overlap of the elemental composition of PE and PC species becomes an issue.

The combination of our SPE fractionation with HPLC-LTQ-FT offers improved separation of co-eluting compounds which leads to a minimization of ion suppression in ESI. SPE allows separation of phospholipids according to their polar headgroups which results in separation of phospholipid classes. This is an important aspect, particularly as the subsequent RP chromatography separates phospholipids due to their non polar fatty acyl chains. Therefore the proposed SPE fractionation has a complementary selectivity to RP chromatography and is able to pre-separate phospholipid classes which would otherwise overlap and elute in the same retention time range. This finally results in higher sensitivity and a higher dynamic range of individual phospholipid species, which is especially helpful for identification of low abundant compounds.

The summary in Table 2 represents the identified phospholipids in the fermentation sample. In total, 22 PA species, 10 PI species, 21 PG species, 6 PC species, 10 SM species and 9 PE species were identified. LPC, LPE, CL and PS were not detected in the fermentation sample. At least 26 species have odd carbon numbered fatty acids due to their odd total side chain carbons number. This indicates apparently the bacterial origin of the phospholipids, because only trace concentrations of odd carbon numbered fatty acids are to be found in mammalian cell systems. Another strong indication for the bacterial origin is the dominating role of PA and PG in the phospholipid distribution, whereas PC is rather a minor class. This is in strong contrast to the phospholipid pattern usually found in mammalian cells (32).

**CONCLUSION**

In conclusion, this study describes an efficient and rapid SPE sample preparation method for separation of 8 phospholipid classes and sphingomyelin into defined fractions by use of aminopropyl and silica gel based cartridges. The method was validated with fermentation samples of organic waste for biogas production. This SPE method offers several advantages: a) reduction of polar and non polar contaminations in expensive and sensitive LC-MS equipment b) enhanced sensitivity for individual phospholipid classes c) separation of overlapping isobaric phospholipid species with identical elemental composition. Together with RP-HPLC coupled to high resolution mass spectrometry, this method offers high identification certainty, selectivity and sensitivity for lipidomic analysis of complex biological samples.

**Table 2.** Lipid classes identified in the fermentation sample of organic waste. The lipid classes are measured either in positive or negative ESI mode. ++ > 5% of the analytes are found in the fractions, + < 5% of the analytes are found in the fractions, - < 1% of the analytes are found in the fractions, n = 3. Percentage expresses the amount of a detected lipid species relatively to the total amount per each single lipid class in the fermentation sample.

| Lipid class | Molecular species | m/z [M+H]$^+$ | m/z [M-H]$^-$ | Fractions | | | | |
|---|---|---|---|---|---|---|---|---|
| | | | | 1 | 3 | 4 | 5 | 6 |
| PA | 29:0 | | 605.41981 | - | - | **++** | - | - |
| | 30:0 | | 619.43524 | - | - | **++** | - | - |
| | 30:1 | | 617.41988 | - | - | **++** | - | - |
| | 31:0 | | 633.45095 | - | - | **++** | - | - |
| | 31:1 | | 631.43525 | - | - | **++** | - | - |
| | 32:0 | | 647.46694 | - | - | **++** | - | - |
| | 32:1 | | 645.45105 | - | - | **++** | - | - |
| | 32:2 | | 643.43524 | - | - | **++** | - | - |
| | 33:0 | | 661.48272 | - | - | **++** | - | - |
| | 33:1 | | 659.46701 | - | - | **++** | - | - |
| | 33:2 | | 657.45157 | - | - | **++** | - | - |
| | 34:0 | | 675.49181 | - | - | **++** | - | - |
| | 34:1 | | 673.48246 | - | - | **++** | - | - |
| | 34:2 | | 671.46626 | - | - | **++** | - | - |
| | 34:3 | | 699.45059 | - | - | **++** | - | - |
| | 34:4 | | 667.42858 | - | - | **++** | - | - |
| | 36:1 | | 701.51351 | - | - | **++** | - | - |
| | 36:2 | | 699.49800 | - | - | **++** | - | - |
| | 36:3 | | 697.48203 | - | - | **++** | - | - |
| | 36:4 | | 695.46611 | - | - | **++** | - | - |

| | | | | | | | | |
|---|---|---|---|---|---|---|---|---|
| | 36:5 | | 693.45071 | - | - | ++ | - | - |
| | 36:6 | | 691.43563 | - | - | ++ | - | - |
| **PC** | 34:1 | 760.58397 | | - | - | - | - | ++ |
| | 34:2 | 758.57001 | | - | - | - | - | ++ |
| | 36:1 | 788.61562 | | - | - | - | - | ++ |
| | 36:2 | 786.60148 | | - | - | - | - | ++ |
| | 36:3 | 784.58576 | | - | - | - | - | ++ |
| | 36:4 | 782.56979 | | - | - | - | - | ++ |
| **PE** | 31:0 | 678.50723 | | - | - | - | ++ | - |
| | 32:0 | 692.52274 | | - | - | - | ++ | + |
| | 32:1 | 690.50712 | | - | - | - | ++ | - |
| | 33:0 | 706.53839 | | - | - | - | ++ | - |
| | 33:1 | 704.52274 | | - | - | - | ++ | - |
| | 34:0 | 720.55407 | | - | - | - | ++ | - |
| | 34:1 | 718.53833 | | - | - | - | ++ | - |
| | 35:1 | 732.55331 | | - | - | - | ++ | - |
| | 36:2 | 744.55406 | | - | - | - | ++ | - |
| **SM** | 16:0 | 703.57541 | | - | - | - | - | ++ |
| | 18:0 | 731.60671 | | - | - | - | - | ++ |
| | 20:0 | 759.63819 | | - | - | - | - | ++ |
| | 21:0 | 773.65369 | | - | - | - | - | ++ |
| | 22:0 | 787.66946 | | - | - | - | - | ++ |
| | 23:0 | 801.68505 | | - | - | - | - | ++ |
| | 23:1 | 799.66905 | | - | - | - | - | ++ |
| | 24:0 | 815.70114 | | - | - | - | - | ++ |
| | 24:1 | 813.68504 | | - | - | - | - | ++ |
| | 24:2 | 811.66964 | | - | - | - | - | ++ |
| **PI** | 31:0 | | 795.50501 | - | - | ++ | - | - |
| | 33:0 | | 823.53606 | - | - | ++ | - | - |
| | 34:0 | | 837.55125 | - | - | ++ | - | - |
| | 34:1 | | 835.53592 | - | - | ++ | - | - |
| | 34:2 | | 833.52019 | - | - | ++ | - | - |
| | 34:3 | | 831.50604 | - | - | ++ | - | - |
| | 35:0 | | 851.56706 | - | - | ++ | - | - |
| | 35:1 | | 849.55212 | - | - | ++ | - | - |
| | 36:1 | | 863.56779 | - | - | ++ | - | - |
| | 36:2 | | 861.55044 | - | - | ++ | - | - |
| **PG** | 30:0 | | 693.47206 | - | ++ | + | - | - |

| | | | | | | |
|---|---|---|---|---|---|---|
| 30:1 | 691.45649 | - | **++** | - | - | - |
| 31:0 | 707.48804 | - | **++** | - | - | - |
| 31:1 | 705.47217 | - | **++** | + | - | - |
| 32:0 | 721.50349 | - | **++** | - | - | - |
| 32:1 | 719.48797 | - | **++** | + | - | - |
| 33:0 | 735.51876 | - | **++** | + | - | - |
| 33:1 | 733.51876 | - | **++** | + | - | - |
| 33:2 | 731.48811 | - | **++** | - | - | - |
| 34:0 | 749.53449 | - | **++** | + | - | - |
| 34:1 | 747.51874 | - | **++** | + | - | - |
| 34:2 | 745.50357 | - | **++** | + | - | - |
| 35:0 | 763.55055 | - | **++** | + | - | - |
| 35:1 | 761.53481 | - | **++** | + | - | - |
| 35:2 | 759.51923 | - | **++** | + | - | - |
| 36:0 | 777.56638 | - | **++** | - | - | - |
| 36:1 | 775.55075 | - | **++** | - | - | - |
| 36:2 | 773.53475 | - | **++** | + | - | - |
| 37:0 | 791.58291 | - | **++** | - | - | - |
| 37:1 | 789.56695 | - | **++** | - | - | - |
| 38:0 | 805.59839 | - | **++** | - | - | - |

## ACKNOWLEDGEMENT

## CONFLICT OF INTEREST STATEMEMENT

The authors have declared no conflicts of interest**.**

**REFERENCES**

1. Ivanova, P. T., S. B. Milne, J. S. Forrester, and H. A. Brown. 2004. Lipid arrays: New tools in the understanding of membrane dynamics and lipid signaling. *Mol Interv* **4**: 86-96.

2. Shevchenko, A., and K. Simons. 2010. Lipidomics: coming to grips with lipid diversity. *Nat Rev Mol Cell Biol* **11**: 593-598.

3. Wenk, M. R. 2005. The emerging field of lipidomics. *Nat Rev Drug Discov* **4**: 594-610.

4. Guo, X., and E. Lankmayr. 2011. Phospholipid-based matrix effects in LC-MS bioanalysis. *Bioanalysis* **3**: 349-352.

5. Griffiths, W. J. 2003. Tandem mass spectrometry in the study of fatty acids, bile acids, and steroids. *Mass Spectrom Rev* **22**: 81-152.

6. Pulfer, M., and R. C. Murphy. 2003. Electrospray mass spectrometry of phospholipids. *Mass Spectrom Rev* **22**: 332-364.

7. Han, X. L., and R. W. Gross. 2005. Shotgun lipidomics: Electrospray ionization mass spectrometric analysis and quantitation of cellular lipidomes directly from crude extracts of biological samples. *Mass Spectrom Rev* **24**: 367-412.

8. Han, X. L., and R. W. Gross. 2003. Global analyses of cellular lipidomes directly from crude extracts of biological samples by ESI mass spectrometry: a bridge to lipidomics. *J Lipid Res* **44**: 1071-1079.

9. Fang, J. S., and M. J. Barcelona. 1998. Structural determination and quantitative analysis of bacterial phospholipids using liquid chromatography electrospray ionization mass spectrometry. *J Microbiol Methods* **33**: 23-35.

10. Taguchi, R., T. Houjou, H. Nakanishi, T. Yamazaki, M. Ishida, M. Imagawa, and T. Shimizu. 2005. Focused lipidomics by tandem mass spectrometry. *J. Chromatogr B Analyt Technol Biomed Life Sci* **823**: 26-36.

11. Smith, P. B. W., A. P. Snyder, and C. S. Harden. 1995. Characterization of bacterial phospholipids by electrospray-ionization tandem mass-spectrometry. *Anal Chem* **67**: 1824-1830.

12. Peterson, B. L., and B. S. Cummings. 2006. A review of chromatographic methods for the assessment of phospholipids in biological samples. *Biomed Chromatogr* **20**: 227-243.

13. Pang, L. Q., Q. L. Liang, Y. M. Wang, L. Ping, and G. A. Luo. 2008. Simultaneous determination and quantification of seven major phospholipid classes in human blood using normal-phase liquid chromatography coupled with electrospray mass spectrometry and the application in diabetes nephropathy. *J. Chromatogr B Analyt Technol Biomed Life Sci* **869**: 118-125.

14. Ogiso, H., T. Suzuki, and R. Taguchi. 2008. Development of a reverse-phase liquid chromatography electrospray ionization mass spectrometry method for lipidomics,

improving detection of phosphatidic acid and phosphatidylserine. *Anal Biochem* **375**: 124-131.

15. Hutchins, P. M., R. M. Barkley, and R. C. Murphy. 2008. Separation of cellular nonpolar neutral lipids by normal-phase chromatography and analysis by electrospray ionization mass spectrometry. *J Lipid Res* **49**: 804-813.

16. Hein, E. M., L. M. Blank, J. Heyland, J. I. Baumbach, A. Schmid, and H. Hayen. 2009. Glycerophospholipid profiling by high-performance liquid chromatography/mass spectrometry using exact mass measurements and multi-stage mass spectrometric fragmentation experiments in parallel. *Rapid Commun Mass Spectrom* **23**: 1636-1646.

17. Taguchi, R., and M. Ishikawa. 2010. Precise and global identification of phospholipid molecular species by an Orbitrap mass spectrometer and automated search engine Lipid Search. *J Chromatogr A* **1217**: 4229-4239.

18. Scherer, M., K. Leuthauser-Jaschinski, J. Ecker, G. Schmitz, and G. Liebisch. 2010. A rapid and quantitative LC-MS/MS method to profile sphingolipids. *J Lipid Res* **51**: 2001-2011.

19. Scherer, M., G. Schmitz, and G. Liebisch. 2010. Simultaneous Quantification of Cardiolipin, Bis(monoacylglycero)phosphate and their Precursors by Hydrophilic Interaction LC-MS/MS Including Correction of Isotopic Overlap. *Anal Chem* **82**: 8794-8799.

20. Houjou, T., K. Yamatani, M. Imagawa, T. Shimizu, and R. Taguchi. 2005. A shotgun tandem mass spectrometric analysis of phospholipids with normal-phase and/or reverse-phase liquid chromatography/electrospray ionization mass spectrometry. *Rapid Commun Mass Spectrom* **19**: 654-666.

21. Sato, Y., T. Nakamura, K. Aoshima, and Y. Oda. 2010. Quantitative and Wide-Ranging Profiling of Phospholipids in Human Plasma by Two-dimensional Liquid Chromatography/Mass Spectrometry. *Anal Chem* **82**: 9858-9864.

22. Burdge, G. C., P. Wright, A. E. Jones, and S. A. Wootton. 2000. A method for separation of phosphatidylcholine, triacylglycerol, non-esterified fatty acids and cholesterol esters from plasma by solid-phase extraction. *Br J Nutr* **84**: 781-787.

23. Kaluzny, M. A., L. A. Duncan, M. V. Merritt, and D. E. Epps. 1985. Rapid separation of lipid classes in high-yield and purity using bonded phase columns. *J Lipid Res* **26**: 135-140.

24. Pinkart, H. C., R. Devereux, and P. J. Chapman. 1998. Rapid separation of microbial lipids using solid phase extraction columns. *J Microbiol Methods* **34**: 9-15.

25. Pernet, F., C. J. Pelletier, and J. Milley. 2006. Comparison of three solid-phase extraction methods for fatty acid analysis of lipid fractions in tissues of marine bivalves. *J Chromatogr A* **1137**: 127-137.

26. Suzuki, E., A. Sano, T. Kuriki, and T. Miki. 1993. Separation and determination of phospholipids in plasma employing thin-layer chromatographic plate with concentration zone or solid-phase extraction. *Biol Pharm Bull* **16**: 77-80.

27. Blunk, H. C., and H. Steinhart. 1990. Separation of phospholipids in bovine tissue with disposable silica-gel extraction columns. *Z. Lebensm.-Unters. Forsch.* **190**: 123-125.

28. Bodennec, J., O. Koul, I. Aguado, G. Brichon, G. Zwingelstein, and J. Portoukalian. 2000. A procedure for fractionation of sphingolipid classes by solid-phase extraction on aminopropyl cartridges. *J Lipid Res* **41**: 1524-1531.

29. Pietsch, A., and R. L. Lorenz. 1993. Rapid separation of the major phospholipid classes on a single aminopropyl cartridge. *Lipids* **28**: 945-947.

30. Hamilton, J. G., and K. Comai. 1988. Rapid separation of neutral lipids, free fatty-acids and polar lipids using prepacked silic Sep-Pak columns. *Lipids* **23**: 1146-1149.

31. Suzuki, E., A. Sano, T. Kuriki, and T. Miki. 1997. Improved separation and determination of phospholipids in animal tissues employing solid phase extraction. *Biol Pharm Bull* **20**: 299-303.

32. Fauland, A., H. Köfeler, M. Trötzmüller, A. Knopf, J. Hartler, A. Eberl, C. Chitraju, E. Lankmayr, and F. Spener. 2011. A comprehensive method for lipid profiling by liquid chromatography-ion cyclotron resonance mass spectrometry. *J Lipid Res* **52**: 2314-2322.

33. Hartler, J., M. Trötzmüller, C. Chitraju, F. Spener, H. C. Köfeler, and G. G. Thallinger. 2010. Lipid Data Analyzer: Unattended Identification and Quantitation of Lipids in LC-MS Data. *Bioinformatics.*

34. Pichler, W. F. 2007. Analyse von flüchtigen Fettsäuren in Fermentationsbrühen zur Optimierung der Biogasproduktion. Graz University of Technology, Graz.

35. Dittmer, J. C., and R. L. Lester. 1964. A simple, specific spray for the detection of phospholipids on thin-layer chromatograms. *J Lipid Res* **15**: 126-127.

36. Kundu, S. K., S. Chakravarty, N. Bhaduri, and H. K. Saha. 1977. Novel spray reagent for phospholipid detection. *J Lipid Res* **18**: 128-130.
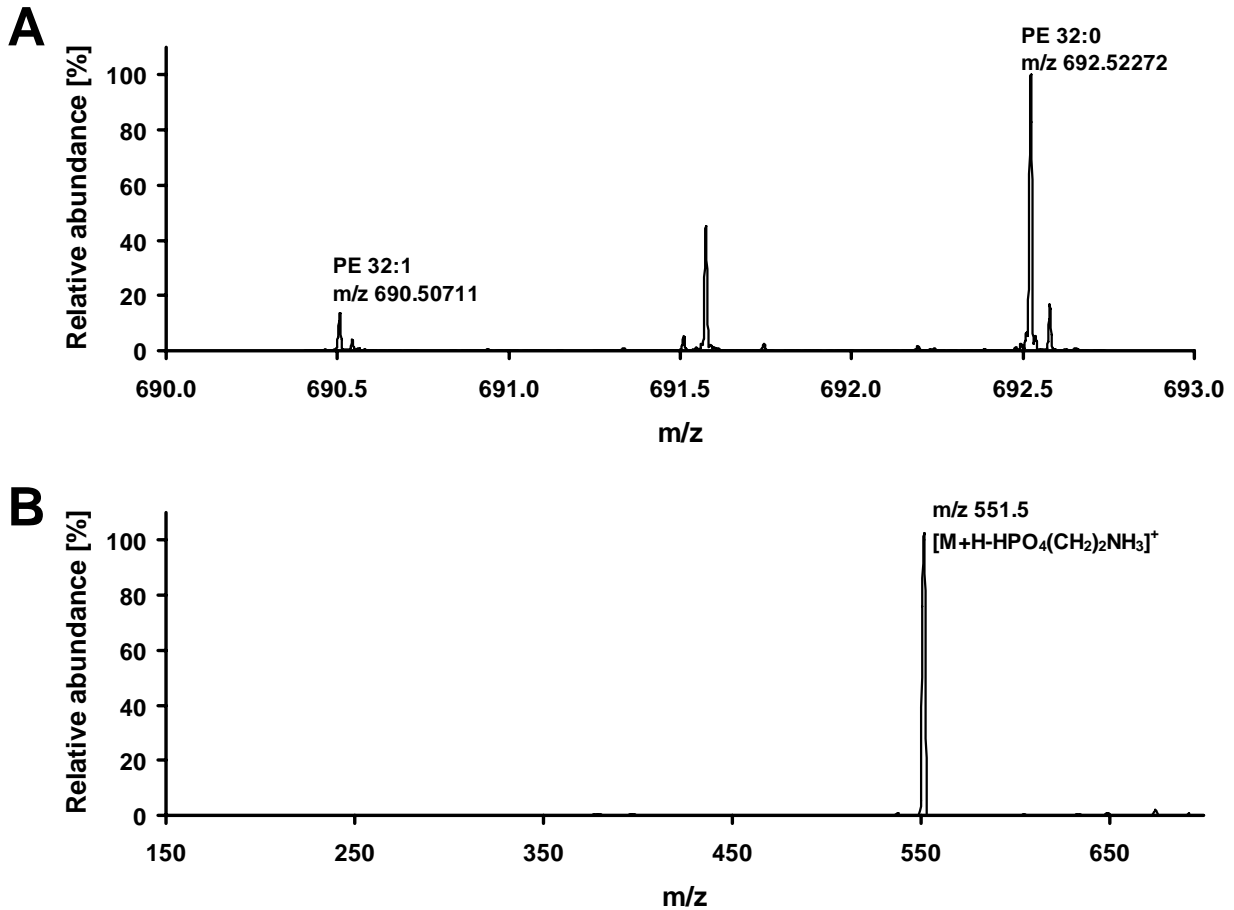
**SUPPLEMENTENTAL DATA**
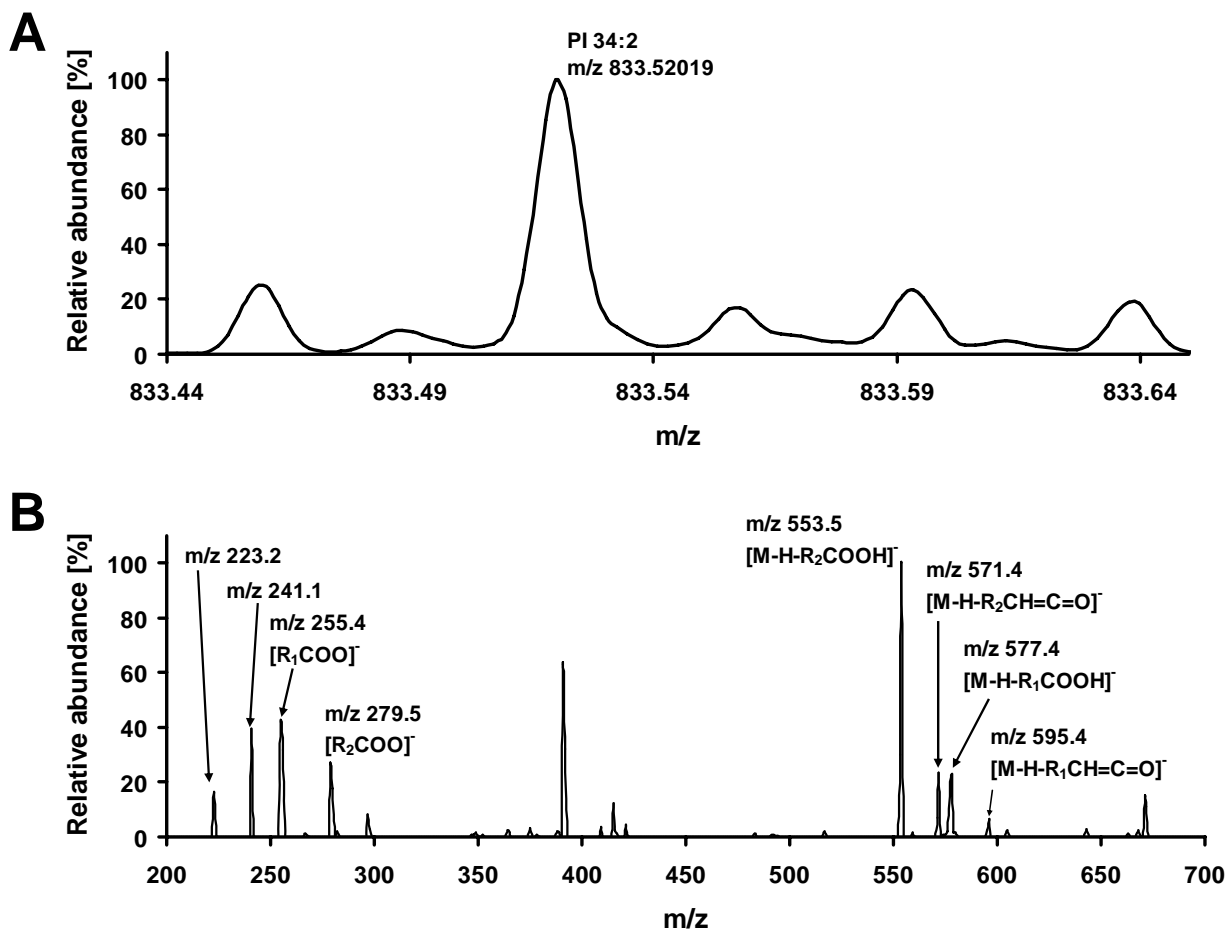


**Supplementary Figure 1S**: Identification and structural elucidation of PI in negative ESI mode (**A**) High resolution LTQ-FT-MS data [M-H]⁻ of m/z 833.52019 corresponding to PI 34:2. Data were generated with a reversed-phase-HPLC/LTQ-FT system. (**B**) Low resolution LTQ-MS/MS spectrum of m/z 255.4 [R$_1$COO]⁻ and 279.4 [R$_2$COO]⁻ depict the fatty acids C16:0 and C18:2 for PI 34:2, respectively. Fragment ions at m/z 553.4 [M-H-R$_2$COOH]⁻ and m/z 577.4 [M-H-R$_1$COOH]⁻ correspond to neutral loss of the respective fatty acyls and m/z 571.4 [M-H-R$_2$CH=C=O]⁻ as well as m/z 595.4 [M-H-R$_1$CH=C=O]⁻ correspond to the respective loss of fatty acids as alkyl ketene. Lipid class characteristic ion m/z 241 derives from H$_2$O loss of the inositol phosphate fragment. The peak at m/z 223 results from dehydration of m/z 241 and the peak at m/z 279 derives from consecutive elimination of two carboxylates at the glycerol backbone.
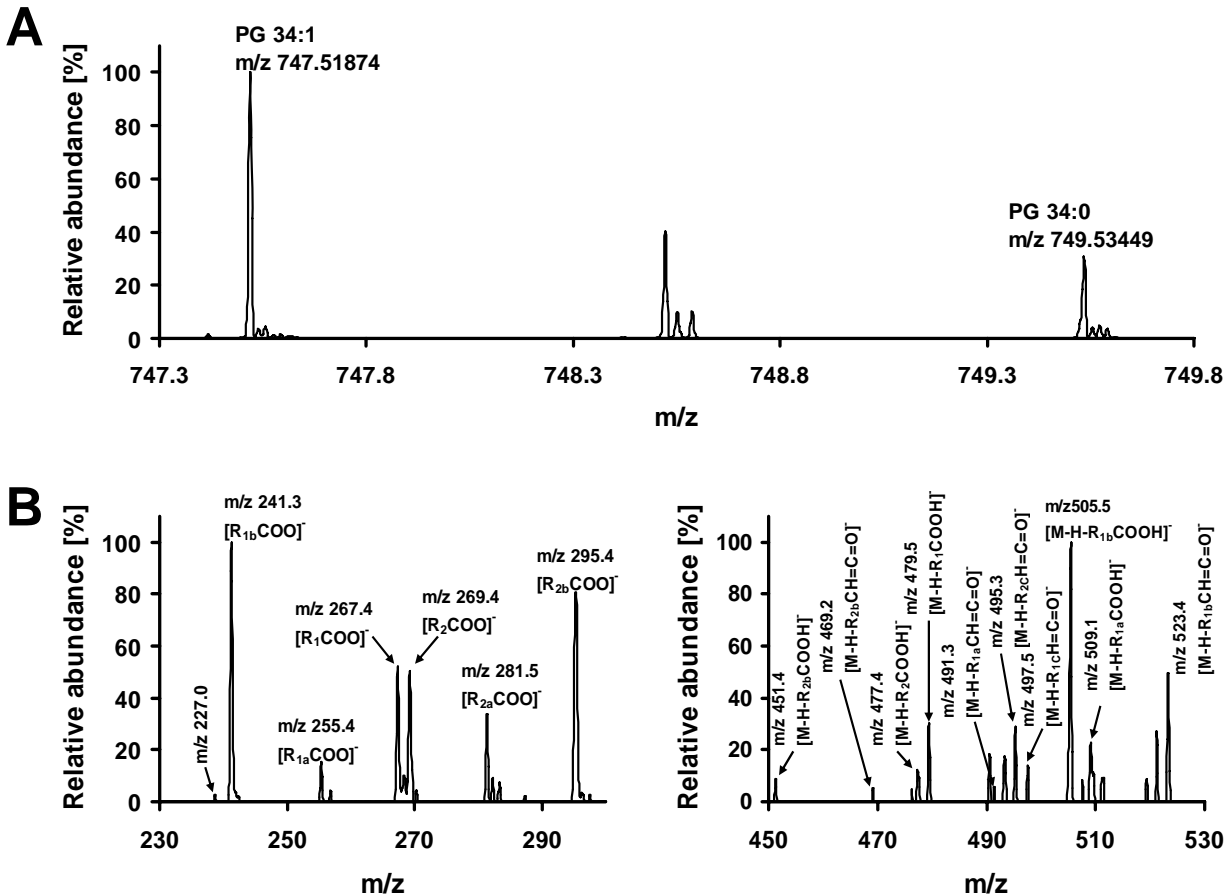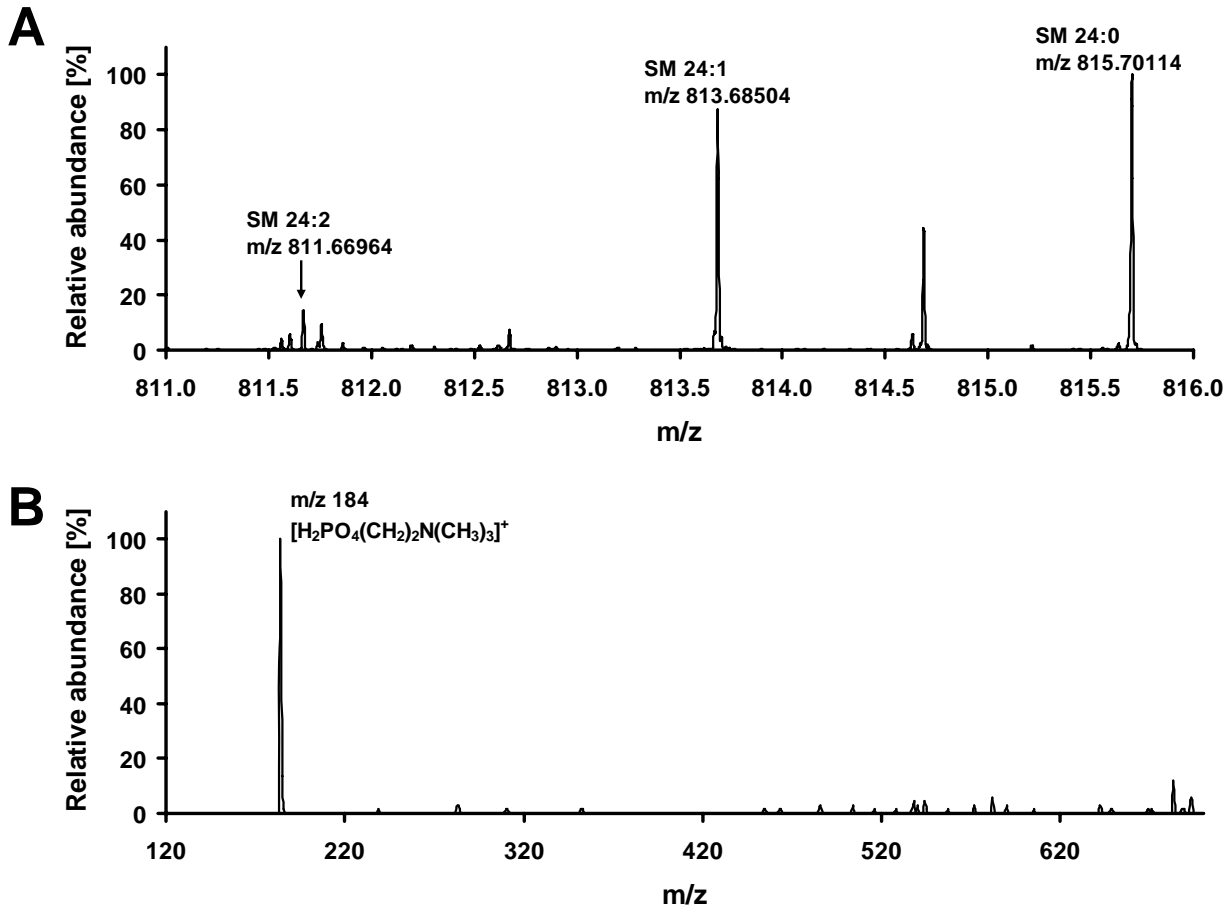
**Supplementary Figure 2S:** Identification and structural elucidation of PG (representative fermentation sample) in negative ESI mode. (**A**) High resolution LTQ-FT-MS data [M-H]⁻ of m/z 747.51874 and 749.53449 representing PG 34:1 and PG 34:0. (**B**) Various fatty acid compositions at the sn-1 and sn-2 position for PG 34:1 are identified by low resolution LTQ-MS/MS. The ions derived from the carboxylate anions are e.g. m/z 267.4 ([$R_1COO$]⁻, C17:1) and m/z 269.4 ([$R_2COO$]⁻ C17:0), or the combination of 255.4 ([$R_{1a}COO$]⁻ C16:0) and m/z 281.4 ([$R_{2a}COO$]⁻ C18:1), or 241.3 ([$R_{1b}COO$]⁻ C15:0) and 295.5 ([$R_{2b}COO$]⁻ C19:1), respectively. The loss of fatty acyl substituents and alkyl ketene formed the following product ions: C15:0 m/z 505.3 [M-H-$R_{1b}COOH$]⁻ and m/z 523.3 [M-H-$R_{1b}CH=C=O$]⁻, C16:0 m/z 491.3 [M-H-$R_{1a}COOH$]⁻ and m/z 509.3 [M-H-$R_{1a}CH=C=O$]⁻, C17:0 m/z 477.3 [M-H-$R_2COOH$]⁻ and m/z 495.3 [M-H-$R_2CH=C=O$]⁻, C17:1 m/z 479.3 [M-H-$R_1COOH$]⁻ and m/z 497.3 [M-H-$R_1CH=C=O$]⁻, C18:1 m/z 465.3 [M-H-$R_{2a}COOH$]⁻ and m/z 483.3 [M-H-$R_{2a}CH=C=O$]⁻, C19:1 m/z 451.2 [M-H-$R_{2b}COOH$]⁻ and m/z 469.2 [M-H-$R_{2b}CH=C=O$]⁻. The diagnostic ion at m/z 227 is lipid class specific for PG.
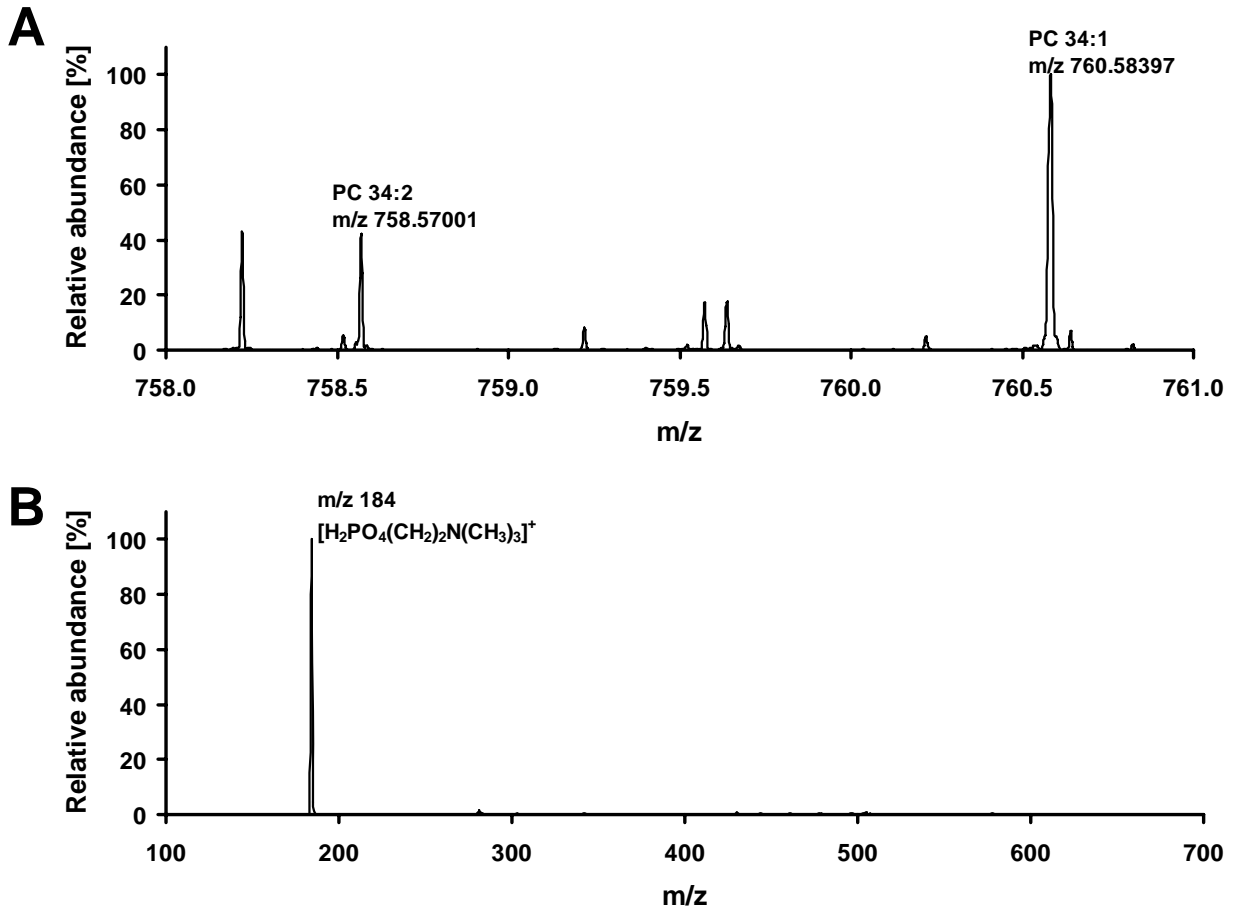
**Supplementary Figure 3S**: Identification and structural elucidation of PC (representative fermentation sample) in positive ESI mode. (**A**) MS spectrum of an LTQ-FT high resolution full scan displays the lipid molecular species of PC 34:1, m/z 760.58397 and PC 34:2, m/z 758.57001, respectively. (**B**) The characteristic dominant fragment ion of PC, m/z 184 [$H_2PO_4(CH_2)_2N(CH_3)_3$]$^+$ in a low resolution LTQ-MS/MS spectrum of PC 34:1 clearly identifies the protonated molecular ion as a phosphatidylcholine.

**Supplementary Figure 4S**: Identification and structural elucidation of PE (representative fermentation sample) in positive ESI mode. (**A**) High resolution LTQ-FT-MS data [M+H]$^+$ of PE 32:0 m/z 692.52272 and PE 32:1 m/z 690.50711. (**B**) The low resolution LTQ-MS/MS spectrum of PE 32:0 highlights fragment ion m/z 551.5 which corresponds to the phosphatidylethanolamine characteristic neutral loss of mass 141 [HPO$_4$(CH$_2$)$_2$NH$_3$].

**Supplementary Figure 5S**: Identification and structural elucidation of SM (representative fermentation sample) in positive ESI mode. (**A**) MS data of m/z 811.66964 (SM 24:2), m/z 813.68504 (SM 24:1) and m/z 815.70114 (SM 24:0) acquired by an LTQ-FT high resolution full scan. SM is detected as [M+H]$^+$ ion. (**B**) Due to the same head group, sphingomyeline has a similar fragmentation pattern as phosphatidylcholine in LTQ-MS/MS experiments. The quaternary nitrogen atom at the head group of SM dominates the fragmentation characteristics of the molecule, resulting in fragment ion m/z 184 [H$_2$PO$_4$(CH$_2$)$_2$N(CH$_3$)$_3$]$^+$.

**Supplementary Table 1S**. SPE fractionation performance control of fermentation samples spiked with reference phospholipids by QTrap mass spectrometer. The ESI source of the QTrap is operated in negative ESI mode in multiple reaction monitoring (MRM). The table depicts the pre-set masses of the quadrupoles Q1 and Q3 for the MRM scan and the compound parameters are optimized for each reference phospholipid class. DP = declustering potential, CE = collision energy / collision cell, CXP = collision cell exit potential.

| Phospholipid species | MRM | Compound parameter | | |
|---|---|---|---|---|
| | | DP | CE | CXP |
| PG 18:1/16:0 | 747.5 / 281.3 | -140 | -52 | -7 |
| PA 16:0/18:1 | 673.5 / 255.2 | -85 | -56 | -3 |
| CL 14:0 | 1239.8 / 227.2 | -150 | -96 | -3 |
| PI 18:2/16:0 | 833.5 / 255.2 | -155 | -68 | -1 |
| PE 18:1/18:1 | 742.5 / 281.3 | -125 | -50 | -5 |
| PS 16:0/16:0 | 734.5 / 255.2 | -55 | -56 | -1 |
| PC 20:0/20:0 | 904.7 / 311.3 | -95 | -64 | -7 |
| LPC 14:0 | 452.3 / 227.2 | -120 | -34 | -5 |
| SM d18:1/16:0 | 761.5 / 687.5 | -95 | -36 | -5 |

## C.4. A comprehensive method for lipid profiling by liquid chromatography - ion cyclotron resonance mass spectrometry

Alexander Fauland[1], Harald Köfeler[2], Martin Trötzmüller[2], Astrid Knopf[2], Jürgen Hartler[3], Anita Eberl[2], Chandramohan Chitraju[4], Ernst Lankmayr[1]and Friedrich Spener[4]

[1]Institute of Analytical Chemistry and Food Chemistry, Graz University of Technology, Graz, Austria

[2]Core Facility for Mass Spectrometry, Center for Medical Research, Medical University of Graz, Graz, Austria

[3]Institute for Genomics and Bioinformatics, Graz University of Technology, Graz, Austria

[4]Departement of Molecular Biology and Biochemistry, Medical University Graz, Austria

**Abbreviations:** BMP: bis(monoacylglycero)phosphates, Cer: ceramides, CID: collision-induced dissociation, CL: cardiolipins, CV: coefficient of variation, DDA: data dependent acquisition, DG: diacylglycerols, ECN: equivalent carbon number, FA: fatty acids, HILIC: hydrophilic interaction liquid chromatography, IS: internal standards, LDA: Lipid Data Analyzer, LM: LIPID MAPS, LOD: limit of detection, LOQ: limit of quantification, LPE: lysophosphatidylethanolamines, LPC: lysophosphatidylcholines, LTQ-FT: hybrid linear ion trap Fourier transform ion cyclotron resonance mass spectrometer, MG: monoacylglycerols, MRM: multiple reaction monitoring, MTBE: methyl *tert.*-butyl ether, NL: neutral loss, PA: phosphatidic acids, PC: phosphatidylcholines, PE: phosphatidylethanolamines, PG: phosphatidylglycerols, PI: phosphatidylinositols, PS: phosphatidylserines, Q-Trap: quadrupole linear ion trap mass spectrometer, RSD: relative standard deviation, SD: standard deviation, SM: sphingomyelins, S/N: signal to noise, TG: triacylglycerols, 1D: one dimensional, 2D: two dimensional, 3D: three dimensional.

Shorthand notation of lipid species: Abbreviation for lipid class is followed by number of acyl carbons: number of double bounds.

**ABSTRACT**

This work aims to combine chromatographic retention, high mass resolution and accuracy, MS/MS spectra, and a package for automated identification and quantitation of lipid species in one platform for lipidomic analysis. The instrumental setup elaborated comprises reversed-phase HPLC coupled to a Fourier transform ion cyclotron resonance mass spectrometer (LTQ-FT), and Lipid Data Analyzer (LDA) software. Data analysis for lipid species quantification in this platform is based on retention time, mass resolution of 200,000, and mass accuracy below 2 ppm. In addition, automatically generated MS/MS spectra provide structural information at molecular level. This LC/MS technology allows analyzing complex biological samples in a quantitative manner as shown here paradigmatically for murine lipid droplets having a huge surplus of triacylglycerol species. Chromatographic pre-separation of the bulk lipid class alleviates the problem of ion suppression of lipid species from other classes. Extension of 1D to 2D chromatography is possible, yet time consuming. The platform affords unambiguous detection of lipid species as low as 0.1‰ within major lipid classes. Taken together, a novel lipidomic LC/MS platform based on chromatographic retention, high mass resolution and accuracy, MS/MS analysis and quantitation software enables analysis of complex samples as demonstrated for lipid droplets.

## INTRODUCTION

Quantitative determination of lipid species provides insights to lipid homeostasis and its dysregulation in diseased states. Thus, lipidomic approaches by mass spectrometry-based technology are attractive for characterization of specific lipids as modulators or disruptors of signaling and metabolic pathways, or as biomarkers in the clinical setting (1-5). Particularly mass spectrometry and advanced bioinformatics tools enable such approaches today (6, 7).

Direct infusion shotgun mass spectrometry is established for 'global' lipidomic analysis (8-13). It is fast and simple, but suffers from inherent ion suppression effects that may however be of advantage in some cases (14). Yet, for certain triacylglycerol - rich samples a pre-cleaning step is necessary (13). As an alternative approach liquid chromatography coupled to mass spectrometry, i.e., LC/ESI-MS, can be used. Here a variety of different reversed-phase and normal-phase liquid chromatographic separation techniques afford higher detection sensitivity in mass spectrometers (15-23). A recent publication describes a HPLC/LTQ-FT system in negative ESI-mode for glycerophospholipids from yeast lipid extracts, featuring a duty cycle time of 5 s at a resolution of 50,000, including 2 data dependent MS/MS spectra per cycle (19). Also, hydrophilic interaction chromatography (HILIC), a modified normal-phase chromatography, coupled to LC/ESI-MS allows analyzing cardiolipins (CL) and bis(monoacylglycero)phosphates (BMP) (22). Increased chromatographic selectivity is obtained by a two dimensional (2D) separation system of normal-phase and reversed-phase chromatography. Moving recently from off- to an on-line 2D LC/MS non-commercial approach, lipid profiles from rat peritoneal surfaces are reported (15).

Taken together, most platforms use either MS/MS spectra and exact mass (10), or retention time and specific fragments (24), or retention time and exact mass (25). It is our goal to combine all these parameters for the highest possible level of confidence in one platform and to link it to a custom-developed software package for automated identification and quantitation (7).

Lipid droplets are long-neglected cell organelles, composed of a hydrophobic lipid core of triacylglycerols (TG) and sterol esters that is surrounded by a monolayer of phospholipids, sphingomyelins (SM) and cholesterol. They emerged as a central hub for TG metabolism among many other metabolic and signaling features (26). The huge concentration difference between TG and the other lipid species (27) makes lipid droplets a highly challenging analytical matrix due to ion suppression effects affected by bulk TG. An efficient chromatographic system and subsequent analysis of lipid species by an ion cyclotron is tested by analyzing this matrix. Moreover, the ultra high mass spectrometric resolution delivered by an ion cyclotron should help to reduce the complexity of lipid droplet samples, which would be a fundamental advantage over systems with lower resolution.

## MATERIALS AND METHODS

### Lipid standards

1,2-dipalmitoyl-*sn*-glycero-3-phosphocholine (PC 16:0/16:0), 1,2-dibehenoyl-*sn*-glycero-3-phosphocholine (PC 22:0/22:0), 1,2-dimyristoyl-*sn*-glycero-3-phosphocholine (PC 14:0/14:0), 1,2-dilauroyl-*sn*-glycero-3-phosphocholine (PC 12:0/12:0), 1,2-diarachidoyl-*sn*-glycero-3-phosphocholine (PC 20:0/20:0), 1,2-distearoyl-*sn*-glycero-3-phosphocholine (PC 18:0/18:0), 1-stearoyl-2-arachidonoyl-*sn*-glycero-3-phosphocholine (PC 18:0/20:4), 1,2-dilignoceroyl-*sn*-glycero-3-phosphocholine (PC 24:0/24:0), 1-palmitoyl-2-oleoyl-*sn*-glycero-3-phospho-L-serine (sodium salt) (PS 16:0/18:1), 1,2-dilauroyl-*sn*-glycero-3-phospho-L-serine (sodium salt) (PS 12:0/12:0), 1-stearoyl-2-arachidonoyl-*sn*-glycero-3-phosphoethanolamine (PE 18:0/20:4), 1,2-dilauroyl-*sn*-glycero-3-phosphoethanolamine (PE 12:0/12:0), 1-octadecyl-*sn*-glycero-3-phosphocholine (LPC 18:0), L-α-lysophosphatidylcholines (chicken egg), 1,2-dilauroyl-*sn*-glycero-3-[phospho-*rac*-(1-glycerol)] (PG 12:0/12:0), 1-palmitoyl-2-oleoyl-*sn*-glycero-3-[phospho-*rac*-(1-glycerol)] (PG 16:0/18:1), L-α-lysophosphatidylethanolamines (chicken egg), sphingolipid mix I, N-lignoceroyl-D-*erythro*-sphingosine ceramide (Cer d18:1/24:0), N-arachidoyl-D-*erythro*-sphingosine ceramide (Cer d18:1/20:0), LIPID MAPS (LM) quantitative lipid standards were supplied by Avanti Polar Lipids (Alabaster, AL, USA). L-α-phospatidylserines (porcine brain), L-α-phosphatidylethanolamines (corn germ), sphingomyelins (bovine brain), L-α-phosphatidylinositols (bovine heart), 1,2,3-tripalmitoyl-glycerol (TG 16:0/16:0/16:0), 1,2,3-tristearoyl-glycerol (TG 18:0/18:0/18:0), 1,2,3-triarachidoyl-glycerol (TG 20:0/20:0/20:0), 1,2,3-heptadecanoyl-glycerol (TG 17:0/17:0/17:0), 1,2-distearoyl-3-palmitoyl-*sn*-glycerol (TG 18:0/18:0/16:0), 1,2-dilauroyl-*sn*-glycerol (DG 12:0/12:0), 1,2-dipalmitoyl-*sn*-glycerol (DG 16:0/16:0), 1,2-distearoyl-*sn*-glycerol (DG 18:0/18:0) were purchased from Larodan (Malmö, Sweden). Standard stock solutions were dissolved in chloroform/methanol 1:1 (v/v) at a concentration of 1 mM and stored at -18°C. Lipid standard mixtures were prepared freshly every day in chloroform/methanol 1:1 (v/v) at a concentration of 3 μM and were used immediately.

Cyclohexane and chloroform were HPLC grade, ammonium acetate and acetic acid were analytical grade, all obtained from Merck KGaA (Darmstadt, Germany). 2-Propanol was LC/MS grade and supplied by Fluka (Steinheim, Germany). Methanol and acetonitrile were LC/MS grade, methyl *tert.*-butyl ether (MTBE) was HPLC grade and 28% ammonia p.a. were all purchased from Sigma-Aldrich Chemie GmbH (Steinheim, Germany). Nitrogen (purity 5.0) was obtained from Air Liquide (Graz, Austria). Ultra pure water purified by a Milli-Q Gradient system (Millipore, Bedford, MA, USA) was used in all experiments (resistivity > 18 MΩcm).

**Isolation of lipid droplets from murine primary hepatocytes**

A pool of lipid droplets isolated from hepatocytes of mice was split into 3 equal parts and used as representative biological examples for lipid droplets. Primary hepatocytes from C57 black mice (C57BL) were isolated according to literature (28). The hepatocyte pellet obtained was re-suspended in 5 ml ice cold disruption buffer (20 mM potassium phosphate pH 7.4, 250 mM sucrose, 1 mM EDTA, 1 mM PMSF) and incubated cells were lysed under nitrogen cavitation at 800 psi for 10 min in a nitrogen bomb (Parr Instrument Company, Moline, IL, USA). The resulting homogenate was centrifuged at 1000 g for 5 min at 4°C to remove cell debris. The supernatant obtained was overlayed with buffer (50 mM potassium phosphate pH 7.4, 100 mM potassium chloride, 1 mM EDTA, 1mM PMSF) and centrifuged at 100,000 g for 1 h at 4°C. Lipid droplets concentrated in a white band at the top of the tube and were used for further experiments.

**Lipid extraction**

Lipid extraction was carried out as described (29). Briefly, 2 mL of the lipid droplet suspension (TG concentration 2.17 mg/mL) were placed in a glass tube with a teflon lined cap. A volume of 3 mL methanol and then 10 mL MTBE were added and tubes were shaken for 1 h at room temperature. Upon addition of 2.5 mL deionized water and shaking, phase separation was induced. The upper organic phase was collected, the lower aqueous phase re-extracted with MTBE and upper phases were combined. The solvent was evacuated in a SpeedVac (Thermo Fisher Scientific, San Jose, CA, USA) and lipids were re-dissolved in 4 mL chloroform/methanol 1:1 (v/v).

**Identification and quantitation**

Dilution factors need to be adapted to expected lipid class concentrations in the sample to be investigated and to instrumental set up in use. In the present case of bulk TG class lipid droplet samples were diluted 1:57 with chloroform/methanol 1:1 (v/v), in case of determination of all other lipid classes together 1:3 with chloroform/methanol 1:1 (v/v). In either case the solvent was evacuated in a SpeedVac and lipids were re-suspended in 100 µL chloroform/methanol 1:1 (v/v) for further analysis. Then lipid extracts were spiked with multiple LM quantitative internal standards (IS) for each lipid class to be monitored. Five replicas of extracted lipid samples were prepared for lipid quantification as well as accuracy and precision analysis. Quantitative IS LM 1000, LM 1002, LM 1003, LM 1004, LM 1601, LM 6002 at 100 pmol/ re-suspended sample for PC, LPC, and sphingolipid classes; LM 1100, LM 1102, LM 1103, LM 1104, LM 1300, LM 1302, LM 1303, LM 1304, LM 1500, LM 1502, LM 1503, LM 1504 at 250 pmol/ re-suspended sample for PE, PS and PI; LM 6001 at 350 pmol/ re-suspended sample for DG; LM 6000 at 150 pmol/ re-suspended sample for TG and

LM 4000 at 800 pmol/ re-suspended sample for cholesterol ester were used. All solutions prepared were stored at -20°C until use.

Accuracy and precision evaluation was performed by spiking five replicas of extracted lipid droplets with 350 pmol TG 17:0/17:0/17:0, 130 pmol PC 12:0/12:0, 270 pmol PE 12:0/12:0 and 220 pmol PS 12:0/12:0. Also, for determination of the dynamic range further three replicas were spiked with these four standards at nine concentration levels each ranging from 0.02 to 328 µmol/µL per standard.

## Chromatographic methods

### High-performance liquid chromatography

The Accela HPLC system was equipped with a reversed-phase C18 column (reversed-phase C18; 100 x 1 mm i.d., 1.9 µm particle size), both from Thermo Fisher Scientific, San Jose, CA, USA. Mobile phase A was 10 mM ammonium acetate containing 0.1% formic acid. Mobile phase B was acetonitrile/2-propanol 5:2 (v/v) containing 10 mM ammonium acetate and 0.1% formic acid. The binary gradient started with 35 to 70% B for 4 min, then was raised up to 100% B in another 16 min and further held for 10 min. The flow rate was 250 µl/min, the oven temperature was 50°C and tray temperature 10°C. For analysis 5 µL sample were injected. After each run the column was flushed 5 min with 35% B before the next run was started.

### High-performance liquid chromatography for 2D chromatographic separation

HILIC-HPLC was carried out in an Agilent 1100 HPLC system (Waldbronn, Germany) consisting of a degasser, a binary pump, a thermostated autosampler and a thermostated column compartment equipped with a semi-preparative column, filled with Nucleosil 100-5 OH, 250 x 10 mm i.d., 5.0 µm particle size (Macherey-Nagel, Düren, Germany). Mobile phase A was cyclohexane and mobile phase B was 2-propanol/deionized water/acetic acid/28% of ammonia 86:13:1:0.12 (v/v). The HPLC flow rate was 1000 µL/min at an isocratic composition of 10% A and 90% B, at 35°C oven and 5°C tray temperature. The injection volume was 100 µL. For online monitoring of lipid fractionation the HPLC system was coupled in positive ESI-mode to a 4000 quadrupole linear ion trap mass spectrometer (Q-Trap) (Applied Biosystem/MDS Sciex, Concord, ON, Canada) with a split of 1:21. Two fractions were manually collected and each subjected to desalting and concentration. For this, 10 mL deionized water was added to each fraction and the organic phase collected. After re-extraction of the aqueous phase with chloroform/methanol 1:1 (v/v), combined organic phases were dried in a SpeedVac and taken up again in 100 µL chloroform/methanol 1:1 (v/v) for further analysis by reversed-phase-HPLC as described before.

**Mass spectrometry**

**LTQ-FT mass spectrometry**

A 7.0 Tesla LTQ-FT hybrid linear ion trap Fourier transform ion cyclotron resonance mass spectrometer (Thermo Fisher Scientific, Bremen, Germany) equipped with an electrospray ion source was used. The instrument was operated in preview mode for parallel MS/MS spectra in the linear ion trap, while running the ion cyclotron in full scan mode at 200,000 resolution (m/z 400) from m/z 400 to 1050 in positive and from m/z 350 to1050 in negative ESI-mode. Helium was used as gas for linear ion trap collision-induced dissociation (CID) spectra. From the LTQ-FT preview scan the 4 most abundant ions were selected in data dependent acquisition (DDA), fragmented in the linear ion trap analyzer and ejected at nominal mass resolution. The following parameters were used for positive and negative ESI-MS/MS experiments: Normalized collision energy was 35%, the repeat count was 2 and the exclusion duration 60 s. The activation Q was at 0.2 and the isolation width 2. For positive ESI spray voltage was set to 5 kV and the tube lens offset was at 120 V. For negative ESI spray voltage was - 4.8 kV and the tube lens offset was - 87 V. The sheath gas flow was set to 50 arbitrary units, auxiliary gas flow to 20 arbitrary units, sweep gas flow to 2 arbitrary units and the capillary temperature to 250°C.

**Data analysis**

Identification and quantitation of lipids was performed by LDA, a platform independent Java application (7). Briefly, the algorithm identifies peaks in the three dimensional LC-MS data space (retention time, m/z and intensity). It determines the peak borders in m/z as well as in time dimension, and integrates the intensities within the borders. Furthermore, the algorithm uses a theoretically calculated isotopic intensity distribution as peak selection criterion in order to improve the specificity.

**RESULTS**

It is the aim of this study to establish an integrated MS-based analytical platform, relying on chromatography, ultra high mass resolution, MS/MS fragmentation and automated data processing (Figure 1). We develop a hyphenated approach by optimizing both reversed-phase-HPLC and subsequent MS parameters. In addition we extend reversed-phase chromatography by a HILIC step (2D LC/MS) that may enhance MS sensitivity for lipid classes through minimizing ion suppression. In this process we test platform performance by analyzing profiles of lipid species present in pooled lipid droplets isolated from mouse hepatocytes.
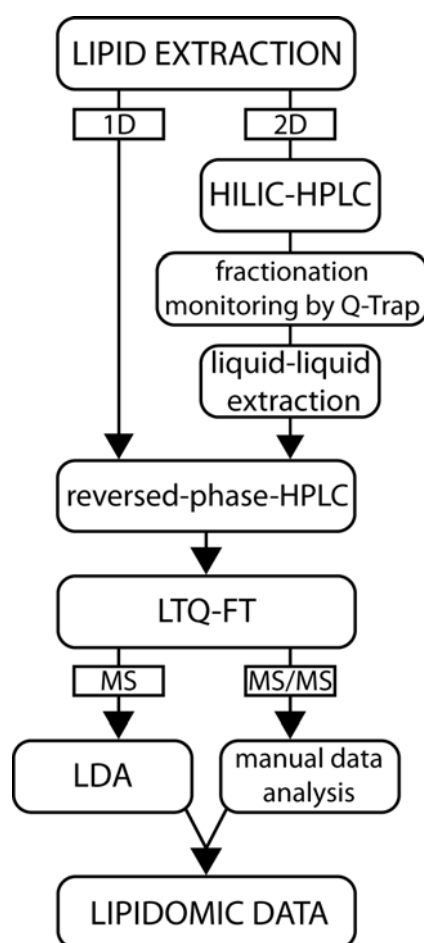


**Figure 1.** Profiling of lipid species by 1D and 2D LC/MS. For 2D LC/MS lipid extracts are first separated in two fractions by normal phase HILIC-HPLC monitored on-line by the Q-Trap mass spectrometer. After liquid-liquid extraction (concentration and desalting) the two fractions are acquired by reversed-phase-HPLC/LTQ-FT (identical to 1D LC/MS). In the last step high resolution MS data are quantitatively evaluated with the LDA software, whereas MS/MS data interpretation is done manually. Retention time is used in data interpretation as additional criterion for identification.

## Reversed-phase-HPLC development

The particular challenge is the high excess of TG in the samples. ESI was used because of its extraordinary sensitivity for monitoring lipid species of TG, diacylglycerols (DG), phosphatidylcholines (PC), lysophosphatidylcholines (LPC), phosphatidylethanolamines (PE), phosphatidylserines (PS) and SM in positive and phosphatidylinositols (PI) in negative mode. Phosphatidic acids (PA), phosphatidylglycerols (PG), CL, lysophosphatidylethanolamines (LPE) and ceramides (Cer) were searched for, but are neither detectable in positive nor in negative ionization mode. Cholesterol and cholesterol esters were not determined, as analysis by a separate silica based normal phase chromatography method with post column addition of a polar solvent is the preferred experimental approach (18) .

The method developed here is a compromise between chromatographic resolution and running time as shown in Figure 2. The chromatogram reveals that in the first 10 min the most polar lipids like LPC elute, followed by a highly crowded range between 10 and 20 min containing most of the phospholipids, SM and DG due to similar interactions of these lipids with the reversed-phase material. Finally, in the retention time window from 20 to 30 min bulk TG elute, the least polar species. Notably, with the help of this reversed-phase-HPLC the class of TG can be separated even in high amounts from the rest of the lipids.

Mobile phase composition and structural features, e.g. chain-lengths and degree of unsaturation of TG species could influence ionization efficiency. However, in a validation experiment with standard LM 6000 (8 deuterated TG species) we found that the HPLC gradient applied and TG structural features have a minor impact only (CV of signal intensities of 8.4% only, data not shown).
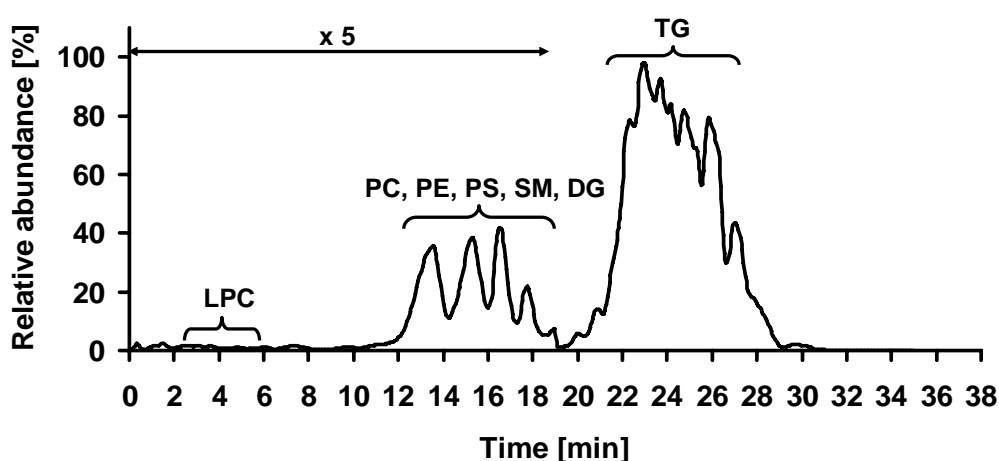


**Figure 2.** Total ion chromatogram of lipids from a representative lipid droplet sample acquired by reversed-phase-HPLC/LTQ-FT. A reversed-phase C18 column is used for separation of lipid species and monitored in positive ESI-mode. The scan range of the LTQ-FT is m/z 350 – 1050.

**Lipid identification and quantitation**

**Accurate mass determination**

The solvent chosen facilitates the formation of ammonia adducts $[M+NH_4]^+$ for TG in positive ESI to yield an elemental fingerprint of $C_xH_yO_6N$. The exact mass of better 2 ppm is sufficient in most cases for unambiguous identification of the elemental composition. The resolution of 200,000 at m/z 400 results in 90,000 at m/z 950, the upper limit for molecular mass of major lipid species in lipid droplets. This resolution does not provide baseline separation of $C_xH_yO_6N$ and $^{13}C_2C_{x-2}H_yO_6N$, yet is still good enough for peak top separation at 80% peak height. The instrument would be able to deliver much higher resolution, but the resolution chosen is a compromise because ion cyclotron sensitivity decreases with increasing resolution on the one hand, and acquisition time increases with increasing resolution resulting in a slower duty cycle on the other hand.

**Determination of lipid molecular species by MS/MS fragmentation**

For interpretation of exact mass data in terms of fatty acid composition of lipid species and also for confirmation of identity by specific fragments, MS/MS spectra were acquired in DDA. In this setup the cyclotron and linear ion trap operate as two separate instruments. This allows acquisition of low resolution MS/MS spectra in the linear ion trap on the most intense peaks in parallel to high resolution spectra acquired by the ion cyclotron (30). The MS/MS coverage of lipid species thus attained in DDA is 66%. The method circumvents the need either to re-run the sample for obtaining MS/MS spectra on precursors identified in a previous high resolution run, or to operate the instrument sequentially in high resolution MS and subsequent MS/MS mode, which would result in a lower duty cycle. This is illustrated paradigmatically in an extracted ion chromatogram shown in Figure 3A for TG 54:5 eluting with a peak maximum at 24.0 min. The respective MS/MS spectrum in positive ionization mode is presented in Figure 3B. The LDA software identifies TG 54:5 by exact mass at m/z 898.78578 ($[M+NH_4]^+$) and the exact mass trace at an isolation width of 0.015 Da shows a main peak at 24.0 min (Figure 3A). The structural elucidation of the detected compound is done by manual analysis of targeted MS/MS data. The MS/MS spectrum (Figure 3B) of m/z of 898.78578 (TG 54:5) depicts fragmentation patterns typically encountered with ammonium adducts of TG. The fragment ion of m/z 881.7 derives from the neutral loss (NL) of $NH_3$ (MW 17) originating from the ammonium adduct of TG 54:5. Moreover Figure 3B clearly shows abundant fragment ions at m/z 599.5 $[M+H-R_1COOH]^+$ and m/z 601.5 $[M+H-R_2COOH]^+$ and the less abundant ion m/z 603.5 $[M+H-R_3COOH]^+$, corresponding to the NL of FA 18:1, 18:2 and 18:3, respectively. This information and combinatorial restrictions arising from elemental composition allows for deducing the molecular species to be TG 18:1/18:2/18:2 and TG 18:1/18:1/18:3.

DG have similar fragmentation behaviour as TG, both having $[M+NH_4]^+$ ions in positive ESI-mode. The characteristic MS/MS fragments are the NL of $NH_3$ and the NL of constituent FA. Similarly, determination of other lipid classes like PC, PE, PS, PI, SM and LPC by MS/MS relies upon specific fragments and neutral losses described in detail in various publications (6, 31). Constituent FA are determined by neutral losses in positive ionization mode and carboxylates in negative ionization mode.
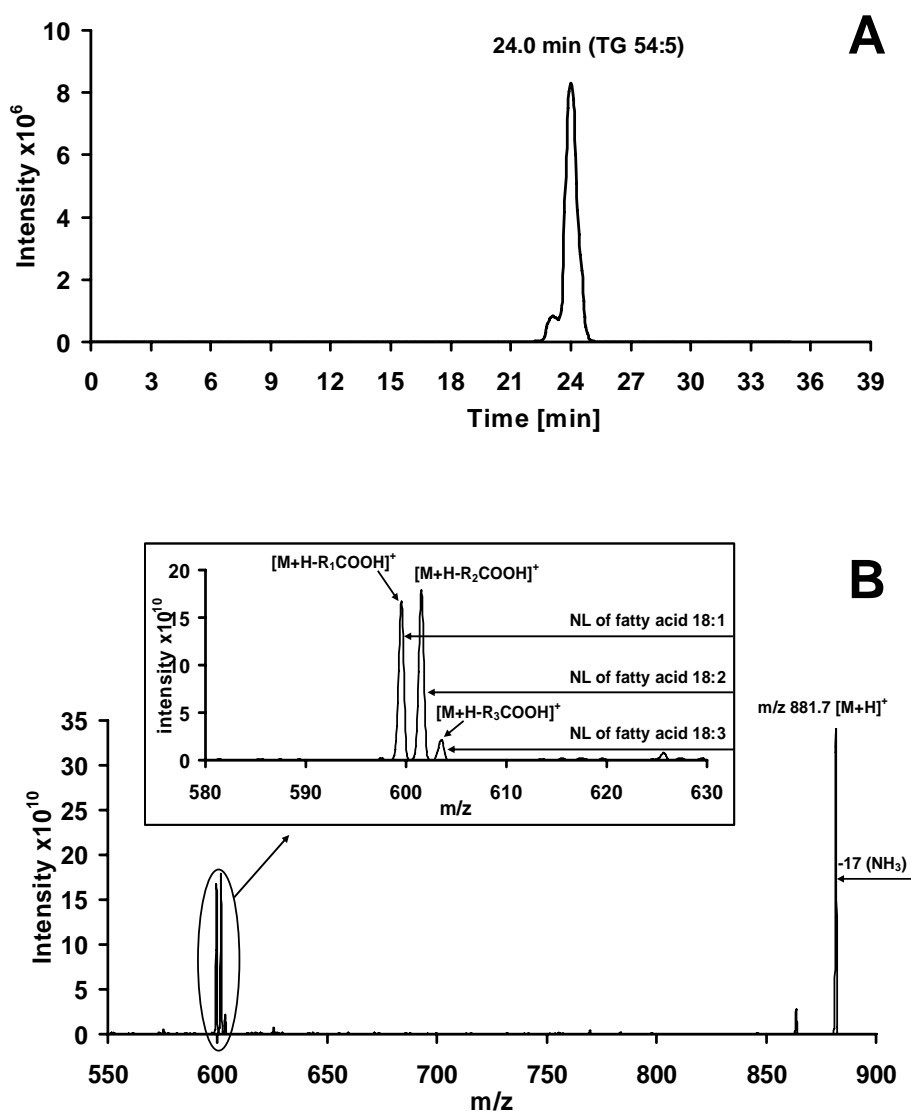


**Figure 3.** Identification and structural elucidation of TG 54:5 (representative lipid droplet sample). (**A**) Exact mass ion chromatogram (isolation width 0.015 Da) of TG 54:5 at m/z 898.78578 extracted from an LTQ-FT high resolution full scan. Data are generated with the reversed-phase-HPLC/LTQ-FT system. The small peak maximum at 23.3 min corresponds to the second isotope of TG 54:6. (**B**) Low resolution LTQ-MS/MS spectrum of m/z 898.8 (TG 54:5) at 24.0 min highlighting the following neutral losses: m/z 599.5 corresponds to NL of fatty acid 18:1, m/z 601.5 corresponds to NL of fatty acid 18:2, m/z 603.5 corresponds to NL of fatty acid 18:3, m/z 881.7 corresponds to NL of $NH_3$.

**Identification of lipid species by retention time**

Low abundant compounds sometimes do not generate reliable MS/MS spectra. In this case accurate retention in addition to accurate mass becomes an important criterion for identification. The method of choice is reversed-phase chromatography where separation of lipid species within one class, expressed by equivalent carbon numbers (32), are mainly based on interaction between hydrophobic stationary phase and acyl carbon chains of the lipid. In fact, chain length and degree of unsaturation of constituent FA of the lipid matter. Consequently, species having FA of same chain lengths (same number of acyl carbons) can be separated by reversed-phase chromatography by their degree of unsaturation in the molecule; the chromatograms shown in Figure 4 illustrate impressively such behavior. Elution times of TG with the same number of acyl carbons decrease by approximately one minute per additional double bond in the lipid. Taking the example of TG having 48 acyl carbons, i.e., TG 48:0 to 48:8, MS/MS data are not available for TG 48:0, 48:1, 48:7 and 48:8. None the less, as shown in Figure 4 and Tables 1S–4S (supplementary data), retention times demonstrate the occurrence of these very minor species by decreasing elution order of these compounds according to number of double bonds. Clearly, identification of lipid species becomes possible by retention time even without availability of reliable MS/MS spectra as long as any other species of the same lipid class with the same carbon number has a reliable MS/MS spectrum.
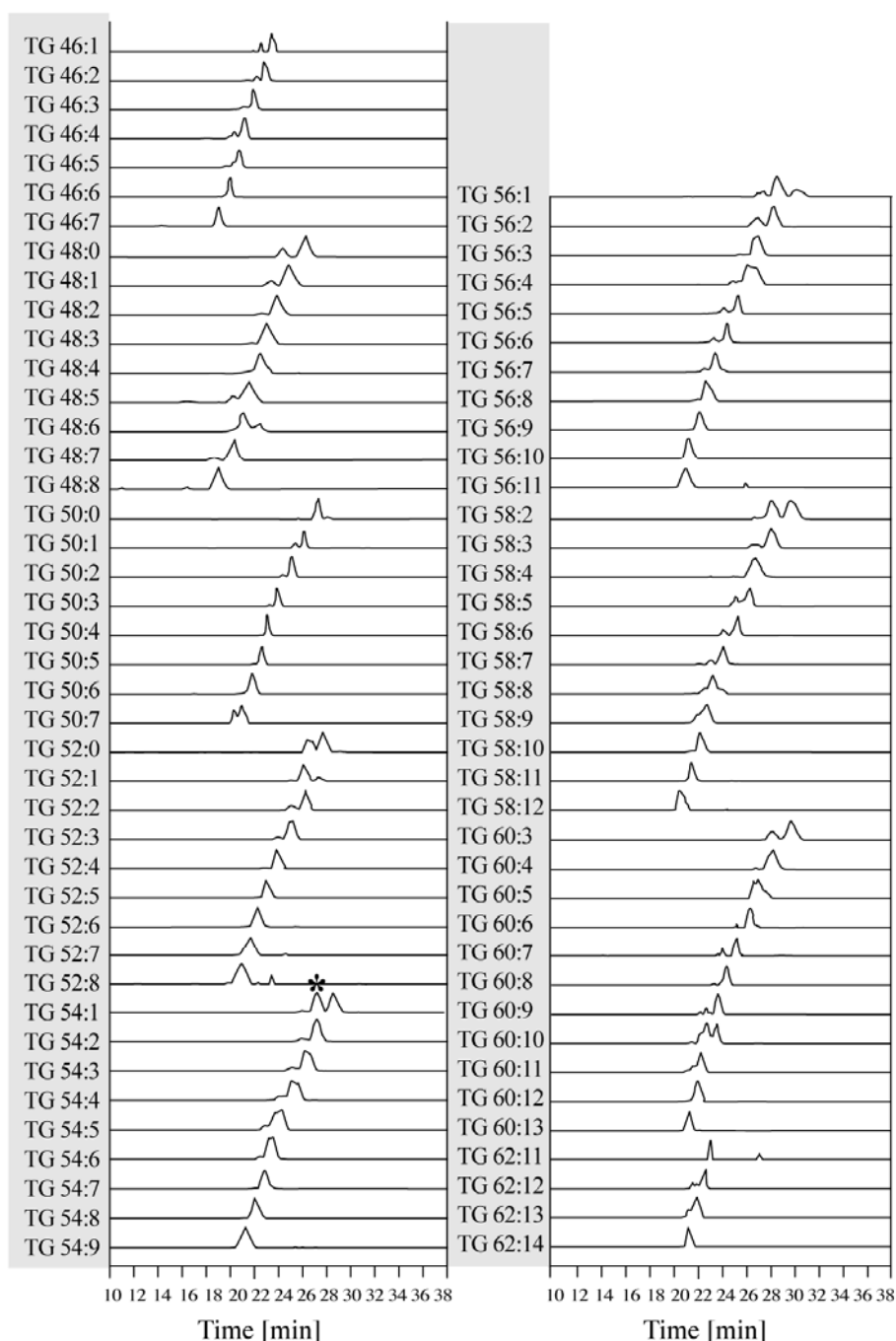
**Figure 4**. Identification of TG species by retention time. Exact mass ion chromatograms extracted from LTQ-FT high resolution full scan of TG species (isolation width 0.015 Da) of a representative lipid droplet sample. Retention time shifts are caused by increasing number of double bonds at the same fatty acyl carbon number. Intensities are normalized to 100% for the highest peak in each trace to show the retention time shift of each species. The real intensities of the TG species are given in Figure 7. The first peak of TG 54:1 marked with * corresponds to the $[M+2]^+$ isotope of the species with one additional double bond (TG 54:2). This is representative for all double peaks seen in these chromatograms.

**2D HPLC approach**

The chromatogram in Figure 2 reveals that in reversed-phase-HPLC/ESI-MS analysis lipid species from different lipid classes overlap, particularly at retention times between 10 and 20 min. A case in point are PC species due to excellent ionization efficiency in positive electrospray mode. They exert a dominating ion suppression on other species of partially co-eluting lipid classes. Thus, a chromatographic selectivity complementary to reversed-phase-HPLC is needed to attain separation of PC species from other polar lipids. Our choice is a diol-based stationary phase allowing for HILIC. The semi-preparative diol column is preconditioned once for 1 h with the isocratic solvent composition as described under methods. The advantage of isocratic elution over gradient elution is that it requires no time-consuming preconditioning between individual runs and has better retention time reproducibility. For method development standards are used as described in "Materials and Methods". During HILIC of lipid droplet samples the eluent of the first 10 min is discarded, then lipids eluting between 10 and 24 min (TG, DG, PS, PE and PI) are collected in fraction 1. The second fraction includes PC, SM and LPC and elutes between 24 and 48 min (Figure 5). The subsequent liquid-liquid extraction after fractionation has two purposes. On the one hand it is necessary to desalt fractions from exceeding ammonium acetate and transfer them into a solvent compatible with the second chromatographic dimension. On the other hand concentrations of lipids in fractions could be increased by a factor of 140 by this procedure.

Our findings indicate that the 2D method elaborated results in a higher sensitivity for certain lipid classes. The data shown in Figure 6A demonstrate that DG species in this sample can be detected by the 2D approach with a higher sensitivity as compared to 1D approach, the same is found for PE species (Figure 6B).
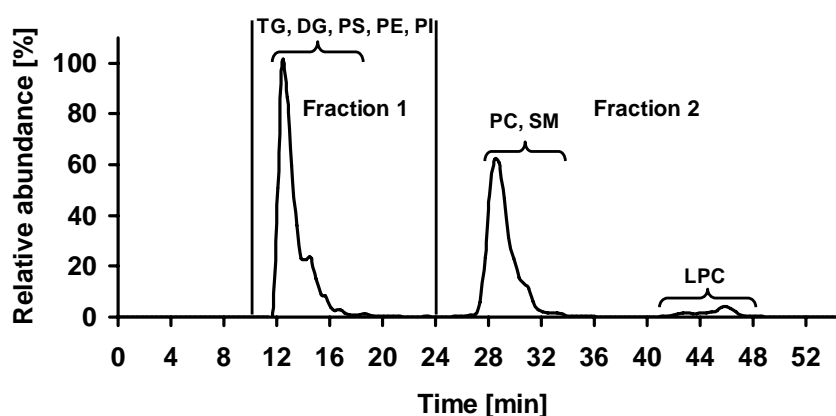


**Figure 5.** Fractionation of lipids of a representative lipid droplet sample on a HILIC column. Pre-separation of lipids in two fractions on this column is obtained by isocratic elution as described in methods. The fractionation process is monitored by a Q-Trap.
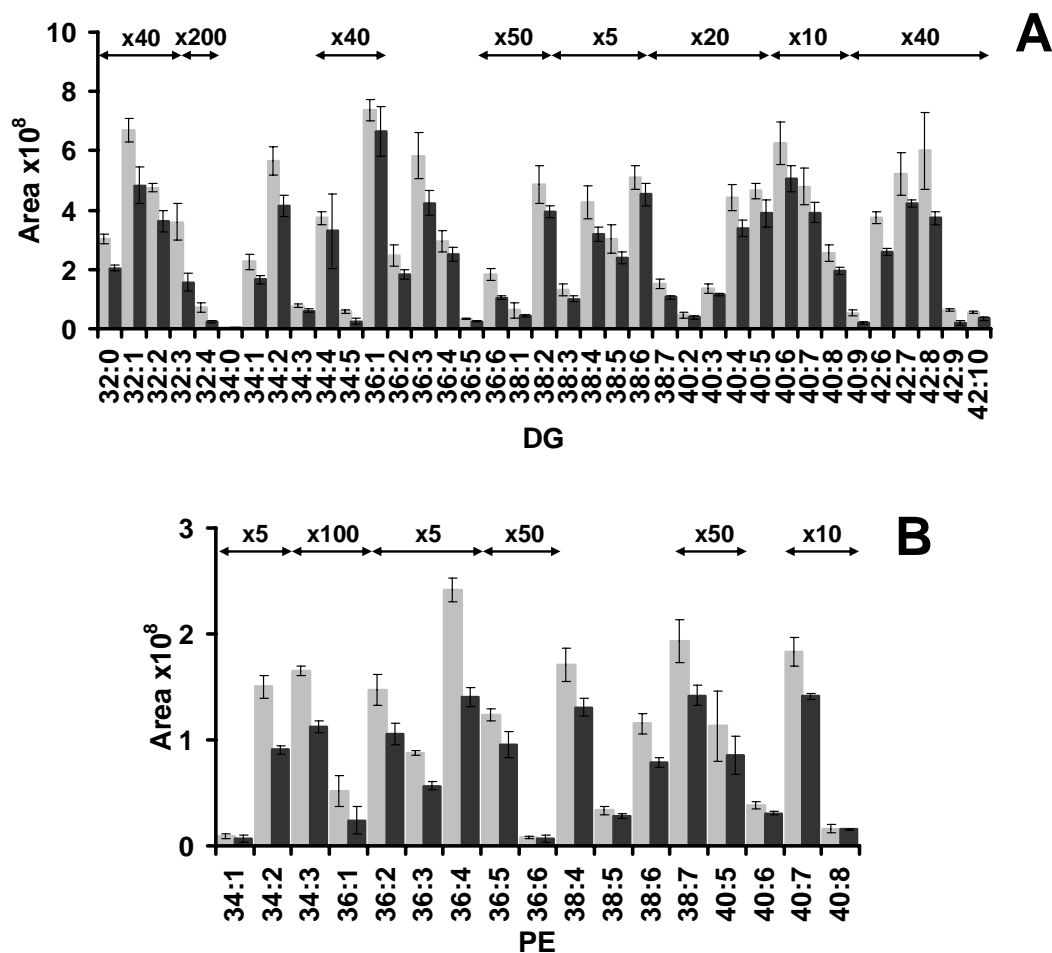
121

**Figure 6.** Comparison of sensitivity in 1D and 2D LC/MS. DG species (**A**) and PE species (**B**) of lipid droplet samples are analyzed by HILIC-reversed-phase-HPLC/LTQ-FT (2D LC; light grey bars) and by reversed-phase-HPLC/LTQ-FT (1D LC; dark grey bars). Chromatographic areas are integrated by LDA and displayed as arbitrary units. Data are means ± SD (n = 3).

**Application of reversed-phase-HPLC/MS to profile lipid species from lipid droplets**

As the gain in significant improvements by 2D chromatography is low in relation to considerable more experimental effort and time needed, our method of choice is reversed-phase HPLC/MS. This allows identification of lipid species by exact mass, MS/MS spectra and retention time in one platform (Figure 1). Exact mass and retention time are then used by LDA for identification and peak integration as described previously (7), whereas MS/MS spectra are inspected manually for confirmation of identity and fatty acid analysis of lipid molecular species. If MS/MS spectra for some species are not available confirmation of identity can be deduced from retention time shifts (Figure 4), a practical example of the latter is given in Figure 7. Due to these procedures the platform is able to identify lipid species as low as 0.1‰ of the respective base peak of a given lipid class with a high degree of certainty,

even besides bulk amounts of a few lipid species. Thus, we were able to identify 103 minor TG species beside 19 major TG species, with each of the minor TG species contributing less than 10‰ of the total amount of TG. The total number of lipids identified account to 122 TG and 41 DG species, 28 PC, 18 PE, 4 PS and 9 PI species (PC compared to the latter three being the dominant phospholipid class), and finally 13 LPC and 7 SM species. Ether-linked phospholipids (e.g. plasmalogens) were searched for but were not detected. Figure 8 shows the molar proportion of each lipid class relative to total lipid amount in the pooled samples. All individual lipid species found in pooled lipid droplets are shown in Tables 1S–3S (supplementary data), presenting data of quantitative analysis including respective retention times. For example, TG 62:14 contributes with as little as 0.066‰ to total amount of TG, in LPC 16:0, 18:2, 18:0, 22:6 and 20:4 fatty acyls predominate, in minor lipid classes PE, PS and PI 38:4 species (18:0/20:4) are the most prominent ones. Very long-chain fatty acyls 22:0, 24:0 and 24:1 predominate in SM species.
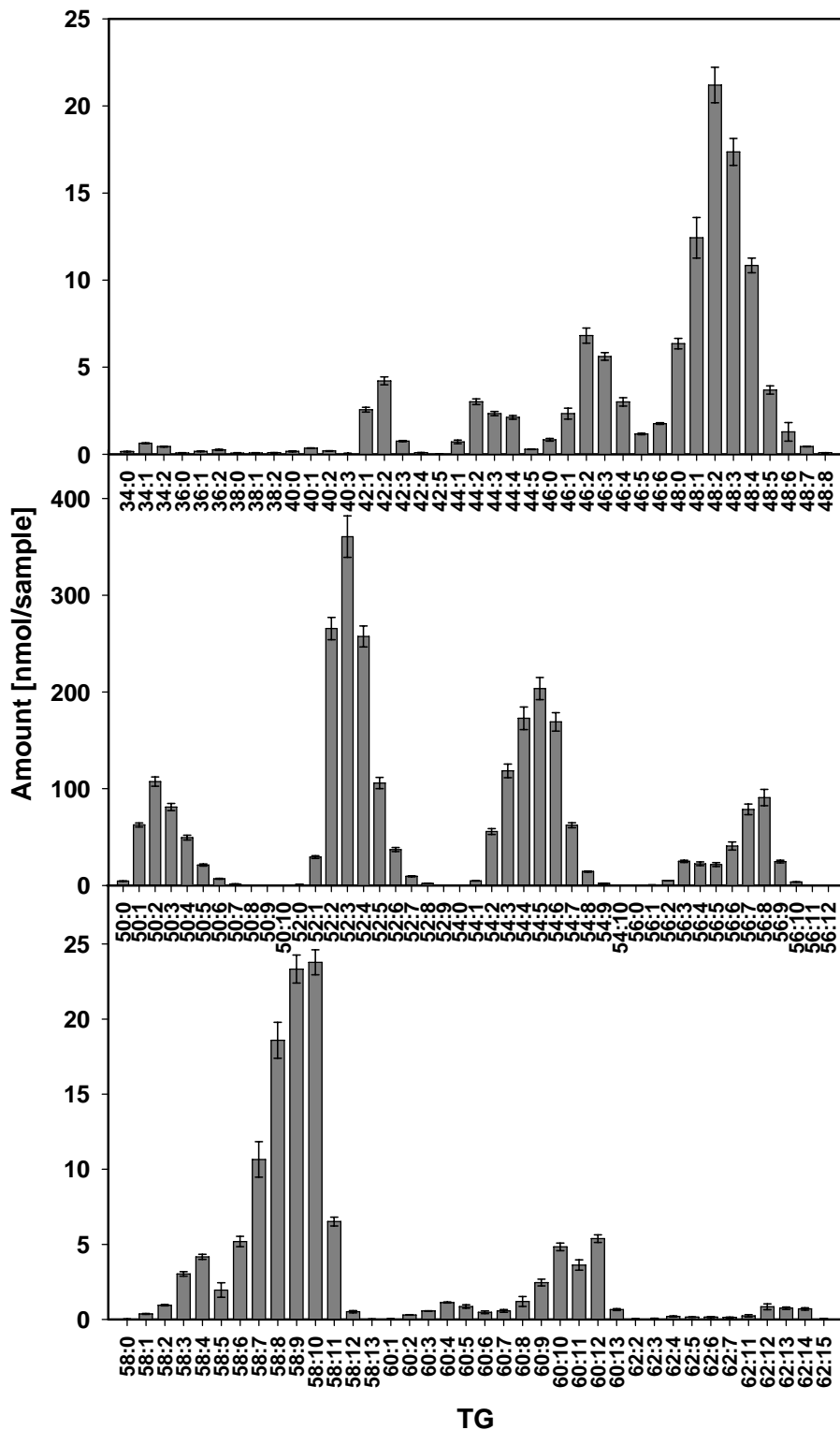
**Figure 7.** Amount of lipid droplet TG species. TG species are determined by reversed-phase-HPLC/LTQ-FT and values are automatically calculated by LDA. Data presented in nmol/sample are means ± SD (n = 5). Please note the larger concentration scale for $C_{50}$ to $C_{56}$ species.
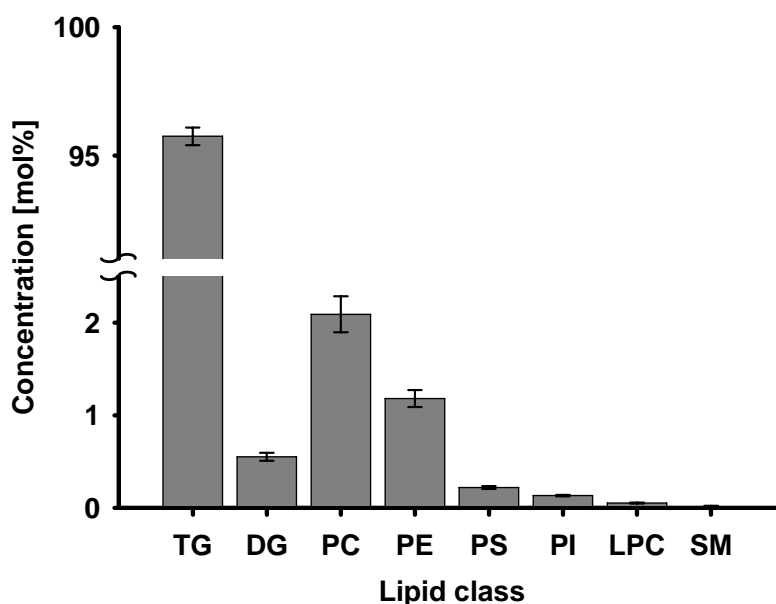
**Figure 8.** Contribution of lipid classes to a pooled lipid droplet sample. Lipid species are determined by reversed-phase-HPLC/LTQ-FT and values are automatically calculated by LDA. Each lipid class is expressed in mol% by their relative molar contribution to total lipids. Data are means ± SD (n = 5).

**Validation of method**

Calibration curves were performed for TG 17:0/17:0/17:0, PC 12:0/12:0, PE 12:0/12:0 and PS 12:0/12:0 showing a linear range of 4 orders of magnitude (Table 4S). The lowest concentration points of the calibration curves are all at a signal to noise (S/N) ratio better than 10:1, a value generally referred to in the literature, thus defining the Limit of Quantitation (LOQ). Accuracy and precision were determined for five replicas spiked with these compounds. The former is within 20% deviation, the latter is below 10% relative standard deviation (Table 4S). All species detected show an S/N ratio of at least 34:1 or better, well above the Limit of Detection (LOD) defined at S/N 3:1. The mean retention time deviation of all acquired lipid species is 0.37% (n=5).

## DISCUSSION

Excellent LC/MS methods were developed based on Orbitrap and LTQ-FT mass spectrometry, though up to date they are restricted exclusively to analysis of phospholipids (19, 20, 33). LC/MS analysis of lipid species by low resolution multiple reaction monitoring (MRM), applicable to a preset list of expected lipids only, was also described (34, 35). In this work, however, a method for comprehensive profiling of lipid species is presented, enabling data acquisition in one HPLC run per ionization polarity. Our platform provides full scan data of high resolution ion cyclotron resonance mass spectrometry. Untargeted MS/MS data, which can be used in an untargeted manner in subsequent bioinformatics analysis are also provided. This is an important aspect when high throughput data generation in 'omics' sciences is required. Flexibility of the platform offers a further advantage, i.e., integration of 'unexpected' lipid species present in a sample into ongoing analysis. Without any need to re-run a sample, this requires only re-analysis by LDA with a database expanded by the unexpected lipid species.

Clearly, shotgun and flow injection lipidomic analysis are closest to high throughput data generation as proven by successful application to biological entities having a more or less common lipid class distribution (8, 10, 36). But in samples containing bulk amounts of a certain lipid class, pre-separation is mandatory (13), due to ion suppression exerted in MS on minor components of the lipidome that would remain undetected. Taking the example of lipid droplet analysis, we demonstrate here that reversed-phase-HPLC coupled to MS monitoring is the method of choice for profiling of glycerolipids, glycerophospholipids and sphingolipids even in the presence of a huge excess of TG species. From the quantitative point of view unambiguous detection of lipid species is possible at a concentration which is 4 orders of magnitude lower than the base peak in the respective lipid class. In fact, the platform is a valuable tool for detection of changes occurring in very low concentration ranges of a lipid species compared to the total amount of lipid species in a given sample.

The limitation of reversed-phase-HPLC is separation of PC from other phospholipid classes. This could be overcome by adding a second chromatographic dimension with complementary selectivity. A separator linking the two chromatographic dimensions for automated analysis was developed recently, but is not commercially available (15). In the case of lipid droplet analysis reported here, we carried out such an approach by manually linking the two chromatographic dimensions and indeed we found enhanced sensitivity for detection of PE and DG species; enhancement of PS species was not significant. Obviously in positive ESI mode these lipid classes benefit particularly from PC removal by the first chromatographic dimension.

Shotgun lipidomics of chromatographically not separated, overlapping M+2 peaks requires isotopic correction (8). This is not necessary here, due to chromatographic resolution and the

extremely high mass resolution delivered by the ion cyclotron. Several combinations of chromatography (retention time), high mass accuracy and MS/MS information are addressed in the literature (15, 19, 20, 25). But the combination of all these parameters including bioinformatic tools integrated in one platform applicable to a wide variety of lipid classes is the novel concept realized in this work. All this results in high identification certainty, sensitivity and selectivity, and contributes significantly to unambiguous detection of minor lipid species.

**ACKNOWLEDGEMENT**

**REFERENCES**

1.  Wenk, M. R. 2005. The emerging field of lipidomics. *Nat Rev Drug Discov* 4: 594-610.

2.  Watson, A. D. 2006. Thematic review series: systems biology approaches to metabolic and cardiovascular disorders. Lipidomics: a global approach to lipid analysis in biological systems. *J Lipid Res* 47: 2101-2111.

3.  Ekroos, K., M. Janis, K. Tarasov, R. Hurme, and R. Laaksonen. 2010. Lipidomics: a tool for studies of atherosclerosis. *Curr Atheroscler Rep* 12: 273-281.

4.  Shevchenko, A., and K. Simons. 2010. Lipidomics: coming to grips with lipid diversity. *Nat Rev Mol Cell Biol* 11: 593-598.

5.  Ivanova, P. T., S. B. Milne, J. S. Forrester, and H. A. Brown. 2004. Lipid arrays: New tools in the understanding of membrane dynamics and lipid signaling. *Mol Interv* 4: 86-96.

6.  Griffiths, W. J. 2003. Tandem mass spectrometry in the study of fatty acids, bile acids, and steroids. *Mass Spectrom Rev* 22: 81-152.

7.  Hartler, J., M. Trötzmüller, C. Chitraju, F. Spener, H. C. Köfeler, and G. G. Thallinger. 2011. Lipid Data Analyzer: unattended identification and quantitation of lipids in LC-MS data. *Bioinformatics* 27: 572-577.

8.  Han, X. L., and R. W. Gross. 2005. Shotgun lipidomics: Electrospray ionization mass spectrometric analysis and quantitation of cellular lipidomes directly from crude extracts of biological samples. *Mass Spectrom Rev* 24: 367-412.

9.  Han, X. L., and R. W. Gross. 2003. Global analyses of cellular lipidomes directly from crude extracts of biological samples by ESI mass spectrometry: a bridge to lipidomics. *J Lipid Res* 44: 1071-1079.

10. Ejsing, C. S., J. L. Sampaio, V. Surendranath, E. Duchoslav, K. Ekroos, R. W. Klemm, K. Simons, and A. Shevchenko. 2009. Global analysis of the yeast lipidome by quantitative shotgun mass spectrometry. *Proc Natl Acad Sci U S A* 106: 2136-2141.

11. Han, X. L., J. Y. Yang, H. Cheng, H. P. Ye, and R. W. Gross. 2004. Toward fingerprinting cellular lipidomes directly from biological samples by two-dimensional electrospray ionization mass spectrometry. *Anal Biochem* 330: 317-331.

12. Han, X. L., and R. W. Gross. 2005. Shotgun lipidomics: multidimensional MS analysis of cellular lipidomes. *Expert Rev Proteomics* 2: 253-264.

13. Stahlman, M., C. S. Ejsing, K. Tarasov, J. Perman, J. Borén, and K. Ekroos. 2009. High-throughput shotgun lipidomics by quadrupole time-of-flight mass spectrometry. *J Chromatogr B Analyt Technol Biomed Life Sci* 877: 2664-2672.

14. Han, X., K. Yang, and R. W. Gross. 2011. Multi-dimensional mass spectrometry-based shotgun lipidomics and novel strategies for lipidomic analyses. *Mass Spectrom Rev.* In press.

15. Nie, H., R. Liu, Y. Yang, Y. Bai, Y. Guan, D. Qian, T. Wang, and H. Liu. 2010. Lipid profiling of rat peritoneal surface layers by online normal- and reversed-phase 2D LC QToF-MS. *J Lipid Res* 51: 2833-2844.

16. Pang, L. Q., Q. L. Liang, Y. M. Wang, L. Ping, and G. A. Luo. 2008. Simultaneous determination and quantification of seven major phospholipid classes in human blood using normal-phase liquid chromatography coupled with electrospray mass spectrometry and the application in diabetes nephropathy. *J Chromatogr B Analyt Technol Biomed Life Sci* 869: 118-125.

17. Ogiso, H., T. Suzuki, and R. Taguchi. 2008. Development of a reverse-phase liquid chromatography electrospray ionization mass spectrometry method for lipidomics, improving detection of phosphatidic acid and phosphatidylserine. *Anal Biochem* 375: 124-131.

18. Hutchins, P. M., R. M. Barkley, and R. C. Murphy. 2008. Separation of cellular nonpolar neutral lipids by normal-phase chromatography and analysis by electrospray ionization mass spectrometry. *J Lipid Res* 49: 804-813.

19. Hein, E. M., L. M. Blank, J. Heyland, J. I. Baumbach, A. Schmid, and H. Hayen. 2009. Glycerophospholipid profiling by high-performance liquid chromatography/mass spectrometry using exact mass measurements and multi-stage mass spectrometric fragmentation experiments in parallel. *Rapid Commun Mass Spectrom* 23: 1636-1646.

20. Taguchi, R., and M. Ishikawa. 2010. Precise and global identification of phospholipid molecular species by an Orbitrap mass spectrometer and automated search engine Lipid Search. *J Chromatogr A* 1217: 4229-4239.

21. Scherer, M., K. Leuthauser-Jaschinski, J. Ecker, G. Schmitz, and G. Liebisch. 2010. A rapid and quantitative LC-MS/MS method to profile sphingolipids. *J Lipid Res* 51: 2001-2011.

22. Scherer, M., G. Schmitz, and G. Liebisch. 2010. Simultaneous quantification of cardiolipin, bis(monoacylglycero)phosphate and their precursors by hydrophilic interaction LC-MS/MS including correction of isotopic overlap. *Anal Chem* 82: 8794-8799.

23. Pettitt, T. R., S. K. Dove, A. Lubben, S. D. J. Calaminus, and M. J. O. Wakelam. 2006. Analysis of intact phosphoinositides in biological samples. *J Lipid Res* 47: 1588-1596.

24. Wagner, S., and E. Richling. 2010. LC-ESI-MS Determination of phospholipids and lysophospholipids. *Chromatographia* 72: 659-664.

25. Yetukuri, L., M. Katajamaa, G. Medina-Gomez, T. Seppanen-Laakso, A. Vidal-Puig, and M. Oresic. 2007. Bioinformatics strategies for lipidomics analysis: characterization of obesity related hepatic steatosis. *BMC Syst Biol* 1.

26. Guo, Y., T. C. Walther, M. Rao, N. Stuurman, G. Goshima, K. Terayama, J. S. Wong, R. D. Vale, P. Walter, and R. V. Farese. 2008. Functional genomic screen reveals genes involved in lipid-droplet formation and utilization. *Nature* 453: 657-661.

27. Blouin, C. M., S. Le Lay, A. Eberl, H. C. Kofeler, I. C. Guerrera, C. Klein, X. Le Liepvre, F. Lasnier, O. Bourron, J. F. Gautier, P. Ferre, E. Hajduch, and I. Dugail. 2010. Lipid droplet analysis in caveolin-deficient adipocytes: alterations in surface phospholipid composition and maturation defects. *J Lipid Res* 51: 945-956.

28. Riccalton-Banks, L., R. Bhandari, J. Fry, and K. M. Shakesheff. 2003. A simple method for the simultaneous isolation of stellate cells and hepatocytes from rat liver tissue. *Mol Cell Biochem* 248: 97-102.

29. Matyash, V., G. Liebisch, T. V. Kurzchalia, A. Shevchenko, and D. Schwudke. 2008. Lipid extraction by methyl-tert-butyl ether for high-throughput lipidomics. *J Lipid Res* 49: 1137-1146.

30. Haas, W., B. K. Faherty, S. A. Gerber, J. E. Elias, S. A. Beausoleil, C. E. Bakalarski, X. Li, J. Villen, and S. P. Gygi. 2006. Optimization and use of peptide mass measurement accuracy in shotgun proteomics. *Mol Cell Proteomics* 5: 1326-1337.

31. Pulfer, M., and R. C. Murphy. 2003. Electrospray mass spectrometry of phospholipids. *Mass Spectrom Rev* 22: 332-364.

32. Brouwers, J., E. Vernooij, A. G. M. Tielens, and L. M. G. van Golde. 1999. Rapid separation and identification of phosphatidylethanolamine molecular species. *J Lipid Res* 40: 164-169.

33. Houjou, T., K. Yamatani, M. Imagawa, T. Shimizu, and R. Taguchi. 2005. A shotgun tandem mass spectrometric analysis of phospholipids with normal-phase and/or reverse-phase liquid chromatography/electrospray ionization mass spectrometry. *Rapid Commun Mass Spectrom* 19: 654-666.

34. Quehenberger, O., A. M. Armando, A. H. Brown, S. B. Milne, D. S. Myers, A. H. Merrill, S. Bandyopadhyay, K. N. Jones, S. Kelly, R. L. Shaner, C. M. Sullards, E. Wang, R. C. Murphy, R. M. Barkley, T. J. Leiker, C. R. H. Raetz, Z. Q. Guan, G. M. Laird, D. A. Six, D. W. Russell, J. G. McDonald, S. Subramaniam, E. Fahy, and E. A. Dennis. 2010. Lipidomics reveals a remarkable diversity of lipids in human plasma. *J Lipid Res* 51: 3299-3305.

35. McAnoy, A. M., C. C. Wu, and R. C. Murphy. 2005. Direct qualitative analysis of triacylglycerols by electrospray mass spectrometry using a linear ion trap. *J Mass Spectrom* 16: 1498-1509.

36. Liebisch, G., B. Lieser, J. Rathenberg, W. Drobnik, and G. Schmitz. 2004. High-throughput quantification of phosphatidylcholine and sphingomyelin by electrospray

ionization tandem mass spectrometry coupled with isotope correction algorithm. *Biochim Biophys Acta* 1686: 108-117.

**SUPPLEMENTENTAL DATA**

**Supplementary Table 1S.** TG species (detected as $[M+NH_4]^+$) of lipid droplets from mouse hepatocytes. Amount of species is calculated per lipid droplet sample and retention times. All data are means ± SD (n = 5).

| Species | m/z | Amount [nmol/sample ±SD] | Retention time [min] | Species | m/z | Amount [nmol/sample ±SD] | Retention time [min] |
|---|---|---|---|---|---|---|---|
| TG 34:0 | 628.55103 | 0.156 ± 0.015 | 19.3 | TG 48:7 | 810.66058 | 0.439 ± 0.015 | 21.0 |
| TG 34:1 | 626.53538 | 0.633 ± 0.025 | 17.8 | TG 48:8 | 808.64493 | 0.090 ± 0.007 | 20.1 |
| TG 34:2 | 624.51973 | 0.438 ± 0.026 | 16.5 | TG 50:0 | 852.80143 | 4.524 ± 0.258 | 27.7 |
| TG 36:0 | 656.58233 | 0.072 ± 0.016 | 20.6 | TG 50:1 | 850.78578 | 62.496 ± 2.154 | 26.6 |
| TG 36:1 | 654.56668 | 0.167 ± 0.023 | 19.3 | TG 50:2 | 848.77013 | 107.402 ± 4.786 | 25.6 |
| TG 36:2 | 652.55103 | 0.257 ± 0.034 | 17.6 | TG 50:3 | 846.75448 | 81.042 ± 3.740 | 24.6 |
| TG 38:0 | 684.61363 | 0.064 ± 0.022 | 21.7 | TG 50:4 | 844.73883 | 49.430 ± 2.406 | 23.9 |
| TG 38:1 | 682.59798 | 0.077 ± 0.012 | 20.6 | TG 50:5 | 842.72318 | 21.173 ± 0.992 | 23.2 |
| TG 38:2 | 680.58233 | 0.092 ± 0.009 | 19.5 | TG 50:6 | 840.70753 | 6.863 ± 0.449 | 22.6 |
| TG 40:0 | 712.64493 | 0.165 ± 0.028 | 22.7 | TG 50:7 | 838.69188 | 1.506 ± 0.065 | 21.8 |
| TG 40:1 | 710.62928 | 0.346 ± 0.020 | 21.7 | TG 50:8 | 836.67623 | 0.185 ± 0.025 | 21.1 |
| TG 40:2 | 708.61363 | 0.197 ± 0.004 | 20.7 | TG 50:9 | 834.66058 | 0.015 ± 0.004 | 20.4 |
| TG 40:3 | 706.59798 | 0.050 ± 0.008 | 19.7 | TG 50:10 | 832.64493 | 0.007 ± 0.002 | 19.6 |
| TG 42:1 | 738.66058 | 2.560 ± 0.139 | 22.8 | TG 52:0 | 880.83273 | 0.971 ± 0.072 | 28.9 |
| TG 42:2 | 736.64493 | 4.212 ± 0.228 | 21.8 | TG 52:1 | 878.81708 | 29.347 ± 1.327 | 27.7 |
| TG 42:3 | 734.62928 | 0.755 ± 0.034 | 20.8 | TG 52:2 | 876.80143 | 265.520 ± 11.528 | 26.6 |
| TG 42:4 | 732.61363 | 0.093 ± 0.008 | 19.9 | TG 52:3 | 874.78578 | 360.535 ± 21.389 | 25.6 |
| TG 42:5 | 730.59798 | 0.010 ± 0.005 | 19.3 | TG 52:4 | 872.77013 | 257.342 ± 10.894 | 24.7 |
| TG 44:1 | 766.69188 | 0.712 ± 0.103 | 23.7 | TG 52:5 | 870.75448 | 105.890 ± 5.817 | 24.0 |
| TG 44:2 | 764.67623 | 3.016 ± 0.160 | 22.8 | TG 52:6 | 868.73883 | 37.164 ± 2.010 | 23.3 |
| TG 44:3 | 762.66058 | 2.339 ± 0.117 | 22.0 | TG 52:7 | 866.72318 | 9.478 ± 0.504 | 22.6 |
| TG 44:4 | 760.64493 | 2.117 ± 0.106 | 21.3 | TG 52:8 | 864.70753 | 2.132 ± 0.174 | 22.1 |
| TG 44:5 | 758.62928 | 0.283 ± 0.012 | 20.2 | TG 52:9 | 862.69188 | 0.311 ± 0.024 | 21.3 |
| TG 46:0 | 796.73883 | 0.829 ± 0.075 | 25.7 | TG 54:0 | 908.86403 | 0.156 ± 0.012 | 30.4 |
| TG 46:1 | 794.72318 | 2.333 ± 0.319 | 24.5 | TG 54:1 | 906.84838 | 4.743 ± 0.205 | 28.8 |
| TG 46:2 | 792.70753 | 6.814 ± 0.438 | 23.7 | TG 54:2 | 904.83273 | 55.791 ± 2.993 | 27.7 |
| TG 46:3 | 790.69188 | 5.614 ± 0.222 | 23.0 | TG 54:3 | 902.81708 | 118.417 ± 7.051 | 26.6 |
| TG 46:4 | 788.67623 | 3.006 ± 0.245 | 22.4 | TG 54:4 | 900.80143 | 172.838 ± 11.679 | 25.6 |
| TG 46:5 | 786.66058 | 1.170 ± 0.043 | 21.4 | TG 54:5 | 898.78578 | 203.479 ± 11.519 | 24.8 |
| TG 46:6 | 784.64493 | 1.762 ± 0.045 | 20.9 | TG 54:6 | 896.77013 | 169.136 ± 9.485 | 24.1 |
| TG 48:0 | 824.77013 | 6.352 ± 0.303 | 26.7 | TG 54:7 | 894.75448 | 62.342 ± 2.540 | 23.4 |
| TG 48:1 | 822.75448 | 12.431 ± 1.163 | 25.5 | TG 54:8 | 892.73883 | 14.365 ± 0.603 | 22.7 |
| TG 48:2 | 820.73883 | 21.199 ± 1.016 | 24.6 | TG 54:9 | 890.72318 | 2.275 ± 0.100 | 22.1 |
| TG 48:3 | 818.72318 | 17.363 ± 0.776 | 23.8 | TG 54:10 | 888.70753 | 0.248 ± 0.071 | 21.7 |
| TG 48:4 | 816.70753 | 10.842 ± 0.422 | 23.1 | TG 56:0 | 936.89533 | 0.085 ± 0.017 | 32.9 |
| TG 48:5 | 814.69188 | 3.690 ± 0.234 | 22.4 | TG 56:1 | 934.87968 | 0.582 ± 0.042 | 30.4 |
| TG 48:6 | 812.67623 | 1.289 ± 0.537 | 21.8 | TG 56:2 | 932.86403 | 5.195 ± 0.138 | 28.8 |

| Species | m/z | Amount [nmol/sample ±SD] | Retention time [min] | Species | m/z | Amount [nmol/sample ±SD] | Retention time [min] |
|---------|-----|--------------------------|----------------------|---------|-----|--------------------------|----------------------|
| TG 56:3 | 930.84838 | 24.947 ± 1.143 | 27.6 | TG 60:1 | 990.94228 | 0.031 ± 0.016 | 34.3 |
| TG 56:4 | 928.83273 | 22.413 ± 1.909 | 26.6 | TG 60:2 | 988.92663 | 0.300 ± 0.018 | 32.1 |
| TG 56:5 | 926.81708 | 21.633 ± 1.988 | 26.1 | TG 60:3 | 986.91098 | 0.561 ± 0.018 | 30.3 |
| TG 56:6 | 924.80143 | 40.797 ± 4.175 | 25.1 | TG 60:4 | 984.89533 | 1.125 ± 0.032 | 28.8 |
| TG 56:7 | 922.78578 | 78.569 ± 5.527 | 24.4 | TG 60:5 | 982.87968 | 0.856 ± 0.117 | 27.6 |
| TG 56:8 | 920.77013 | 90.798 ± 8.416 | 23.8 | TG 60:6 | 980.86403 | 0.470 ± 0.090 | 27.0 |
| TG 56:9 | 918.75448 | 24.669 ± 1.378 | 23.1 | TG 60:7 | 978.84838 | 0.568 ± 0.090 | 26.2 |
| TG 56:10 | 916.73883 | 3.622 ± 0.231 | 22.4 | TG 60:8 | 976.83273 | 1.195 ± 0.328 | 25.4 |
| TG 56:11 | 914.72318 | 0.321 ± 0.013 | 21.8 | TG 60:9 | 974.81708 | 2.454 ± 0.224 | 24.3 |
| TG 56:12 | 912.70753 | 0.043 ± 0.013 | 21.1 | TG 60:10 | 972.80143 | 4.831 ± 0.251 | 23.7 |
| TG 58:0 | 964.92663 | 0.023 ± 0.007 | 34.5 | TG 60:11 | 970.78578 | 3.623 ± 0.345 | 23.5 |
| TG 58:1 | 962.91098 | 0.368 ± 0.028 | 32.3 | TG 60:12 | 968.77013 | 5.380 ± 0.255 | 23.0 |
| TG 58:2 | 960.89533 | 0.946 ± 0.045 | 30.3 | TG 60:13 | 966.75448 | 0.656 ± 0.059 | 22.2 |
| TG 58:3 | 958.87968 | 3.032 ± 0.152 | 28.8 | TG 62:2 | 1016.95793 | 0.031 ± 0.018 | 34.2 |
| TG 58:4 | 956.86403 | 4.166 ± 0.167 | 27.6 | TG 62:3 | 1014.94228 | 0.073 ± 0.008 | 32.2 |
| TG 58:5 | 954.84838 | 1.951 ± 0.483 | 27.1 | TG 62:4 | 1012.92663 | 0.193 ± 0.038 | 29.0 |
| TG 58:6 | 952.83273 | 5.188 ± 0.349 | 26.1 | TG 62:5 | 1010.91098 | 0.150 ± 0.008 | 28.6 |
| TG 58:7 | 950.81708 | 10.656 ± 1.180 | 25.1 | TG 62:6 | 1008.89533 | 0.153 ± 0.031 | 28.1 |
| TG 58:8 | 948.80143 | 18.592 ± 1.193 | 24.4 | TG 62:7 | 1006.87968 | 0.131 ± 0.030 | 27.4 |
| TG 58:9 | 946.78578 | 23.334 ± 0.937 | 23.9 | TG 62:11 | 998.81708 | 0.236 ± 0.081 | 24.2 |
| TG 58:10 | 944.77013 | 23.783 ± 0.830 | 23.2 | TG 62:12 | 996.80143 | 0.840 ± 0.197 | 23.6 |
| TG 58:11 | 942.75448 | 6.517 ± 0.299 | 22.6 | TG 62:13 | 994.78578 | 0.747 ± 0.079 | 23.1 |
| TG 58:12 | 940.73883 | 0.510 ± 0.076 | 21.9 | TG 62:14 | 992.77013 | 0.697 ± 0.077 | 22.4 |
| TG 58:13 | 938.72318 | 0.022 ± 0.005 | 21.3 | TG 62:15 | 990.75448 | 0.050 ± 0.008 | 21.8 |

**Supplementary Table 2S**. DG species (detected as [M+NH$_4$]$^+$) and PC species (detected as [M+H]$^+$) of lipid droplets from mouse hepatocytes. Amount of species is calculated per lipid droplet samples and retention times. All data are means ± SD (n = 5).

| Species | m/z | Amount [nmol/sample ±SD] | Retention time [min] | Species | m/z | Amount [nmol/sample ±SD] | Retention time [min] |
|---|---|---|---|---|---|---|---|
| DG 32:0 | 586.54047 | 300.38 ± 24.54 | 18.3 | DG 40:9 | 680.52482 | 49.35 ± 2.52 | 14.0 |
| DG 32:1 | 584.52482 | 695.84 ± 25.00 | 16.9 | DG 42:6 | 714.60307 | 91.38 ± 5.53 | 18.1 |
| DG 32:2 | 582.50917 | 573.59 ± 13.27 | 15.6 | DG 42:7 | 712.58742 | 237.37 ± 12.4 | 16.5 |
| DG 32:3 | 580.49352 | 94.73 ± 14.55 | 14.2 | DG 42:8 | 710.57177 | 179.09 ± 6.45 | 15.5 |
| DG 32:4 | 578.47787 | 20.44 ± 9.62 | 13.0 | DG 42:9 | 708.55612 | 19.10 ± 8.79 | 15.5 |
| DG 34:0 | 614.57177 | 124.21 ± 10.02 | 19.7 | DG 42:10 | 706.54047 | 65.06 ± 14.65 | 14.9 |
| DG 34:1 | 612.55612 | 8298.71 ± 686.49 | 18.5 | PC 32:0 | 734.56939 | 386.03 ± 12.10 | 16.4 |
| DG 34:2 | 610.54047 | 20221.90 ± 419.74 | 17.2 | PC 32:1 | 732.55374 | 321.63 ± 20.15 | 14.4 |
| DG 34:3 | 608.52482 | 4087.52 ± 196.49 | 15.8 | PC 32:2 | 730.53809 | 101.63 ± 7.55 | 13.0 |
| DG 34:4 | 606.50917 | 486.11 ± 18.18 | 14.5 | PC 32:3 | 728.52299 | 6.45 ± 1.15 | 11.4 |
| DG 34:5 | 604.49352 | 94.98 ± 5.61 | 13.6 | PC 34:0 | 762.60069 | 40.62 ± 7.44 | 18.9 |
| DG 34:6 | 602.47787 | 10.04 ± 1.15 | 12.5 | PC 34:1 | 760.58504 | 5229.24 ± 125.97 | 16.5 |
| DG 36:0 | 642.60307 | 14.32 ± 1.41 | 20.9 | PC 34:2 | 758.56939 | 17464.93 ± 510.93 | 14.9 |
| DG 36:1 | 640.58742 | 658.78 ± 77.87 | 19.8 | PC 34:3 | 756.55374 | 1032.61 ± 20.49 | 13.4 |
| DG 36:2 | 638.57177 | 9087.16 ± 763.71 | 18.7 | PC 34:4 | 754.53809 | 65.75 ± 4.95 | 11.7 |
| DG 36:3 | 636.55612 | 18979.12 ± 533.24 | 17.4 | PC 36:1 | 788.61634 | 601.92 ± 39.32 | 18.9 |
| DG 36:4 | 634.54047 | 12996.29 ± 510.59 | 16.1 | PC 36:2 | 786.60069 | 6568.78 ± 197.38 | 17.0 |
| DG 36:5 | 632.52482 | 1781.85 ± 45.91 | 14.9 | PC 36:3 | 784.58504 | 3584.64 ± 151.56 | 15.1 |
| DG 36:6 | 630.50917 | 208.32 ± 12.36 | 13.8 | PC 36:4 | 782.56939 | 8762.38 ± 203.00 | 14.5 |
| DG 36:7 | 628.49352 | 10.85 ± 2.38 | 13.2 | PC 36:5 | 780.55374 | 402.84 ± 23.43 | 12.8 |
| DG 38:1 | 668.61872 | 31.33 ± 8.61 | 21.0 | PC 36:6 | 778.53809 | 36.73 ± 4.18 | 11.3 |
| DG 38:2 | 666.60307 | 380.64 ± 30.51 | 19.9 | PC 38:2 | 814.63199 | 73.20 ± 8.68 | 19.1 |
| DG 38:3 | 664.58742 | 1006.75 ± 69.15 | 18.9 | PC 38:3 | 812.61634 | 349.59 ± 73.74 | 18.2 |
| DG 38:4 | 662.57177 | 2584.82 ± 138.45 | 18.4 | PC 38:4 | 810.60069 | 5111.87 ± 194.42 | 16.4 |
| DG 38:5 | 660.55612 | 2071.09 ± 121.93 | 17.0 | PC 38:5 | 808.58504 | 2201.14 ± 299.2 | 14.6 |
| DG 38:6 | 658.54047 | 4338.53 ± 215.67 | 16.3 | PC 38:6 | 806.56939 | 7006.83 ± 329.74 | 14.0 |
| DG 38:7 | 656.52482 | 299.14 ± 22.70 | 14.7 | PC 38:7 | 804.55374 | 178.81 ± 12.85 | 12.0 |
| DG 38:8 | 654.50917 | 17.57 ± 1.23 | 13.6 | PC 38:8 | 802.53864 | 4.11 ± 0.32 | 11.1 |
| DG 40:2 | 694.63437 | 21.26 ± 7.03 | 21.1 | PC 40:3 | 840.64764 | 1.66 ± 0.78 | 19.5 |
| DG 40:3 | 692.61872 | 41.90 ± 11.56 | 20.1 | PC 40:4 | 838.63199 | 63.11 ± 4.63 | 18.4 |
| DG 40:4 | 690.60307 | 333.57 ± 40.92 | 18.3 | PC 40:5 | 836.61634 | 169.05 ± 10.12 | 17.9 |
| DG 40:5 | 688.58742 | 579.54 ± 28.59 | 18.2 | PC 40:6 | 834.60069 | 2211.6 ± 120.07 | 15.9 |
| DG 40:6 | 686.57177 | 1704.28 ± 55.62 | 17.2 | PC 40:7 | 832.58504 | 662.78 ± 28.13 | 14.1 |
| DG 40:7 | 684.55612 | 1374.55 ± 111.13 | 16.4 | PC 40:8 | 830.56939 | 221.08 ± 11.82 | 12.8 |
| DG 40:8 | 682.54047 | 944.67 ± 34.94 | 15.2 | | | | |

134

**Supplementary Table 3S.** SM, PS, PE, LPC species (detected as [M+H]$^+$) and PI species (detected as [M-H]$^-$) of lipid droplets from mouse hepatocytes. Amount of species is calculated per lipid droplet sample and retention times. All data are means ± SD (n = 5).

| Species | m/z | Amount [nmol/sample ±SD] | Retention time [min] | Species | m/z | Amount [nmol/sample ±SD] | Retention time [min] |
|---|---|---|---|---|---|---|---|
| SM 16:0 | 703.57481 | 494.39 ± 33.84 | 13.6 | PE 40:6 | 792.55374 | 3240.33 ± 208.36 | 15.6 |
| SM 16:1 | 701.55916 | 29.79 ± 2.65 | 11.5 | PE 40:7 | 790.53809 | 1207.82 ± 22.30 | 14.0 |
| SM 18:0 | 731.60611 | 48.29 ± 5.74 | 15.9 | PE 40:8 | 788.52244 | 203.58 ± 14.30 | 11.7 |
| SM 22:0 | 787.66871 | 1047.31 ± 97.21 | 20.3 | LPC 16:0 | 496.33973 | 3017.9 ± 404.99 | 3.5 |
| SM 22:1 | 785.65306 | 100.64 ± 35.58 | 18.5 | LPC 16:1 | 494.32408 | 85.29 ± 13.76 | 2.5 |
| SM 24:1 | 813.68436 | 1210.75 ± 687.52 | 20.2 | LPC 18:0 | 524.37103 | 1345.24 ± 202.65 | 4.9 |
| SM 24:2 | 811.66871 | 199.41 ± 29.25 | 18.5 | LPC 18:1 | 522.35538 | 724.01 ± 98.41 | 3.8 |
| PS 36:4 | 784.51226 | 332.46 ± 67.62 | 13.4 | LPC 18:2 | 520.33973 | 1636.58 ± 57.23 | 2.9 |
| PS 38:4 | 812.54356 | 3655.80 ± 166.55 | 15.1 | LPC 18:3 | 818.32408 | 9.56 ± 7.75 | 2.2 |
| PS 38:6 | 808.51226 | 425.47 ± 26.16 | 12.8 | LPC 20:0 | 552.40233 | 8.80 ± 5.02 | 6.3 |
| PS 40:6 | 836.54356 | 1906.75 ± 148.91 | 14.6 | LPC 20:1 | 550.38668 | 13.42 ± 3.96 | 5.1 |
| PE 34:1 | 718.53809 | 237.95 ± 26.58 | 16.2 | LPC 20:2 | 548.37103 | 7.01 ± 2.82 | 4.1 |
| PE 34:2 | 716.52244 | 2148.73 ± 106.8 | 14.6 | LPC 20:3 | 546.35538 | 58.03 ± 15.41 | 3.7 |
| PE 34:3 | 714.50679 | 159.86 ± 15.97 | 13.1 | LPC 20:4 | 544.33973 | 879.22 ± 99.66 | 2.8 |
| PE 36:1 | 746.56939 | 58.85 ± 9.00 | 17.9 | LPC 22:5 | 570.35538 | 105.21 ± 15.72 | 3.0 |
| PE 36:2 | 744.55374 | 2063.50 ± 89.43 | 16.5 | LPC 22:6 | 568.33973 | 1018.52 ± 73.71 | 2.7 |
| PE 36:3 | 742.53809 | 989.45 ± 44.84 | 14.9 | PI 34:1 | 835.53414 | 128.05 ± 10.67 | 12.8 |
| PE 36:4 | 740.52244 | 2686.55 ± 81.03 | 14.3 | PI 34:2 | 833.51849 | 21.58 ± 1.96 | 10.8 |
| PE 36:5 | 738.50679 | 260.04 ± 8.55 | 12.7 | PI 36:2 | 861.54979 | 65.89 ± 3.49 | 12.5 |
| PE 36:6 | 736.49114 | 23.41 ± 8.75 | 11.5 | PI 36:3 | 859.53414 | 44.17 ± 1.08 | 11.1 |
| PE 38:3 | 770.56939 | 84.50 ± 10.71 | 17.1 | PI 36:4 | 857.51849 | 158.79 ± 9.70 | 10.6 |
| PE 38:4 | 768.55374 | 11675.36 ± 223.25 | 16.1 | PI 36:5 | 855.50284 | 2.66 ± 0.49 | 10.4 |
| PE 38:5 | 766.53809 | 2289.52 ± 245.28 | 14.6 | PI 38:4 | 885.54979 | 3287.86 ± 233.71 | 12.2 |
| PE 38:6 | 764.52244 | 6159.77 ± 327.64 | 13.8 | PI 38:5 | 883.53414 | 113.95 ± 8.32 | 11.1 |
| PE 38:7 | 762.50679 | 241.68 ± 37.81 | 11.6 | PI 38:6 | 881.51849 | 8.65 ± 1.43 | 10.2 |
| PE 40:5 | 794.56939 | 214.63 ± 48.39 | 16.8 | | | | |

**Supplementary Table 4S.** Calculation of accuracy and precision, and linear range for major lipid classes TG, PC, PE and PS. Lipid droplet samples are spiked with 350 pmol TG 17:0/17:0/17:0, 130 pmol PC 12:0/12:0, 270 pmol PE 12:0/12:0 and 220 pmol PS 12:0/12:0 for determination of accuracy and precision, concentration range of standards tested for determination of linear range is given in the table.

| Lipid species | Accuracy | Precision | Linear range | |
|---|---|---|---|---|
| | [%]<br>n=5 | [%, RSD]<br>n=5 | [fmol/µL]<br>n=3 | Correlation coefficient<br>n=3 |
| TG 17:0/17:0/17:0 | 105.0 | 7.4 | 0.02 - 328 | 0.952 |
| PC 12:0/12:0 | 85.8 | 4.0 | 0.02 - 328 | 0.981 |
| PE 12:0/12:0 | 90.0 | 6.3 | 0.02 - 328 | 0.956 |
| PS 12:0/12:0 | 116.1 | 9.6 | 0.02 - 328 | 0.977 |

## C.5. Characteristics and origins of common chemical noise ions in negative ESI LC-MS

Martin Trötzmüller[1], Xinghua Guo[2], Alexander Fauland[2], Harald Köfeler[1] and Ernst Lankmayr[2]

[1]Core Facility for Mass Spectrometry, Center for Medical Research, Medical University of Graz, Graz, Austria
[2]Institute of Analytical Chemistry and Food Chemistry, Graz University of Technology, Graz, Austria

**ABSTRACT**

Ionic chemical background noise in LC-MS has been one of the major problems encountered in trace analysis. In this study, the typical negative background ions in ESI LC-MS are investigated exemplarily. It was carried out using tandem mass spectrometry to study the products and precursors of the major background ions to examine their structures and structure relationship. Various typical LC eluents with different compositions and additives such as ammonium formate / formic acid and ammonium acetate/acetic acid have been studied. Several types of negative noise ions are concluded, which include the cluster chemical background ions only from mobile phase components and additives. Furthermore, there are also abundant clusters resulting from the solvation of some typical individual contaminants (e.g. additives and degradation products from tubing, and impurities in the mobile phase, etc.), accompanied by some minor contribution from contaminants. The elemental composition of some selected ions were confirmed using the FT-ICR-MS accurate mass measurement. This work provides us insight information about the structures and types of common negative background ions and will help to understand their formation and origins. More importantly, it will guide us to prevent chemical noise interference in practice and also contribute to develop methods for noise reduction based on selective ion-molecule reactions.

## INTRODUCTION

Chemical background noise ions are omnipresent by-products of atmospheric pressure ionization liquid chromatography-mass spectrometry (API LC-MS) (1, 2), resulting from the efficient and generic nature of this soft ionization technique. In mass spectrometry, any trace of ionized contaminants and stable cluster ions, which survive under mild de-clustering conditions, can contribute to chemical background noise. The consequent drawbacks observed in qualitative as well as quantitative studies include, e.g. the contribution to the high and drifting baseline in the total ion current (TIC) chromatogram, and the effect on the limits of detection or quantification (LOD/LOQ) due to the resulting low signal-to-noise ratio (S/N) and/or isobaric ion interferences. Furthermore, poor quality MS or MS/MS spectra complicate qualitative studies for identification of trace components, such as unknown metabolites, where the chemical background ions may completely overshadow the target analytes in chromatograms and even in mass spectra.

Chemical noise reduction and prevention have been as an important and interesting research topic as the exploration of the ionization technique itself. Neither hardware (3-5) nor software approaches (6-8) developed in the past decades could solve this problem completely due to the intrinsic soft and generic feature of the atmospheric pressure ionization. Most efforts of the hardware improvements for noise reduction were focused on either efficient ionization or transportation of ions into the mass analyzer. (3) The interference is almost unavoidable in LC-MS (9) due to the complex natures of the origins of the chemical background interferences as well as their mechanisms of formation, even when improved interfaces for de-clustering and desolvation have been developed and high-purity HPLC solvents and additives were applied. Moreover, it is known that the chemical interference varies sometimes significantly with HPLC mobile phases, matrices and MS ionization conditions. The contaminants can result from HPLC solvents as well as additives, tubing materials, MS ion sources and even laboratory air. The best solution is probably the selective removal or reduction of chemical background ions before they reach the MS-detector, rather than post-acquisition data processing.

Recently we have reported a novel technique of chemical noise reduction in LC-MS, which is based on selective and efficient reactions of background ions with a chosen reagent such as dimethyl disulfide, (10) ethylene oxide or butadiene monoxide. (11) The involvement of chemical reactions and resolution is the key issue for the successful noise reduction, which requires the extensive knowledge of the structures of major noise ions. An earlier study (12) has shown that, in positive mode, common chemical background ions in LC-MS can be classified into three groups: 1) cluster ions derived from mobile phase constitutes and additives; 2) clusters from the solvation of some typical contaminants (e.g. additives and degradation products from tubing, impurities in mobile phase, etc.), and accompanied by 3)

some contribution from individual contaminants. Additionally, it is concluded that there is a striking difference in structures between these chemical noise ions and (predominantly) protonated analyte ions generated using positive API. This result has contributed directly to the development of the above-mentioned noise reduction approach, (13) since it indicates further that these two types of ions (analytes and chemical noise) may have different reactivities with a chosen neutral reagent for noise reduction.

It should be noticed that the background ions in the positive mode are very different from those in the negative mode, which points out that the discovered reagents for positive noise reduction (10, 11) may not be suitable for this purpose in the negative mode because of the different chemistry involved. For the continuation of this development, it is very important to study the natures of background anions with regard to their structures and origins. For the purpose of an automatic identification and data interpretation, Tong et al. (14) has published an extensive listing of typical artifacts and cluster ions in API mass spectrometry for both positive and negative modes. Besides this, although the interference of background ions has been a serious problem even in modern mass spectrometry, (15, 16) to our knowledge, there has not been any detailed studies about the nature of negative noise ions in LC-MS. In this study, we will present a systematic characterization of typical common negative chemical background interferences using tandem mass spectrometry by classifying them into a few major groups according to their structures. The obtained information can surely help to understand the formation of negative chemical noise in LC-MS and also contribute to develop methods for noise reduction as already carried out for the positive mode(10, 11).

## EXPERIMENTAL

The unit resolution ESI-MS and ESI-MS/MS experiments were carried out using a triple quadrupole API-2000 system (MDS Sciex, Concord, ON, Canada) coupled with either a 1100 HPLC system (Agilent, Waldbonn, Germany) or an infusion pump. The turbo Ionspray ionization with the heater gas assistance under the negative mode was used with the spray voltage (IS) setting to 4500 V. The ultra-pure nitrogen (5.0) without further purification was used as the curtain and collision gases and the synthetic air as the nebulizer gas. The direct infusion flow was set to 10-50 µl/min, and the flow rate of the isocratic LC-MS experiments was 200 µl/min. For a comparison purpose, the LC-MS curtain gas was operated either normally (about 25 arbitrary units) or with a lower value (10 arbitrary units). The typical representative LC eluents with different compositions and additives were investigated, which include 1) 1 mM $CH_3COONH_4$ and/or 0,1 % $CH_3COOH$, and 2) 1 mM $HCOONH_4$ and/or 0,1 % $HCOOH$ in $ACN/H_2O$ or $MeOH/ H_2O$ (1:1, v/v) under different ionization conditions (mainly by varying the curtain gases for de-clustering) respectively. Before starting the experiments and also changing the mobile phases, the syringe and the complete tubing were flushed sufficiently until the chemical background was constant with regard to the ion intensities and types of the ions.

After inspecting the negative background ions in the full scan mode, MS/MS precursor ion scan and product ion scan with collision energies ranging from 5 to 40 eV were acquired for the major noise ions in order to draw a structure-relationship between them. In order to improve the detection of the low abundant background ions and their fragments, an average of 20-50 mass spectra was generally needed.

The accurate mass measurements were carried out on a 7.0 Tesla LTQ-FT hybrid linear ion trap Fourier transform ion cyclotron resonance (ICR) mass spectrometer (Thermo Fisher Scientific, Bremen, Germany) equipped with an electrospray ion source. The FT-ICR-MS was operated in full scan mode at a 200,000 resolution (m/z 400) for m/z 50 - 600 to obtain an overview of the background ions. For the highly sensitive detection of some specific background masses the mass range was selected as ± 1 Daltons of the mass of interest. The following parameters were used: the ESI spray voltage - 4.8 kV and the tube lens offset was - 87 V. The sheath gas flow was set to 3 or 5, and sweep gas flow to 0, 2 or 4 arbitrary units and the capillary temperature set to 250°C. The same mobile phases as for the low resolution experiments at a flow of 5 µL/min were used.

Acetonitrile and MeOH (HPLC gradient grade) were obtained from Karl Roth GmbH (Karlsruhe, Germany). Formic acid (98-100 %, p.a) and acetic acid (100 %, p.a) were purchased from Merck (Darmstadt, Germany). Furthermore, ammonium acetate (> 99 %, p.a) and ammonium formate (> 99 %, p.a) were obtained from Sigma-Aldrich Chemie GmbH

(Buchs, Switzerland). The ultra-pure water was supplied by an in-house ion-exchange Milli-Q Gradient system (Millipore, Bedford, USA).

## RESULTS AND DISCUSSION

The focus of this study is to investigate typical negative background ions derived from common HPLC solvents and additives as well as different interface conditions in API LC-MS. In the practice and literature it has been evident that chemical background interferences depend slightly on different suppliers of the used chemicals. However, the intention of this study is not to compare the supplier-dependent impurities of the chemicals, but to comprehensively characterize a few typical LC-MS mobile phase conditions with regard to the negative chemical background noise. Therefore, the result may be universally valid and provides insights into the sources of chemical background interferences under the negative mode. This study is realized by investigating the products and precursors of the major background ions to find out their structure relationship using tandem mass spectrometry.

### Typical negative background mass spectra in LC-MS

The typical negative ESI LC-MS background mass spectra obtained from the two frequently used LC eluents are compared in Figure 1. It is known that the abundances of the background ions are closely related to the de-clustering conditions of the LC-MS interface such as the curtain gas flow, the de-clustering potential, the ring focusing potential and the temperature of the heater gas on a Sciex triple quadrupole instrument. A similar observation of the variation of the background on the interface temperature with a heated capillary on other instruments is also well recognized in practice. Although the overall abundances of the negative background ions are lower than that in positive mode, (12) it is still a crucial interfering factor in negative LC-MS trace analysis. In order to study the very low abundant background ions, some experiments were also carried out under a relatively low curtain gas condition. A typical example of such a full mass spectrum is shown in Figure 1b, where more abundant distinct background ions become visible. They are mainly related to the clusters of mobile phase components, e.g. water or $CH_3COOH$ as being discussed later in the text. It can be seen in Figure 1 that, over the mass range of m/z 30-300, there are significant background ions in all cases. They may not only contribute to the high level of the background baseline in LC-MS but also interfere with analytes in this region by completely overshadowing the appearance of analytes in chromatograms and even as isobaric ions in mass spectra.
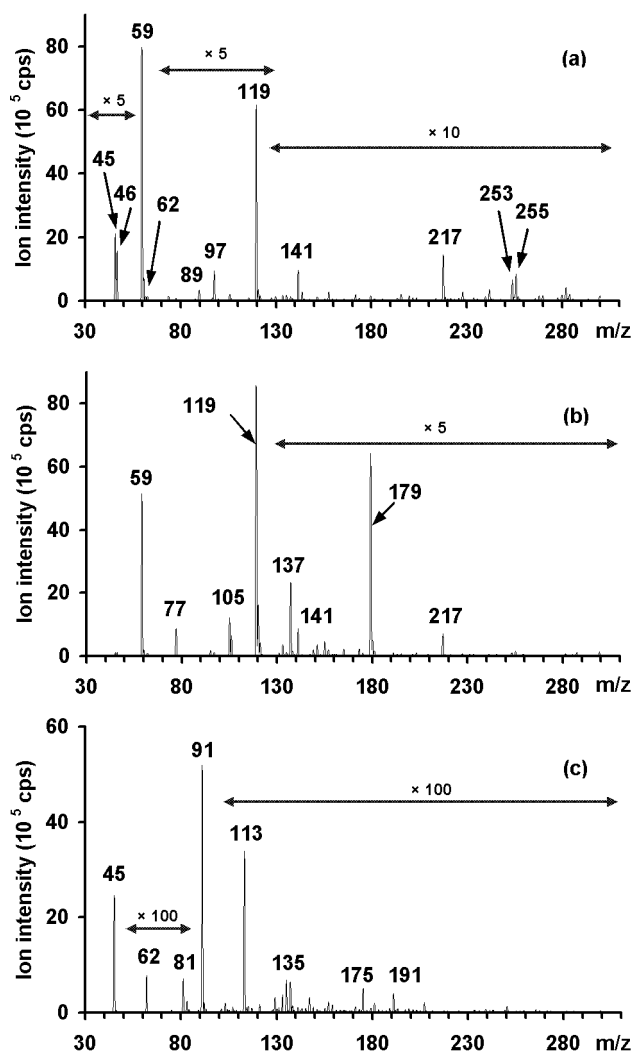
**Figure 1.** Typical negative ESI-MS full-scan mass spectra of (**a**) the eluent with 1 mM CH₃COONH₄ and 0,1 % CH₃COOH in ACN/H₂O (1:1, v/v); (**b**) the same eluent as in (**a**), but under the condition of a relatively low curtain gas flow; and (**c**) the eluent with 1 mM HCOONH₄ and 0,1 % HCOOH in ACN/H₂O (1:1, v/v).

**Cluster ions involving the mobile phase components when ammonium acetate and acetic acid are used as the additives**

As already mentioned and shown in Figure 1, the main abundant background ions of the investigated eluents result from the added acids and/or salts, which are used as ionization agents under the negative mode. Actually the background spectrum remains rather similar when acetonitrile is changed to methanol due to their limited involvement. However, further clustering with water plays an important role in the generation of the background noise. Some important clusters of mobile phase components were studied using precursor and product ion scans and are discussed below in detail.

The precursor ion scan mass spectra of the two major background ions m/z 59 [CH$_3$COO]$^-$ and m/z 119 [(CH$_3$COOH)$_2$-H]$^-$ are shown in Figure 2, where the clear involvement of acetic acid CH$_3$COOH (*mw.* 60) and H$_2$O (*mw.* 18) molecules for clustering is indicated in these partially magnified mass spectra. The ions observed here make up to the major background contribution both in intensity and entities. A summary of the possible typical clusters of mobile phase components and clusters of contaminants with mobile phase components is given in Table 1.

**Table 1.** Summary of typical cluster related background ions involving mobile phase components

| Mobile phase additives or possible origins | Type of background ions |
|---|---|
| | Pure cluster ions of mobile phase components |
| CH$_3$COONH$_4$ and / or CH$_3$COOH | [(**CH$_3$COOH)$_a$** + **(H$_2$O)$_b$** + (CH$_3$COONa)$_c$ + (CO$_2$)$_d$ + $^\alpha$(HCOOH)$_e$ + $^\beta$(CH$_3$CN)$_f$ - H]$^-$ <br> (a = 1-6; b = 0-12; c = 0,3; d = 0-1; e = 0-1; f = 0-2) |
| HCOONH$_4$ and / or HCOOH | [(**HCOOH)$_a$** + **(H$_2$O)$_b$** + (HCOONa)$_c$ + (CO$_2$)$_d$ + $^\gamma$(NaHCO$_3$)$_e$ - H]$^-$ <br> (a =1-3; b = 0-3; c = 0-3; d = 0-2; e = 0,1) |
| | Other cluster ions of mobile phase components |
| Contaminants and additives | [$^\delta$46 + (CH$_3$COOH)$_b$ + (HCOOH)$_c$ + (CH$_3$COONa)$_d$ + (H$_2$O)$_e$]$^-$ <br> (a = 1,2; b = 0-2; c = 0-2; d = 0,1; e = 0-4) <br> [$^\varepsilon$62 + (CH$_3$COOH)$_a$ + (HCOOH)$_b$ + (CH$_3$COONa)$_c$ + (HCOONa)$_d$ + (H$_2$O)$_e$ + $^\beta$(CH$_3$CN)$_f$ + $^\varepsilon$(85)$_g$ + $^\zeta$(98)$_h$]$^-$ <br> (a = 0,1; b = 0,1; c = 0,1; d = 0,1; e = 0-3; f = 0-2; g = 0,1; h = 0,1) <br> [$^\eta$89 + (CH$_3$COOH)$_a$ + (HCOOH)$_b$ + (CH$_3$COONa)$_c$ + (HCOONa)$_d$]$^-$ <br> (a = 0-3; b = 0,1; c = 0-2; d = 0-2) |

| | Clustering between contaminants and mobile phase components |
|---|---|
| Contaminants and additives | $[^\zeta\textbf{(98)}_a + \textbf{(CH}_3\textbf{COOH)}_b + \textbf{(HCOOH)}_c + \textbf{(CH}_3\textbf{COONa)}_d +$ $\textbf{(H}_2\textbf{O)}_e + {}^\beta\textbf{(CH}_3\textbf{CN)}_f + \textbf{(63)}_g + {}^\gamma\textbf{(74)}_h - \text{H}]^-$ (a = 1-3; b = 0-3; c = 0,1; d = 0-2; e = 0-5; f = 0-2; g = 0,1; h = 0,1) |
| | $[\textbf{Cl} + \textbf{(CH}_3\textbf{COOH)}_a + \textbf{(HCOOH)}_b + \text{(CH}_3\text{COONa)}_c +$ $\text{(HCOONa)}_d + \text{(44)}_e]^-$ (a = 0-3; b = 0,1; c = 0-3; d = 0-2; e = 0-2) |
| | $[{}^\theta 74 + \text{(CH}_3\text{COOH)}_a -\text{H}]^-$ (a = 0-2) |

$^{\alpha)}$    The presence of the formic acid or formate-related clusters is most probably not a contamination of the eluent, rather possibly a product of the ESI process.

$^{\beta)}$ The low abundant clusters with $CH_3CN$ can only be detected under low de-clustering conditions.

$^{\gamma)}$    $NaHCO_3$ can also be considered as $NaOH + CO_2$.

$^{\delta)}$    The ions at m/z 46 are probably related to the electron attached species $[HCOOH]^-$; and the ions at m/z 62 correspond to $[HCOOH+O]^-$ or deprotonated ammonium formate $[HCOO+NH_3]^-$ (less likely).

$^{\epsilon)}$    The neutral *mw.* 85 is likely related to $CH_3CN + 44$ ($CO_2$).

$^{\zeta)}$    The neutral *mw.* 98 mainly refers to $H_3PO_4$.

$^{\eta)}$    The ions at m/z 89 may correspond to deprotonated lactic acid $[CH_3CH(OH)COO]^-$ or $[CO_2+HCOO]^-$ respectively.

$^{\theta)}$    The neutral *mw.* 74 presumably corresponds to dimethyloxosilane $Si(CH_3)_2O$ and the deprotonated form $[Si(CH_3)_2O - H]^-$ (m/z 73) was also observed.

Only very minor contribution of clustering with the neutral molecule $CH_3CN$ (*mw.* 41) was observable even under the low de-clustering conditions (Figure 2). For instance, this refers to the precursor ions of $[CH_3COO]^-$ (m/z 59) at m/z 100 (addition of 41) and 141 (addition of 82) in Figure 2a and m/z 141 in Figure 3. The product ion scan mass spectrum of m/z 141 in Fig. 3a shows the loss of a neutral of 82 (to form m/z 59 back). This indicates that the cluster ions $[(ACN)_2+CH_3COO]^-$ contribute to produce the background ions m/z 141, which is also confirmed by the elemental composition studies using accurate mass measurements (see,

Table S1 in the Supporting information). Another possibilities are the formation of clusters [CH₃COONa+CH₃COO]⁻ by addition of one CH₃COONa molecule (*mw.* 82) to [CH₃COO]⁻ and some minor isobaric contribution from [CH₃COOH+HCOOH+2H₂O-H]⁻ respectively. This sodium contribution may depend highly on its availability in mobile phases or samples. The ions at m/z 141 further form clusters with the solvent components and contaminants (Figure 3b). Furthermore, m/z 157 and m/z 217 (Fig. 2a) are mainly related to clusters between neutral molecule CH₃COOH and deprotonated phosphoric acid [H₂PO₄]⁻ (m/z 97) - a well-known contaminant derived from the plasticizer phosphates, which will be discussed in detail later in this paper. A minor portion of [(CH₃COOH)₂+³⁷Cl]⁻ (m/z 157) was also confirmed with accurate mass measurement.
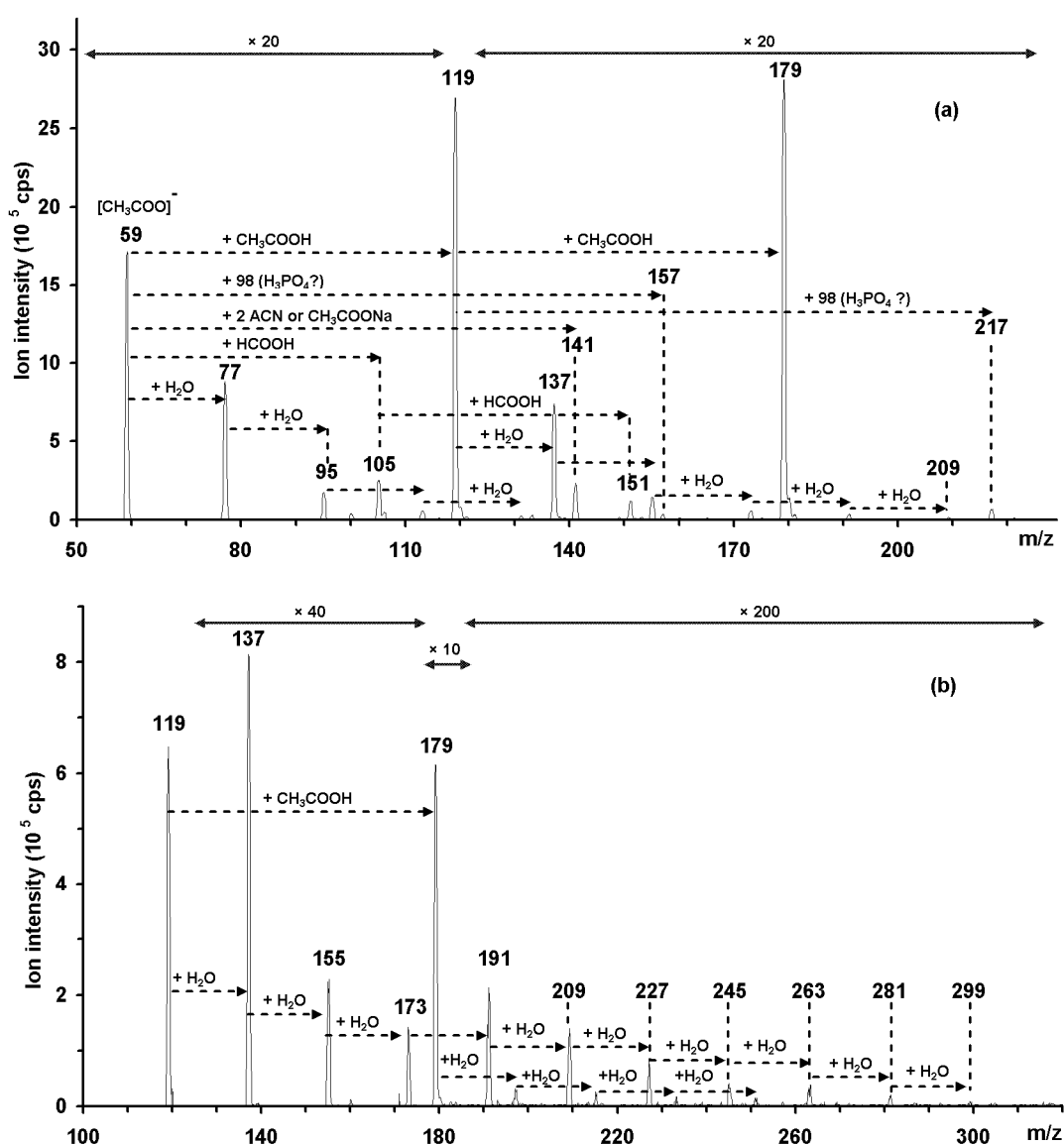


**Figure 2.** Precursor ion scan mass spectrum of (**a**) m/z 59 [CH₃COO]⁻ at a collision energy of 15 eV and (**b**) m/z 119 [(CH₃COOH)₂-H]⁻ at a collision energy of 5 eV under a relatively low curtain gas condition.
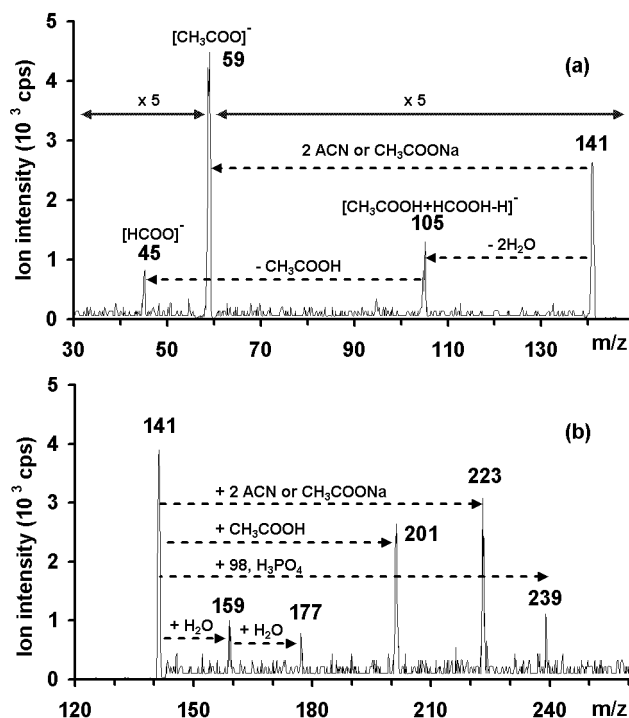
**Figure 3.** (**a**) Product ion scan (collision energy 8 eV) and (**b**) precursor ion scan (collision energy 5 eV) mass spectra of m/z 141 at a relatively low curtain gas condition.

In negative electrospray ionization mode using the given MS parameters (curtain gas, de-clustering potential and focusing potential), neither $CH_3COONH_4$ (*mw.* 77, a mobile phase additive) nor $HCOONH_4$ (*mw.* 63 in the other one discussed later) clusters could be detected. Instead of these ions, $CH_3COONa$ (*mw.* 82) and $HCOONa$ (*mw.* 68) adducts were observed. The presence of sodium as contaminant can be explained due to its ubiquitous nature. The corresponding adducts between formic acid and sodium were also shown in Figure 1c (m/z 113) and the further product and precursor ions indicating the involvement of $HCOONa$ are given later in Figure 5 and Figure 6 respectively. Therefore, most components of the mobile phase including $CH_3COOH$, $HCOOH$, $H_2O$, 44 ($CO_2$), $CH_3CN$ and $CH_3COONa$ are more or less involved in the cluster formation and the possible cluster-related noise ions are summarized in Table 1.

In Figure 1b, the ions at m/z 179 are assigned as $[(CH_3COOH)_3-H]^-$. This contribution appears to be the main species, and further tandem mass spectrometric experiments indicate that only minor isobaric $[97+CH_3COONa]^-$ (or, $[97+(ACN)_2]^-$, m/z 179) are present (data not shown). This is additionally confirmed by the precursor ion scan of m/z 97 as discussed later in the text.

148

The small background ions at m/z 45, 46 and 62 in Figure 1 do not directly interfere much in most tandem LC-MS studies (only contribute to the full-scan chromatogram baseline), however, their further clusters with other mobile phase components make significant contribution to the background noise. The presence of the ion [HCOO]$^-$ at m/z 45 in the full-scan mass spectrum when $CH_3COONH_4$ and $CH_3COOH$ as the additives (Figure 1a and b) is most probably not only a contamination of the eluent with formic acid or formate, but also likely due to the formation of [HCOO]$^-$ during the ESI process (heat, discharge and high voltage). The ions at m/z 46 may result from only a very small amount (ca. 1 %) of the $^{13}$C-isotope of the [HCOO]$^-$ anion but the major contribution might be related to an electron attached anion [HCOOH]$^-$ formed during discharge processes. The other discharge related species is [HCOOH+O]$^-$ (m/z 62), which underwent neutral loss of 16 *a.m.u.* in its product ion scan spectrum.

The ions at m/z 89 comprise of mainly deprotonated lactic acid [$CH_3$-CH(OH)-COO]$^-$, which can result from the contamination of lactic acid-related plastic (polylactide and polylactic acid) materials or detergents. This is in accordance with the two fragment ions at m/z 43 (likely an enolate anion [$CH_2$=CH-O]$^-$ by loss of a neutral formic acid molecule HCOOH) and 45 (deprotonated formic acid [HCOO]$^-$) respectively (see, Fig. S1a in the Supporting information). This assignment is also supported by its accurate mass as also shown in Table S1 in the supporting information. The other possible structures for m/z 89 such as the cluster [HCOO+$CO_2$]$^-$ (formed during ionization) and the contribution from ethylene glycol derivatives (contamination from detergents) can not be excluded either. All above-mentioned small ions are the original nuclei for further clustering with the eluent components as summarized in Table 1. As another example for cluster formation, the precursor ion scan mass spectrum of m/z 89 is also given in the supporting information (Fig. S1b), where further clustering with $CH_3COOH$, HCOOH and $CH_3COONa$ were observed and confirmed by elemental composition.

A comparison of the background noise ions in the range of m/z 220-350 in the full-scan mass spectra and that in the precursor ion scans of m/z 59 and m/z 119 is given in Figure 4. It is obvious that many other background ions, which are not related to the clusters of m/z 59 [$CH_3COO$]$^-$ or m/z 119 [($CH_3COOH$)$_2$-H]$^-$, are also present in the full-scan spectra. Some of them are included in the classification of other clusters. Anyway, there are still many minor contributions, which are not studied in detail due to their low abundances. However, all these noise ions with low abundances will also surely contribute to the chemical background and interfere LC-MS studies.
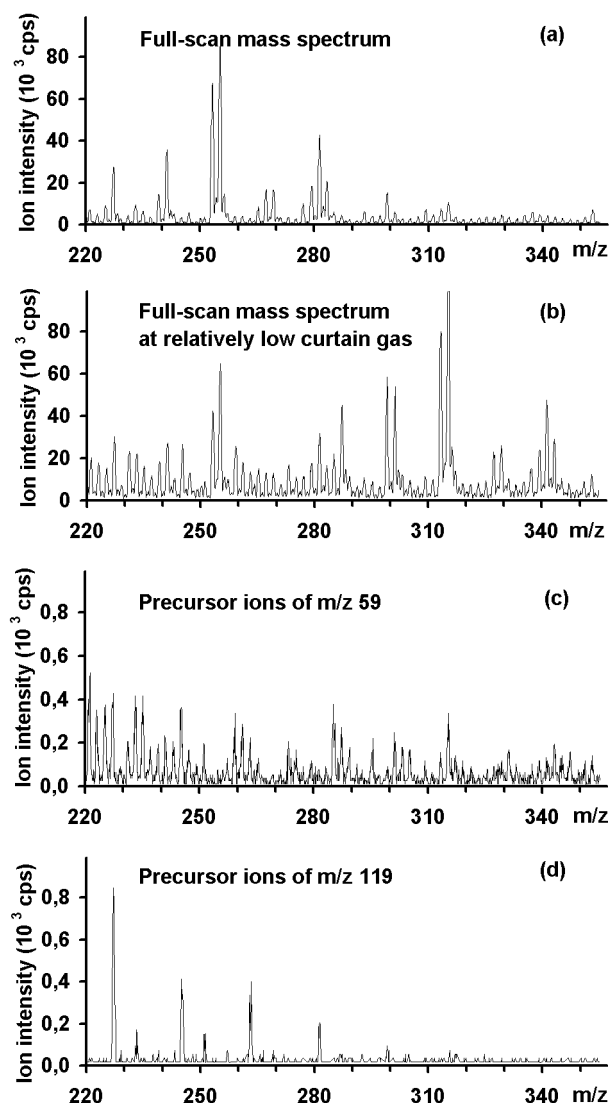
**Figure 4**. ESI-MS partial full-scan mass spectra of the eluent with 1 mM CH$_3$COONH$_4$ and 0,1 % CH$_3$COOH in ACN/H$_2$O (1:1, v/v) under (**a**) the standard curtain gas and (**b**) the low curtain gas conditions. For comparison, the precursor ion scan mass spectra of the ions at (**c**) m/z 59 and (**d**) m/z 119 obtained using the standard curtain gas are given. The result indicates that, although most ions in the whole spectra can be found in the precursors of m/z 59 and 119, there are always ions which are not related to either of them.

## Cluster ions involving the mobile phase components while ammonium formate and formic acid are used as the additives

Generally the mobile phase eluents investigated in this study are very alike with respect to the types of background ions. In Figure 1c two dominant peaks of [HCOO]$^-$ (m/z 45) and [(HCOOH)$_2$-H]$^-$ (m/z 91) are similar to m/z 59 and 119 in Figure 1a and b as the typical cluster-related species from mobile phase components. The precursor ion scan mass spectrum of m/z 45 showing the background ions derived from [HCOO]$^-$ is given in Figure 5.

Besides the pure cluster ions from the mobile phase components HCOOH and water, what also worth-mentioned is the formation of the significant cluster ions [HCOONa+HCOO]$^-$ at m/z 113, which has also been reported as a possible artifact peak in the negative ESI in the literature. (14) Their analogous clusters [CH$_3$COONa+CH$_3$COO]$^-$ at m/z 141 derived from acetic acid have already been discussed above in Figure 3. In addition, the further clustering of the ions at m/z 45, 113 and 137 with a neutral species of 44 *a.m.u.* was only detected when HCOOH was used as an additive, which indicates that the addition of 44 might relate to CO$_2$ or ethylene glycol oxide C$_2$H$_4$O from contamination. Both the elemental composition (as shown in Table S1 in the Supporting information) and the product ion scan mass spectrum of m/z 113 in Figure 6a confirm this assignment, where the product ions at m/z 69 and 45 by loss of the neutrals 44 and 68 (HCOONa) are present. And the precursor ion scan mass spectrum of m/z 113 in Figure 6b shows its further clustering with the molecules HCOONa and 44. Moreover, the involvement of sodium in clustering can also be observed in another form as in m/z 129 in Figure 5. The separate accurate mass FT-ICR-MS experiment confirms that at least the ions with a composition equivalent to [NaHCO$_3$+HCOO]$^-$ were found. Although here the ions at m/z 129 can also due to potassium salt [HCOOK+HCOO]$^-$ similar to [HCOONa+HCOO]$^-$ (m/z 113), no direct evidence was obtained from its product ion spectrum as shown in Fig. S2 in the supporting information, where the formation of the fragment ions at m/z 111 and 83 can only be explained better by [NaHCO$_3$+HCOO]$^-$.

As a summary, the background ions resulting from solvation / clustering reactions of mobile phase components and additives are given in Table 1. The contribution of the cluster ions purely derived from the mobile phase components to chemical background noise can be relatively easily reduced by improving de-clustering conditions such as higher curtain gas flow and temperature, high de-clustering potential, and high temperature of the heated capillary. An alternative is the choice of a different mobile phase, which at least offers the possibility to avoid specific eluent-dependent interfering noise ions. Hence, the knowledge about the identity of these eluent-related chemical background ions can assist us in the prevention/reduction of chemical interference during ESI LC-MS method development for trace analysis. However, the background ions discussed below are non-solvent- and non-additive-specific chemical interference ions, which are present persistently in negative ESI mass spectrum.
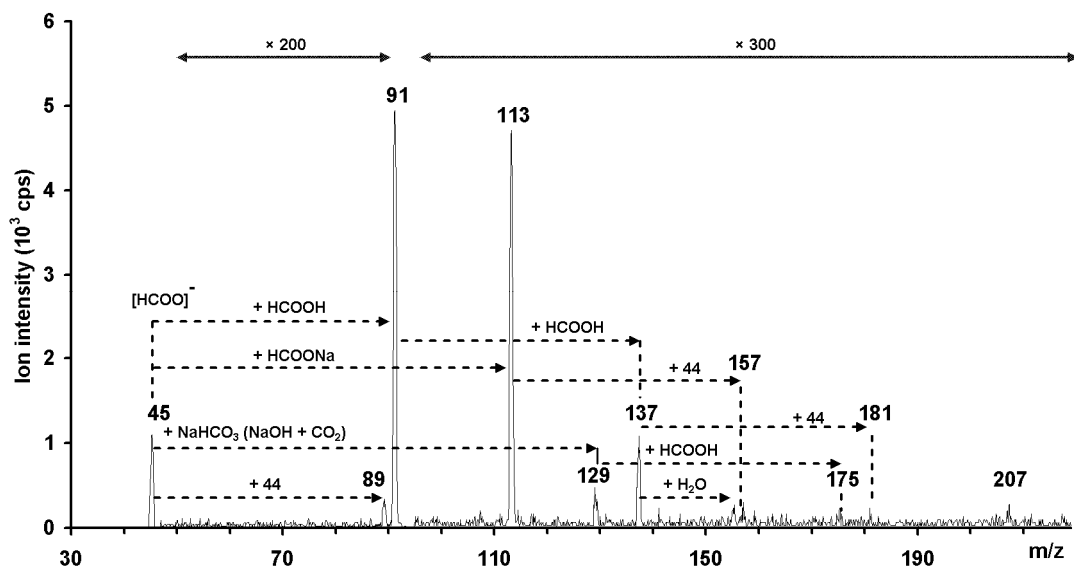
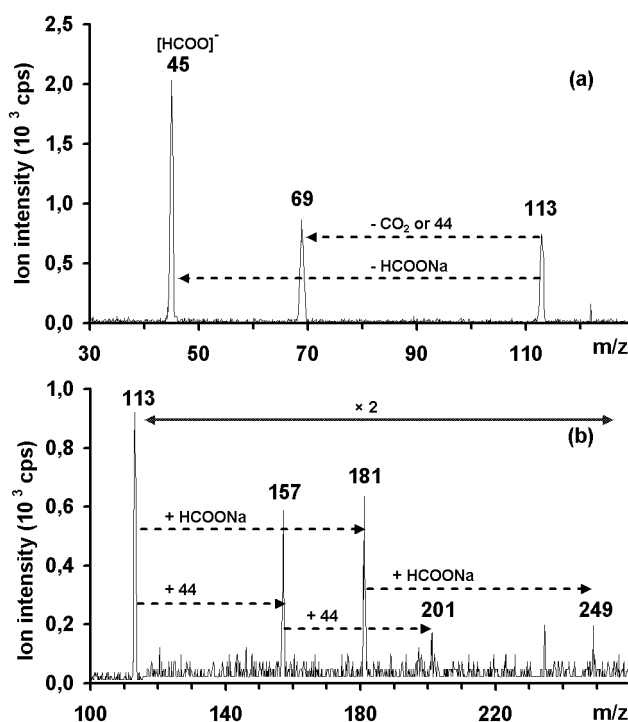**Figure 5.** Precursor ion scan mass spectrum of m/z 45 at a collision energy of 15 eV.



**Figure 6.** (**a**) Product ion scan and (**b**) precursor ion scan mass spectra of m/z 113 at a collision energy of 10 eV.

## Clustering between contaminants and mobile phase components

Besides the common negative background ions derived from solvent/additives exemplarily discussed above, abundant chemical background ions, which are not or not only originated from the mobile phase components, are also often observed in ESI LC-MS. These ions are

presumably originated from the mobile phase or ion source contaminants including plasticizers and silicones.

As demonstrated in the full-scan mass spectrum in Figure 1a and some precursor and product ion spectra while $CH_3COONH_4$ and $CH_3COOH$ were used as the additives, for example, the involvement of an anion with m/z 97 (or a neutral mass of 98) was often observed. The product ion scan mass spectrum of m/z 97 generated under a relatively high curtain gas condition and collision energy (25 eV) shows predominately the loss of water as a detectable fragment (mass spectrum given as Fig. S3 in the Supporting information), which at least excludes a possible contribution of $[HSO_4]^-$ (m/z 97) as however suggested by Tong *et al.* (14). Increasing the collision energy did not induce any further dissociation. This indicates that the majority of m/z 97 is likely from deprotonated phosphoric acid $[H_2PO_4]^-$ derived from a typical plasticizer triphenyl phosphate, which is also supported by our previous studies (12) in positive mode where the cations at m/z 99 are assigned as $[H_4PO_4]^+$. However, in this study, the product ion spectrum of m/z 97 formed under a relatively low curtain gas condition and low collision energy (5 eV) particularly shows the typical trace contribution of clusters between the mobile phase components and contaminants (Figure 7a) besides $[H_2PO_4]^-$. For instance, one small portion of m/z 97 consists probably of an adduct of an anion (m/z 37) with $CH_3COOH$, which is likely the [37]Cl isotope of $[CH_3COOH+Cl]^-$ (m/z 95) according to the high resolution measurement. This is further confirmed by loss of 38 H[37]Cl from m/z 97 to form anions at m/z 59, which is apparently $[CH_3COO]^-$. Accordingly, the loss of 36 (which could be interpreted as H[35]Cl) from m/z 97 to form an anion product at m/z 61 may be explained by the ^{13}C isotope contribution from m/z 59 due to its overwhelmingly high abundance.
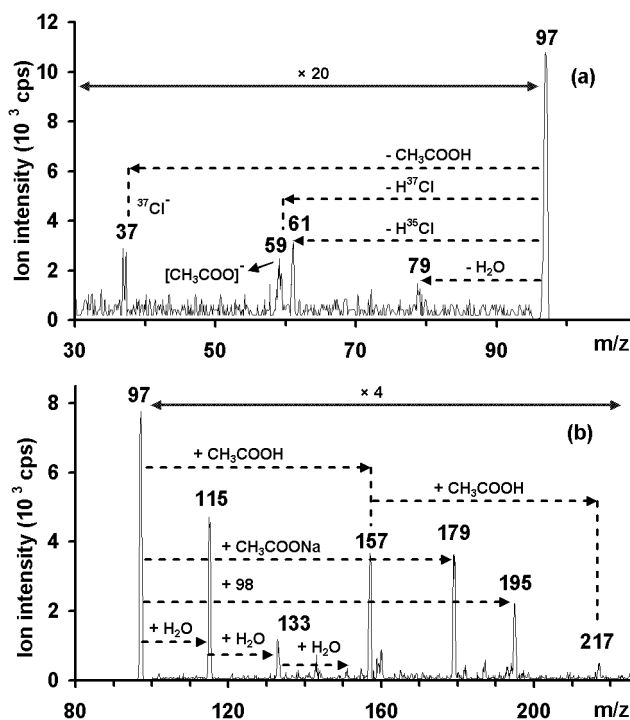
**Figure 7**. (**a**) Product ion scan mass spectrum of m/z 97 at a collision energy of 5 eV and (**b**) precursor ion scan mass spectrum of m/z 97 at a collision energy of 8 eV under a relatively low curtain gas condition when $CH_3COONH_4$ and $CH_3COOH$ were used as the additives.

Based on the above-mentioned mixed contributions at m/z 97, further clustering with the mobile phase components $CH_3COOH$, $H_2O$ and $CH_3COONa$ were observed both under the low and high de-clustering conditions as shown in its precursor ion scan mass spectrum in Figure 7b. A portion of the ions at m/z 195 correspond to $[98+H_2PO_4(97^-)]^-$ (supported by product ion scan) and $[CH_3COOH+(H_2O)_5+HCOO]^-$ (supported by the elemental composition) respectively. However, the presence of $[CH_3COOK+H_2PO_4]^-$ can not be supported by the accurate mass measurement. Although the ions at m/z 179 in Figure 2a are no doubt as $[(CH_3COOH)_2+CH_3COO]^-$, that as the precursors of m/z 97 in Figure 7b certainly have a different structure (likely $[CH_3COONa+H_2PO_4]^-$) as suggested by its product ion spectrum. A summary of possible background ions between the contaminants and mobile phase components is given in Table 1. Summary of typical cluster related background ions involving mobile phase components.

In addition, other contaminants and their clusters with mobile phase additives are also identified in the investigated eluents. For example, the product ion scan mass spectrum of m/z 133 represents the contribution of the typical silicon rubber related contaminant $Si(CH_3)_2O$ (*mw.* 74), where both the anion $[Si(CH_3)_2O - H]^-$ at m/z 73 and its cluster with acetic acid molecules were observed. Similar evidence is also shown in the product ion scan

mass spectrum of m/z 171 (tandem MS data of m/z 133 and 171 not shown). This anion at m/z 73 has also been reported in a previous investigation. (14)

## CONCLUSIONS

In this study the characteristics as well as their structure relationship of the most common chemical background ions under the negative ESI LC-MS mode have been investigated systematically. The result provides a general overview about the interfering background ions in negative ESI with regard to their classification and characteristics depending on their origins. The knowledge about the background ions of the investigated typical ESI-MS eluents can partially be transferred accordingly to other mobile phases due to the similarity of clustering. The main negative interference in the negative mode results from the cluster ions of solvents and additives. Additionally, there are also the clusters arising from the solvation of some typical contaminants (e.g. additives and degradation products from tubing, impurities in mobile phase, etc.), and accompanied by some minor contribution from individual contaminants. This differs somehow from the typical chemical background interferences in the positive ESI mode, where much significant contribution of chemical background noise derived from contaminants including plasticizers (phthalates, phenyl phosphates, adipates, etc.) and silicones are concluded. (12)

Since the aim of this study is to give a general overview about the correlation of background ions in negative ESI mode, not all ions discussed here were structurally identified. However, based on the current tandem mass spectrometric experiments, elemental compositions and literature, most structurally related ions are successfully classified into groups. Furthermore, it should be mentioned that, in general, the negative background cluster ions have significantly different structures compared with deprotonated analytes. This distinction may possibly contribute to developing a novel noise reduction technique using selective chemical reactions in LC-MS as already discussed in the positive mode. (10)

## ACKNOWLEDGMENT

**REFERENCES**

1. Fenn, J. B., M. Mann, C. K. Meng, S. F. Wong, and C. M. Whitehouse. 1989. Electrospray ionization for mass spectrometry of large biomolecules *Science* 246: 64-71.

2. Covey, T. R., E. D. Lee, A. P. Bruins, and J. D. Henion. 1986. Liquid-chromatography mass-spectrometry. *Anal Chem* 58: 1451A-1461A.

3. Applied Biosystems/MDS Sciex. 2006. Product Brochure: API 5000$^{TM}$ LC-MS/MS-System: Publication 114BR115-102.

4. Purves, R. W., R. Guevremont, S. Day, C. W. Pipich, and M. S. Matyjaszczyk. 1998. Mass spectrometric characterization of a high-field asymmetric waveform ion mobility spectrometer. *Rev Sci Instrum* 69: 4094-4105.

5. Sparkman, O. D. 2006. Mass spectremetry PittCon®. *J Am Soc Mass Spectrom* 17: 873-884.

6. Visentini, J., E. C. Kwong, A. Carrier, D. Zidarov, and M. J. Bertrand. 1995. Comparison of softwares used for the detection of analytes present at low-levels in liquid chromatographic mass spectrometric experiments. *J Chromatogr A* 712: 31-43.

7. Windig, W., J. M. Phalp, and A. W. Payne. 1996. A noise and background reduction method for component detection in liquid chromatography mass spectrometry. *Anal Chem* 68: 3602-3606.

8. Muddiman, D. C., A. L. Rockwood, Q. Gao, J. C. Severs, H. R. Udseth, R. D. Smith, and A. Proctor. 1995. Application of sequential paired covariance to capillary electrophoresis electrospray-ionization time-of-flight mass spectrometry-unraveling the signal from the noise in the electropherogram *Anal Chem* 67: 4371-4375.

9. Olsen, J. V., L. M. F. de Godoy, G. Q. Li, B. Macek, P. Mortensen, R. Pesch, A. Makarov, O. Lange, S. Horning, and M. Mann. 2005. Parts per million mass accuracy on an orbitrap mass spectrometer via lock mass injection into a C-trap. *Mol Cell Proteomics* 4: 2010-2021.

10. Guo, X., A. P. Bruins, and T. R. Covey. 2007. Method to reduce chemical background interference in atmospheric pressure ionization liquid chromatography-mass spectrometry using exclusive reactions with the chemical reagent dimethyl disulfide. *Analytical Chemistry* 79: 4013-4021.

11. Guo, X., A. P. Bruins, T. R. Covey, M. Trötzmüller, and E. Lankmayr. 2009. Alternative Reagents for Chemical Noise Reduction in Liquid Chromatography-Mass Spectrometry Using Selective Ion-Molecule Reactions. *J Am Soc Mass Spectrom* 20: 105-111.

12. Guo, X., A. P. Bruins, and T. R. Covey. 2006. Characterization of typical chemical background interferences in atmospheric pressure ionization liquid chromatography-mass spectrometry. *Rapid Commun Mass Spectrom* 20: 3145-3150.

13. (a) X.H. Guo, A.P. Bruins, T.R. Covey. Chemical noise reduction for mass spectrometry. *U.S. Patent* 7528365. (b) X.H. Guo, A.P. Bruins, T.R. Covey. Chemical noise reduction for mass spectrometry. *International Patent* 2007/092873.

14. Tong, H., D. Bell, K. Tabei, and M. M. Siegel. 1999. Automated data massaging, interpretation, and E-mailing modules for high throughput open access mass spectrometry. *J Am Soc Mass Spectrom* 10: 1174-1187.

15. Keller, B. O., J. Suj, A. B. Young, and R. M. Whittal. 2008. Interferences and contaminants encountered in modern mass spectrometry. *Anal Chim Acta* 627: 71-81.

16. New Objective, Inc. 2011. Technical Note PV-3: *Common Background Ions for Electrospray*. Online available at: www.newobjective.com/downloads/technotes/PV-3.pdf.

**SUPPORTING INFORMATION**

**Supplementary Table 1S.** List of some negative background ions encountered in ESI LC-MS with possible structure / composition assignments based on MS/MS and selected elemental composition measurements in this study. It should be noted that the ions accompanied with an elemental composition were studied and confirmed so far by FT-ICR-MS accurate mass measurements, and those without were either not investigated or not possible to be confirmed because the differences between the two MS instruments do exist.

| M/z | Possible structures / elemental compositions [a] | Found mass (a.m.u.) [b] | Error (ppm) [b] | Remarks |
|-----|-----|-----|-----|-----|
| 35 | $^{35}Cl^-$ | | | |
| 37 | $^{37}Cl^-$ | | | |
| 43 | $[C_2H_3O]^-$ ? | | | |
| 45 | $[HCOO]^-$ | | | Mainly when formic acid used |
| 46 | $[H^{13}COO]^-$, $[HCOOH]^{-\bullet}$ | | | Mainly when formic acid used. The abundance of m/z 46 is much higher than the $^{13}C$ contribution alone. No further MS/MS fragments were detectable. The electron attachment possibly occur during ESI. |

| 59 | $[CH_3COO]^-$ | 59,013850 | + 0,1 ppm | |
| 62 | $[HCOOH+O]^{-\bullet}$ | | | Mainly when formic acid used |
| 63 | $[H_2O+HCOO]^-$ | 63,008760 | + 0,1 ppm | Mainly when formic acid used |
| 64 | $[H_2O+H^{13}COO]^-$, $[H_2O+HCOOH]^{-\bullet}$ | | | Mainly when formic acid used |
| 69 | No assignment yet | | | |
| 73 | $[Si(CH_3)_2O - H]^-$ | | | |
| 77 | $[H_2O+CH_3COO]^-$ | 77,024460 | + 0,7 ppm | |
| 80 | $[HCOOH+H_2O+O]^{-\bullet}$ | | | Mainly when formic acid used |
| 81 | $[(H_2O)_2+HCOO]^-$ | | | Mainly when formic acid used |
| 82 | $[(H_2O)_2+H^{13}COO]^-$, $[HCOOH+(H_2O)_2]^{-\bullet}$ | | | Mainly when formic acid used |
| 89 | $[CH_3CH(OH)COO]^-$ | 89,024450 | + 0,5 ppm | |
| 91 | $[HCOOH+HCOO]^-$ | 91,003720 | + 0,6 ppm | Mainly when formic acid used |
| 92 | $[HCOOH+H^{13}COO]^-$, $[HCOOH+HCOOH]^{-\bullet}$ | 92,007080 | + 0,7 ppm | Mainly when formic acid used |
| 95 | $[CH_3COOH+^{35}Cl]^-$, $[(H_2O)_2+CH_3COO]^-$ | 94,990610 | + 0,9 ppm | |
| 97 | $[CH_3COOH+^{37}Cl]^-$, $[H_2PO_4]^-$, $[62+^{35}Cl]^-$ | 96,987650 | + 0,9 ppm | |

| 100 | [ACN+CH$_3$COO]$^-$ | 100,040450 | + 0,6 ppm | |
|---|---|---|---|---|
| 105 | [CH$_3$COOH+HCOO]$^-$ | 105,019410 | + 0,9 ppm | |
| 106 | [CH$_3$COOH+H$^{13}$COO]$^-$, [CH$_3$COOH+HCOOH]$^{-\bullet}$ | 106,022760 | + 0,9 ppm | |
| 113 | [HCOONa+HCOO]$^-$, [(H$_2$O)$_3$+CH$_3$COO]$^-$, [69+44]$^-$ | 112,985870 | + 2,3 ppm | |
| 115 | [H$_2$O+97]$^-$, [71+44]$^-$ | | | |
| 116 | No assignment yet | | | |
| 119 | [CH$_3$COOH+CH$_3$COO]$^-$ | 119,035060 | + 0,8 ppm | |
| 120 | [CH$_3$COOH+$^{13}$CH$_3$COO]$^-$ | 120,038430 | + 0,9 ppm | |
| 121 | [H$_2$O+CO$_2$+CH$_3$COO]$^-$ | | | |
| 123 | [CH$_3$COOH+H$_2$O+HCOO]$^-$ | | | Mainly when formic acid used |
| 124 | [CH$_3$COOH+H$_2$O+H$^{13}$COO]$^-$, [CH$_3$COOH+H$_2$O+HCOOH]$^{-\bullet}$ | | | Mainly when formic acid used |
| 127 | [CH$_3$COONa+HCOO]$^-$ | | | |
| 128 | [CH$_3$COONa+H$^{13}$COO]$^-$, [CH$_3$COONa+HCOOH]$^{-\bullet}$ | | | Mainly when formic acid used |
| 129 | [NaHCO$_3$+HCOO]$^-$ | 128,980850 | + 2,5 ppm | Mainly when formic acid used |

| | | | | |
|---|---|---|---|---|
| 131 | $[(H_2O)_4+CH_3COO]^-$ | 131,056430 | + 2,6 ppm | |
| 133 | $[Si(CH_3)_2O+CH_3COO]^-$ | 133,032480 | - 1,1 ppm | |
| | $[(H_2O)_2+ CH_3COOH+^{37}Cl]^-$ | 133,008850 | + 1,2 ppm | |
| 135 | $[HCOOH+44+HCOO]^-$, | | | Mainly when formic acid used |
| 136 | No assignment yet | | | |
| 137 | $[CH_3COOH+H_2O+CH_3COO]^-$, | 137,045660 | + 1,0 ppm | |
| | $[(HCOOH)_2+HCOO]^-$, | 137,009230 | + 0,7 ppm | Mainly when formic acid used |
| | $[93+44]^-$ | | | |
| 138 | $[CH_3COOH+H_2O+^{13}CH_3COO]^-$ | | | |
| 141 | $[(ACN)_2+CH_3COO]^-$, $[CH_3COOH+(H_2O)_2+HCOO]^-$, $[CH_3COONa+CH_3COO]^-$ | 141,067390 | + 3,2 ppm | |
| 142 | $[CH_3COOH+(H_2O)_2+H^{13}COO]^-$ | | | Mainly when formic acid used |
| 143 | $[HCOOH+97]^-$ | | | Mainly when formic acid used |
| 149 | $[CH_3COOH+CH_3CH(OH)COO]^-$, $[(H_2O)_5+CH_3COO]^-$ | 149,045770 | + 1,6 ppm | |
| 151 | $[(H_2O)_3+CH_3COOH+^{37}Cl]^-$, | 151,019250 | + 0,1 ppm | |
| | $[CH_3COOH+HCOOH+HCOO]^-$ | 151,025070 | + 1,9 ppm | |

| | | | | |
|---|---|---|---|---|
| 155 | $[CH_3COOH+CH_3COOH+^{35}Cl]^-$, <br> $[(H_2O)_2+CH_3COOH+CH_3COO]^-$ | 155,011670 | + 0,2 ppm | |
| 156 | $[CH_3COOH+(H_2O)_2+^{13}CH_3COO]^-$ | | | |
| 157 | $[(CH_3COOH)_2+^{37}Cl]^-$, <br> $[CH_3COOH+H_2PO_4]^-$, <br> $[119+38]^-$, $[HCOONa+44+HCOO]^-$, $[69+(44)_2]^-$ | 157,008860 | + 1,1 ppm | |
| 159 | $[CH_3COOH+(H_2O)_3+HCOO]^-$ | | | |
| 160 | $[CH_3COOH+ACN+CH_3COO]^-$, | 160,061780 | + 1,7 ppm | |
| | $[CH_3COOH+(H_2O)_3+H^{13}COO]^-$ | 160,053810 | - 3,4 ppm | Mainly when formic acid used |
| 165 | $[CH_3COOH+HCOOH+CH_3COO]^-$, | 165,040720 | + 1,7 ppm | |
| | $[HCOONa+CH_3COOH+^{37}Cl]^-$, | 164,975340 | + 2,2 ppm | |
| | $[121+44]^-$ | | | |
| 166 | $[CH_3COOH+H^{13}COOH+CH_3COO]^-$ | 166,044070 | + 1,7 ppm | Mainly when formic acid used |
| 167 | $[(H_2O)_6+CH_3COO]^-$ | 167,077240 | + 0,2 ppm | |
| 171 | $[CH_3COONa+CH_3CH(OH)COO]^-$ <br> $[97+74]^-$ | 171,027730 | + 1,5 ppm | |
| 173 | $[CH_3COONa+HCOOH+HCOO]^-$, <br> $[CH_3COOH+(H_2O)_3+CH_3COO]^-$ | 173,007020 | + 1,7 ppm | Mainly when formic acid used |

| | | | | |
|---|---|---|---|---|
| 174 | $[CH_3COOH+(H_2O)_3+{}^{13}CH_3COO]^-$ | | | |
| 175 | $[CH_3COOH+H_2O+CH_3COOH+{}^{37}Cl]^-$, | 175,019270 | + 0,1 ppm | |
| | $[NaHCO_3+HCOOH+HCOO]^-$ | 174,986250 | + 1,5 ppm | Mainly when formic acid used |
| 177 | $[CH_3COOH+(H_2O)_4+HCOO]^-$ | | | |
| 178 | $[CH_3COOH+(H_2O)_4+H^{13}COO]^-$ | | | Mainly when formic acid used |
| 179 | $[(CH_3COOH)_2+CH_3COO]^-$, | 179,056360 | + 1,5 ppm | |
| | $[CH_3COONa+97]^-$, or $[(ACN)_2+97]^-$ | | | |
| 181 | $[93+(44)_2]^-$, $[137+44]^-$, | | | |
| | $[(HCOONa)_2+HCOO]^-$ | | | |
| 185 | $[(H_2O)_7+CH_3COO]^-$ | 185,087850 | + 0,5 ppm | |
| 189 | No assignment yet | | | |
| 191 | $[CH_3COOH+(H_2O)_4+ CH_3COO]^-$ | 191,077050 | - 0,8 ppm | |
| 192 | $[CH_3COOH+(H_2O)_4+{}^{13}CH_3COO]^-$ | | | |
| 193 | $[CH_3COOH+(H_2O)_2+CH_3COOH+{}^{37}Cl]^-$ | 193,029110 | - 3,6 ppm | |
| 195 | $[CH_3COOH+(H_2O)_5+HCOO]^-$, | 194,965040 | - 1,9 ppm | |
| | $[H_3PO_4+CH_3COOH+{}^{37}Cl]^-$, | 194,965040 | - 3,1 ppm | |
| | $[CH_3COOH+HCOOH+44+HCOO]^-$, | | | |
| | $[141+54]^-$, | | | |

| | | | |
|---|---|---|---|
| 196 | $[CH_3COOH+(H_2O)_5+H^{13}COO]^-$ | | |
| 197 | $[(CH_3COOH)_2+H_2O+CH_3COO]^-$ | 197,066320 | - 1,7 ppm |
| 201 | $[(CH_3COOH)_2+(H_2O)_2+HCOO]^-$, $[69+(44)_3]^-$ | 201,061200 | - 1,8 ppm |
| 203 | $[(H_2O)_8+CH_3COO]^-$, $[HCOOH+157]^-$ | | |
| 209 | $[(CH_3COOH)_2+CH_3CH(OH)COO]^-$, $[CH_3COOH+(H_2O)_5+CH_3COO]^-$, $[165+44]^-$ | 209,066250 | - 1,9 ppm |
| 210 | $[CH_3COOH+(H_2O)_5+{}^{13}CH_3COO]^-$ | | |
| 211 | $[CH_3COOH+(H_2O)_3+97]^-$, $[(CH_3COOH)_2+HCOOH+HCOO]^-$ | | |
| 215 | $[(CH_3COOH)_2+(H_2O)_2+CH_3COO]^-$ | 215,076780 | - 2,0 ppm |
| 217 | $[(CH_3COOH)_2+97]^-$, $[173+44]^-$, $[175+42]^-$ | | |
| 219 | No assignment yet, $[175+44]^-$, | | |
| 221 | $[(H_2O)_9+CH_3COO]^-$ | | |
| 223 | $[CH_3COOH+(H_2O)_4+HCOOH+HCOO]^-$ $[(CH_3COONa)_2+CH_3COO]^-$, $[CH_3COONa+(ACN)_2+CH_3COO]^-$ | 223,066840 | - 0,8 ppm |

| | | | |
|---|---|---|---|
| 225 | $[(CH_3COOH)_2+HCOOH+CH_3COO]^-$ | | |
| 227 | $[CH_3COOH+(H_2O)_6+CH_3COO]^-$ | 227,098680 | - 1,6 ppm |
| 228 | $[CH_3COOH+(H_2O)_6+^{13}CH_3COO]^-$ | | |
| 231 | $[CH_3COONa+CH_3COOH+CH_3CH(OH)COO]^-$ | | |
| 233 | $[(HCOOH)_2+(ACN)_2+CH_3COO]^-$ <br> $[(CH_3COOH)_2+(H_2O)_3+CH_3COO]^-$, <br> $[CH_3COOH+CH_3COONa+HCOOH+HCOO]^-$, <br> $[136+97]^-$, $[(HCOOH)_2+141]^-$, $[189+44]^-$ | 233,078080 | - 0,9 ppm |
| 235 | $[CH_3COOH+NaHCO_3+HCOOH+HCOO]^-$, <br> $[(CH_3COOH)_2+H_2O+97]^-$, <br> $[(H_2O)_4+CH_3COOH+44+CH_3COO]^-$ | 235,006720 | - 1,7 ppm |
| 237 | No assignment yet | | |
| 239 | $[(CH_3COOH)_3+CH_3COO]^-$, <br> $[CH_3COOH+CH_3COONa+97]^-$, <br> $[(H_2O)_{10}+CH_3COO]^-$, $[142+97]^-$ | 239,076850 | - 1,5 ppm |
| 241 | $[182+CH_3COO]^-$, No assignment yet | | |
| 243 | No assignment yet | | |
| 245 | $[CH_3COOH+(H_2O)_7+CH_3COO]^-$ | | |
| 246 | $[CH_3COOH+(H_2O)_7+^{13}CH_3COO]^-$ | | |

| | |
|---|---|
| 249 | [(HCOONa)$_3$+HCOO]$^-$ |
| 251 | [(CH$_3$COOH)$_2$+(H$_2$O)$_4$+CH$_3$COO]$^-$ |
| 253 | No assignment yet |
| 255 | [CH$_3$COOH+195]$^-$ |
| 259 | [200+CH$_3$COO]$^-$ |
| 263 | [CH$_3$COOH+(H$_2$O)$_8$+CH$_3$COO]$^-$ |
| 269 | [CH$_3$COOH+209]$^-$ |
| 277 | [CH$_3$COOH+217]$^-$ |
| 281 | [CH$_3$COOH+(H$_2$O)$_9$+CH$_3$COO]$^-$ |
| 285 | [(H$_2$O)$_8$+CH$_3$COONa+CH$_3$COO]$^-$ |
| 287 | [(CH$_3$COOH)$_2$+(H$_2$O)$_6$+CH$_3$COO]$^-$ |
| 291 | [CH$_3$COONa+(CH$_3$COOH)$_2$+CH$_3$CH(OH)COO]$^-$ |
| 293 | [CH$_3$COOH+233]$^-$ |
| 299 | [CH$_3$COONa+217]$^-$, [126+173]$^-$, [76+223]$^-$, |
| 301 | [182+ CH$_3$COOH+CH$_3$COO]$^-$, [HCOOH+255]$^-$ |
| 305 | [(CH$_3$COOH)$_2$+(H$_2$O)$_7$+CH$_3$COO]$^-$ |
| 313 | [96+217]$^-$, [CH$_3$COOH+253]$^-$ |
| 315 | [H$_3$PO$_4$+217]$^-$, [CH$_3$COONa+233]$^-$ |

| | |
|------|-------------------------------------|
| 315 | [CH$_3$COOH+255]$^-$ |
| 319 | [200+CH$_3$COOH+CH$_3$COO]$^-$ |
| 323 | [182+CH$_3$COONa+CH$_3$COO]$^-$ |
| 347 | [(CH$_3$COOH)$_3$+(H$_2$O)$_6$+CH$_3$COO]$^-$ |
| 359 | [CH$_3$COOH+299]$^-$ |
| 361 | [CH$_3$COOH+301]$^-$ |
| 373 | [CH$_3$COOH+313]$^-$ |
| 375 | [H$_3$PO$_4$+CH$_3$COOH+217]$^-$ |
| 381 | [164+217]$^-$, [CH$_3$COONa+299]$^-$ |
| 391 | [174+217]$^-$ |
| 457 | [H$_3$PO$_4$+CH$_3$COOH+ CH$_3$COONa+217]$^-$ |

When the ^{13}C contribution is assigned or assumed, this ^{13}C atom can be at any other possible positions as well;

The found accurate mass and error correspond to the structure / elemental composition in the same row with the same color.
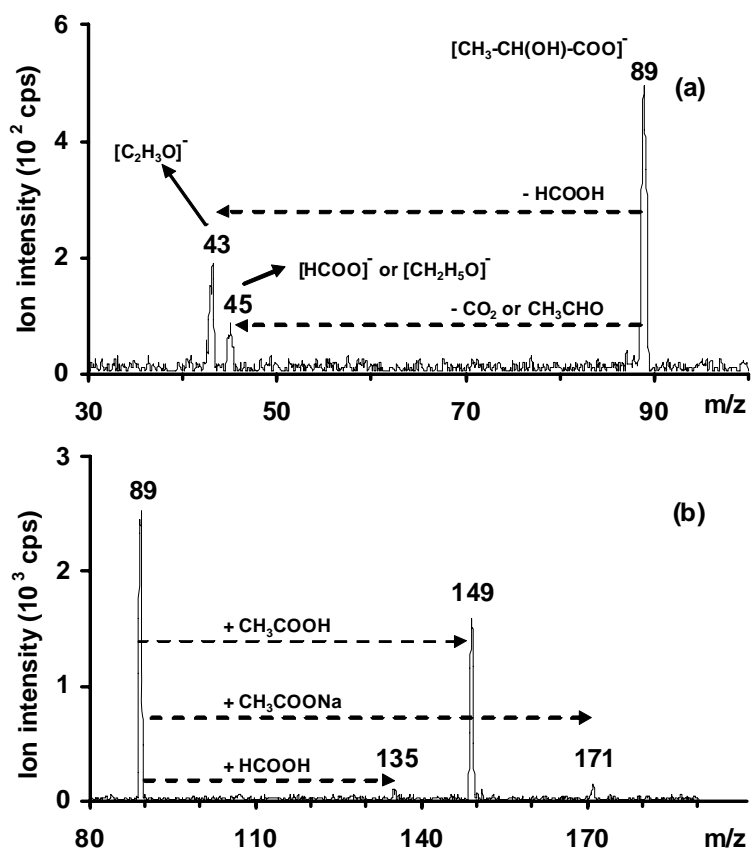
Figure S1. (a) Product ion scan (collision energy 15 eV) and (b) precursor ion scan (collision energy 8 eV) mass spectra of m/z 89.
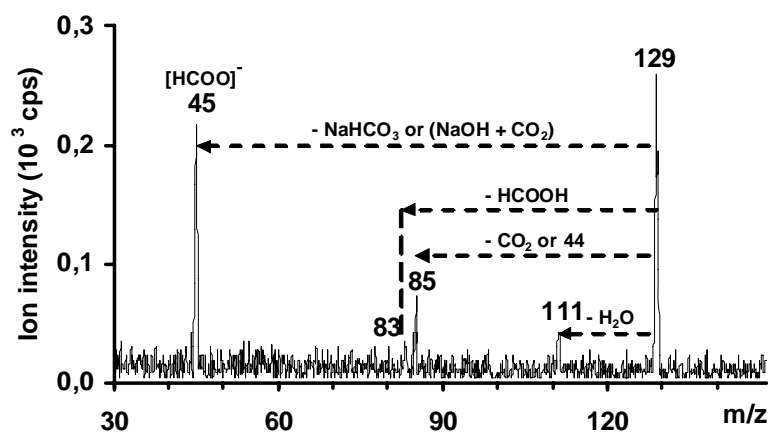
**Figure S2.** Product ion scan mass spectrum of m/z 129 at a collision energy of 10 eV.
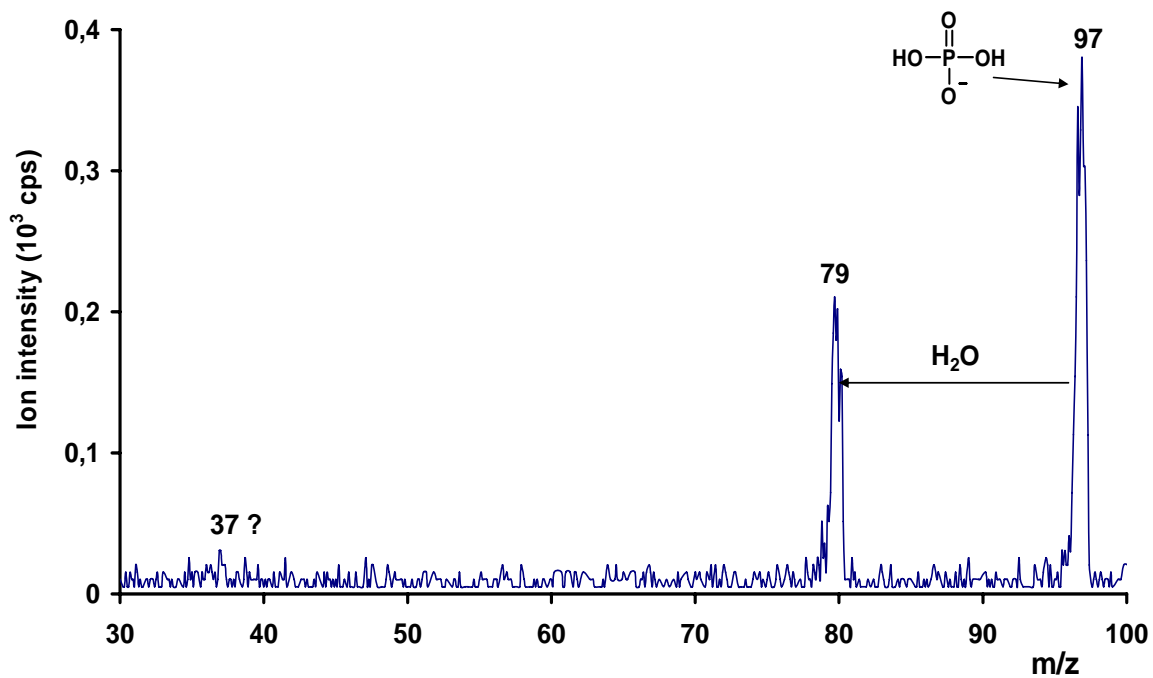
**Figure S3.** The product ion scan mass spectrum of m/z 97 generated under a relatively high curtain gas condition (which means after removing the contribution of the most cluster type ions) and high collision energy (25 eV) shows predominately the loss of water as a detectable fragment. Increasing the collision energy did not induce further fragmentation.

## C.6.  References

1.  Guo, X. 2011. Habilitation Thesis: Developments of Liquid Chromatography (LC-MS) for Trace Bioanalysis. Graz University of Technology.
2.  Shevchenko, A., and K. Simons. 2010. Lipidomics: coming to grips with lipid diversity. *Nat Rev Mol Cell Biol* 11: 593-598.
3.  Wenk, M. R. 2005. The emerging field of lipidomics. *Nat Rev Drug Discov* 4: 594-610.
4.  Watson, A. D. 2006. Thematic review series: systems biology approaches to metabolic and cardiovascular disorders. Lipidomics: a global approach to lipid analysis in biological systems. *J Lipid Res* 47: 2101-2111.
5.  The LIPID MAPS–Nature Lipidomics Gateway, 2012. http://www.lipidmaps.org.
6.  Lipid Library, 2012. http://lipidlibrary.aocs.org.
7.  Christie, W. W. 2003. LIPID ANALYSIS - Isolation, Separation, Identification, and Structural Analysis of Lipids, 3rd ed. Amer Oil Chemists Society.

# D. SUMMARY

Lipids are not regarded anymore as unimportant and uninteresting oily material only being cell membrane constituents and energy storing agents. The high diversity of molecular lipid species in living systems fulfils several different essential biological functions including structural roles or mediator molecules in cell signaling. In addition, imbalance of lipid metabolism and lipid-related pathways leads to a number of severe human diseases. Innovations in lipidomic technology greatly enhance our knowledge about lipid functions at the level of individual species. Thus, selective and sensitive mass spectrometry has become the ultimate tool for the characterization of different lipid species. Identification of lipid molecular species at very low trace levels with unusual fatty acid combinations such as for example TG 64:14 has become now manageable in combination with chromatographic separation systems.

Despite the high selectivity and sensitivity provided by modern mass spectrometers, which can be even increased if MS is coupled to LC, sample preparation still remains an integral part in organic trace analysis. Innovative techniques such as SPE can be used either for the separation of contaminants and the enrichment of low concentrated components or for the chromatographic separation of individual target analytes. An improved SPE separation of phospholipids based on their classes prior to LC-MS measurement is described in chapter C.3. In complex biological samples, the identification of phospholipid species by means of LC-MS might result in complications due to ion suppression and isobaric mass overlapping effects. The SPE approach developed for this purpose enables the separation of phospholipids species according to their headgroups into four fractions using two different kinds of sorbent material. Additionally, undesirable compounds are separated into an extra fraction. It is not worthwhile to separate each phospholipid species in a single fraction since it would on one hand be extremely time-consuming and on the other hand also other kinds of sorbent material would be required. The importance of the SPE approach is the separation of isobaric phospholipid species with the same elemental composition like PC 32:1 and PE 35:1 prior to LC-MS. A decrease of co-eluting analytes with the same exact mass on LC-MS finally results in higher sensitivity and a higher dynamic range of individual phospholipid species. The performance of the SPE procedure was validated by reference phospholipids spiked in the fermentation sample. Identification of phospholipids in the fermentation sample is performed on an ultra-high mass resolution and high mass accuracy mass spectrometer coupled online to an HPLC approach. In total 22 PA species, 10 PI species, 21 PG species, 6 PC species, 10 SM species and 9 PE species could be identified in the fermentation sample.

The main part of this work describes the development of a high throughput analytical platform for lipidomic research with an instrumental setup including reversed-phase HPLC coupled to a Fourier transform ion cyclotron resonance mass spectrometer, and Lipid Data Analyzer software (chapter C.4). We aimed to ensure the highest possible level of confidence for lipid profiling in pooled lipid droplets isolated from mouse hepatocytes. For this purpose, the distinct parameters being chromatographic retention, high mass resolution and accuracy as well as MS/MS spectra were combined. Especially the overwhelming amount of triacylglycerol species in murine lipid droplet samples increases the difficulties of a successful determination of all minor lipid species. Thus, the proposed 1D reversed-phase HPLC method enables the separation of highly concentrated TG species from the rest of the lipids. Nevertheless the chromatography is limited to the separation of isobaric compounds which can only be achieved by stretching the gradient significantly. However, the optimized HPLC method is a compromise between sufficient chromatographic resolution and short analysis times. Subsequent online detection of separated target analytes is performed on a high resolution LTQ-FT mass spectrometer. The instrument is operated in DDA mode where mass analyzers, the cyclotron and the linear ion trap, can be regarded as two separate instruments. This enables acquisition of low resolution MS/MS spectra in the linear ion trap on the most intense peaks in parallel to high resolution spectra acquired by the ion cyclotron. The DDA allows obtaining MS/MS spectra without the need to first identify the precursor in a previous high resolution full scan. Furthermore, the acquired untargeted MS/MS data offers the advantage to detect "unexpected" lipid species present in the sample. Besides high mass resolution and accuracy from full scans and MS/MS data, the chromatographic retention time also contributes to the selectivity for the identification and quantification of various lipid species. At very low abundant analytes often no MS/MS data are generated during DDA. Consequently, the retention time shift can be used as selective criterion for proper identification, since with reversed-phase chromatography the chromatographic separation within one class follows a general scheme. Additionally to the 1D also a 2D chromatographic approach has been investigated to improve the poor separation of PC from other phospholipid classes. PC tends to suppress co-eluting analytes due to its high ionization efficiency in positive ESI. To overcome this limitation, two complementary chromatographic dimensions, first HILIC followed by a reversed-phase approach, are employed. Thus, a clear separation of PC from the rest of the analytes can be achieved. This results finally in enhanced sensitivity especially for the detection of PE and DG species. Automated identification and quantification of high resolution LC-MS data is performed by the LDA software, whereas MS/MS data interpretation is still done manually.

One of the main drawbacks in organic trace analysis using ESI MS or ESI LC-MS is the ubiquitous chemical background noise. This unavoidable ionic chemical background derives from different sources e.g. abundant cluster ions from the mobile phase constituents and additives in LC-MS, cluster formation from solvation of typical contaminants or from other individual minor contaminants. Typical contaminants originate from additives and degradation products of tubing and from impurities in the mobile phase. Especially in trace analysis, background ions tend to overshadow low abundant target analytes in chromatograms or mass spectra. This results in poor quality MS and MS/MS spectra and complicates identification and quantitative studies. Thus, the characterization and the structure relationship of typical background ions in negative ESI deriving for example from HPLC solvents and additives are investigated systematically (chapter C.5). Different interface conditions in negative ESI LC-MS are examined, which leads to altered formation of cluster ions involving mobile phase components, additives and contaminants. Interface settings like curtain gas flow, de-clustering potential, ring focusing potential and temperature of the heater gas are varied which is helpful for proper identification of background ions. In addition, the elemental composition of several identified ions is confirmed by FT-ICR-MS measurements. In general the results provide an overview about the interfering background ions in negative ESI with regard to their classification and characteristics depending on their origins. The knowledge about detailed information of chemical background noise facilitates its prevention. This is not only relevant in lipid research but generally in organic trace analysis.

Within the past decades mass spectrometry and chromatographic technologies have underwent several developments. Due to the increasing sensitivity and selectivity provided by these technologies, they can be regarded as method of choice for qualitative and quantitative lipidomic analysis. Consequently, this emerging research field has been pushed forward by these techniques. However, detection and quantification of all individual lipids is not yet possible in a given cellular system because of analytical limitations. Each lipid class has its own rules for fragmentation and its specific ionization efficiency which makes development of one standardized 'all inclusive' method a daunting challenge. It is also impractical to stick to a single "golden standard" mass spectrometry approach since the advantage of a combination of various technologies provides better possibilities for successful lipidomic analysis. But the real bottleneck within several analytical platforms in lipidomics is the lack of automated data analyzing software tools. In order to deal with the huge amount of acquired data from various advanced MS instruments, automated and reliable software tools are required. Nevertheless, ongoing new developments and analytical methods including new software tools, improved shotgun approaches as well as online

coupled 1D and 2D chromatographic methods are very promising for the future in the relatively young research field of lipidomics.

# E. Curriculum Vitae

**Alexander Fauland, Dipl.-Ing.**

**Curriculum vitae**



## Personal

**Birth :** 7 October 1983, in Graz, Austria

**Affiliation :** Institute of Analytical Chemistry and Food Chemistry

Graz University of Technology

Stremayrgasse 9

A-8010 Graz, Austria

Tel.: +43 (316) 873 – 32512

Mobile: +43 (650) 5682778

E-mail: Alexander.Fauland@tugraz.at

http://www.analytchem.tugraz.at/

## Education

**since 2008:** PhD study at the Institute of Analytical Chemistry and Food Chemistry, Graz University of Technology, Austria. Supervisor: Prof. Dr. Ernst Lankmayr

**2008:** Diploma thesis: "*SPE fractionation of phospholipids in fermentation samples and their determination by ESI HPLC-MS/MS*" Supervisor: Prof. Dr. Ernst Lankmayr, Institute of Analytical Chemistry and Food Chemistry, Graz University of Technology, Austria.

**2002 - 2008:** Diploma study in Technical Chemistry – General Technical Chemistry, Graz University of Technology, Austria.

## Research experience

*2008 - 2012:* Organic trace analysis of various biological and industrial samples - customized analysis with different sample preparation and separation techniques (LLE, SPE, HPLC, GC...) were used in combination with detection methods, e.g. mass spectrometry, tandem mass spectrometry, UV-VIS, FTIR, photometry…

*2009 - 2012:* Development of LC-MS- and MS/MS-based lipidomic platforms for lipid profiling of various biological samples. Co-supervisor: Dr. Harald Köfeler, Core Facility of Mass Spectrometry in the Center of Medical Research, Medical University of Graz.

## Teaching experience

*2008 - 2012:* Lab practical course in Instrumental Analytics - Graz University of Technology

*2009 - 2012:* Lab practical course in Analytical Chemistry - Graz University of Technology

*2009 - 2012*: Lab practical course in Analytical Chemistry (Microbiology Study) - University of Graz

## Co-supervision of students

*2012:* BSc. Bernadette Reiter - Bachelor thesis (still in process).

*2011:* BSc. Johanna Schlaminger - Bachelor thesis: Determination of caffeine in chocolate by HPLC-UV

*2011:* MSc. Sandra Pötz - Master thesis: Method development for the analysis of oxidized phospholipids by 2D HPLC and mass spectrometry

**Peer-reviewed research articles**

*2012*

Köfeler H, **Fauland A**, Rechberger G, Trötzmüller M. Mass Spectrometry Based Lipidomics: An Overview of Technological Platforms. *Metabolites 2012; 1:19 - 38.*

*2011*

**Fauland A**, Koefeler H, Trötzmüller M, Knopf A, Hartler J, Eberl A, Chitraju C, Lankmayr E, Spener F. A comprehensive method for lipid profiling by liquid chromatography-ion cyclotron resonance mass spectrometry. *Journal of Lipid Research. 2011; 52:2314 - 2322.*

Trötzmüller M, Guo X, **Fauland A**, Köfeler H, Lankmayr E. Characteristics and origins of common chemical background noise ions in negative ESI LC-MS. *Journal of Mass Spectrometry 2011; 46: 553 - 560.*

Koc M, Donten M, Musijowski J, Guo X, **Fauland A**, Lankmayr E, Trojanowicz M. Applications of gas chromatography to determination of total organic fluorine after defluorination of perfluorooctanoic acid as a model compound**.** *Croatica chemica acta 2011; 3:399 - 406.*

**Publications in progress**

**Fauland A**, Trötzmüller M, Eberl A, Afiuni-Zadeh S, Köfeler H, Guo X, Lankmayr E. An improved SPE sample preparation method for fractionation of phospholipids. - s*ubmitted to The Journal of Separation Science*

Pabst M, Fischl R.M, Brecker L, Morelle W, **Fauland A**, Köfeler H, Altmann F, Léonard R. Rhamnogalacturonan II diversity results from fucose exchange, side chain length, methyletherification and methylesterification. - s*ubmitted to The Plant Journal*

**Oral Presentations**

*2012*

**Fauland A**, Trötzmüller M, Köfeler H, Lankmayr E. A comprehensive analytical system for lipid profiling of biological samples. - at Doctoral Days, NAWI Graz, Graz, Austria, 21.06.2012

Lankmayr E, **Fauland A**. Lipid profiling by LC/MS. - at CEEPUS Seminar on Analytical Chemistry. Bratislava, Slovakia, 21.05.2012

*2010*

**Fauland A**, Guo X, Lankmayr E. Shotgun Mass Spectrometry under Information Dependent Acquisition Control for Automated Lipidomic Analysis. - at Young Investigators Seminar on Analytical Chemistry. Venice, Italy, 29.06.2010

*2009*

**Fauland A**, Guo X, Lankmayr E. SPE fractionation of phospholipids in fermentation samples and their determination by ESI HPLC-MS/MS. - at Young Investigators Seminar on Analytical Chemistry. Graz, Austria, 29.06.2009

*2008*

Guo X, **Fauland A**, Trötzmüller M, Lankmayr E. SPE Fractionation for Phospholipids in Bacterial Cell- Membrane and Determination by HPLC- MS/MS. - at 9th Symposium on Instrumental Analysis. Pecs, Hungary, 29.06.2008

**Posters**

*2012*

Hartler J, Trötzmüller T, **Fauland A**, Büschl C, Schuhmacher R, Köfeler H, Thallinger G. Lipid Data Analyzer: automated identification and quantitation of lipid species in LC-MS data. - at ACIB Science Days. Vienna, Austria, 2.07.2012

Hartler J, Trötzmüller T, **Fauland A**, Büschl C, Schuhmacher R, Köfeler H, Thallinger G.

Automated and Reliable Detection and Quantitation of Low Abundant Lipid Species and Other Metabolites in LC-MS Data. - at 60th ASMS Conference on Mass Spectrometry and Allied Topics. Vancouver, Canada, 20.05.2012

**Fauland A**, Trötzmüller M, Guo X, Köfeler H, Lankmayr E. A simplified SPE procedure combined with HPLC-ESI/MS for phospholipid determination. -  at 2$^{nd}$ Graz Lipid Mass Spec Meeting. Graz, Austria at, 06.03.2012

*2011*

**Fauland A**, Trötzmüller M, Hartler J, Köfeler H, Lankmayr E. Lipid Profiling by Reversed Phase Chromatography Coupled to Fourier Transform Mass Spectrometry. - at ASMS Conference on Mass Spectrometry and Allied Topics. Denver, USA, 05.06.2011

*2010*

**Fauland A**, Trötzmüller M, Köfeler H, Lankmayr E. Infromation Dependent Aquisition Control for Automated Lipidomic Analysis. - at 3$^{rd}$ International Symposium on Lipid and Membrane Biology. Graz, Austria, 18.03.2010

*2009*

**Fauland A**, Trötzmüller M, Guo X, Lankmayr E. Combination of SPE, Shotgun ESI/MS and HPLC ESI/MS for thr determination of different classes of phospholipids. - at 1$^{st}$ Styrian Conference on Lipid Mass Spec. Graz, Austria, 21.10.2009

Dzimbova T, **Fauland A**, Guo X, Lankmayr E, Pajpanova T. Comparative Studies on Conventional and Microwave Sythesis of Peptide Nucleic Acid Monomers and Peptide Conjugates. - at 11$^{th}$ International Congress on Amino Acids, Peptides and Proteins. Vienna, Austria, 03.08.2009

*2008*

**Fauland A**, Trötzmüller M, Fauler G, Guo X, Lankmayr E. SPE fractionation of phospholipids in bacterial cell-membrane and determination by HPLC-MS/MS. - at 9$^{th}$ Symposium on Instrumental Analysis. Pecs, Hungary, 29.06.2008